

**Role of nuclear localized effectors of
Thecaphora thlaspeos in modulation
of host defense responses during
infection**

Inaugural-Dissertation

For the attainment of the title of doctor
in the Faculty of Mathematics and Natural Sciences
at the Heinrich Heine University Düsseldorf

Presented by

Summia Gul

From Mansehra, Pakistan

Düsseldorf, January 2023

From the institute for Microbiology
in the Faculty of Mathematical and Natural Sciences
of the Heinrich Heine University Düsseldorf

Published by the permission
of the Faculty of Mathematics and Natural Sciences at
Heinrich Heine University Düsseldorf

Supervisor: Prof. Dr. Michael Feldbrügge

Institute for Microbiology
Heinrich Heine University Düsseldorf

Co-supervisor: Prof. Dr. Laura Rose

Institute for Population Genetics
Heinrich Heine University Düsseldorf

Date of examination: 12.05.2023

The research detailed in this thesis was conducted from November 2017 until December 2022 in Düsseldorf at the Heinrich Heine University Düsseldorf in the institute for Microbiology under the supervision of Prof. Dr. Michael Feldbrügge.

I hereby confirm that for the published manuscript included in this thesis, my specific contribution has been accurately stated.

Statutory declaration

I, Summia Gul, hereby declare that I have fully and independently written the submitted dissertation without additional unauthorized support and consultation beyond that permitted and specified in the dissertation. Experimental work for this thesis has been conducted at Heinrich Heine University Düsseldorf according to the "Principles for Safeguarding and Good Scientific Practice". I performed a key role in the preparation of the experimental work, data analysis, interpretation, preparation of figures and writing of dissertation. This dissertation has not been submitted in the current or similar form to other institutions or faculties. I have not previously failed a doctoral examination procedure.

The work was done under the guidance and the supervision of **Prof. Dr. Michael Feldbrügge** and **Dr. Vera Göhre**

Institute for Microbiology

Heinrich Heine University Düsseldorf

Düsseldorf, January 2023

Eidesstattliche Erklärung

Ich, Summia Gul, versichere hiermit an Eides Statt, dass ich selbst und eigenständig die vorliegende Dissertation geschrieben habe, ohne der Zuhilfenahme von unautorisierter Hilfe. Die Experimente dieser Arbeit wurden an der Heinrich-Heine-Universität Düsseldorf durchgeführt, gemäß der "Grundsätze zur Sicherung guter wissenschaftlicher Praxis". Ich hatte die Schlüsselrolle in der Durchführung der Experimente, der Datenanalyse und Interpretation, sowie Herstellung der Abbildungen und dem Schreiben der Dissertation. Die Dissertation wurde in ihrer jetzigen oder ähnlichen Form noch bei keiner anderen Hochschule eingereicht. Ich habe zuvor keine erfolglosen Promotionsversuche unternommen.

Düsseldorf, den _____

Summia Gull

Table of Contents

Table of contents.....	I
Summary.....	1
Zusammenfassung.....	2
Abbreviations.....	4
1. Introduction.....	7
1.1 Pathogen born plant diseases: Economic importance and impact on global food security.....	7
1.2 Smut fungi and their relevance to important crop plants.....	8
1.2.1 <i>Ustilago maydis</i>	9
1.3 Plant-pathogen interactions.....	9
1.3.1 Fungal lifestyle.....	10
1.3.1.1 Necrotroph and hemibiotroph.....	10
1.3.1.2 Biotrophs.....	10
1.3.1.3 Endophytes.....	11
1.4 Plant immune system.....	11
1.4.1 PTI (Pathogen-triggered immunity).....	11
1.4.2 ETI (Effector-triggered immunity).....	12
1.5 Molecular events leading to plant hormone regulation during defense.....	13
1.5.1 Salicylic acid (SA).....	14
1.5.2 Jasmonic acid (JA).....	15
1.5.3 Ethylene.....	16
1.5.4 Modulation of SA-JA crosstalk during pathogen infection.....	17
1.6 Fungal effectors.....	19
1.6.1 Translocation of the effectors.....	20
1.6.2 Host proteins interaction of effectors.....	21
1.6.3 Nuclear-localized effectors.....	22
1.7. <i>Thecaphora thlaspeos</i> as a novel pathogen.....	24
2. Aims of this thesis.....	25
2.1 Hypothesis.....	25
2.2 Aims.....	25
3. Functional characterization of conserved effector <i>TtStp1</i>	26
3.1 Results.....	26
3.1.1 Revision of the <i>T. thlaspeos stp1</i> gene model.....	26
3.1.2 <i>T. thlaspeos</i> conserved effector <i>Stp1</i> is not functional in <i>U. maydis</i>	28
3.1.2.1 <i>U. maydis</i> strain generation and infection assay.....	28
3.1.2.2 Verification of <i>stp1</i> expression.....	30
3.2 Discussion.....	32

4. Summary and personal contribution to Courville et al., 2019	33
5. Functional characterization of nuclear localized effectors	54
5.1 Results	54
5.1.1 Inventory of <i>T. thlaspeos</i> NLS effectors.....	54
5.1.2 Effectors candidates are targeted to the nuclei of the plant cells in both stably transformed <i>A. thaliana</i> and in a heterologous expression system.....	55
5.3 Predicted NLS sequence is responsible for both nuclear and nucleolar localization of effectors.	57
5.4 NLS effectors delivered via <i>Pst</i> -LUX enhances bacterial proliferation in <i>A. thaliana</i>	59
5.5 Expression of <i>TtTue1</i> -Gfp in <i>A. thaliana</i> results in pronounced phenotypes in both early and late growth phases.....	61
5.6 Genetic modification of <i>TtTue1</i> in <i>T. thlaspeos</i>	63
5.6.1 <i>TtTue1</i> deletion strain.....	63
5.6.2 Translocation of <i>TtTue1</i> to the host plant.....	63
5.7 <i>TtTue1</i> interaction screening by using <i>A. thaliana</i> root library	64
5.8 <i>TtTue1</i> interaction screening identifies potential plant targets by using stress-induced cDNA library.....	66
5.9 Targeted Y2H verifies strong interaction of <i>TtTue1</i> with the 12 candidates.	68
5.10 Strength of interaction of full length CPK28 and JAS1 full-length proteins do not affect the strength of interaction with <i>TtTue1</i>	70
5.11 <i>In planta</i> confirmation of <i>TtTue1</i> interaction with CPK28 and JAS1	73
5.12 <i>In vitro</i> analysis of <i>TtTue1</i> interaction with CPK28 and JAS1	74
5.12.1 <i>AtJAS1</i> and <i>ArhJAS1</i> bind <i>TtTue1</i>	75
5.12.2 CT- <i>AtJAS1</i> has a slightly strong binding affinity for <i>TtTue1</i>	75
5.12.3 <i>AtCPK28</i> and <i>ArhCPK28</i> bind <i>TtTue1</i>	75
5.13 Quantitative analyses of <i>TtTue1</i> binding to JAS1 and CPK28.....	77
5.14 <i>ArhJAS1</i> localized to the nucleus while <i>ArhCPK28</i> is targeted to both nucleus and plasma membrane of plant.....	79
5.15 PTI response remain unchanged in presence of <i>TtTue1</i>	81
5.16 <i>TtTue1</i> triggered the secondary metabolite accumulation in plants.	82
5.17 Effect of CPK28 on colonization of <i>T. thlaspeos</i> upon culture infection	84
5.18 CPK28 is degraded while JAS1 remains unaffected upon incubation with <i>T. thlaspeos</i>	86
5.19 <i>TtTue1</i> has binding affinity towards host plant DNA	88
6. Discussion.....	91
6.1 Effectors accumulate in the plant nucleus	92
6.2 Nuclear effectors promote susceptibility and act as virulence factors	95
6.3 Identification of plant proteins targeted by <i>TtTue1</i>	97
6.4 Modification of plant hormone signaling in response to <i>TtTue1</i>	100
6.4.1 SA and JA/ET signaling and related transcriptional profile of <i>TtTue1</i>	100

6.4.2 The Hormonal modification and the developmental phenotype of <i>TtTue1</i> is interconnected.....	107
6.5 Conclusion and outlook.....	110
7. Materials and Methods	113
7.1 Materials.....	113
7.1.1 Plant lines	113
7.1.2 Strains	113
7.1.2.1 Bacteria	113
7.1.2.2 Yeast.....	114
7.1.2.3 <i>Thecaphora. thlaspeos</i>	114
7.1.2.4 <i>Ustilago. maydis</i>	114
7.1.3 Plasmids	114
7.1.3.1 Plasmids for protein expression in <i>U. maydis</i> and <i>T. thlaspeos</i>	114
7.1.3.2 Plasmids for protein expression in plants.....	115
7.1.3.3 Plasmids for protein expression in <i>S. cerevisiae</i>	117
7.1.3.4 Plasmids for protein expression in <i>E. coli</i>	118
7.1.4 Oligonucleotides	119
7.1.5 Antibiotics	121
7.1.6 Enzymes	121
7.1.7 Antibodies	121
7.1.8 Kits.....	121
7.1.9 Ladders.....	121
7.1.10 Media	122
7.2 Methods	123
7.2.1 Bacterial and fungal species	123
7.2.1.1 <i>E. Coli</i>	123
7.2.1.2 <i>Pseudomonas syringae</i>	123
7.2.1.3 <i>Agrobacterium tumefaciens</i>	124
7.2.1.4 <i>Saccharomyces cerevisiae</i>	124
7.2.1.5 <i>Thecaphora. thlaspeos</i>	125
7.2.1.6 <i>Ustilago. maydis</i>	126
7.2.2 Infection assays	127
7.2.2.1 Infection of <i>A. thaliana</i> with <i>P. syringae</i> (<i>Pst-LUX</i>).....	127
7.2.2.2 Infection of <i>A. thaliana</i> with <i>T. thlaspeos</i> culture	127
7.2.2.3 Infection of <i>Z. mays</i> with <i>U. maydis</i> SG200 strain.....	127
7.2.3 Plant growth condition and assays.....	128
7.2.3.1 <i>Arabidopsis</i> seed sterilization	128
7.2.3.2 <i>Arabidopsis</i> plant growth	128
7.2.3.3 <i>Arabidopsis</i> transgenic line generation	128

7.2.3.4 <i>N. benthamiana</i> infiltration with <i>A. tumefaciens</i>	128
7.2.4 Isolation of nucleic acids	129
7.2.4.1 Plasmid DNA extraction.....	129
7.2.4.2 <i>A. thaliana</i> gDNA extraction.....	129
7.2.4.3 <i>A. thaliana</i> RNA extraction.....	130
7.2.4.4 cDNA synthesis	130
7.2.4.5 Polymerase chain reaction (PCR).....	130
7.2.4.6 Restriction digestion	131
7.2.4.7 Gel extraction/PCR purification.....	131
7.2.4.8 DNA sequencing.....	131
7.2.4.9 Gene expression analysis (Semi quantitative RT-PCR).....	131
7.2.4.10 Southern blot analysis	131
7.2.5 Isolation of protein.....	133
7.2.5.1 Protein extraction from plant.....	133
7.2.5.2 Protein extraction from yeast	133
7.2.5.3 Western blot analysis.....	134
7.2.6 Cloning.....	134
7.2.6.1 Classical cloning.....	134
7.2.6.2 GoldenGate cloning	135
7.2.6.3 GreenGate cloning	135
7.2.6.4 Gateway cloning	136
7.2.7 <i>E. coli</i> protein expression and purification	137
7.2.7.1 Expression.....	137
7.2.7.2 Purification.....	137
7.2.7.3 Size exclusion chromatography (SEC)	138
7.2.8 GST pull down assay	138
7.2.9 MicroScale Thermophoresis (MST).....	138
7.2.10 Bimolecular fluorescence complementation (BiFC)	139
7.2.11 Chromatin immunoprecipitation (ChiP).....	139
7.2.12 ROS assay.....	141
7.2.13 Microscopy.....	141
7.2.14 Bioinformatic tool	141
7.2.15 Data analysis, writing and graphical design.....	142
8. References.....	143
9. Supplementary figures.....	167
10. Acknowledgement.....	181

Summary

Summary

Smut fungi present a prevalent group of plant pathogenic fungi that infect crop plants. Despite the vast information and tools that exist in the model smut fungus *Ustilago maydis*, the host plant responses to such fungal infection is difficult to study due to complexity of the genome. *Thecaphora thlaspeos* is the only smut fungus that infects Brassicaceae and colonizes the model plant *Arabidopsis thaliana* under the lab condition. Fungi establish their interaction with the host plant by deploying secreted molecules referred to as effectors. Effectors either promote virulence of fungal pathogens by suppressing plant defense responses or alter plant physiology for the fungal benefit. They manipulate a variety of host cellular functions and accordingly act in different cellular compartments. Nuclear-localized effectors often target proteins involved in transcriptional regulation, phytohormone signaling and programmed cell death. However, we have limited knowledge on the molecular mechanism of nuclear effectors.

Presented in this thesis, the characterization of nuclear localized effectors of *T. thlaspeos* with a focus on the non-conserved and novel effector *TtTue1*. This project was driven by the hypothesis that effectors of *T. thlaspeos* perform their function according to spatial distribution upon delivery into the host cell, where the nucleus is considered a hub for regulation of basic cellular processes. Effector delivery is still enigmatic for fungi, and the Stp-complex is the only evidence. Therefore, I investigated whether *T. thlaspeos* has a conserved system. However, *TtStp1* could not restore the function of *UmStp1* in complementation assays. Next, the characterization of nuclear localized effectors that might interfere with regulation of the host immune responses was the main focus of this study. A first transcriptome analysis of infected *Arabidopsis hirsuta* revealed 40 effector candidates. Among these, prediction of seven nuclear localized effectors has set the foundation of this investigation. Using heterologous approaches, an accumulation of NLS effectors in the plant nucleus with exclusive and dual localization patterns was shown. Furthermore, deletion of the predicted NLS results in exclusion from the nucleus for *TtTue1* indicative of its NLS mediated nuclear transport. In parallel, the candidates were tested in a bacterial heterologous delivery system to gain first insight into their virulence activity. This revealed that four candidates have significant effect on bacterial proliferation and thus seem to have virulence activity. Additionally, expression of *TtTue1* in *A. thaliana* leads to morphological phenotypes such as dwarf rosettes and induction of late flowering. These developmental phenotypes suggest that *TtTue1* might interfere with fundamental plant regulatory mechanisms and its similarity to auto-immune mutants point towards activation of plant immune responses.

TtTue1 was prioritize as top NLS effector candidate on basis of these observations. The investigation on *TtTue1* function was started by yeast-two-hybrid screens that revealed several potential plant targets of *TtTue1*, indicated its multi targeting function. *AtJAS1* and *AtCPK28* were identified as top plant targets of *TtTue1* and verified for full-length homologs of JAS1 and CPK28 of *Ar. hirsuta* both *in vivo* and *in vitro*. The well-known role of JAS1 strongly suggest that *TtTue1* alters the host hormone signaling. Furthermore, induction of genes associated with salicylic acid signaling, non-induced Jasmonic acid-responsive genes and accumulation of stress related hormones that include high level of salicylic acid in *TtTue1* overexpression line pointed toward interference with hormone cross-talk. Based on this study, I proposed that *TtTue1* interact with JAS1 in order to stabilize it and repress the activity of downstream MYC transcription factor. The second interaction partner, CPK28, is a negative regulator of BIK1-

Summary

mediated PAMP induced calcium burst. It might undergo degradation upon *TtTue1* interaction, but further characterization is required.

Taken together, the findings of this thesis contribute to our knowledge on the effector biology of *T. thlaspeos*. Verification of plant targets provides a working model for the molecular analysis of *TtTue1*. Identification of JAS1 and evidence towards its stabilization by *TtTue1* provide novel insight in to Jasmonic acid-mediated signaling pathway. Most importantly, *TtTue1* is found to be a first novel smut fungal effector that interacts with CPK28 to date. Interactions with JAS1 and CPK28 can be used to investigate the contribution of *TtTue1* to infection of *T. thlaspeos*.

Zusammenfassung

Brandpilze sind eine weit verbreitete Gruppe pflanzenpathogener Pilze, die Kulturpflanzen befallen. Trotz der umfangreichen Informationen und Hilfsmittel, die für den Modell- Brandpilz *Ustilago maydis* zur Verfügung stehen, ist die Reaktion der Wirtspflanze auf eine solche Pilzinfektion aufgrund der Komplexität des Wirtgenoms schwer zu untersuchen. *Thecaphora thlaspeos* ist der einzige Brandpilz, der Brassicaceae infiziert und die Modellpflanze *Arabidopsis thaliana* unter Laborbedingungen kolonisieren kann. Um eine stabile Interaktion mit der Pflanze einzugehen, werden vom Pilzpathogen sogenannte Effektoren eingesetzt. Diese kleinen Moleküle fördern entweder die Virulenz von Pilzpathogenen, indem sie pflanzliche Immunreaktionen unterdrücken, oder sie verändern die Pflanzenphysiologie zu Gunsten des Pilzes. Sie beeinflussen eine Vielzahl zellulärer Funktionen des Wirts und wirken dementsprechend in verschiedenen zellulären Kompartimenten. Im Zellkern lokalisierte Effektoren beeinflussen häufig pflanzliche Proteine, die an der Transkriptionsregulation, der Phytohormonsignalisierung und dem programmierten Zelltod beteiligt sind. Jedoch ist über die molekularen Mechanismen der nukleären Effektoren nur wenig genaueres bekannt.

In dieser Arbeit wird der im Zellkern der Wirtspflanze lokalisierende Effektor von *T. thlaspeos* *TtTue1* genauer untersucht. Er gehört zu einer nicht konservierten, für *T. thlaspeos* einzigartigen Gruppe von Effektoren an. Als Grundidee wird davon ausgegangen, dass die Effektoren von *T. thlaspeos* ihre Funktion entsprechend ihrer räumlichen Verteilung in der Wirtszelle ausüben, wobei der Zellkern das zentrale Element für die Regulierung grundlegender zellulärer Prozesse ist. Wie die Übertragung von Effektoren von Pilzen in die Wirtszelle funktioniert ist immer noch ungeklärt, der Stp-Komplex ist der einzige Anhaltspunkt für solch eine Übertragung. Daher wurde zunächst untersucht, ob der Stp-Komplex in *T. thlaspeos* konserviert ist. Allerdings konnte *TtStp1* die Funktion von *UmStp1* in Komplementationsversuchen nicht wiederherstellen. Als Nächstes wurden im Kern lokalisierte Effektoren, die in die Regulierung der Immunantwort des Wirts eingreifen könnten, genauer untersucht. Eine erste Transkriptomanalyse von infiziertem *Arabis hirsuta* Gewebe ergab 40 Effektor-Kandidaten. Die Vorhersage von sieben kernständigen Effektoren bildete die Grundlage für folgende Experimente. Mit Hilfe heterologer Expressionsansätze konnte die Akkumulation von NLS-Effektoren im Pflanzenkern mit exklusiven und dualen Lokalisierungsmustern nachgewiesen werden. Darüber hinaus führte die Deletion der vorhergesagten NLS zu einem Ausschluss von *TtTue1* aus dem Zellkern, was auf einen NLS-vermittelten Transport in den Zellkern hinweist. Parallel dazu wurden die Effektor-Kandidaten in einem bakteriellen heterologen System getestet, um einen ersten Einblick in ihre Virulenzaktivität zu gewinnen. Dabei zeigte sich, dass vier Kandidaten eine signifikante Wirkung auf die bakterielle Vermehrung haben und somit eine Virulenzaktivität besitzen.

Summary

Darüber hinaus führt die Expression von *TtTue1* in *A. thaliana* zu morphologischen Phänotypen wie Zwergrosetten und der Induktion einer späten Blüte. Diese Entwicklungsphänotypen deuten darauf hin, dass *TtTue1* in grundlegende pflanzliche Regulationsmechanismen eingreifen könnte, Ähnlichkeit mit Autoimmunmutanten deutet auf eine Aktivierung der pflanzlichen Immunantwort hin.

Aufgrund dieser Beobachtungen wurde *TtTue1* als wichtigster NLS-Effektor-Kandidat eingestuft. Die Untersuchung der Funktion von *TtTue1* erfolgte durch Hefe-Zwei-Hybrid-Screens, die mehrere pflanzliche Protein Interaktionspartner von *TtTue1* aufzeigten, was darauf hindeutet, dass *TtTue1* mehrere Ziele haben könnte. *AtJAS1* und *AtCPK28* wurden als wichtigste pflanzliche Ziele identifiziert und sowohl *in vivo* als auch *in vitro* wurde die Interaktion mit den Volllängenhomologe von *JAS1* und *CPK28* von *Ar. hirsuta* bestätigt. Die bekannte Rolle von *JAS1* deutet stark darauf hin, dass *TtTue1* die Wirtshormonsignalisierung verändert. Darüber hinaus deuten die Induktion von Genen, die mit der Salicylsäure-Signalisierung assoziiert sind, die nicht-induzierten Jasmonsäure-reaktiven Gene und die Akkumulation von stressbezogenen Hormonen, die eine Hochregulierung von Salicylsäure in der *TtTue1*-Überexpressionslinie einschließen, auf eine Störung des Hormon-Cross-Talks hin. Auf der Grundlage der in dieser Arbeit erzielten Daten habe ich vorgeschlagen, dass *TtTue1* mit *JAS1* interagiert, um es zu stabilisieren und die Aktivität des nachgeschalteten Transkriptionsfaktors *MYC* zu unterdrücken. Der zweite Interaktionspartner, *CPK28*, ist ein negativer Regulator des *BIK1*-vermittelten PAMP-induzierten Kalzium-Ausbruch. Er könnte durch die Interaktion mit *TtTue1* abgebaut werden, was jedoch noch weitergehend charakterisiert werden muss.

Zusammenfassend tragen die Ergebnisse dieser Arbeit zu unserem Wissen über die Effektorbiologie von *T. thlaspeos* bei. Die Verifizierung der pflanzlichen Zielproteine liefert ein Arbeitsmodell für die molekulare Analyse von *TtTue1*. Die Identifizierung von *JAS1* und die Hinweise auf seine Stabilisierung durch *TtTue1* liefern neue Erkenntnisse über den Jasmonsäure-Signalweg. Am wichtigsten ist jedoch, dass *TtTue1* der erste neuartige Brandpilz-Effektor ist, der mit *CPK28* interagiert. Die Wechselwirkungen mit *JAS1* und *CPK28* können genutzt werden, um den Beitrag von *TtTue1* zur Infektion von *T. thlaspeos* zu untersuchen.

Abbreviations

Abbreviations

<i>At</i>	<i>Arabidopsis thaliana</i>
<i>Arh</i>	<i>Arabis hirsuta</i>
AOC	ALLENE OXIDE CYCLASE
BiFC	Bimolecular fluorescence complementation
BIK1	BOTRYTIS-INDUCED KINASE 1
°C	Degree Celsius
CERK1	CHITIN ELICITOR RECEPTOR KINASE 1
Chip	Chromatin immunoprecipitation
µl	Microliter
µM	Micromolar
aa	Amino acid
AM	Arbuscular mycorrhizal
ATP	Adenosine triphosphate
BLAST	Basic Local Alignment Search Tool
bp	Base pairs
BIC	Biotrophic interfacial complex
<i>CaMV35S</i>	35S promoter of Cauliflower Mosaic Virus
cDNA	Complementary DNA
CDS	Coding sequence
Col-0	Columbia
COR	Coronatine
CO11	CORONATINE INSENSITIVE1
Cep	Conserved effector protein
CPK28	Calcium dependent protein kinase 28
DAMPs	Damage-associated molecular patterns
DNA	Desoxyribonucleic acid
dpi	Days post infection
<i>EDS1</i>	Enhanced disease susceptibility1
EDV	Effector detector vector
eGFP	Enhanced GFP
GA	Gibberillic acid
GST	Glutathione S-transferase
ER	Endoplasmic reticulum
ETI	Effector triggered immunity
ET	Ethylene
ERF	ETHYLENE RESPONSE FACTOR
EIN3	Ethylene-insensitive3
gDNA	Genomic DNA
GFP	Green fluorescent protein
JAZ	JASMONATE-ZIM DOMAIN
<i>Hpa</i>	<i>Hyaloperonospora arabidopsidis</i>
HR	Hypersensitive response
<i>hsp70</i>	Heat shock protein 70
His	Histidine
JA	Jasmonic acid
kb	Kilo base

Abbreviations

LF1	<i>T. thlaspeos</i> strain LF1
LF2	<i>T. thlaspeos</i> strain LF2
LRR	Leucine-rich-repeat
Leu	Leucine
M	Molar (mol/l)
MAPK	Mitogen-activated protein kinase
ml	Millilitre
mM	Millimolar
mRNA	Messenger RNA
NLS	Nuclear localization signal
NB-LRR	Nucleotide binding, leucine rich repeat
NCBI	National Center for Biotechnology Information
NPC	Nuclear pore complex
NPR1	NONEXPRESSOR OF PATHOGENESIS-RELATED GENES 1
NHP	N-hydroxypipicolinic acid
NHPG	NHP glycoside
OD	Optical density
OE	Over expression
ORF	Open reading frame
ORA59	Octadecanoid-responsive arabidopsis 59
<i>PAD4</i>	Phytoalexin deficient4
PCWDEs	Plant cell wall degrading enzymes
PAMP	Pathogen associated molecular pattern
PBS	Phosphate buffered saline
PCR	Polymerase chain reaction
<i>PDF1.2</i>	Plant defensin 1.2
PEG	Polyethylene glycol
PFAM	Protein Families
PI	Propidium iodide
PR1	Pathogenesis-related 1
PRRs	Pattern recognition receptors
PTI	PAMP triggered immunity
R protein	Resistance protein
ROS	Reactive oxygen species
RNA	Ribonucleic acid
RNAseq	RNA sequencing
RPM	Revolutions per minute
RT	Room temperature
rRNA	Ribosomal RNA
SA	Salicylic acid
SAG	Salicylic acid O- β -glucoside
sec	Second(s)
SP	signal peptide
T-DNA	Transfer DNA
TMHMM	TransMembrane prediction using hidden Markov models
<i>Tt</i>	<i>T. thlaspeos</i>
Tue	<i>Thecaphora</i> unique effector
Tae	<i>Thecaphora</i> Anothracocystis effector
TGA	TGACG SEQUENCE-SPECIFIC BINDING PROTEIN

Abbreviations

T3SS	Type 3 secretion system
Trp	Tryptophan
U	Unit (enzyme activity)
UF	Upstream flank
<i>Um</i>	<i>U. maydis</i>
Ura	Uracil
V	Volume
v/v	Volume per volume
VSP2	<i>VEGETATIVE STORAGE PROTEIN2</i>
w/v	Weight per volume
WGA	Wheat germ agglutinin
WT	Wild type
YL	YEPSlight
Y2H	Yeast two-hybrid
Δ	Delta, symbolizes a deletion
μm	Micrometer

Introduction

1. Introduction

1.1 Pathogen born plant diseases: Economic importance and impact on global food security

Plants are considered as primary source of nutrition and provider of more than 80% of food consumable for humans (Rizzo et al., 2021). Major crops that feed the world population are subjected to attacks by numerous biotic threats such as phytopathogenic fungi, bacteria, viruses, and oomycetes, as well as various insects and parasitic plants. Plant diseases lead to about 30% loss of global food production which cost hundreds of billions of US dollars (Rizzo et al., 2021). Another type of loss is productivity lost due to the abandoning of fields for growing favored crops in favor of less profitable ones, or to non-crop plants, weeds, or trees (Saharan and Mehta, 2008). The economic impact of a disease stems from productivity losses, disease control costs (disease management cost), and the economic penalty incurred for having to cultivate less profitable alternative crops. For an individual producer, this means less money due to decreased yields and a higher expense of disease management (Chakraborty et al., 1998). The losses are caused by a direct loss of yield and an indirect loss of quality. In addition to reduction in crop yield, plant diseases impair crop quality and economic value, and can also cause toxicosis in humans and animals (Rizzo et al., 2021).

According to a recent global survey, yield losses of major crops to pests and pathogens can range from 24.6% to 40.9% in rice (*Oryza sativa*), 19.5% to 41.1% in maize (*Zea mays*), 10.1% to 28.1% in wheat (*Triticum aestivum*), 8.1% to 21.0% in potato (*Solanum tuberosum*), and 11.0% to 32.4% in soybean (*Glycine max*) (Schultink et al., 2017; Savary et al., 2019). In surveys conducted by the journal, *Molecular Plant Pathology*, hundreds of international researchers working on fungal, bacterial, and viral pathogens were asked to identify the most scientifically and economically important plant pathogens. Among those deemed to be the most important were: *Magnaporthe oryzae* (rice blast), which causes severe destruction to rice an important staple food feeding half of the population of the world; *Botrytis cinerea* (grey mould), which causes cell death to the host and is known to infect more than 200 plant species; *Puccinia spp.* (wheat rust), the most severe threat to global wheat production, which can cause about 70% yield losses in wheat; *Pseudomonas syringae*, the causative agent of diseases such as bacterial speck of tomato and bleeding canker of horse-chestnut (Dean et al., 2012). Importantly, the smut fungi *U. maydis* is the causative agent of the corn smut disease and represents a major threat to maize crop, which lead to substantial economical losses around the world (Reyes-Fernández et al., 2021).

Modern agriculture developed varieties of practices to tackle the constant threat impose by pathogens. From the early twentieth century, fungicides were used as a key tool to reduce the crop losses. However, over time, fungicides resistance against several pathogen was an ever worse issue (Brent & Hollomon, 2007; Ellis et al., 2014). Development of highly resistant cultivars is a cost-effective and an ecologically benign alternative to costly and damaging chemical controls of plant diseases. For that purpose, the selection and identification of resistant genes (*R* genes) is a priority (Li et al., 2020). The most economical and effective strategy is using *R* genes based resistant cultivars for controlling crop diseases (Mundt, 2014). Because of their significant impact and ease of selection, plant breeders have depended on single dominant or recessive resistance (*R*) genes. Most *R* genes offer race-specific resistance against a single or a few pathogen strains; nevertheless, mutation and virulence shifts in the pathogen population render these race-specific *R* genes ineffective (Li et al., 2020). Stacking

Introduction

multiple *R* genes, that are resistant against single or multiple pathogens in the same genetic background and offer different and broad resistant spectra has offered an effective strategy for achieving BSR (Li et al., 2020). Broad-spectrum resistance (BSR) is resistance to more than one pathogen species or to the majority of races or strains of the same pathogen (Kou and Wang, 2010). Pyramiding *R* genes are successfully applied in important crop plants include rice, wheat and soybean. In wheat, several *R* genes such as *Sr22*, *Sr23*, *Sr25*, *Sr33*, *Sr45* and *Sr50* have been decided to stacked against many harmful races of stem rust include the most devastating race Ug99 (Ellis et al., 2014; Singh et al., 2015).

All in all, plant diseases pose a major threat to global food security. The rate of increase in food production cannot keep up with the rate of increase in food demand due to many reasons including pathogen-born plant diseases. To overcome the challenges that modern agriculture is facing, scientist, farmers, and other members of the community has to fight on many different fronts like climate change, deforestation, and urbanization.

1.2 Smut fungi and their relevance to important crop plants

With over 1,500 identified species, smut fungi are the biggest group of phytopathogenic fungi after the rust fungi. Smut fungi are biotrophic plant pathogens that mostly infect monocot plants, including economically significant cereal crops such as maize, wheat, barley, sorghum, and sugarcane and some can infect the dicot family Caryophyllaceae and genus *Persicaria*. Smut fungi are distinguished by their ability to produce large quantities of black or dark brown teliospores. These cells are typically formed in the floral organs of the host, affecting reproduction of the infected plants (Zuo et al., 2019).

Generally different stages of the life cycle such as the development of teliospores are a common feature among many smuts (Laurie et al., 2012; Begerow et al., 2014). Teliospores are resting structures that allow the fungus to overwinter and persist for years in the soil. Teliospores germinate and go through meiosis under humid, favorable environmental conditions, resulting in the production of the promycelium, from which haploid cells called sporidia are produced (Begerow et al., 2014; Rabe et al., 2016). The sporidia grow in the yeast form and remain non-pathogenic unless they come into contact with a haploid cell of a compatible mating type (Kämper et al., 2006). The fusion of two haploid cells in a mating event initiates pathogenic development, resulting in the formation of a dikaryotic mycelium required for the infection (Brefort et al., 2009; Matei and Doehlemann, 2016).

Smut fungi such as *U. hordei*, the causative agent of covered smut in barley and oats, and *S. reilianum*, which causes head smut in maize and sorghum, spread systemically throughout the host plant (Laurie et al., 2012; Poloni and Schirawski, 2016). They colonize the host vascular system asymptotically until they reach the apical meristem and form teliospores. Sporulation appears to affect the development of reproductive organs and to take place mostly in floral tissues. For instance, it has been demonstrated that fungal teliospores in *Sporisorium* sp. may completely replace the plant seed, leaving only vascular tissue in the host hull, whereas *U. hordei* teliospores are intermingled with the host seeds in the same seed husk (Thomas, 1988). At some point, mature sori rupture, producing spores that are easily distributed to start a new infection.

Introduction

1.2.1 *Ustilago maydis*

The *U. maydis* evolved as the dominant model organism for smut fungus and biotrophic fungal pathogens due to its quick symptom identification, a highly compact genome, ease of in vitro culture, and accessible genetic manipulation. Several biological processes of broad scientific significance were explored in *U. maydis*. Mechanism of homologous recombination and the Holliday junction were discovered as a result of a series of investigations on genetic recombination and DNA repair carried out between the 1960s and the mid-1980s (Holliday, 1974). The cloning of mating genes made possible to examine the recognition between haploid cells (Bölker et al., 1992; Spellig et al., 1994) and how smut fungi control this process to stimulate the biotrophic development (Gillissen et al., 1992; Kämper et al., 1995). Transformation, gene knockouts through homologous recombination and existence of solopathogenic strains SG200 were the key properties to established *U. maydis* as a model organism (Bölker et al., 1995). The *U. maydis* system was further developed by successful implementation of CRISPR-Cas9 system for rapid generation of gene knockout strains (Schuster et al., 2016; Schuster et al., 2018).

All aerial tissues of maize plant are susceptible to infection by *U. maydis*, which causes localized tumor growth in 4–7 days after infection and lead to teliospores generation in later phases (Zuo et al., 2019). A cell cycle arrested dikaryotic filament forms upon fusion of different mating type of haploid cells (Bölker et al., 1995; Benevenuto et al., 2018). These pathogenic filaments differentiate into infection structures known as appressoria. Infection caused by *U. maydis* show symptoms in all green parts of the plant which is localized and characterized by small and large tumors and induction of anthocyanin (Lanver et al., 2017).

It should be highlighted that *U. maydis*, despite being clearly useful for molecular analyses, has certain limitations in terms of representing smut fungi. In some cases, its biology exhibits characteristics that are not common for other smut fungi. First off, an atypical infection style and sporulation in all aerial tissues is contrast to other smut fungus, which spread systemically after infection but only generate disease symptoms in reproductive organs of the plants (Zuo et al., 2019). Similarly, all other smut genomes that have been examined so far have the RNAi machinery while *U. maydis* is missing the RNAi machinery including Dicer and Argonaute proteins (Yoshimoto et al., 2022).

Due to the genetic complexity of the host crop plants, molecular research on plant responses to smut fungi have been difficult to conduct (Frantzeskakis et al., 2017). Given that maize has a large genome and genetic manipulation is not trivial (Schnable et al., 2009), it was beneficial to identify a smut fungus that can infects the model plant *Arabidopsis thaliana*. This strategy would still allow for the use of tools developed for *U. maydis* but would additionally offer a plant host with a relatively small genome (The Arabidopsis Genome Initiative, 2000).

1.3 Plant-pathogen interactions

A broad range of microorganisms affect plants throughout their lifetimes and the nature of their interactions can range from beneficial to harmful (Thrall et al., 2007; Rodriguez et al., 2019). Plants can modulate their innate immune systems to cope with both mutualistic and pathogenic microorganisms differently (Pieterse et al., 2014). They retain immunological memory of previous infections and, unlike mammals, completely rely on a static innate immune system. Fungi are a dominant group of plant pathogens with a huge impact on agriculture and they

Introduction

established a plethora of strategies to colonize the host plant (Gunther et al., 2017). During the initial stage of infection, fungal spores or sporidia adhere to the plant surface, then form germ tubes which differentiate into specialized infection structures such as appressoria or hyphopodia in the later stages. Such appressorium-like structures are common to many plant-colonizing pathogens, many fungi, such as *Colletotrichum graminicola*, *Alternaria alternata*, *Magnaporthe oryzae*, *Pyrenophora teres*, and many oomycetes, such as *Phytophthora infestans* and *Phytophthora cinnamomi* penetrate plant cuticle directly by appressorium formation.

1.3.1 Fungal lifestyle

Plant pathogens have evolved diverse strategies and lifestyles. These strategies can be classified as necrotrophic, biotrophic, and hemibiotrophic, regarding their ability to colonize living or dead host cells.

1.3.1.1 Necrotroph and hemibiotroph

Necrotrophic fungi actively kill the colonized host cells and feed on them. A well-known example of necrotrophic fungi is *B. cinerea* and *Sclerotinia sclerotiorum* grow subcuticularly and kill epidermal cells by secreting toxic metabolites and proteins. Their hyphae eventually replace large parts of the plant epidermis (Williamson et al., 2007). Hemibiotrophs such as *M. oryzae* and *Colletotrichum* spp. typically form bulged hyphae during the biotrophic phase, then switch to thinner necrotrophic hyphae (Lo Presti et al., 2015). These pathogens develop close contact with the host by penetrating the epidermal and subepidermal layer. This contact established through specialized hyphae which invaginate the host cell membrane and form true biotrophic interphase. After certain period of time (which can last from 1 to several days) fungal life style switch from biotrophic to necrotrophic phase. This transition period comprises modification of hyphae, production of toxins and enzymes and secretion of specialized effectors (Doehlemann et al., 2017).

1.3.1.2 Biotrophs

Biotrophic fungal pathogens infect plants without killing the cells (Green et al., 1995; Heath and Skalamera, 1997). This group is further divided into obligate and facultative biotrophs on basis of their mode of contact establishment with the host plant. Obligate biotroph includes Basidiomycota and Ascomycota causing rust and powdery mildew respectively (Doehlemann et al., 2017). They are completely dependent on the host plant for energy source due to less ability of consumption of common substrates (Schulze-Lefert and Panstruga, 2003; Wernegreen, 2005). Spores of rust fungi germinate in to a hyphal structure that invade the leaf surface of host plant and proliferate into mesophyll space through stomata. In powdery mildews, fungal conidia penetrate the epidermal cell after germination on leaf surface with the addition of appressoria (Spanu et al., 2010; Hüchelhoven and Panstruga, 2011). After entering in the internal plant space, fungi cross the wall of mesophyll and epidermal cells and develop a haustoria which serve as a mediator for extracting the plant nutrients. This haustoria do not rupture the cell membrane and instead their pushing cause invagination of the membrane and establish a viable “cell within cell” complex (Heath and Skalamera, 1997). Following the complex establishment, the haustoria initiate nutrient acquisition from the infected plant through a range of transporters (Voegelé et al., 2001; Struck, 2015). Facultative biotrophs can find in a broad range of genera and taxonomically more variable. Their wide range of genera

Introduction

include smuts (*Ustilaginales*, Basidiomycota) and some *Claviceps* species (*Claviceptacea*, Ascomycota) (Doehlemann et al., 2017). Facultative biotrophs can live and survive without the host plant such as *Claviceps purpurea*, fungus of ergot disease can easily survive in axenic culture as well as live in planta as a true biotroph (Tudzynski and Scheffer, 2004). Among them smut fungi *U. maydis* stands out due to its small genome and genetic manipulation, it infects maize by entering the primordia of all aerial organs, induces the tumor formation and spore development (Doehlemann et al., 2017).

1.3.1.3 Endophytes

Endophytes are microbes that colonize plant tissues without causing any obvious visible symptoms. They can colonize all plant tissues (Vega, 2008), throughout the complete life cycle of plants (Haridim et al., 2015; Puri et al., 2016). Studies on endophytes showed that this group of pathogens arises due to switching of mutualism to a host-pathogen interaction, which resulted in a balance between the pathogen and host plant up to some extent e.g endophytic association between *C. magna* and its host plant species (Redman et al., 2001). Fungal endophytes generally help crop plant to grow while some can have pathogenic effect after an incubation period and cause diseases in host plant. Few species have neutral life style neither offer benefits nor damaging the host plant (Sikora et al., 2007; Sikora et al., 2008). Saprophytic fungi such as *N. crassa* can also become endophytes on pine species depending on the availability of a suitable host (Perkins and Turner, 1988; Kuo et al., 2014). *Fusarium* species infects banana cultivar develop no symptoms in its cord root and identified as asymptomatic (Niere, 2001; Sikora et al., 2008). Some pathogenic fungi can behave like an endophyte and colonize host plants asymptotically, then only produce symptoms when a specific stage is reached. Other examples are root endophyte *Piriformospora indica* and a grass genus *Epichloë* which stay inside the host all over the growing season (Rodriguez et al., 2009; Franken, 2012). Members of endophytes genus *Epichloë* promote growth of temperate grasses by improving their nutrient acquisition. Additionally, they also increase the resistance of grasses against drought and diseases (Scott, 2001; Schardl and Leuchtman, 2005). In some cases, the fungal endophyte remains dormant or inactive but become active again in the late growth phase of plant, due to environmental changes or during the stress (Petrini, 1991) which was observed by (Alvarez-Loayza et al., 2011) as well. (Agrios, 1997) has described that host plant is infected during the latent infection stage without showing any symptoms. *T. thlaspeos* systemically colonize the host plant *Ar. hirsuta* without causing any macroscopic symptoms throughout the prolong growth phase which resembles the broad definition of endophytes in regards to its infection biology. On other hand transcriptome profile of *T. thlaspeos* has revealed activation of typical defense responses of plant and induces fungal effector gene which shows virulence function therefore, it is not completely clear yet that *T. thlaspeos* belong to pathogen or non-pathogen side of the endophyte continuum (Courville PhD thesis 2018).

1.4 Plant immune system

1.4.1 PTI (Pathogen-triggered immunity)

Most of the pathogens that invade plants are recognized by the plant immune system and trigger host defense responses (Lo Presti et al., 2015). Plants display constitutive and induced defense responses pathogen attack (Anderson et al., 2010; Doughari, 2015). Pre-formed constitutive responses mainly are physical and chemical barriers which can decrease the

Introduction

spread of diseases by limiting the entry of the microbes (Chassot et al., 2008; Underwood, 2012). The pre-existing physical barriers are rigid cell wall and the waxy cuticle layer, while callus formation can be induced once these barriers are breached. Phytoanticipins are pre-existing chemical defences. Such mechanisms are in place to resist and terminate the colonization process of invading pathogenic microbes (Michalski and Conrath, 2016).

Induced defense response consist of two major defense strategies. First line of defense is activated by recognition of pathogen/microbe-associated molecular patterns (PAMPs/MAMPs) such as fungal chitin. PAMPs are recognized by plasma membrane-associated pattern recognition receptors (PRRs) which lead to the first layer of defense called PAMP triggered immunity (PTI) (Jones and Dangl, 2006). The PRR signaling activates a cascade of downstream responses which include accumulation of ROS, activation of defense related MAPK pathway, ion channel activation and extensive changes in gene expression and activation of stress hormones signaling. Cumulative responses of PRR signaling leads to the production of antimicrobial proteins such as chitinases, proteinases, and glucanases and antimicrobial peptide including cyclotides, defensins, snakins and thionins (Lyapina et al., 2019) which are detrimental to pathogen structures (Dodds and Rathjen, 2010; Macho and Zipfel, 2014). The fungal chitin receptor of *A. thaliana* is the LysM-RLK (receptor-like kinase) CERK1/RLK1/LYK1 which perceives chitin through its three extracellular LysM domains. Two CERK1 molecules bind to chitin octamers and lead to homodimerization of receptors which play vital role in activation of downstream signaling (Miya et al., 2007; Liu et al., 2012). GHs-elicitors were found in many plant pathogenic fungi that include *F. graminearum*, *B. cinerea*, *R. solani*, and *V. dahlia*. *BcCrh1*, a GH16 transglycosylase of *B. cinerea* that catalyzes the crosslinking of glucan polymers and chitin of fungal cell wall. It has been proven an atypical elicitor of fungi that perform function in the plant cytoplasm (Guo and Cheng, 2022).

1.4.2 ETI (Effector-triggered immunity)

In order to suppress and overcome PTI responses, pathogens secrete effectors or inactivate toxic plant metabolites. If pathogen effectors are recognized by plant specialized receptors (R proteins), a second layer of defense strategy called effector triggered immunity (ETI) is activated. There are two conserved features of R proteins, nucleotide-binding and leucine-rich repeat, termed as NLRs. Pathogen effector proteins are usually recognized by host nucleotide-binding leucine-rich repeat (NB-LRR) or NLRs immune receptors (Cui et al., 2015). Recognition of an effector by plant receptors often restrict the fungal proliferation by triggering localized cell death response called hypersensitive response (Giraldo and Valent, 2013; Cui et al., 2015). Both PRRs and NLRs elicit the same immune responses however, amplitude and duration of ETI responses are greater than PTI responses (Peng et al., 2018). Interestingly, the most recent findings showed that NLR-mediated ETI have a substantial linkage with PRR-mediated PTI (Ngou et al., 2021; Yuan et al., 2021). It is also reported that PTI and ETI responses overlap each other at transcriptional level (Tao et al., 2003; Navarro et al., 2004). In addition to localized cell death, various PAMPs trigger the transport of defense-related signals across the rest of the plant and result in broad spectrum of resistance called systemic acquired resistance (SAR) (Gao et al., 2015). On the other hand, in absence of R protein or effectors bypass the R proteins of plants and successfully suppress PTI responses, colonize the susceptible host and eventually leading to effector triggered susceptibility (ETS) (Naveed et al., 2020).

Introduction

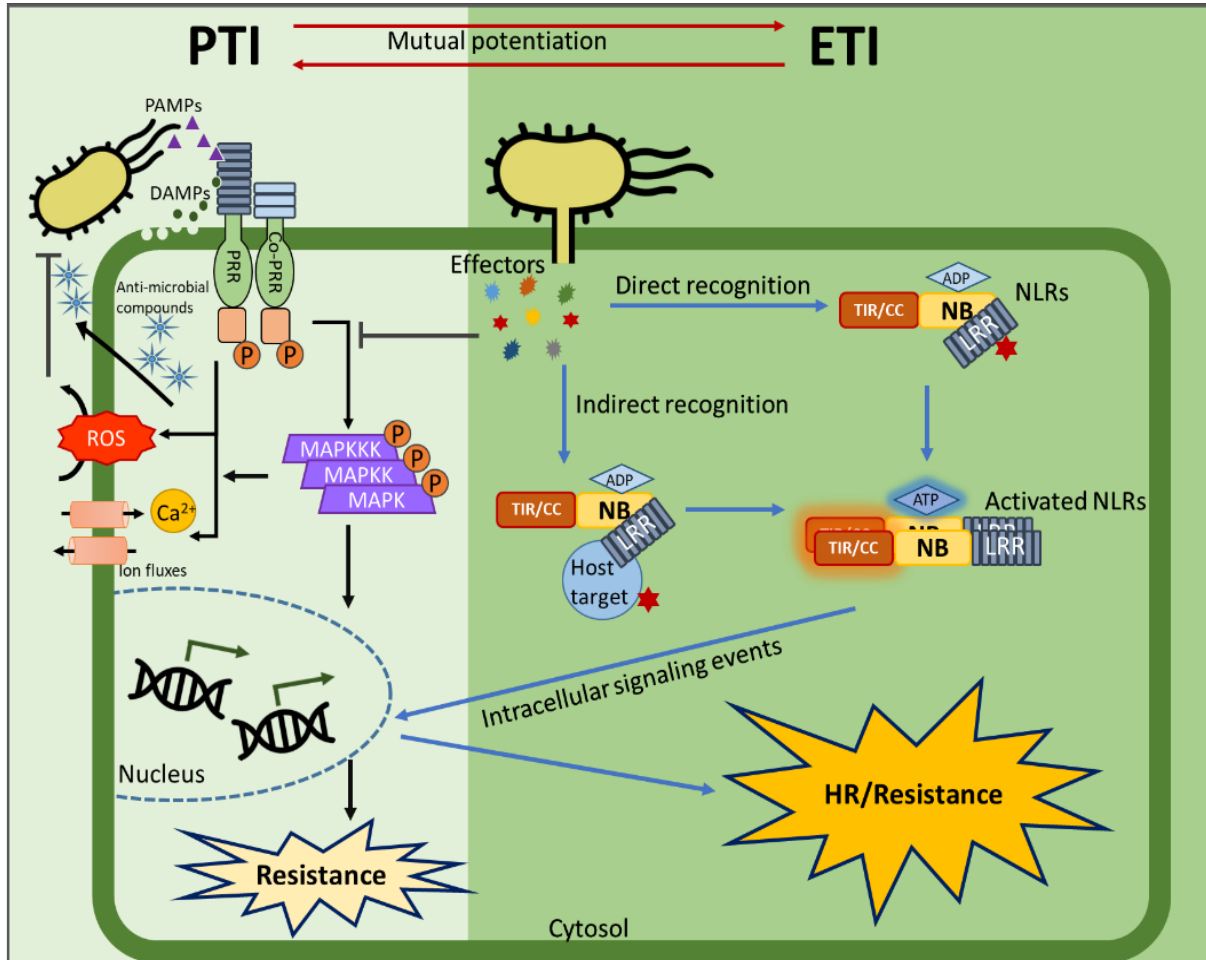


Fig. 1-1. Pattern-triggered immunity (PTI) and effector-triggered immunity (ETI) in plants are depicted schematically. The identification of pathogen-associated molecular patterns (PAMPs) or damage-associated molecular patterns (DAMPs) by pattern recognition receptors (PRRs) activates the first layer of induced immunity, known as PTI (black arrows). Activation of the mitogen-activated protein kinase (MAPK) kinase cascades, an influx of Ca^{2+} into the cytosol, and the generation of reactive oxygen (ROS) species are just a few examples of PTI signaling events that take place. The production of antimicrobial substances and activation of defense genes takes place. However, the pathogens use their effectors to repress PTI. The second layer of defense, known as ETI (blue arrows), begins when effectors are detected by nucleotide-binding (NB) and leucine-rich-repeat (LRR)-containing receptors (NLRs). A conformational shift brought on by NLRs direct or indirect perception of pathogenic effectors, along with a number of intracellular signaling processes, ultimately results in the hypersensitive response (HR) or other defensive reactions. Unexpectedly, the most recent research revealed that PTI and ETI are connected and, when combined, strengthen the immune response (red arrows) (Adopted from (Ngou et al., 2021).

1.5 Molecular events leading to plant hormone regulation during defense

As described in the plant immunity section, microbes produce PAMPs and activate the plant immune system, which involves surface-localized PRRs and intracellular NB-LRRs. Upon recognition of microbial molecules, these plant receptors activate an array of immune responses and produce various defense signaling molecules, including phytohormones, that play a vital role in enabling the downstream defense responses (Pieterse et al., 2012).

Introduction

Salicylic acid (SA), jasmonic acid (JA), and ethylene (ET) are classical examples of defensive phytohormones. They are major players in plant immunity and their signaling play a vital role in defence against biotrophic and necrotrophic pathogens. SA and JA each have their own signaling pathways that include biosynthetic enzymes, receptors, transcription factors, and downstream responsive genes. These SA and ET/JA signaling pathways are intricately linked, forming integrated networks. While SA and ET/JA mediated signals frequently work antagonistically (SA-JA crosstalk), they may sometimes collaborate synergistically, giving plants robust and controllable immune regulation (Li et al., 2019).

Pathogens, however, can take advantage of antagonistic interactions to increase their virulence (Erb and Reymond, 2019). Several filamentous fungal pathogens have evolved protein or toxin effectors that target hormonal pathways. Furthermore, some filamentous plant pathogens can themselves synthesize phytohormones and derivatives as a host mimicry to influence or hijack host hormone homeostasis (Chanclud and Morel, 2016). A bacterial JA mimic and bacterial toxin coronatine (COR), which forcefully open the stomata of plants, is a well-characterized example of this phenomenon (Melotto et al., 2006; Lee et al., 2013). Besides that, some infected plants exhibit different developmental changes such as stunted growth, elongation and late or early flowering that often outcome of pathogen-mediated modification of host hormonal regulation (Kazan and Lyons, 2014).

1.5.1 Salicylic acid (SA)

SA is a phenolic molecule that is involved in a variety of plant activities such as growth, flowering, senescence, and responses to abiotic and biotic stresses. The significance of SA in local and systemic acquired resistance (LAR and SAR) against biotrophic and hemibiotrophic pathogens has been thoroughly researched (Vlot et al., 2009; Dempsey et al., 2011). Previous studies provide convincing evidences for supporting SA as a critical signal in plant defense responses. A bacterial enzyme salicylate hydroxylase (NahG) cause exclusion of endogenous SA through transient expression and make the plant susceptible to bacteria, fungi and viruses (Gaffney et al., 1993; Reuber et al., 1998). Furthermore, isochorismate compromised mutant Sid (SA induction-deficient) is not able to produce SA during pathogen attack and more prone to fungal and bacterial pathogens (Nawrath and Métraux, 1999; Wildermuth et al., 2001). SA also assist in triggering hypersensitive response upon pathogen effector recognition by R proteins (Brodersen et al., 2005; Raffaele et al., 2006).

Two different biosynthetic pathways are used to produce SA from chorismate, the end product of the shikimate pathway. The isochorismate (IC) pathway is mainly serve a key source of SA biosynthesis in both infected and non-infected plants (Dempsey et al., 2011; Seyfferth and Tsuda, 2014). The precursor chorismate is converted to isochorismate which leads to the production of SA through an enzymatic reaction in the chloroplast (Garcion and Métraux, 2008; Dempsey et al., 2011).

NONEXPRESSOR OF PATHOGENESIS-RELATED GENES 1 (NPR1) serves as a receptor of SA and central regulator of immune responses mediated by SA (Dong, 2004; Wang et al., 2006). After the pathogen attack, SA synthesis causes phosphorylation of NPR1 and subsequent monomerization, allowing it to translocate into the nucleus and trigger *PR* gene expression (Mou et al., 2003; Lee et al., 2015). The active monomers in the nucleus work with several transcription factors to induce the expression of SA-responsive genes, for example NPR1 targets many TGA transcription factors and histone acetyltransferases to regulate the expression of *PR* genes and activate SA-induced transcriptional reprogramming (Kesarwani et

Introduction

al., 2007; Fu and Dong, 2013). Because of its importance in plant immunity, NPR1 is an intriguing effector target for subverting SA-mediated defenses (Lorang et al., 2012; Kazan and Lyons, 2014). The proteasome inhibitors Syla and XopJ secreted by bacteria diminish the co-transcriptional activity of NPR1 by inhibiting the proteasome-mediated degradation of its phosphorylated form thereby affecting the SA signaling pathway (Schellenberg et al., 2010; Üstün and Börnke, 2015).

1.5.2 Jasmonic acid (JA)

JA is ubiquitously found in plants as a natural plant growth regulator (Ahmad et al., 2016; Wasternack and Strnad, 2016). It has long been believed that the JA pathway enables plants to resist numerous environmental challenges, such as attacks from herbivores and necrotrophic pathogens (Thomma et al., 1999; Glazebrook, 2005). More recently, it became evident that JA-mediated defenses also play an important role in resistance to both biotrophic and hemibiotrophic pathogens (Riemann et al., 2013; Lemarié et al., 2015). A few hemibiotrophic fungi may break down JA produced by their host plants. For example, *Magnaporthe oryzae* produces the antibiotic biosynthetic monooxygenase (Abm), which can change JA into 12-OH-JA to inhibit JA signaling and facilitate colonization (Patkar et al., 2015; Zhang et al., 2017).

JA biosynthesis initiates from chloroplast lipids in *A. thaliana* (Klessig et al., 2018; Ghorbel et al., 2021). In chloroplast, an unsaturated fatty acid converts to deoxymethylated vegetable dienoic acid (dm-OPDA) and 12-oxo-phytodienoic acid (12-OPDA) which subsequently lead to the formation of JA by β -oxidation in peroxisome. The final conversion to structurally different forms of JA occurs in cytoplasm such as JA-isoleucine (JA-Ile), methyl jasmonate (MeJA) and 12-hydroxyjasmonic acid (12-OH-JA) (Yang et al., 2019).

The main active form is JA-Ile, which is sensed by the Skp-Cullin-F-box E3 ubiquitin ligase CORONATINE INSENSITIVE1 (SCF-COI1) receptor complex (Sheard et al., 2010; Wasternack and Feussner, 2018). Upon stress, the active JA-Ile binds to COI1 to facilitate the formation of COI1-JAZs complex, resulting in degradation of JAZ by the 26S proteasome. JAZ proteins are transcriptional repressors that suppresses the transcription activity of MYC genes (Chini et al., 2007; Wasternack and Feussner, 2018). Hence, JAZ degradation allows the MYC2 and its homologs, as well as other factors like the mediator component MED25, to induce the JA-responsive genes containing G-box motif (CACATG) (Li et al., 2021). Downstream of COI1-JAZ perception, JA signaling pathway has two major branches, namely MYC branch and ET response factor (ERF) branch. The MYC branch is under control of MYC2, MYC3 and MYC4 transcription factor and their activation upon degradation of JAZ protein lead to expression of JA responsive genes including *VSP2* and *LOX2*. The ERF branch is controlled by transcription factors of APETALA2/ETHYLENE RESPONSE FACTOR (AP2/ERF) family such as *ETHYLENE RESPONSE FACTOR 1 (ERF1)* and *OCTADECANOID-RESPONSIVE ARABIDOPSIS AP2/ERF 59 (ORA59)* and lead to the induction of JA/ET signaling marker *PLANT DEFENSIN1.2 (PDF1.2)*. This branch controls the defense responses against necrotrophic pathogens and co-regulated by JA and ET signaling (McGrath et al., 2005; Dombrecht et al., 2007). JAZ proteins can also regulate the ethylene signaling pathway via the transcription factor ETHYLENE INSENSITIVE 3 (EIN3) and its homolog. It directly interacts with EIN3 and downregulate the EIN3 that induces *ORA59* and *ERF1* expression (Zhu et al., 2011).

Introduction

1.5.3 Ethylene

Ethylene, a gaseous hormone has a role in fruit ripening and senescence (Grbić and Bleecker, 1995; Bleecker and Kende, 2000) and is also known as a plant growth regulator (Li et al., 2019). ET signaling plays a significant role in defense responses as evident from the finding that ethylene suppressive *A. thaliana* and soybean mutants are more prone to pathogen attack and lead to susceptibility of the plant (Berrocal-Lobo et al., 2002; Yang et al., 2017). The role of ethylene in plant defense was revealed by studying in soybean root rot the interaction between *PsAvh238* and Type2 ACSs (*GmACSs*) in which *PsAvh238* repress ethylene synthesis through destabilizing *GmACSs* to assist infection (Yang et al., 2019). While an elevated resistance response has been detected upon overexpression of *GmACSs* in *Nicotiana benthamiana* which is consistent with the finding of downregulation of ET-mediated defense responses in hemibiotrophic pathogens. Both jasmonic acid and ethylene signaling pathways are essential for the stimulation of plant defense responses against necrotrophs.

The 1-aminocyclopropane-1-carboxylic acid (ACC) serve as precursor for biosynthesis of ethylene in a reaction catalyze by ACC synthase (ACS) (Wang et al., 2002). ET biosynthesis is tightly regulated and controlled due to its gaseous and diffusible properties. Therefore, the enzymatic activity of ASC is strictly regulated and tightly control the production of ET (Li et al., 2019). After accumulation, ET is perceived by receptors which is localized to endoplasmic reticulum and act as negative regulator of ET signaling pathway (Ju and Chang, 2015). ET binding lead to dephosphorylation of ER-localized EIN2 which eventually releases its C-terminal domain (CEND) to enter the nucleus and transfer signals to EIN3 (Alonso et al., 1999; Qiao et al., 2012). EIN3 activates the expression of ET responsive transcription factors including *ERF1* and *ORA59* which stimulate the ET response (Solano et al., 1998; Pré et al., 2008)

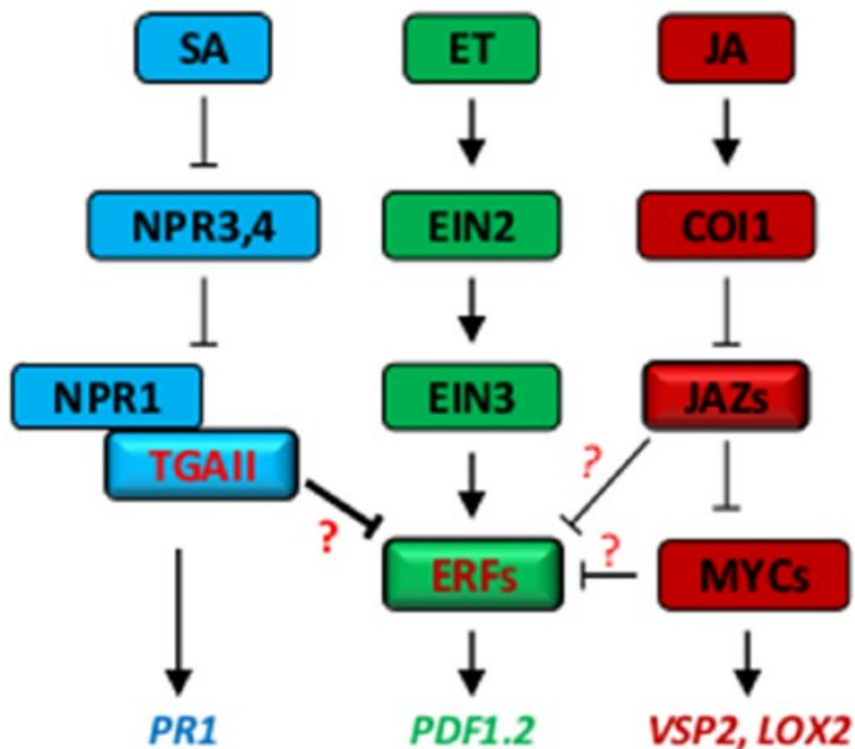


Fig. 1-2. A schematic representation of the signaling pathway of defense hormones. In uninfected plant, basal SA detection occur by low binding affinity receptor NPR4 that target NPR1 for degradation

Introduction

while high SA level result in interaction between NPR3 and NPR1 during infection. SA stimulation lead to the NPR1-TGA1 mediated expression of *PR1*. Accumulation of ethylene perceive by a receptor EIN2 by dephosphorylation and send signals to transcription factor EIN3 which directly induce the expression of several ethylene responsive transcription factors (ERFs) that responsible for activation of marker gene *PDF1.2*. An active form of JA sensed by a receptor complex including COI1 and result in proteasome mediated degradation of JAZs proteins and result in expression of JA responsive genes *VSP2*, *LOX2*. Question marks shows unknown mechanism of inhibition of ERFs by JAZs, MYCs and TGAs. Arrows indicate the activation of genes/transcription factors and blunt end line shows repression of the targets. Adopted from (Li et al., 2019).

1.5.4 Modulation of SA-JA crosstalk during pathogen infection

SA and JA signaling pathways act antagonistically (Hou and Tsuda, 2022). SA causes suppression of JA signaling at multiple levels. The major SA receptor NPR1 mediated suppression of JA-responsive genes by SA was shown to take place in the cytoplasm (Spoel et al., 2003) however, Nomoto et al showed that NPR1 is essential for downregulation of JA responsive genes by targeting MYC2 and its homologs in the nucleus (Nomoto et al., 2021) Together, both cytoplasmic and nuclear NPR1 can suppress JA signaling through different mechanism. Indeed, the author showed that MYC2 suppression via nuclear NPR1 is the key mechanism for NPR1 based immunity against hemibiotrophic pathogen *Pseudomonas syringae* pv. *maculicola* ES4326. However, the molecular mechanism of inhibition of MYC2 transcription through NPR1 is still unknown. Moreover, a heterodimeric complex of two lipase-like proteins EDS1 and PAD4 involved in SA accumulation and signaling also inhibits MYC2 activity in the nucleus to elevate the SA level which eventually lead to immunity against *P. syringae* pv. *tomato* DC3000 (*Pto*) (Bhandari et al., 2019; Lapin et al., 2020). All these observations showed importance of MYC2 inhibition for downregulation of JA level. In addition to NPR1, TGAs are also involved in suppression of JA responsive genes via SA which is shown by SA-mediated repression of JA marker genes *VSP2* and *PDF1.2* through *TGA2*, *TGA3*, *TGA5* and *TGA6* (Leon-Reyes et al., 2010). TGAs directly target the master regulator ORA59, of ERF branch of JA signaling (Zander et al., 2014). ET also play a role in enhancing the binding between promoter of ORA59 and TGAs, thus give an insight into activation and regulation of SA antagonism with JA/ET responsive genes. Therefore, it is concluded that SA can transcriptionally modulate the clade II TGAs to control the JA/ET pathways (Li et al., 2019).

Pathogens exploit the extensive antagonistic crosstalk between SA and JA pathways to meet their requirements (Kazan and Lyons, 2014). SA signaling as well as immune-related mitogen-activated protein kinases (MAPKs) are both suppressed by enhanced JA signaling (Mine et al., 2017; Xin et al., 2018). The COI1-JAZs complex mediated MYC2 expression also induces the transcription of three NAC transcription factor genes including ANAC019, ANAC055, and ANAC072 (Zheng et al., 2012). These three genes suppress the activity ICS1 and downregulate the SA signaling pathway. AvrB, HopB1, HopZ1a, and HopX1 are examples of other *P. syringae* effectors that target JAZs to stimulate JA signaling, which in turn suppresses SA signaling that would otherwise be effective against pathogens (Zhou et al., 2015; Yang et al., 2017). Conversely, *B. cinerea*, a necrotrophic fungal pathogen, secrete an exopolysaccharide (EPS) that leads to the induction of *NPR1* and activation of SA signaling which suppresses JA signaling to facilitate necrotrophic infection (El Oirdi et al., 2011). These examples amply demonstrate how pathogens take advantage of the SA-JA antagonism to increase their pathogenicity/virulence.

Introduction

1.6 Fungal effectors

A very broad definition of an effector is a small, secreted protein from a microbe which has a physiological effect on the plant host during the interaction. These small secretory proteins are often less than 300 amino acids in size (Gan et al., 2013; Martín et al., 2018). However, some larger effector proteins have also been characterized (Djamei et al., 2011) therefore, a cutoff of 300 amino acids is considered rather inconsistent (Lo Presti et al., 2015). Most of the effector proteins consist of cysteine rich sequence which stabilize the protein tertiary structure by disulfide bridges (Stergiopoulos et al., 2013). A frequently used criterion for identifying effector protein is the absence of orthologues outside the same genus (O'Connell et al., 2012; Wicker et al., 2013), although some effector proteins have conserved domains (Gan et al., 2013; Stergiopoulos et al., 2014). The majority of effector proteins characterized to date are secreted via the conventional endoplasmic reticulum–Golgi apparatus route. The pre-secretory proteins harbor an N-terminal signal peptide for ER targeting, which is also one of the criteria used for identification effector proteins.

Effectors either help in elevating the virulence of a fungal pathogen or assist in plant colonization by symbionts (Lo Presti et al., 2015). Virulence function of effectors can be tested by reverse genetics approaches in the pathogen, that can result in less infected plant tissue upon deletion which leads to reduced disease severity (Lo Presti et al., 2015). Plant contact stimulates the expression of effectors and this expression profile is tightly regulated at different stages of infection which can be affected by the type of organ or cell that the fungus comes in contact (Ökmen and Doehlemann, 2014). Some fungal effectors might suppress the PTI responses even before penetration, therefore their expression is required directly after plant surface contact (O'Connell et al., 2012; Lanver et al., 2014). The effector repertoires of a fungal pathogen can depend on its lifestyle and adaptations to the host plant species (Lo Presti et al., 2015). Fungal effectors can perform their functions in various locations once secreted. They can play a role at the fungal cell wall e.g Avr4 of *C. fulvum*, in the apoplast e.g Tom1 and Avr2 of *C. fulvum*, Pep1 and Pit2 of *U. maydis* and CSEP0055 of *B. graminis* or it can translocate into the plant cell and localize to the plant organelles that include cytoplasmic effectors Cmu1, Tin2 and nuclear effector See1 and Nkd1 of *U. maydis*, chloroplastic effector ToxA of *S. nodorum* (Lo Presti et al., 2015).

In comparison to oomycetes and bacterial effectors, not many fungal effectors have been characterized. Some of the fungal species e.g rust fungi are difficult to genetically manipulate which is the one of the major reasons for limited fungal effector research. Another problem of equal significance is that reverse genetics of effectors do not show a clear loss-of-function phenotype. Possible reasons for this may be functional redundancy or not having a suitable assay or detection system. For example, a large scale disruption analysis of 78 effector genes of *M. oryzae* resulted in the identification of only one effector, MC69, which contributed to virulence (Saitoh et al., 2012). Similarly, deletion of an entire effector gene cluster in *U. maydis* did not contribute to any change in the virulence (Farfing et al., 2005). However, advancements in the techniques such as host and virus-induced gene silencing, bimolecular fluorescence complementation and several transient expression systems facilitate functional characterization of fungal effectors (Lo Presti et al., 2015).

Introduction

1.6.1 Translocation of the effectors

The effector translocation mechanism into the host cell is well described for bacterial system, while the mechanisms of fungal effector translocation are poorly understood. Pathogenic bacteria possess six well-characterized secretion systems, of which type three secretion system T3SS is essential for virulence and plays a role in translocation of effectors to the host plant (Akagi et al., 2009; Albert, 2013). The first evidence of migration of fungal effector to the host cells was provided by cell death phenotypes upon co-expression of an effector Avr and its cognate R protein, that suggest a function for the fungal protein in the host cells (Stergiopoulos and de Wit, 2009). However, the molecular mechanism of this uptake is not well understood (Rafiqi et al., 2012). More than 26 fungal Avr genes encoding for effector candidates (Rouxel and Balesdent, 2010), and their interacting plant R protein have been studied (Stergiopoulos and de Wit, 2009; Gururani et al., 2012; Ali et al., 2014). Plant R proteins are mostly localized in the cytoplasm, which suggests that corresponding fungal effectors are also translocated from the fungus to the plant (Stergiopoulos and de Wit, 2009).

Bioinformatic prediction of conserved motifs for fungal effector translocation had limited success so far. Absence of conserved sequence domains might point towards lack of a universal entry mechanism. Furthermore, different fungal pathogens may have evolved different effector delivery mechanisms. Nonetheless, there are a few exceptions such as the powdery mildew fungi and the root endophyte *P. indica*, which have conserved motifs. Approximately 80% of the effector candidate proteins in powdery mildew share the same N-terminal motif Y/F/WxC downstream of the signal peptide (Godfrey et al., 2010). Similarly, the C-terminal conserved motif RSIDEED is shared by a group of 25 small effectors of *P. indica* (Zuccaro et al., 2011). However, the role of these motifs in effector translocation into plant cells is still not proven.

Secretion and uptake of effectors into plant cells can be analyzed by live cell imaging of fluorescently-tagged effectors. AFP-tagged effector of *C. orbiculare* localized to a ring like structure during the early biotrophic stage (Irieda et al., 2014). This structure surrounds the neck of the hyphae between the plant plasma membrane and fungal cell wall. Such interface localization of effectors depends on their expression and the conventional secretion pathway. To increase the efficiency and better detection of FP-tagged protein, an NLS signal can fused along the FP-tagged protein for concentrating the signal in the plant nucleus which has been effectively done for translocation of *M. oryzae* effectors (Lo Presti et al., 2015).

In the rice pathogen *M. oryzae*, cytoplasmic effectors follow a Golgi-independent unconventional secretory pathway and accumulate at the biotrophic interfacial complex (BIC) before entering the rice cells (Khang et al., 2010; Giraldo et al., 2013). The BIC is a focal membrane-rich plant structure. Primary biotrophic hyphae first show the BIC appearance at the tip then change its position to the side of fully developed invasive hyphae (Khang et al., 2010). A cytoplasmic effector Rbf1 has a role in differentiation of invasive hyphae and it contributes to the formation of proper foci of the BIC (Nishimura et al., 2016). Still, the requirement of the BIC for the entry of cytoplasmic effectors into the host cells and the movement of these effectors from the BIC to the plant compartments are unanswered questions (Lanver et al., 2017). A recently discovered Stp complex of *U. maydis* seems to target maize aquaporin and assist in effector delivery. Plasma membrane associated ATPases of plant and other interaction partners of Stp complex promote membrane transport processes and could facilitate the effector delivery. Identification of fungal structure carrying Stp complex

Introduction

and its extension in to the host cells pointed towards such a system for delivery of effectors in vesicles (Ludwig et al., 2021).

To assess the cytoplasmic function and avirulence activity of the effector candidates, heterologous expression in bacteria and delivery of a fungal fusion proteins via the bacterial type III secretion system has been used. This system worked effectively for delivery of fungal effectors into wheat, rice, and barley cells but their application to the other pathosystems still needs to be investigated (Upadhyaya et al., 2014). In this so-called Effector-Detector-Vector system (EDV), a phytopathogenic bacterial strain *P. syringae* (*Pst*DC3000) is used to translocate the effectors to the host cell via T3SS (Cornelis, 2010). The N-terminal 1-136 amino acids sequence of AvrRPS4 is necessary for effector secretion (Sohn et al., 2007). A luciferase expressing strain (*Pst*-LUX) of *Pst*DC3000 assist in detection of disease promoting activity of an effector through measurement of bioluminescence signals (Fabro et al., 2011). As a proof-of-concept, ATR13, an effector of the filamentous oomycete *H. parasitica* was delivered to host plant by N-terminal fusion to AvrRps4 and AvrRpm1 of *P. syringae*. ATR13 suppresses PTI responses and significantly contribute to disease progression inside the host plant cell (Sohn et al., 2007).

1.6.2 Host proteins interaction of effectors

It is possible to demonstrate an effector's involvement in virulence or anticipate the host manipulation by preliminary screenings; however, the molecular function of an effector could only be postulated after finding its interacting partner. Identification of pathogen effector targets opens up the possibility to increase our understanding of plant defense mechanisms. Only a few fungal effectors, in contrast to oomycete and bacterial effectors, have been functionally described. The main challenges in studying fungal effectors stems from the challenges of working with fungi in a lab setting, particularly obligate biotrophs like rust fungus. The fact that many effector mutations lack corresponding phenotypes, maybe as a result of functional redundancy, subpar assay techniques, or the difficulty to precisely assess minute phenotypic changes, adds to these difficulties (Selin et al., 2016). Despite these challenges several effectors have been described in different pathogens such as numerous powdery mildew effector targets have been discovered through direct investigation of their interaction. During infection, the powdery mildew effector CSEP0064 interacts with the host's *PR10* (pathogenesis-related protein) and interferes in the host ribosomal RNA degradation (Pennington et al., 2019). Stripe rust's PEC6 effector inhibits PTI through interacting with wheat adenosine kinases. However, it is still unknown how PEC6's interaction with adenosine kinases affects the host's immune system (Liu et al., 2016).

A significant progress has been made in understanding the functional roles of secreted fungal effectors utilizing technologies like bimolecular fluorescent complementation (BiFC) (Kerppola, 2008; Kodama and Hu, 2012), immunocolocalization (Dunn et al., 2011), yeast-two hybrid systems (Brückner et al., 2009), and gene expression assays. Ideally, the native host system is a priority but it often is found challenging, therefore heterologous expression techniques using *N. benthamiana* and *A. thaliana* are employed to find interaction partners of pathogen proteins (Ahmed et al., 2018; Lorrain et al., 2018). Expression of 20 putative effectors of the poplar rust fungus in *N. benthamiana* revealed their potential target proteins and cellular localization. This study identified an interaction between the host's TOPLESS-related protein 4 and the poplar effector MLP124017 (Petre et al., 2015; Lorrain et al., 2019). In a related work, Petre *et al.*, 2016 employed *N. benthamiana* to express sixteen potential *P. striiformis*

Introduction

effectors in order to determine the interaction partners (Petre et al., 2016). PST02549, one of the study's effectors, interacts with the host's EDC4 (ENHANCER OF mRNA DECAPPING PROTEIN 4) protein in *N. benthamiana* and wheat (Petre et al., 2016; Lorrain et al., 2018). These investigations showed that the alternate host system can be used to identify effectors' interaction partners and unravel their molecular activity.

The biotrophs are the ones where fungal effector proteins have been functionally studied most. *U. maydis* and related smut fungi secrete Pep1, an effector that is located in the apoplast. The deletion of *pep1* completely stops fungal proliferation at the level of the maize epidermal cells, and causes a strong accumulation of reactive oxygen species H₂O₂ at the cell wall. The *pep1* mutant stimulates defense responses of the host and activates its immune system (Doehlemann et al., 2009). In wild type fungal strains, plant immunity is suppressed due to interaction between Pep1 and its target POX12. POX12 is a secreted maize peroxidase that is a conserved part of the plant's reactive oxygen species (ROS)-generating machinery (Hemetsberger et al., 2012).

Avr2, an effector that was first recognized as an Avr protein in resistant plants but was subsequently demonstrated to be a true virulence factor of non-obligate biotrophic fungus *C. fulvum* in susceptible plants, targets secreted cysteine proteases that are crucial in plant immunity (van Esse et al., 2008). The interaction between Avr2 and apoplastic proteases PIP1 and RCR3 was identified by fluorescent protease activity profiling which showed that Avr2 specifically inhibits these proteases upon interaction (Rooney et al., 2005; Shabab et al., 2008).

1.6.3 Nuclear-localized effectors

Microbial effectors manipulate a variety of host cellular functions upon their delivery to the plant cell, and a subset of them move from cytosol into the nucleus of host plant. (Win et al., 2012). Nuclear-localized effectors might target proteins involved in chromatin remodeling, transcription, DNA replication, and nuclear import and export of mRNAs and proteins (De Mandal and Jeon, 2022).

Ralstonia solanacearum cause bacterial wilt in many crops of Solanaceae family. PopP2 is a multi-plant target effector encoded by *R. solanacearum* that suppress the host plant immunity by acetyltransferase activity. RD19, RRS1, some of WRKY transcription factors and recently characterized EDS1 and PAD4 physically interact with PopP2 (Huh, 2021). A Y2H screen using a cDNA library of infected *A. thaliana* root tissue identified cysteine protease RD19 which re-localized from vacuoles to the plant nucleus and might activate the plant defense responses (Bernoux et al., 2008). PopP2 interaction with both immune regulator EDS1 and PAD4 identified by CoIP and BiFC that lead to the suppression of plant immunity (Huh, 2021). EDS1 and PAD4 are SAR responsive genes that make a heterodimeric complex to elevate the basal defense signaling (Baggs et al., 2020) through accumulation of salicylic acid.

Laccaria bicolor is an ectomycorrhizal fungus which colonizes poplar specie *Populus trichocarpa*. A diffusible signal from plant roots stimulate the induction of MiSSP7, which is necessary for the establishment of symbiotic relationship (Plett et al., 2014). Nuclear localized MiSSP7 interacts with JAZ protein (*PtJAZ6*) which in turn negatively regulates JA induced genes (Plett et al., 2014). Plant JAZ proteins are responsible for repressing the transcriptional components in the jasmonic acid signaling pathway. MiSSP7 interaction with *PtJAZ6* stabilizes

Introduction

this repressor and thus prevents activation of JA-induced genes that can modify the cell wall and have roles in cell wall modification assist hyphal entry into the roots (Plett et al., 2014).

Interestingly, an opposite role has been found for biotrophic pathogens that facilitate JA signaling during host colonization (Doehlemann et al., 2008; López-Ráez et al., 2010). One such example is type III effector HopZ1a of *P. syringae* that localized to both cytoplasm and nucleus. HopZ1a causes degradation of AtJAZ1 upon interaction and activate of the JA signaling pathway, which ultimately leads to increased bacterial growth (Jiang et al., 2013).

Bacterial and oomycete effectors can also interfere with host immune responses by manipulating the SA-induced gene expression (Nomura et al., 2011; Caillaud et al., 2013). HaRxL44 from the downy mildew *H. arabidopsidis* localizes to the nucleus and interacts with the mediator complex subunit protein MED19a, and leads to its proteosomal degradation which results in lowered expression of SA-related defense response genes (Caillaud et al., 2013). In addition to suppressing SA, HaRxL44 also induces expression of JA/ET responsive genes (Dean et al., 2005). These studies indicate that each organism differently target the SA and JA signaling pathway depended on the requirement of the pathogen.

See1 is an effector of the smut fungus *U. maydis*, it localizes to both host cell nucleus and cytoplasm and has a role in tumor formation in infected maize leaves by inducing plant cell division (Matei and Doehlemann, 2016). See1 interacts with a highly conserved maize protein SGT1 and block the phosphorylation of SGT1 (Doehlemann et al., 2011). SGT1 is a cell cycle regulator and involved in protein ubiquitination, kinetochore assembly, and pathogen-induced responses (Ghareeb et al., 2011; Hemetsberger et al., 2012).

In the examples above, nuclear-targeted effectors interacted with host plant proteins, but they can also directly bind to DNA in order to modulate the host transcription machinery. PsCRN108 is a DNA binding effector of *P. sojae*, which has a role in disease progression. PsCRN108 binds to the promotor region of plant *HSP* (heat shock protein) via its predicted HhH (helix-hairpin-helix) motif, which is considered to be essential for the interaction. A large number of Hsp protein encoded by *A. thaliana* are directly involve in offering resistance against diseases such as Hsp90 complexes assist in R protein-mediated disease resistance in various plants. The interaction between PsCRN108 and the plant *HSP* promotor inhibits the plant heat shock transcription factor in *A. thaliana*, *N. benthamiana* and soybean. Therefore, the expression of *HSP* gene remains suppressed and promotes plant susceptibility to *P. sojae* (Song et al., 2015).

AvrBs3, the TAL effector of the bacterial pathogen *X. campestris pv. vesicatoria*, is the prototypic member of a large effector family (Gürlebeck et al., 2006). AvrBs3 dimerizes after entering the host cytoplasm and uses its C terminal nuclear localization signals (NLS) for nuclear import (Szurek et al., 2002; Gürlebeck et al., 2005). An acidic activation domain and a putative leucine zipper domain is present in AvrBs3 family members. AvrBs3 binds to a conserved promotor region of *upa20* which regulate cell size. This binding ultimately causes an induction of hypertrophy in susceptible genotypes (Kay et al., 2007). AvrBs3 binds to the promotor of its R protein Bs3 in a resistant pepper cultivar and activates Bs3 transcription in the nucleus (Römer et al., 2007). It was concluded that AvrBs3 and other members of this family act as transcription factors and play roles in the promotion of bacterial virulence in susceptible genotypes, while they are avirulence factors in the resistant genotypes. In addition, TAL effectors have successfully used to generate site-specific gene-editing tools by fusing the specific TAL effector to nucleases (TALENs), transcription factors (TALE-TFs) and several

Introduction

other functional domains. Thus, the TAL effectors based application allows researchers to specifically target any required sequence (Cermak et al., 2011).

1.7. *Thecaphora thlaspeos* as a novel pathogen

Although grass smuts are used to investigate the molecular basis of various important aspects e.g pathogenicity, signaling pathways and mating events of pathogen (Bölker, 2001; Basse and Steinberg, 2004), the host plant responses to such fungal infection is difficult to study. Conversely, *A. thaliana* is great source of information for the underline mechanisms of plant responses to fungal infection and modulation of plant immune system. Therefore, it would be advantageous to combine the available resources and molecular tool of smut fungi and *A. thaliana* to readily investigate cellular processes.

T. thlaspeos is the only known smut fungus that can infect the Brassicaceae family (Vánky and Lutz, 2007). It has been identified in at least 15 host species which include *Arabidopsis hirsuta*, *Arabidopsis lyrata* (Vánky et al., 2008) and genetically tractable, perennial and annual model plants *Ar. alpina* and *A. thaliana* though the infection is not completed in *A. thaliana*. However, colonization and early events of *A. thaliana* is similar to the infection pattern of natural host *Ar. hirsuta* which makes model plant *A. thaliana* an ideal experimental host (Frantzeskakis et al., 2017). *T. thlaspeos* belongs to *Thecaphora* clade and it is the first member which has been study at molecular level. Fungal species of this clade cause yield loss to agronomically important non grain food crop e.g 80% of yield loss of potato occur due to *T. solani* in South America (Conforto et al., 2013).

Similar to *S. reilianum* and *U. hordei*, *T. thlaspeos* can infect the entire plant by growing systemically along the whole vasculature, and similar to *U. esculenta* it maintains the infection over several years (Frantzeskakis et al., 2017). This systemic infection is not detrimental to the plant development except that seeds of host plant are cover or replace by fungal teliospores at the end of flowering stage each growing season (Frantzeskakis et al., 2017). Interestingly, germination of mature teliosopres needs a plant signal which is heat stable. This suggests a novel perception pathway might be involved in breaking spore dormancy. In contrast, teliospores of all other smut fungi germinate in water and do not require any special signal. In comparison to other biotrophic fungi, *T. thlaspeos* can also grow in haploid axenic culture as filaments, and their manokaryotic infectious filament is not arrested in cell cycle. However, the yeast-like sporidial form typical for the grass smut fungi is not present in *T. thlaspeos* (Frantzeskakis et al., 2017).

Long lasting asymptomatic systemic infection of *T. thlaspeos* is a characteristic feature of plant endophytes. Similarly, *T. thlaspeos* has evolved with its perennial host plant in such a life-style. Investigating molecular and cellular event of *T. thlaspeos* will give more insight into how it establishes and maintains its systemic growth (Frantzeskakis et al., 2017).

Transcriptional changes in infected host plants induced by *T. thlaspeos* indicated biotic stress responses, as exemplified by induction of *PR-1*. *T. thlaspeos* has a repertoire of unique and conserved secretory proteins found in transcriptome analysis (Courville et al., 2019). Functional characterization of these effector proteins can reveal the molecular basis of host plant interaction with *T. thlaspeos*.

Aims

2. Aims of this thesis

2.1 Hypothesis

Effector repertoire of *T. thlaspeos* was identified in (Courville et al., 2019) and opened up questions for their functional characterization. These questions arise on base of following hypothesis: Effectors translocate from fungus to host plant during infection upon secretion, and their function determines the specific sub-cellular localization in plant cells. One important compartment is the nucleus that a hub for transcriptional regulation of basic cellular processes. Here, nuclear localized effectors can interfere with the host immune responses and contribute to disease progression by changing plant gene expression.

2.2 Aims

Functional characterization of *TtStp1*.

The genome and a transcriptome study of systemically infected *Ar. hirsuta* identified *Stp1* as a potential secreted effector. The functional analysis of *U. maydis* *Stp1* revealed its importance in the disease progression and as a part of *Stp* complex (Ludwig et al., 2021). As genetic modifications were not yet possible for *T. thlaspeos*, *TtStp1* was characterized here in a complementation analysis in comparison to its homologue *UmStp1* in *U. maydis*.

Identification and Initial characterization of nuclear targeted effectors.

To address the questions in the first part of my hypothesis, this study aimed at a detailed scanning of the secretome including induced effector candidates of *T. thlaspeos* for identification of nuclear localized effectors and their validation in independent systems. To prioritize the functionally interesting candidates from the list of 7 putative NLS effectors, their virulence activity was examined to find the potential influence of effectors in disease progression.

Molecular characterization of *TtTue1* as a top NLS effector candidate.

The host plant immune system and their associated regulatory components could be the targets of *TtTue1* which were not yet explored. To address the questions related to the molecular function of the effectors, a large scale screen was performed to identify the host plant targets of *TtTue1*. Identification of interacting partners of *TtTue1 in planta* provides a route for finding hints for the molecular basis of host interaction and possible pathway involved. Involvement of stress induced hormones during pathogen attack is a common phenomenon, which could functionally describe for *TtTue1*. Furthermore, *TtTue1* protein has DNA binding residues and it could bind to promotor of host plant DNA. The DNA binding affinity of *TtTue1* has provided the base for analyzing its interference with host transcription machinery.

Results

3. Functional characterization of conserved effector *TtStp1*

3.1 Results

3.1.1 Revision of the *T. thlaspeos stp1* gene model

Stp1 is a secreted effector of *U. maydis* that is crucial for the establishment of biotrophic interaction between *U. maydis* and its host plant maize. As this effector is conserved among different smut fungi and was initially characterized in the *maydis* (Liang, 2013), we planned to verify the function of *Ttstp1* via complementation of *U. maydis*.

To investigate *stp1* in *T. thlaspeos*, we first carried out sequence comparisons. THTG_02966 is a homolog of *Umstp1* but the protein alignment only showed 26% identity and gene size is much shorter than *Umstp1*. According to the predicted gene model (Courville et al., 2019), THTG_02966 is 957 bp long while *Umstp1* has 1548 nucleotides. There was a short predicted gene (THTG_02967) 127 bp upstream of THTG_02966. The RNA-seq data showed high read coverage in this short intergenic region and no clear sign of splicing, which suggests that THTG_02966 may have an upstream start codon and be longer in reality (Fig. 3-1a). Therefore, I manually looked for an alternative open reading frame (ORF). There was an ORF that starts 82 bp upstream of the originally annotated THTG_02967 and covers the entire *Ttstp1* gene. The ORF was 1359 bp long and did not have any intron. Checking the genomic sequence further upstream, I could not find any other in frame start codons. In addition, there were stop codons present upstream of the new start codon in all three frames, which suggest that this newly defined ORF is the accurate and full-length *stp1*. To verify this new annotation, I did sequence alignments of the predicted proteins, compared with the characterized domains of *UmStp1*. The function of Stp1 mainly depends on its structural domains. Previous studies revealed that the N- and C-terminal conserved domains of Stp1 (Fig. 3-1c) are necessary for the protein function, while the central variable domain is dispensable. Deletion analysis had previously shown that N- and C-terminal domains could be separately expressed but are both crucial for virulence activity (Liang, 2013). Accordingly, the N- and C-termini of Stp1 are conserved among different smut fungi, while the central glycine-rich domain is highly variable. The N-terminal region includes a predicted signal peptide. In the *T. thlaspeos* gene models, a signal peptide was only present in the new annotation, and lacking from the old version (Fig. 3-1c). Furthermore, RT-PCR was carried out on RNA extracted from infected tissue to identify the mature mRNA. Primers were design in a way that should cover the falsely predicted intergenic region and the intron (Fig 3-1a). Amplification on both cDNA and gDNA produced PCR products of the same length (Fig 3-1b) confirmed that the new gene model is correct.

Based on the RNA-seq read coverage (Fig. 3-1a), the transcript comprises of 163 nucleotides in the 5' UTR and 156 nucleotides in the 3'UTR. Thus I have corrected the gene model of *Ttstp1*.

Results

Fig. 3-1 Gene model and RNA-seq based read coverage of THTG_02966 and *Ttstp1*. (a)

The old annotation around the gene locus THTG_02966, shows of a small upstream gene THTG_02967 of size 192 bp with a small intergenic sequence of 127 bp. There was high and continuous read coverage across the intergenic region and both annotated genes, indicating that there may be a single longer gene, rather than two shorter genes. The new gene model of full-length *Ttstp1* was verified by PCR amplification with a forward primer from upstream part of THTG_02967 and reverse primer binds in the middle of THTG_02966. Colour dots indicate stops codon in frame 1 (green), 2 (yellow), 3 (pink). (b) RT-PCR amplification of *Ttstp1*. Both cDNA and gDNA were used as a template. Primer pairs are indicated with arrows in (a), resulting in a product size of 922bp for both templates. The same length of the PCR amplicon from cDNA indicated that 127 bp were a part of *Ttstp1* and there is no gap in between the two genes in the previous annotation (c) Protein alignment of the newly annotated, longer THTG_02967 (*TtStp1*) and the previously annotated THTG_02966. Domain structure of Stp1, Blue box: signal peptide, Red boxes: N-terminus and C-terminus conserved regions. Green colour represents conserved amino acids. Red arrow shows the missing signal peptide and N-terminal conserved region of THTG_02966. Alignment showed the conserved N and C-terminal part of Stp1 among different smut fungi while the central region was dispensable. Scoring matrix BLOSUM 62 was used for alignment.

3.1.2 *T. thlaspeos* conserved effector Stp1 is not functional in *U. maydis*

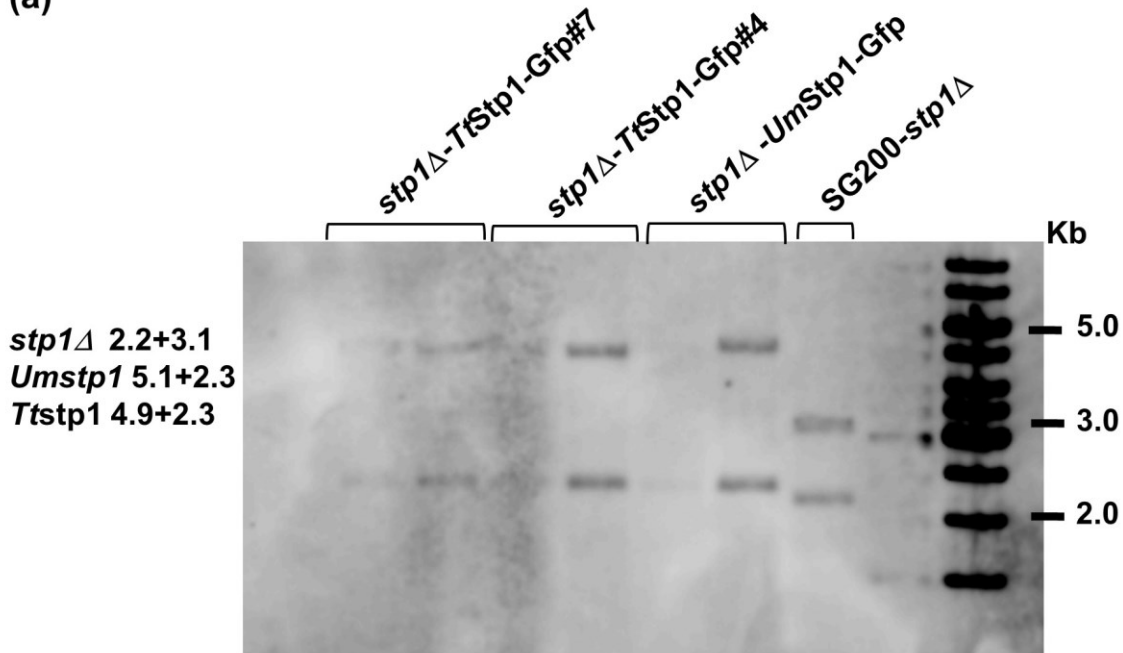
3.1.2.1 *U. maydis* strain generation and infection assay

To find out if *TtStp1* is performing the same function as *UmStp1* in assisting fungal growth after initial penetration of epidermal cell in maize, a complementation analysis was carried out. First, the deletion strain of *U. maydis* in SG200 wild type background was generated by replacing the *stp1* with the hygromycin resistance cassette. An *stp1* deletion mutant of *U. maydis* was generated and complemented with *Ttstp1*. Five independent transformants of SG200 *stp1Δ* strain were verified by Southern blot analysis. Transformant #1 was further used for generation of a complementation strain. *Ttstp1-gfp* was inserted in the *Umstp1* locus (UMAG_024759) so that it is placed under the *Umstp1* promotor, and fused to a nourseothricin resistance cassette. The *stp1Δ-UmStp1-Gfp* complementation strain was used as a positive control. Similarly, two independent transformants were selected for both *stp1Δ-UmStp1-Gfp* and *stp1Δ-TtStp1-Gfp* complementation strains (Fig. 3-2a). Previously, it had been shown that the GFP-tagged fusion protein of *UmStp1* was functional in *U. maydis* (Schipper, 2009). Therefore, we expected full virulence of both complementation strains.

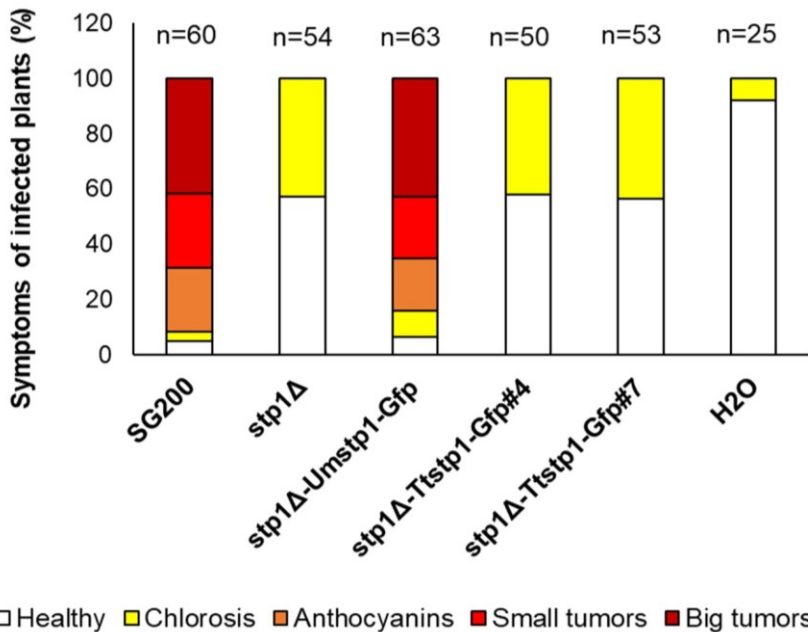
To confirm the virulence phenotype of *stp1Δ*, *stp1Δ-UmStp1-Gfp* and *stp1Δ-TtStp1-Gfp*, infection assays were performed with 8-9 days old maize plants using the progenitor strain SG200 (solo-pathogenic (Kämper et al., 2006)) as wild type. My main interest was to show that *Ttstp1* restores the fungal proliferation after initial penetration of epidermal cell in maize. No disease symptoms were detected on plants infected with *stp1Δ* while SG200 profusely colonized the plant and developed the infection symptoms (Fig. 3-2b). The *stp1* deletion strain lost virulence which confirmed that *stp1* is crucial for the establishment of biotrophic interaction between *U. maydis* and its host plant maize, and the complementation strains *stp1Δ-UmStp1-Gfp* regained virulence with disease scores similar to wild type strain (Fig. 3-2b). By contrast, *stp1Δ-TtStp1-Gfp* did not cause any obvious disease symptoms and their phenotype was similar to the deletion strain, although the fusion protein was expressed *in planta* (Fig. 3-3), which might be due to the inability of *TtStp1* to do networking with interaction partners of *UmStp1*.

Results

(a)



(b)



(c)

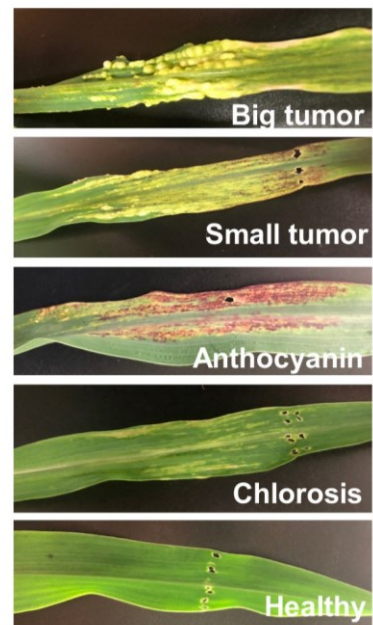


Fig. 3-2 Generation of *stp1* deletion and complementation strain and infection assay. (a)

Confirmation of *Umstp1* deletion and complementation strains by Southern blot analysis. *stp1*Δ was generated in SG200 background. This deletion strain was complemented with both *Ttstp1* and *Umstp1*. Strains were verified by Southern Blot analysis with probes directed against the upstream and downstream flanking regions of *Umstp1*. Band sizes were 2.2, 3.1 kb for *stp1*Δ 5.1, 2.3 kb for *stp1*Δ-*UmStp1* and 4.9, 2.3 kb for *stp1*Δ-*TtStp1*. Expected sizes confirmed the generation of independent deletion and complementation strains. (b) Disease rating of maize plants 7 days post inoculation with H₂O and *U. maydis* strains. SG200 has developed all the symptoms chlorosis, anthocyanins, as well as big and small tumors. *stp1*Δ did not show any disease symptom except chlorosis. The complementation strain *stp1*Δ-*UmStp1*-Gfp produces comparable symptoms to wild type SG200, while both strains with

Results

TtStp1 did not complement the *stp1Δ* phenotype. *stp1Δ-TtStp1-Gfp* showed only chlorosis and behaves completely like *stp1Δ*. The values above the bars indicate the total number of plants inoculated in three independent experiments. (c) Disease symptoms of infected plants were classified in to big tumor, small tumor, anthocyanin, chlorosis, and healthy.

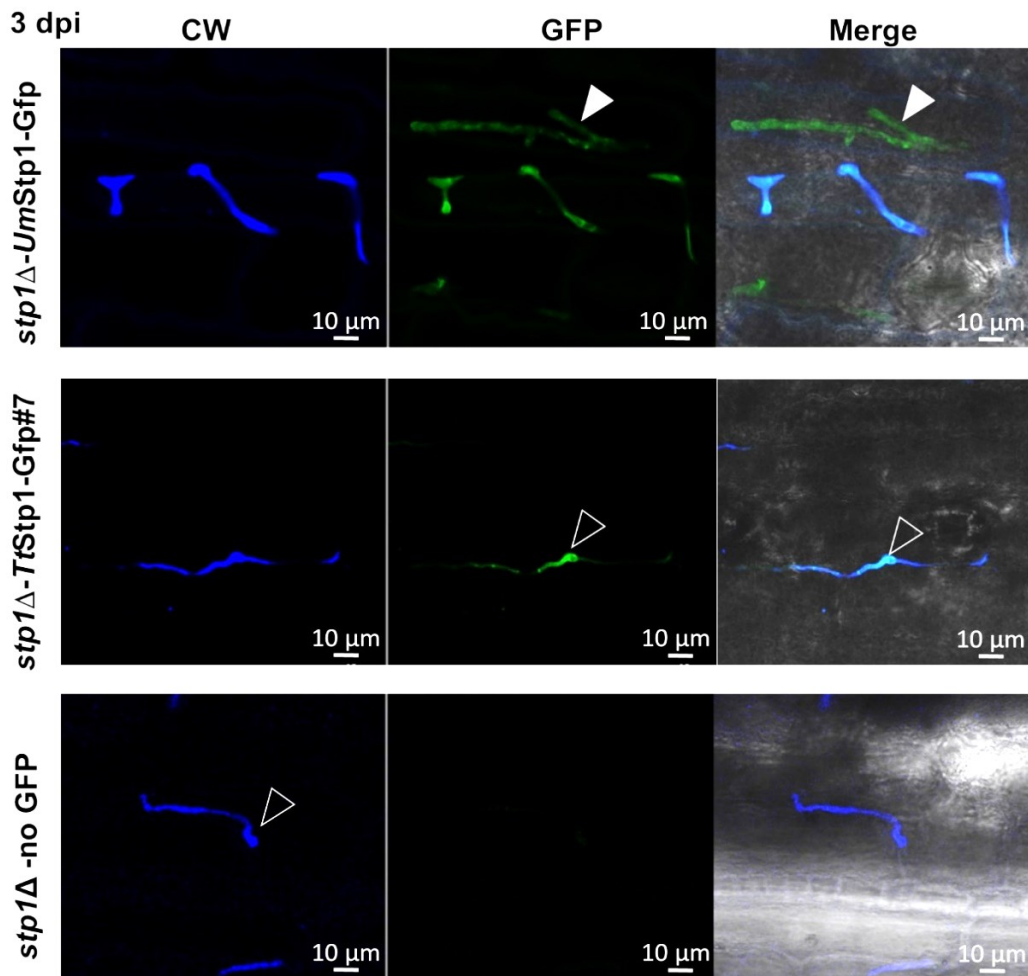
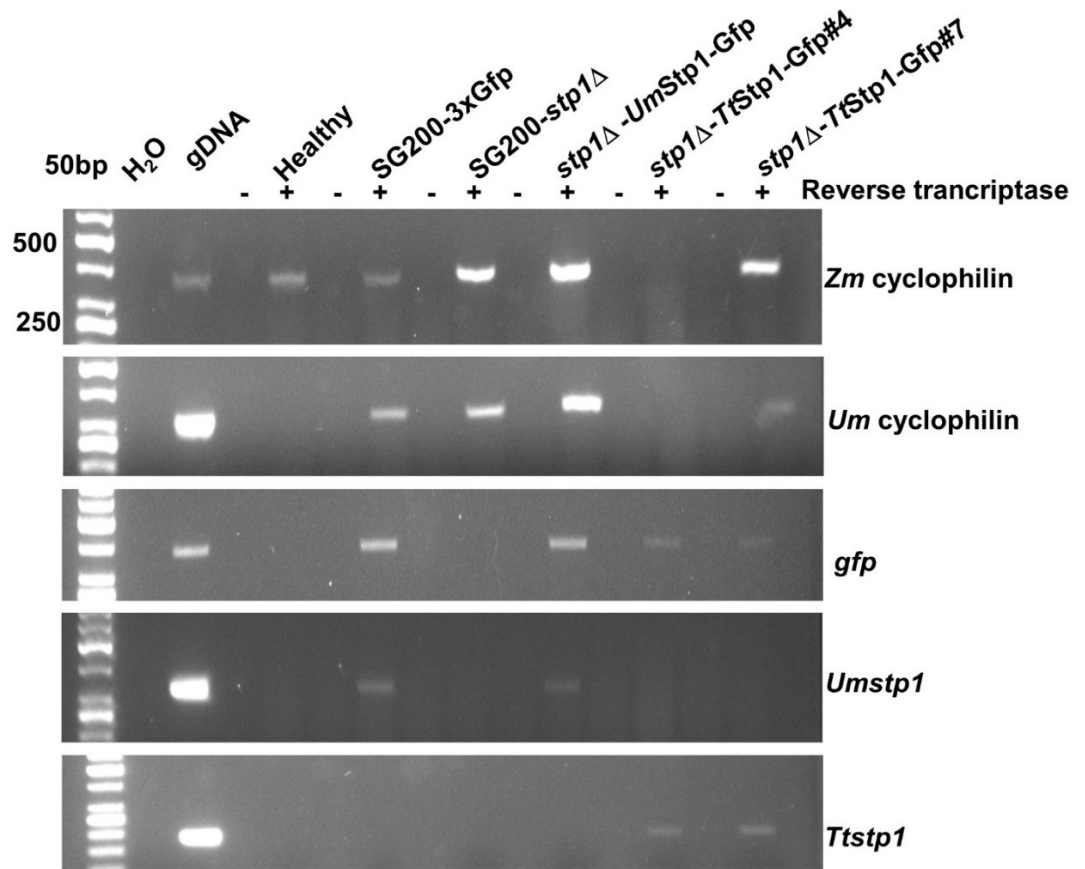
3.1.2.2 Verification of *stp1* expression

As virulence was not restored in the strain where *Umstp1* was replaced by *Ttstp1*, it was necessary to confirm the expression of *Ttstp1* at both the transcriptional and protein level. To verify expression, semi-quantitative RT-PCR was carried out on cDNA generated from RNA of infected maize leaf samples three days post infection (dpi). According to a time-course of gene expression during *U. maydis* infection of maize (Lanver et al., 2018), *stp1* is strongly induced from 0.5 to 2 dpi and expression is largely maintained up to 12 dpi. Therefore, leaves were harvested at 7 dpi. Maize and *U. maydis* cyclophilin were used as reference genes for transcript normalization (Lin et al., 2014; Panzer et al., 2019). Both reference gene transcripts were detected in all infected samples except *stp1Δ-TtStp1-Gfp#4*, although expression of *TtStp1* indicated that respective sample has enough fungal mass for detecting the expression (Fig. 3-3a). In comparison to controls, a low level of both *Umstp1* and *Ttstp1* were detected in the respective strains. Band intensities showed that expression level of *Umstp1* and *Ttstp1* were almost the same and *gfp* expression showed the presence of fusion protein. The amount of fungal tissue differs between the samples therefore a difference in the expression levels was observed. Overall results clearly indicated that both *Ttstp1-gfp* and *Umstp1-gfp* were expressed in all complementation strains.

The second approach for detecting the *stp1-gfp* expression was monitoring the protein level via confocal microscopy. For this purpose, plant samples were harvested at 3 dpi and leaves were stained with calcofluor-white (CW) which binds with fungal chitin on the surface of the plant. *stp1Δ* formed appressoria on the leaf surface, but did not penetrate (Fig. 3-3b, bottom). There was no GFP tag in *stp1Δ* strain so we were not expecting any GFP signal. Plants infected with *stp1Δ-UmStp1-Gfp* showed proliferation of fungal cells in the form of hyphae. Filaments and appressorium-like structures on the plant surface were stained with CW and display GFP signal, while hyphae growing in planta were not stained with CW and express GFP only. The growth of intracellular hyphae *in planta* therefore indicates restoration of *stp1* function (Fig 3-3b, top). In contrast, *stp1Δ-TtStp1-Gfp* resembles the *stp1*-deletion strain, the filaments clearly formed appressoria, but no hyphal penetration and proliferation was observed, which was consistent with the results from the infection assay. However, I still detected the accumulation of GFP signal showing that the fusion protein is expressed.

In summary, *Ttstp1* did not complement the *stp1Δ* phenotype, even though the protein was expressed. We speculated that *stp1* could be functionally conserved in *T. thlaspeos* as they had sequence homology with *Ustilago maydis*, but surprisingly it did not show the expected results. It might be interesting to further characterize diverged functionality of *Ttstp1*.

Results



Discussion

Fig. 3-3 Gene and protein expression analysis of *stp1* (a) Gene expression was checked by RT-PCR on maize leaf tissues infected with different *U. maydis* strains. -/+ indicates the no-RT control and reverse transcribed cDNA. A gDNA controls from maize tissue, SG200-3xGfp and LF1 were used to verify the primers amplification. Maize and *U. maydis* cyclophilin were used as positive controls and they were not expressed only in the leaves infected with *stp1* Δ -*TtStp1*-Gfp#4 while expression of *TtStp1* showed sufficient fungal material for the detection. Maize leaf samples infected with *stp1* Δ -*TtStp1*-Gfp and *stp1* Δ -*UmStp1*-Gfp have low expression of *Umstp1* and *Ttstp1* in comparison to controls. *gfp* was expressed in samples infected with both complemented strains while slightly low band intensity was observed in samples infected with *stp1* Δ -*TtStp1*-Gfp strain. *Zm* cyclophilin 368bp, *Um* cyclophilin 312bp, *gfp* 365bp, *Umstp1* 324bp, *Ttstp1* 317bp. (b) Protein expression analysis of Stp1. Maize variety Amadeo was infected with *U. maydis* complementation strains. Confocal microscopy images of *stp1* Δ , *stp1* Δ -*UmStp1*-Gfp and *stp1* Δ -*TtStp1*-Gfp#7 were taken at 3dpi. *stp1* Δ -*UmStp1*-Gfp showed hyphal growth in maize leaf tissues, while CW staining was seen in appresoria and small hyphae attached to the surface. There were no proper hyphal growth found inside the leaf infected with the *TtStp1* complementation strain, except a small appressorium-like structure. Empty arrowheads indicate the appresoria on the surface of plant and filled arrowheads show hyphal growth inside the plant. Left panel show fungal filaments stained with CW, middle panel indicate accumulation of GFP and right panel show overlay of two channels. CW: calcofluor white. The scale bar: 10 μ m.

3.2 Discussion

Stp1 is conserved among different smut fungi and considering an important role of Stp1 in disease progression of *U. maydis*, its homolog in *T. thlaspeos* was characterized via complementation analysis in *U. maydis*. Nonetheless, *TtStp1* showed similarity with *UmStp1* but their corrected gene model did not carry any NLS signal while *UmStp1* was localized to both cytoplasm and nucleus. Besides that, *TtStp1* could not complement the *UmStp1* and did not restore the virulence function. In a similar complementation analysis of a virulence factor *TtPit1*, no functional complementation of *UmPit1* was observed after correcting the *pit1* gene model (Lesley Plücker, Master thesis 2017). *Pit1* is essential for tumor formation in *U. maydis* infected maize plants (Doehlemann et al., 2011). *Pep1*, a functionally conserved secreted protein that interacts with maize peroxidase POX12 and inhibits the ROS burst. *TtPep1* is an apoplastic secreted effector and placed among top10 induced proteins of *T. thlaspeos*. Functional complementation analysis showed that *TtPep1* partially complemented the infection phenotype in SG200 Δ *pep1* background, hence pointed towards a rather distinct function (Courville et al., 2019). Ludwig et al found that *UmStp1* is a part of complex. This complex consists of 7 members including *Pep1*. These components are co-regulated and specifically required for the plant colonization. *T. thlaspeos* might differently regulate these genes although the cross species complementation of 7 members of the complex suggested their conserved function (Ludwig et al., 2021). Additionally, the partial complementation of *TtPep1* might be due to no interaction with the complex members of *U. maydis*. Similarly, *TtStp1* might not interact with *UmPep1* and probably other members of the complex as well. Therefore, role of *TtStp1* can be identify through reverse genetics or by expressing other members of complex of *T. thlaspeos* in *U. maydis*. Furthermore, It has been shown that Stp complex could promote membrane transport processes and might involve in effector translocation (Ludwig et al., 2021). Therefore, the confirmation of Stp1 function and investigation of Stp complex in *T. thlaspeos* could be an interesting addition to the effector biology of *T. thlaspeos*.

4. Summary and personal contribution to Courville et al., 2019

Biotrophic fungal plant pathogens can develop a delicate balance with their host plant and give rise to a successful, long-lasting infection to complete their life cycles. During the establishment of a long colonization phase, *T. thlaspeos* can utilize many ways to manipulate the host responses. To gain a deeper understanding of this pathogen and how it infects the plant, genomic and transcriptomic analyses were carried out. Transcriptional response of the plant to infection cause by *T. thlaspeos* showed typical biotic stress observed during infection with plant pathogens. To gain insight into the virulence function of *T. thlaspeos*, the effector repertoire of the fungus was defined and initial attempts were made to characterise them. Identification of novel and unique effectors in *T. thlaspeos* is a significant contribution to investigating the molecular basis of smut fungus-host interactions.

T. thlaspeos genome assembly gave rise to a genome size of 20 Mb and 6239 predicted gene models. The predicted functional categories and gene content of *T. thlaspeos* are comparable to other grass-infecting smut fungi. There were known domains present in 81% of protein models and 355 genes were identified as putative secreted proteins. Effectors perform their role after having contact with the host plant and often get induced during infection therefore for a more in-depth analysis of the biotrophic phase of *T. thlaspeos*, an RNA-seq experiment was performed on infected plant material, axenic *T. thlaspeos* culture, and healthy plant tissues. Expression of 988 fungal genes were detected in total, while 132 were differentially expressed between culture and infected plants. Interestingly, more than half of the upregulated genes could not be functionally annotated. The lack of functional annotation is a standard criterion used to define effectors. Further evaluation has found signal peptides in 51 (39%) upregulated genes. *T. thlaspeos* effector candidates contain few orthologs in other smut fungi which suggests that it has a somewhat different effector repertoire to maintain its long lasting biotrophic phase of life in dicot plant species. Less conservation of *T. thlaspeos* effectors with other smut fungi suggested independent adaptation to its lifestyle. Besides the low number of orthologs, out of the 51 effector candidates, 19 are unique to *T. thlaspeos* called *Thecaphora*-unique effector candidates (Tue). In addition to conserved and unique effectors, there was another group of candidates which were found to be conserved among *T. thlaspeos* and its closest homolog and an epiphytic biocontrol agent *A. flocculosa*. Interestingly their synteny showed larger overlap in gene content and several conserved genes were identified as effector candidates.

To investigate the effector function in more detail, the growth phenotype was observed for a set of 6 effectors overexpressed in *A. thaliana*. *TtTue1* from the unique effector category shown stunted growth and small rosette in vegetative growth phase. I have contributed to the paper by performing an experiment for assessment of virulence activity of selected 6 effector candidates including *TtTue1*. To investigate the role of effectors in promoting the virulence of a pathogen, I used *Pseudomonas syringae* pv. *tomato* DC3000-LUX (*Pst*-LUX) and observed contribution of different effectors in bacterial proliferation. Wild type *Arabidopsis thaliana* plants and transgenic lines expressing *TtTue1*, *TtNlp1*, and 4 other effector candidates were spray-inoculated with *Pst*-LUX. These transgenic lines were previously produced by Kaitlyn Courville. The *TtTue1* line showed significantly enhanced bacterial proliferation upon inoculation and the bacterial growth level was same as the positive control line *bak1-5* (Chinchilla et al., 2007). However, the other effector-expressing lines did not show increased bacterial proliferation compared to the wild type plants (Fig. 6c from Courville et al., 2019). This experiment has

Publication

shown that *TtTue1* possesses virulence activity and significantly increases the bacterial proliferation. Therefore, it was concluded from the previous transcriptomic data and later characterization that *TtTue1* is a novel virulence factor which might transcriptionally activate the host immune responses. Additionally, a transcriptome analysis of the *TtTue1* transgenic line resulted in 93 upregulated and 12 downregulated genes which mainly belong to different stress stimuli according to GO term enrichment analysis. Enrichment of GO term for cold acclimation is the main highlight.

Identification of the effector repertoire of *T. thlaspeos* provided a strong basis for a detailed characterization of effector candidates. Additionally, the identification of *TtTue1* as a virulence factor developed my interest to further look in to detailed effector biology. Therefore, I have started a project on identification and characterization of nuclear localized effectors. It was found from the literature search that nuclear localized effectors are still the least studied part of pathogen effectoromes. Additionally, to investigate the modulation of host transcription regulation by effectors of *T. thlaspeos* was the main interest to specifically focus on nuclear localized effectors.



Smut infection of perennial hosts: the genome and the transcriptome of the Brassicaceae smut fungus *Thecaphora thlaspeos* reveal functionally conserved and novel effectors

Kaitlyn J. Courville^{1*}, Lamprinos Frantzeskakis^{1*} , Summia Gul¹, Natalie Haeger¹, Ronny Kellner^{1,2} , Natascha Heßler¹, Brad Day³ , Björn Usadel⁴ , Yogesh K. Gupta⁵ , H. Peter van Esse⁵ , Andreas Brachmann⁶ , Eric Kemen² , Michael Feldbrügge¹ and Vera Göhre¹

¹Institute for Microbiology, Cluster of Excellence on Plant Sciences, Heinrich-Heine University, Building 26.12.01, Universitätsstr. 1, Düsseldorf 40225, Germany; ²Max Planck Institute for Plant Breeding Research, Carl-von-Linné-Weg 10, Cologne 50829, Germany; ³Department of Plant, Soil, and Microbial Sciences, Michigan State University, East Lansing, MI 48824-6254, USA; ⁴Unit of Botany and Molecular Genetics, Institute for Biology I, BioSC, RWTH Aachen University, 52074 Aachen, Germany; ⁵The Sainsbury Laboratory, Norwich, NR4 7UH, UK; ⁶Faculty of Biology, Genetics, Ludwig-Maximilians-Universität München, Großhaderner Str. 2-4, Planegg-Martinsried 82152, Germany

Summary

Author for correspondence:

Vera Göhre

Tel: +49 211 81 11529

Email: vera.goehre@uni-duesseldorf.de

Received: 21 December 2018

Accepted: 9 January 2019

New Phytologist (2019) **222**: 1474–1492

doi: 10.1111/nph.15692

Key words: effector, fungal endophyte, genome sequencing, infection, plant immune responses, RNA-seq.

- Biotrophic fungal plant pathogens can balance their virulence and form intricate relationships with their hosts. Sometimes, this leads to systemic host colonization over long time scales without macroscopic symptoms. However, how plant-pathogenic endophytes manage to establish their sustained systemic infection remains largely unknown.
- Here, we present a genomic and transcriptomic analysis of *Thecaphora thlaspeos*. This relative of the well studied grass smut *Ustilago maydis* is the only smut fungus adapted to Brassicaceae hosts. Its ability to overwinter with perennial hosts and its systemic plant infection including roots are unique characteristics among smut fungi.
- The *T. thlaspeos* genome was assembled to the chromosome level. It is a typical smut genome in terms of size and genome characteristics. *In silico* prediction of candidate effector genes revealed common smut effector proteins and unique members. For three candidates, we have functionally demonstrated effector activity. One of these, *TtTue1*, suggests a potential link to cold acclimation. On the plant side, we found evidence for a typical immune response as it is present in other infection systems, despite the absence of any macroscopic symptoms during infection.
- Our findings suggest that *T. thlaspeos* distinctly balances its virulence during biotrophic growth ultimately allowing for long-lived infection of its perennial hosts.

Introduction

The *Thecaphora thlaspeos*-Brassicaceae pathosystem is a remarkable example of a sustained systemic plant–microbe interaction. *T. thlaspeos* establishes an infection of the entire plant, which can be maintained over several years (Vanky *et al.*, 2008; Frantzeskakis *et al.*, 2017). After penetration, intercellular hyphae of *T. thlaspeos* proliferate along the vasculature throughout the entire plant without visible impact on plant development. When the host plant develops siliques each year, fungal hyphae differentiate into spores that replace the developing seeds. In addition, fungal hyphae keep proliferating in the newly growing vegetative tissue. The capability of *T. thlaspeos* to overwinter with its perennial hosts and sustain the systemic infection within the entire plant is a unique characteristic among smut fungi studied to date.

T. thlaspeos is a relative of the well studied grass smut *Ustilago maydis*, which is adapted to Brassicaceae hosts (Vanky

et al., 2008; Frantzeskakis *et al.*, 2017). Closely related sister species of *T. thlaspeos* comprise devastating crop pathogens such as *T. solani* on potato (up to 85% losses, Andrade *et al.*, 2004) or *T. frezii* on peanut (Andrade *et al.*, 2004; Conforto *et al.*, 2013). In addition to its *Arabidopsis* hosts, *T. thlaspeos* can colonize the model plant *Arabidopsis thaliana*. Therefore, the *T. thlaspeos*-Brassicaceae pathosystem benefits from the well developed resources of *A. thaliana* research that overcome experimental constraints of grass smuts due to the genetic complexity of their hosts (Frantzeskakis *et al.*, 2017). While plant–fungus interactions of pathogens and symbionts are well studied (Gutjahr & Parniske, 2013; Lo Presti *et al.*, 2015), the molecular mechanisms that enable *T. thlaspeos* to establish and maintain its remarkably long biotrophic interaction with Brassicaceae over years are completely unknown. A deeper understanding of this pathosystem therefore might unveil molecular processes related to the endophytic phase of fungal infections.

*These authors contributed equally to this work.

Biotrophic pathogens have evolved distinct mechanisms to evade plant immunity and establish genetic interactions with their host (Brefort *et al.*, 2009). During invasion, plant cell wall-degrading enzymes are secreted, which promote fungal penetration of the plant cell (Choi *et al.*, 2013). Subsequently, fungal hyphae proliferate inside the apoplast and/or grow through host cells, establishing an intimate contact zone for the exchange of nutrients and proteins. Functional genomic analyses of the grass smut fungi *U. maydis*, *Sporisorium reilianum* and *U. hordei* have greatly contributed to our understanding of smut infection and the associated host responses (Kämper *et al.*, 2006; Brefort *et al.*, 2009; Ghareeb *et al.*, 2015; Lanver *et al.*, 2018). In short, these studies have revealed different repertoires of conserved and host-adapted effector proteins (Okmen & Doehlemann, 2014; Lanver *et al.*, 2017). In *U. maydis* and *S. reilianum*, effector-encoding genes are clustered as exemplified by a locus of 26 genes named 'Cluster 19A' (Kämper *et al.*, 2006; Schirawski *et al.*, 2010). When the entire cluster is deleted, tumor formation in maize is impaired and ultimately spore formation is defective (Kämper *et al.*, 2006). However, clustering of effector genes is not always conserved, as exemplified by *U. bromivora*, the false brome (*Brachypodium* sp.) smut (Rabe *et al.*, 2016). In addition, functional analysis in *U. maydis* confirmed the contribution of single effector proteins to fungal virulence (Lanver *et al.*, 2017). For example, Pep1, a protein essential for fungal penetration, was initially identified outside of the effector clusters and was characterized as an apoplastic peroxidase inhibitor (Doehlemann *et al.*, 2009; Hemetsberger *et al.*, 2012), which is conserved in several grass smut species as well as the dicot-infecting smut *Melanopsichium pennsylvanicum* (Hemetsberger *et al.*, 2015).

In response to fungal colonization, plants have evolved mechanisms to inhibit pathogen infection and proliferation (Dodds & Rathjen, 2010). To detect invading pathogen, plants deploy two major strategies. First, plasma membrane-located pattern-recognition receptors (PRR) recognize conserved microbial elicitors, called pathogen-associated molecular patterns (PAMPs), and induce PAMP-triggered immunity (PTI, Zipfel, 2014). Second, pathogen effector molecules are recognized by intracellular host nucleotide-binding leucine-rich repeat (NLR) immune receptors that induce effector-triggered immunity (ETI, Gassmann & Bhattacharjee, 2012; Białas *et al.*, 2017). PTI and ETI involve similar immune responses including the activation of signaling cascades, massive transcriptional reprogramming, and the accumulation of the two defense hormones, salicylic acid and jasmonic acid (Thomma *et al.*, 1998; Tsuda & Somssich, 2015). In addition, and specific to R-protein activation, ETI induces a local programmed cell death response referred to as the hypersensitive response, as well as systemic acquired resistance (Giraldo & Valent, 2013; Lo Presti *et al.*, 2015).

While factors conferring resistance to smut infection are of agronomic importance, to date, the only known resistance gene is the maize wall-associated kinase *ZmWAK* which protects maize against the head smut *S. reilianum* (Zuo *et al.*, 2014). In addition, the barley smut *U. hordei* encodes three dominant avirulence genes, but the corresponding resistance genes remain undiscovered (Linning *et al.*, 2004). In the current study, we investigate

the systemic and long-lasting smut infection in Brassicaceae. Using a combination of genomic DNA and RNA sequencing of the recently described smut fungus *T. thlaspeos*, we present a functional characterization of its first effector candidates. These give a first insight into how *T. thlaspeos* balances its virulence during biotrophic growth and provide an inventory of effector candidates for future studies.

Materials and Methods

Cloning of expression vectors

Standard USER cloning procedures (NEB) were followed to generate the AvrRPS4-*TnNlp1* construct. *TnNlp1* was amplified from cDNA from start codon to stop codon excluding the signal peptide and inserted in frame after the AvrRPS4 leader sequence in the pEDV3 expression vector (Sohn *et al.*, 2007). Standard Golden Gate cloning (Engler *et al.*, 2014; Patron *et al.*, 2015) procedures were followed to generate binary expression vectors for *in planta* expression. From left border to right border, expression cassettes contained kanamycin resistance, an olesin *AtOLE1*-RFP protein fusion (Shimada *et al.*, 2010), and the *T. thlaspeos* effector gene controlled by the cauliflower mosaic virus (CaMV) 35S promoter and g7 terminator. Standard Gateway cloning procedures were used to generate pEarley Gate 103-*TnNlp1*-Gfp and pEarley Gate 103-*PsojNIP*-Gfp expression vectors (Karimi *et al.*, 2002; Qutob *et al.*, 2002; Earley *et al.*, 2006). Cloning of *Tipep1* into plasmid p123-pep1 (Aichinger *et al.*, 2003) and transformation into solo-pathogenic strain SG200Δpep1 was carried out according to Hemetsberger *et al.* (2015).

Strains, transgenic *A. thaliana* lines, and infection assays

Pseudomonas syringae pv. *tomato* DC3000-LUX (*Pst-LUX*) was transformed with pEDV3-*TnNlp1* and pEDV3_empty (Katagiri *et al.*, 2002). Four-wk-old plants were spray inoculated with the bacterial strains as described in Fabro *et al.* (2011). At 3 d post infection, total photon counts – a measure of *Pst-LUX* growth – were quantified and normalized to the foliar area or leaf fresh weight.

Transgenic *A. thaliana* Col-0 effector-expressing lines were generated via the floral dipping method using the *A. tumefaciens* AGL1 strain expressing the effector constructs (Koncz & Schell, 1986). Primary *A. thaliana* transformants (T1) for two independently transformed lines per effector were selected based on RFP-marker-fluorescence of the seeds (Shimada *et al.*, 2010). Rosette areas were measured 4-wk post sowing. One leaf per plant was harvested for RNA extraction.

Transient expression of *TnNlp1*-Gfp and *PsojNIP*-Gfp in *Nicotiana benthamiana* was assessed using a Zeiss LSM780 confocal microscope (Bleckmann *et al.*, 2010) 2 d after infiltration of *A. tumefaciens* strain GV3101 (pMP90 RK) containing the respective effector. All bacterial strains in this study were grown overnight at 28°C in Luria-Bertani (LB) medium.

U. maydis growth, infection of maize, and microscopy of maize infection was performed as previously described (Hemetsberger *et al.*, 2015; Bösch *et al.*, 2016). *T. thlaspeos* infection of *Arabidopsis*

hirsuta was performed by co-germination of seeds and spores on soil (Frantzeskakis *et al.*, 2017).

T. thlaspeos genome assembly, annotation and comparative genomics

For genomic DNA (gDNA) sequencing of the *T. thlaspeos*, high-molecular-weight gDNA was prepared from pure cultures using phenol extraction (Bösch *et al.*, 2016). LF1 gDNA was sequenced by PacBio long-read sequencing (P6-C4, Max Planck Genome Centre, Cologne, Germany) and by Illumina short-read sequencing (2 × 300 bp; Illumina MiSeq, v3 chemistry, Genomics Service Unit at the Biocenter of Ludwig-Maximilians University, Munich, Germany). Long reads were assembled with CANU v.1.3 (Koren *et al.*, 2017) and short reads trimmed with TRIMMOMATIC v.0.32 (Bolger *et al.*, 2014) were used with Pilon (Walker *et al.*, 2014) for error correction. LF2 gDNA was sequenced by short-read sequencing (2 × 150 bp; Illumina HiSeq, Biomedical Research Center, HHU). The LF2 short reads were assembled using SPADes v.3.8.0 (Bankevich *et al.*, 2012). REPEATMASKER v.4.0.5 was subsequently used to report and mask repetitive regions in the genome (Jurka *et al.*, 2005; Tempel, 2012).

Annotation of both genomes was performed using MAKER2 (Holt & Yandell, 2011) as previously described (Campbell *et al.*, 2014). Briefly, for the LF1 genome, an annotation was generated providing as evidence to MAKER assembled transcripts of LF1 in nutrient-rich culture conditions (Complete Medium; Holliday, 1961), proteomes of several Ustilaginales species (Supporting Information Table S1), and data from the UniProt protein reference database. After two iterations, 397 gene models were manually curated and used to train AUGUSTUS v.3.0.3 (Stanke & Morgenstern, 2005) and SNAP v2006-07-28 (Korf, 2004). For assessing the completeness of the datasets BUSCO v1.1b1, was used (Simão *et al.*, 2015).

Functional annotation was carried out using INTERPROSCAN 5.19 (Jones *et al.*, 2014). dbCAN (Yin *et al.*, 2012) and ANTI-SMASH v.4.0 (Weber *et al.*, 2015) were used to mine the genome for CAZymes and secondary metabolism-related genes. Genome to genome alignments were performed using MUMMER v.3.23 (Delcher *et al.*, 2003) using default user settings and the results were processed using auxiliary scripts provided with the package (e.g. SHOW-COORDS, DNADIFF). Search for orthologues between the Ustilaginales genomes used here (Table S1) and the generation of a multilocus based phylogeny tree was done utilizing ORTHOFINDER v.1.1.1.2 (Emms & Kelly, 2015).

Data availability

The data generated were deposited in ENA (PRJEB24478).

Quantitative RNA sequencing

Samples from LF2, *T. thlaspeos* spore-infected *Ar. hirsuta* (spores and seed collected in Ronheim, Germany in 2015), and healthy *Ar. hirsuta* were snap frozen in liquid nitrogen. Leaves from *A. thaliana* Tue1 lines were harvested following phenotyping.

Total RNA was extracted using the RNeasy Plant Mini kit (Qiagen) including a DNaseI treatment (NEB). cDNA for RT-PCRs was generated using the Protoscript II First Strand cDNA Synthesis kit (NEB) and cDNA libraries were generated using the TruSeq RNA Library Prep kit v2 (Illumina) and sequenced on an Illumina HiSeq 3000 platform (Biomedical Research Center, HHU).

RNA-seq data for *Ar. hirsuta* were assembled using Trinity (Grabherr *et al.*, 2011). The transcript models were added to the ones derived from the genome release. Subsequently, *Ar. hirsuta* RNA-seq data from infected plants were mapped against this transcriptome set using BOWTIE (Langmead *et al.*, 2009). Reads that did not map to *T. thlaspeos* were retained and merged with RNA-seq data from healthy *Arabis* plants. This combined set was then used to generate a transcriptome using Trinity either using a relatively standard pipeline or correcting errors in the reads using Rcorrector (Song & Florea, 2015) and assembling the data using minimal coverage of 2. Both assemblies were filtered and analyzed using transrate (Smith-Unna *et al.*, 2016). As the standard approach yielded better transrate values, the resulting transrate filtered standard Trinity assembly was used in the subsequent analysis. These *Ar. hirsuta* gene models were pooled with those from the *T. thlaspeos* genome assembly and all RNA-seq data from healthy and infected *Ar. hirsuta* plants were mapped against this combined set using subread. The data were summarized using eXpress (Roberts *et al.*, 2011), but only uniquely mapped reads were extracted. Data were split and separately analyzed for the plants using edgeR (Robinson *et al.*, 2009). Gene ontology enrichment assessment was carried out using GORILLA (Eden *et al.*, 2009) and visualizations were generated with REVIGO (Supek *et al.*, 2011).

For the analysis of the fungal transcriptome short reads were mapped to the genome using STAR 2.5.2 (Dobin *et al.*, 2013), tables with raw read counts were parsed and analyzed with DESeq2 (Love *et al.*, 2014). For the analysis of the Tue1 line, short reads were mapped to the genome using HISAT2 (Kim *et al.*, 2015), and analyzed with STRINGTIE (Pertea *et al.*, 2016) and DESeq2.

Results

Assembly and annotation of *T. thlaspeos* LF1 and LF2 genomes

To assemble the reference genome for *T. thlaspeos*, gDNA from the haploid strain LF1 of the mating type *a1b1* (Frantzeskakis *et al.*, 2017) was sequenced using both long-read (PacBio, *c.* 40× coverage) and short-read (Illumina MiSeq, *c.* 53× coverage) platforms. The two approaches resulted in 332 950 single long reads and 5433 377 paired short reads, respectively. PacBio long reads were assembled into 33 scaffolds and further polished using short Illumina reads. The resulting assembly is of high continuity, reaching chromosome level. The mitochondrial genome was fully assembled in a single scaffold of 108.2 kb (Fig. S1). Here, 19 out of the 32 nuclear scaffolds have telomeric repeats (TTAGGG) at both ends, five have repeats at one end (Tables 1, S2). Hence,

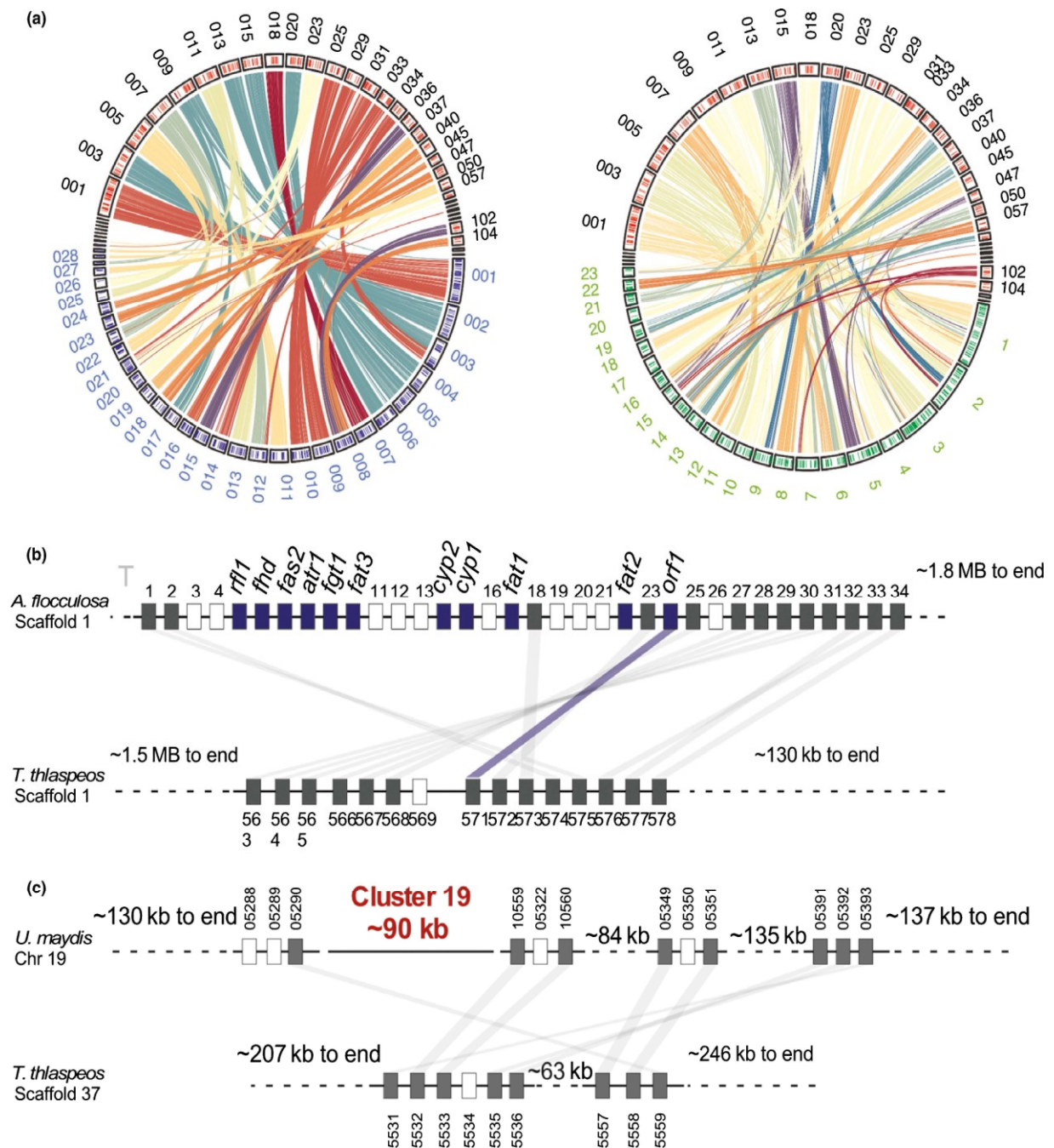


Fig. 1 Synteny is higher between *Thecaphora thlaspeos* and *Anthracocystis flocculosa* than *T. thlaspeos* and *Ustilago maydis*. (a) Circos plots between *T. thlaspeos* and *A. flocculosa* (left) or *U. maydis* (right). Colored lines depict syntenic blocks larger than 2 kb. Outer ring depicts the location of secreted proteins in the corresponding scaffold or chromosome. Scaffolds of *A. flocculosa* are in blue, while scaffold of *U. maydis* are in green (b) Synteny of the flocculosin secondary metabolite cluster in *A. flocculosa* and *T. thlaspeos*. Blue boxes depict genes involved in flocculosin production, white boxes depict genes with no orthologues in the compared genome. (c) Synteny of the effector Cluster 19A between *U. maydis* and *T. thlaspeos*. White boxes depict genes with no orthologues in the compared genome.

we used whole-genome alignments (Fig. S3). Overall, *T. thlaspeos* scaffolds align best to *A. flocculosa* with an average alignment rate of 51.4% and an average similarity ranging from 74.2% to 78% (Fig. 1a; Table S11). By contrast, alignment rate and sequence similarity between *T. thlaspeos* and the model smut fungus

U. maydis drops to averages of 32.4% and 73.4%, respectively (Fig. 1a; Table S11).

Loss of synteny between genomes of fungal plant pathogens has been shown to increase with genetic distance and, moreover, involves genomic regions that are often enriched for virulence-

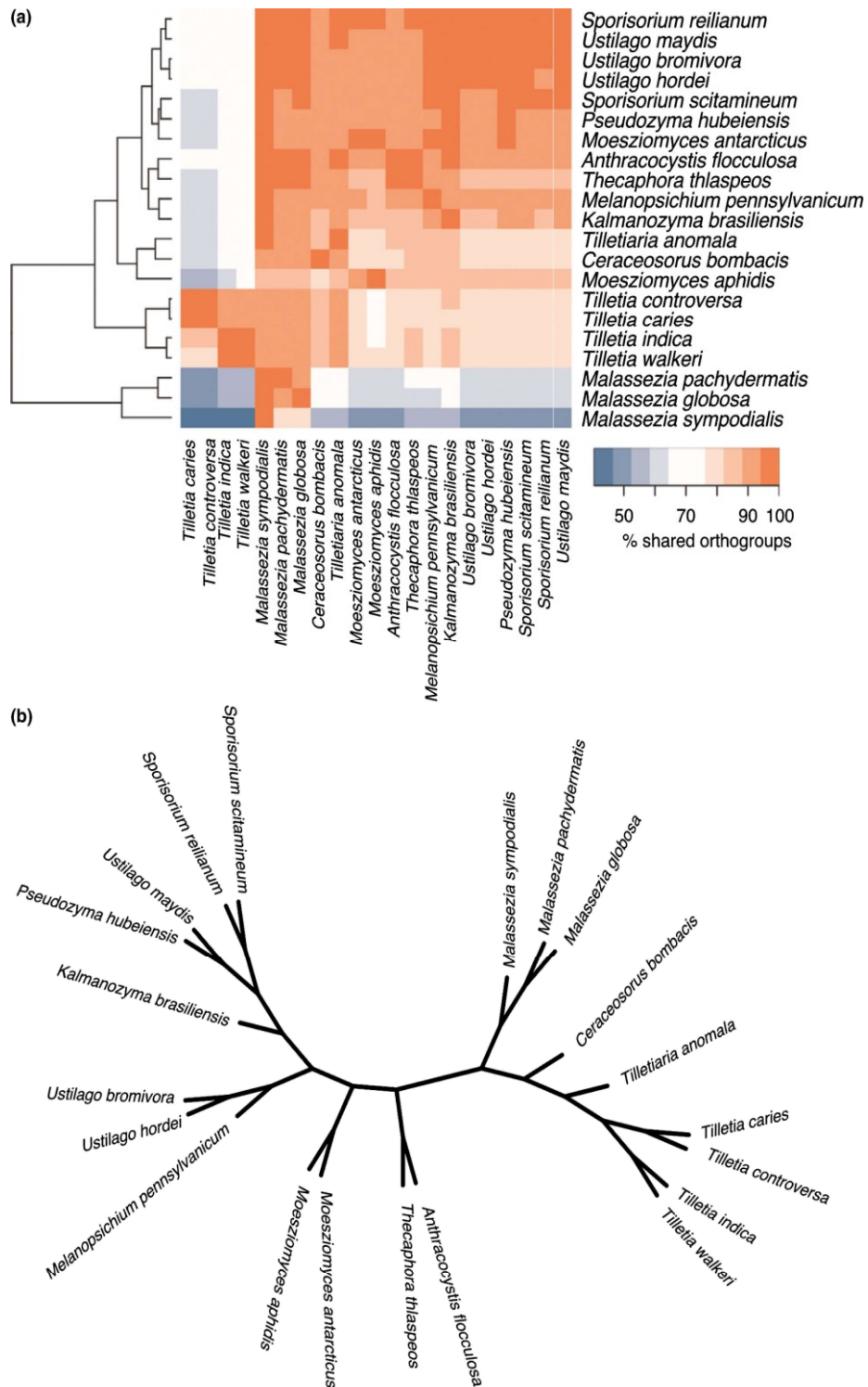


Fig. 2 *Thecaphora thlaspeos* and *Anthracozytis flocculosa* are genetically separate from the grass smuts. (a) Orthology analysis of all *T. thlaspeos* predicted genes in comparison to the predicted genes of other Ustilaginales species. The heatmap depicts the % overlap of orthologous groups. Cladogram on the left is based on hierarchical clustering (Euclidean method). (b) Multilocus phylogeny of the Ustilaginales species used for the analysis based on 1307 single-copy orthologues.

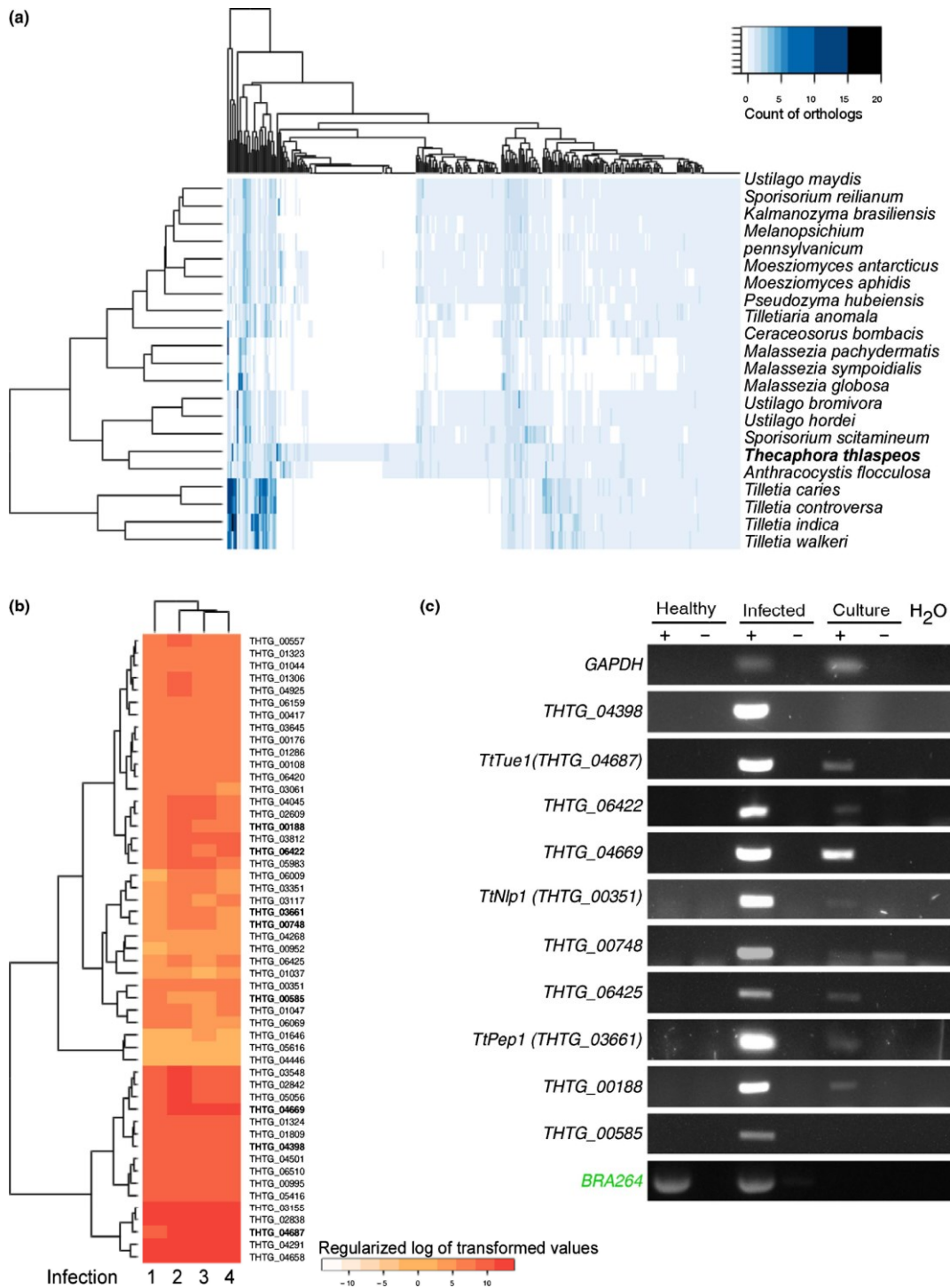


Fig. 3 Candidate effectors of *Thecaphora thlaspeos* are identified via differential expression analysis during infection and confirmed by RT-PCR. (a) Orthology analysis of the *T. thlaspeos* predicted secretome in comparison to the predicted secretomes of other Ustilaginales species. Cladogram on the left and on top is based on hierarchical clustering (Euclidean method). Color-coding depicts the amount of orthologues in other species for every *T. thlaspeos* secreted protein-coding gene. (b) Expression values of 51 differentially expressed secreted protein-coding genes during the infection of *Arabidopsis hirsuta*. Each column represents a biological replicate. Cladogram on the left is based on hierarchical clustering (Euclidean method) and effector candidates verified by RT-PCR are highlighted in bold. Color code represents regularized log transformed values derived from the DESeq2 analysis. (c) Effector candidates have visibly higher mRNA accumulation during infection compared with in culture. Effector mRNA accumulation is normalized by that of *gapdh*. Plant marker *BRA264* (Stockenhuber *et al.*, 2015) was used to verify samples containing plant tissue cDNA. RT, Reverse transcriptase, reaction: 35 cycles.

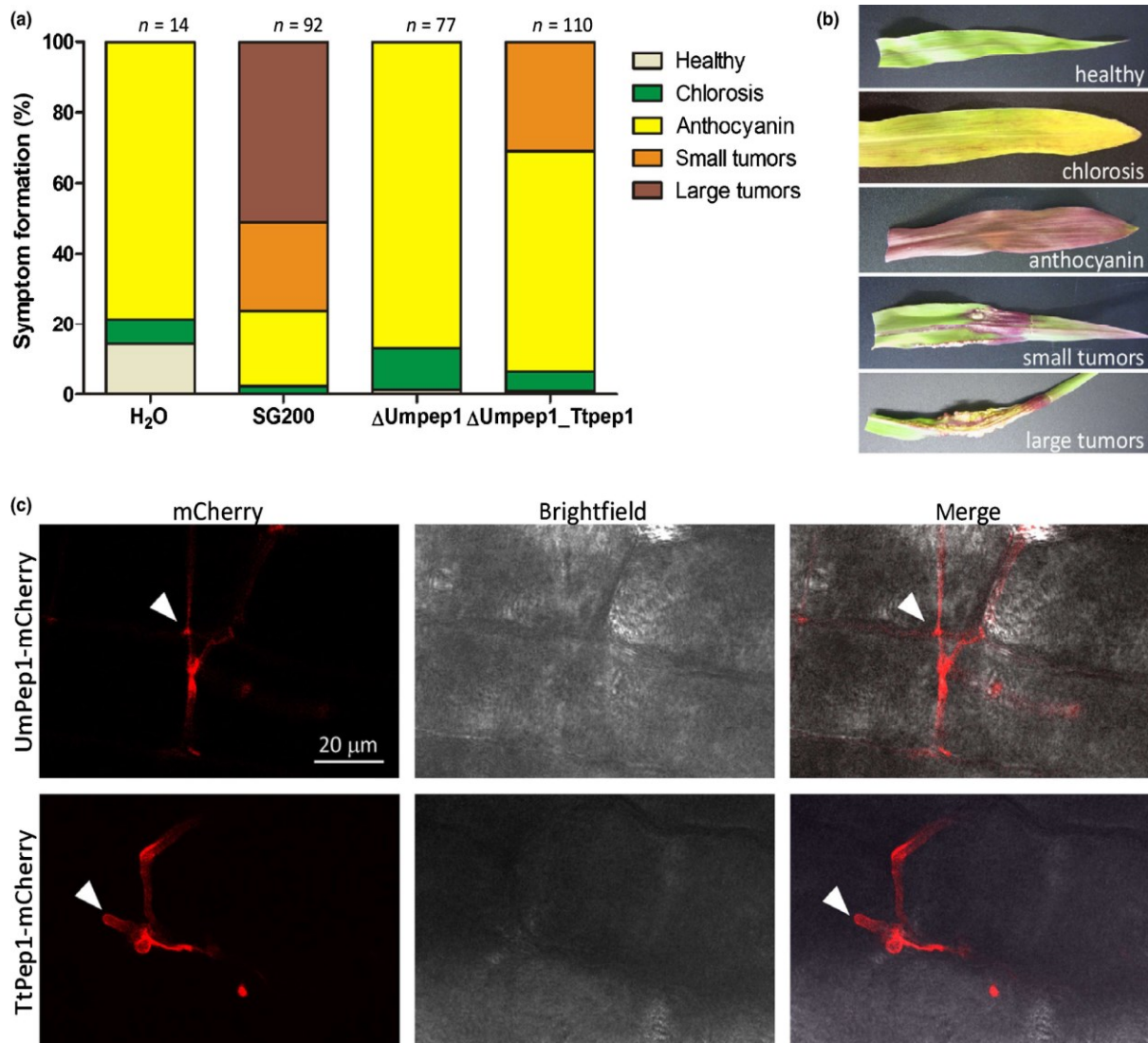


Fig. 4 *Ttpep1* partially complements deletion of *Umpep1* in maize infection. (a) Disease rating of 1-wk-old Early Golden Bantam maize plants 3 d post infection (dpi) with H₂O (mock) and *Ustilago maydis* strains SG200_Δ*pep1* (Δ*Umpep1*), SG200, and SG200_Δ*pep1*_Tt*pep1* (Δ*Umpep1*_Tt*pep1*). The values indicate the total number of plants infected in three independent experiments. (b) A representation of each disease category. (c) Confocal imaging of maize leaves infected with *UmPep1*-mCherry (SG200_Δ*pep1*_Um*Pep1*-mCherry), top, and *TtPep1*-mCherry (SG200_Δ*pep1*_Tt*Pep1*-mCherry), bottom. Arrows indicate apoplastic regions into which *UmPep1* is secreted, as shown by Doeblemann *et al.* (2009), and therefore where *TtPep1* is also likely secreted.

second class of Nlp proteins are noncytotoxic and induce immune responses, but do not elicit HR-related cell death (Santhanam *et al.*, 2012; Oome *et al.*, 2014). To date, the role of the noncytotoxic class of Nlps during infection remains elusive.

In addition to the induced *Ttnlp1*, the genome of *T. thlaspeos* encodes two *nlp* genes with predicted NPP1-domains (Pfam accession PF05630): THTG_00343 = *nlp2*, and THTG_04815 = *nlp3*. *Ttnlp1* and *Ttnlp2* are located on scaffold 1 and have predicted signal peptides. This *nlp* locus contains additional genes with predicted signal peptides and, hence, might comprise the first *T. thlaspeos* effector gene cluster (Fig. 5a). *Ttnlp3*, located on scaffold 33, is substantially shortened at the N-terminus and

does not have a signal peptide. Amino acids in the necrosis-inducing heptapeptide are not conserved in the three *T. thlaspeos* proteins suggesting they are noncytotoxic (Fig. 5b). In line with these findings, transient expression assays in *N. benthamiana* confirmed that *TtNlp1* fails to cause necrosis (Fig. 5c). To test whether *TtNlp1* plays a role in virulence, we utilized *Pseudomonas syringae* pv. *tomato* DC3000-LUX (*Pst-LUX*) for pathogen-mediated delivery of *TtNlp1* into *A. thaliana*. As expected, this noncytotoxic protein does not cause HR. However, bacterial growth significantly increased in the presence of *TtNlp1*, suggesting a virulence function for this candidate effector (Fig. 5d,e). In the future, it will be important to confirm this

Table 2 Features of *Thecaphora thlaspeos* effector candidates investigated in *Arabidopsis thaliana*.

Candidate effector protein	Protein length (aa)	Signal peptide length (aa)	Upregulation in infection (RT-PCR)	Phenotype when expressed in <i>A. thaliana</i>
THTG_04398	235	27	Yes	–
THTG_04687 (<i>TtTue1</i>)	294	22	Yes	Small rosettes
THTG_06422	162	18	Yes	–
THTG_04669	269	22	Yes	Few transformants in <i>A. thaliana</i>
THTG_00351 (<i>TtNlp1</i>)	292	19	Yes	–
THTG_00748	137	25	Yes	–
THTG_06425	271	18	Yes	No effector mRNA accumulation
THTG_03661 (<i>TtPep1</i>)	142	22	Yes	Few transformants in <i>A. thaliana</i>
THTG_00188	252	23	Yes	No <i>Agrobacterium tumefaciens</i> strains
THTG_00585	449	22	Yes	–

Phenotype refers to macroscopically detectable changes in growth or morphology 4 wk post sowing. Candidate effectors are listed from most upregulated during infection to least and those in gray were not further analyzed in phenotype screen.

our dataset, we cannot yet evaluate whether these responses contribute to limiting *T. thlaspeos* hyphae to the vasculature.

Discussion

T. thlaspeos has a typical smut genome with unique effectors that suggest adaptation to dicot hosts

With a size of *c.* 20 Mb, a low repeat content, and 6239 predicted gene models, the genome of *T. thlaspeos* has the typical characteristics of most sequenced smut fungi. Despite the adaptation to a dicot host, its absolute gene content and predicted functional categories largely overlap with grass-infecting smut fungi (Sharma *et al.*, 2015; Dutheil *et al.*, 2016). However, two unique features stand out from the genome assembly and annotation. First, synteny between *T. thlaspeos* and the grass smuts is low and second, *T. thlaspeos* shares only few known effector candidate genes with its grass smut relatives. Hence, *T. thlaspeos* seems to deploy a different repertoire of effectors to establish and maintain its biotrophic lifestyle. Remarkably, *M. pennsylvanicum*, the only example of grass smuts that underwent a host jump from grasses to the dicot genus *Persicaria*, has maintained its typical grass smut effector repertoire and accordingly has a very low number of *T. thlaspeos* orthologues suggesting independent dicot adaptation in *Thecaphora* and *M. pennsylvanicum* (Sharma *et al.*, 2015; Fig. 2a; Table S13). For example, the Nlps are well known effectors that distinguish *T. thlaspeos* from other smut fungi. Notably, these are also absent in earlier diverging species of the Ustilaginales such as *Ceraceosorus bombacis* (Sharma *et al.*, 2015), suggesting independent acquisition for example by horizontal gene transfer.

More closely related to *T. thlaspeos* is the epiphytic biocontrol agent *A. flocculosa* which has a significantly higher degree of synteny and a larger overlap in gene content including 17 candidate effector genes. Interestingly, *A. flocculosa* also carries Nlp domain encoding genes (Lefebvre *et al.*, 2013), yet these are nonorthologous to the *T. thlaspeos* Nlps. The close genetic distance to *T. thlaspeos*, along with the presence of these candidate effectors, supports the previously raised hypothesis that *A. flocculosa* besides

being a mycoparasite of powdery mildews (Laur *et al.*, 2017), could also be a yeast anamorph of a dicot-infecting smut species (Begerow *et al.*, 2014).

Comparing the two *T. thlaspeos* isolates, LF1 and LF2, revealed the first isolate-specific smut effectors. This is particularly interesting as the infectious form of smut fungi is a dikaryon. Considering that *T. thlaspeos* genetically contains the capacity for mating and that haploid isolates of opposite mating types form fusion hyphae (Frantzeskakis *et al.*, 2017), genetic exchange during mating in *T. thlaspeos* provides the potential to bring together certain virulence-related genes of the single strains. Hence, the combination of different mates could result in distinct fitness levels of the fungus due to alterations in effector dosage and/or content or due to complementation of effector gene losses. In the future, population genetics approaches can reveal distribution of effectors throughout populations and the stability of such populations over the years.

T. thlaspeos infection strategy enables perennial biotrophy

In addition to pathogens, fungal endophytes also possess an astonishing diversity of host colonization strategies that independently evolved in several taxonomic groups (Rodriguez *et al.*, 2009; Brader *et al.*, 2017). Endophytes are microorganisms that colonize the inner plant tissues of macroscopically healthy host plants (Schulz & Boyle, 2005). Some fungal endophytes establish long-lasting interactions such as the generalist root endophyte *Piriformospora indica* or members of the grass endophyte genus *Epichloë* that remain inside their host throughout the growing season (Rodriguez *et al.*, 2009; Franken, 2012). As for biotrophic pathogens, successful colonization requires complex molecular mechanisms. For example, the basidiomycete *P. indica* establishes biotrophy in *A. thaliana* and barley in a host species-dependent manner with distinct transcriptional responses (Lahrman *et al.*, 2013). Despite a few well studied examples, it remains largely unknown how plant-pathogenic endophytes manage to establish and maintain such sustained systemic infections and what determines the type of interaction and host specificity.

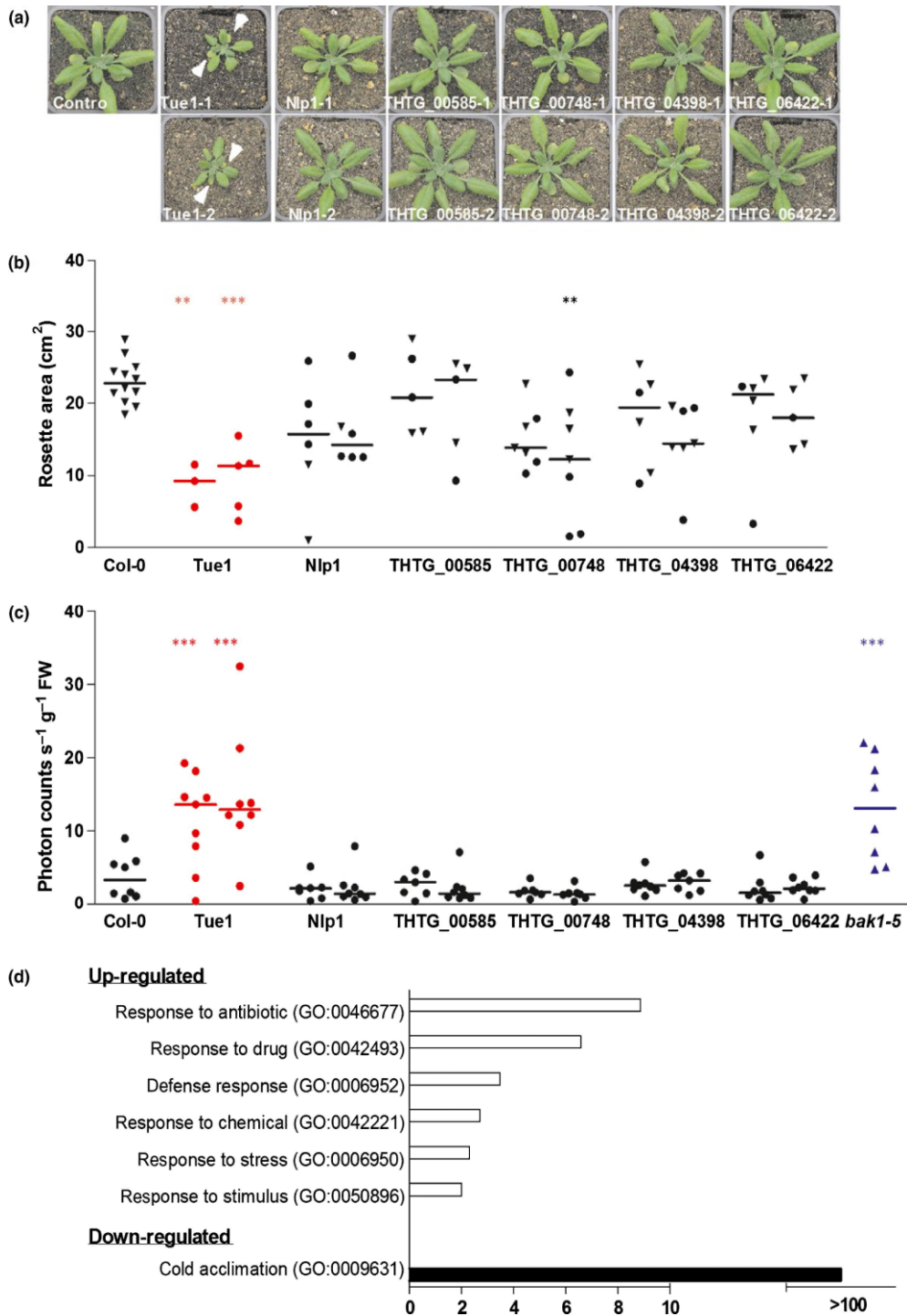


Fig. 6 Transgenic *Arabidopsis thaliana* accumulating mRNA of *Tttue1* are small with slightly chlorotic first true leaves. (a) Representative images of two independent plant lines (1 and 2) expressing the upregulated effector candidate. *TtTue1*-lines are clearly smaller and show signs of chlorosis (arrowheads). (b) Quantification of rosette area confirms that *TtTue1* plants are significantly smaller than the controls. Circles indicate plants whose effector mRNA accumulation was confirmed via RT-PCR (25 cycles), triangles indicate additional individuals. (c) *Pst-LUX* proliferation significantly increases in lines expressing *Tue1* and reaches the same level as in the susceptible *bak1-5* mutant. (d) GO term enrichments of differentially expressed genes (DEGs) in the *Tue1*-line reveals upregulation of categories related to response to stress and environment, while cold-stress acclimation seem reduced. (b, c) Individual replicates and median are shown, statistical analysis was carried out by one-way analysis of variance (ANOVA) followed by Bonferroni's post tests; ***, $P < 0.001$; **, $P < 0.01$.

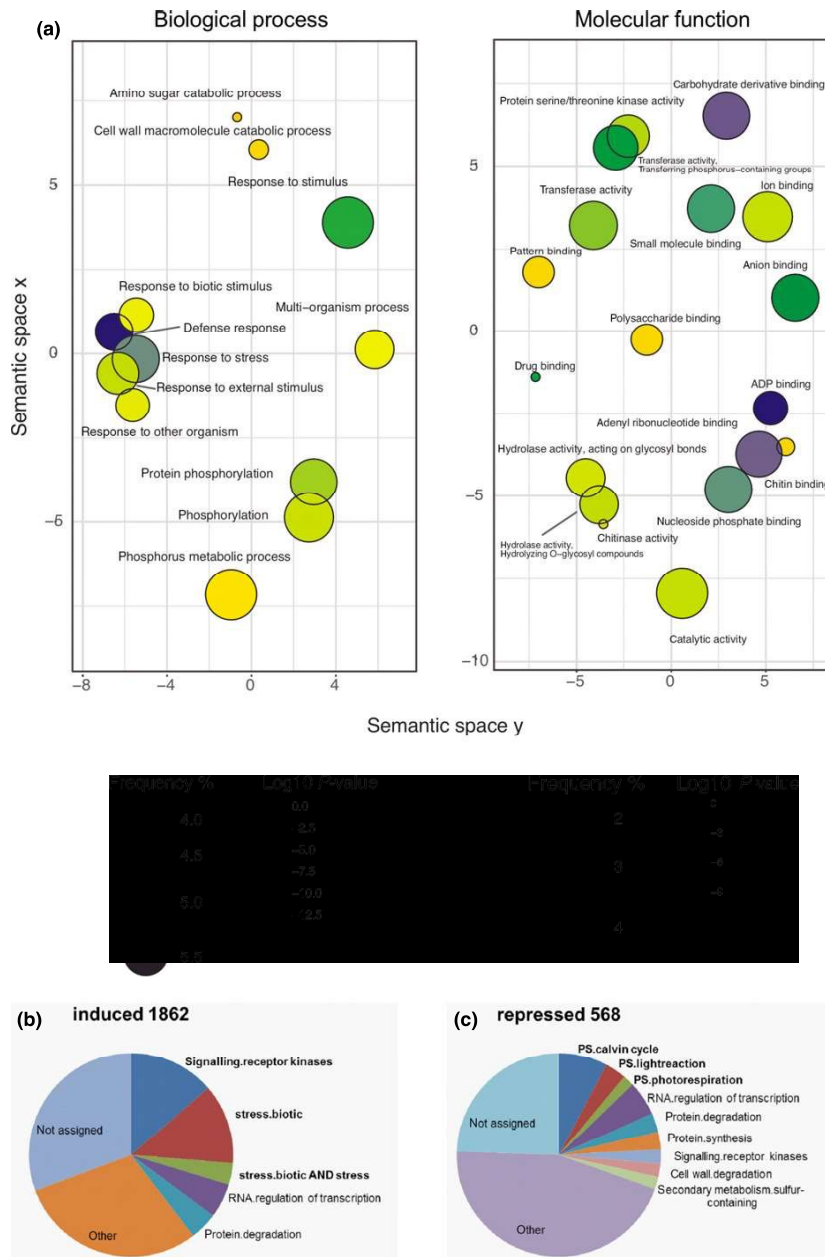


Fig. 7 Over-represented gene ontology (GO) terms and MapMan categories during the infection of *Arabis hirsuta* by *Thecaphora thlaspeos* show prevalence of biotic stress. (a) Two-dimensional semantic space scatterplots to describe over-represent GO terms were generated with GORILLA and REVIGO (P -value < 0.001). Circle sizes represent the frequency of the GO term in the Arabidopsis genome while the color indicates the P -value for the enrichment. (b) MapMan analysis of induced transcript revealed a strong overrepresentation of biotic stress-related categories (bold) in the induced transcripts. About one-third of the transcripts fall into signaling, receptor kinases, or stress/biotic. (c) MapMan analysis of repressed genes indicates a downregulation of photosynthetic genes.

Here, we characterized the biotrophic phase of *T. thlaspeos*. To maintain this ‘hidden’ growth without macroscopic symptoms, it employs typical effector proteins such as Pep1 and Nlps, but also unique effectors such as *TTue1*. The latter, when overexpressed in *A. thaliana*, causes a growth defect reminiscent of the

phenotypes observed in several *HaNlps* expressed in *A. thaliana* as well as autoimmune mutants (Bowling *et al.*, 1994, 1997; Oome *et al.*, 2014), which transcriptionally activate host immune responses and suppress cold acclimation. Overall, the identification of these novel smut effectors opens the door to study the

Table 3 Expression of salicylic acid (SA)-dependent defense signaling genes in healthy and infected *Arabis hirsuta* plants.

<i>A. thaliana</i> homologue	Trinity transcript ID	logFC	logCPM	<i>P</i> -value	FDR
PR-1 (At2g14610)*	TRINITY_DN13170_c0_g1_i1	4.51	11.88	1.2E-49	5.1E-45
PR-2 (At3g57260)	TRINITY_DN17095_c0_g1_i3	1.07	6.28	1.0E-06	2.0E-04
EDS1 (At3g48090)	TRINITY_DN27010_c2_g5_i1	0.92	6.07	3.3E-06	5.6E-04
	TRINITY_DN27010_c2_g5_i3	0.71	5.02	3.4E-04	2.8E-02
	TRINITY_DN27010_c2_g5_i6	0.96	3.63	1.2E-05	1.7E-03
	TRINITY_DN27010_c2_g5_i2	0.74	4.33	0.00088	0.06
EDS5/SID1 (At4g39030)	TRINITY_DN27010_c2_g7_i4	-0.40	1.14	0.335903	1
	TRINITY_DN25779_c1_g4_i6	2.23	2.56	5.84E-09	1.9E-06
	TRINITY_DN6765_c0_g1_i1	2.12	1.89	5.8E-08	1.5E-05
PAD4 (At3g52430)	TRINITY_DN25779_c1_g4_i9	-0.63	2.99	0.01	0.40
	TRINITY_DN20844_c0_g1_i1	1.21	5.16	1.4E-07	3.3E-05
	TRINITY_DN20844_c0_g1_i2	0.74	4.58	0.00019	1.7E-02
NDR1 (At3g20600)	TRINITY_DN15989_c0_g1_i1	1.48	4.99	2.8E-09	9.7E-07
	TRINITY_DN15989_c0_g1_i2	1.44	4.33	1.8E-10	7.5E-08
NPR1/NIM1 (At1g64280)	TRINITY_DN27057_c1_g2_i1	1.02	3.73	4.4E-05	5.2E-03
	TRINITY_DN27057_c1_g1_i11	0.54	5.81	5.8E-03	0.23
	TRINITY_DN27057_c1_g1_i18	0.93	1.38	7.4E-03	0.27
	TRINITY_DN27057_c1_g3_i1	0.30	3.82	0.15	1
	TRINITY_DN17408_c0_g3_i1	0.36	0.66	0.45	1

Arabidopsis thaliana genes with a role in SA-signaling were selected based on literature (see text). Homologues in the *Ar. hirsuta* transcript assembly were identified. For some genes, more than one transcript was assembled and those with good coverage (logCPM > 0) were considered. Significant FDR values are shown in bold and these transcripts were all induced during infection pointing at upregulation of SA-signalling. PR-5, SAG101, TGA1 and TGA2 were identified in several transcript isoforms, but none on these was induced.

*For PR-1 several fungal reads from culture mapped to the transcript. These reads likely belong to TtPry1 (THTG_03812), a putative sterol binding protein and member of the CAP protein superfamily, which is induced during infection.

specific activity of the *Thecaphora* clade effectorome and how, or when, it is utilized to manipulate the host's responses.

On the host side, transcriptional changes reflect a typical response to infection and register as a biotic stress event in the plant's transcriptome. This resembles the plant responses to a majority of microbes, which have effects on their host plant's transcriptomes to various degrees and establish a balance with the plant immune system leading to colonization and infection (Brader *et al.*, 2017). This observation also agrees with previous studies on smut fungi in which an overall upregulation of stress-related gene expression during early infection is kept at bay by effectors (Doehlemann *et al.*, 2008; Djamei & Kahmann, 2012). This effective balance and continuous interaction between *T. thlaspeos* and the host's immune system may therefore limit excessive fungal proliferation to the vasculature which could undermine plant fitness.

In summary, *T. thlaspeos* colonizes Brassicaceae hosts using a unique set of secreted proteins, different from both monocot infecting species but also the dicot-infecting *M. pennsylvanicum*. Excitingly, we find smut-typical effectors such as Pep1, dicot-typical effector genes such as the Nlps but also novel effector candidates such as *TtTue1* that seem to integrate abiotic stress factors, that is cold-stress response into the fungal infection mechanism. In addition, we show that the effector repertoire likely differs between *T. thlaspeos* isolates. Further studies on *T. thlaspeos* will elucidate whether the secreted protein-coding genes identified here present different expression patterns in various tissues or at different points during its long-term biotrophic stage. Finally, using the information and the resources provided

here, more extensive studies could address the pathogen-endophyte continuum using *T. thlaspeos* as a model organism.


Acknowledgements

We warmly thank our colleagues at the Institute of Microbiology, The Sainsbury Laboratory (TSL), the John Innes Centre (JIC), and Michigan State University (MSU) for great discussions. We greatly thank the TSL plant transformation team for their work in generating our transgenic *A. thaliana* lines, the JIC horticultural team for excellent plant care services, and the TSL support team for media preparation. Special thanks to Simone Esch, Lesley Plücker and Merve Öztürk for technical assistance. Research in the laboratory of VG is funded by the Cluster of Excellence in Plant Sciences (CEPLAS, DFG EXC 1028) and the Bioeconomy Science Center (BioSC). The scientific activities of the BioSC were financially supported by the Ministry of Innovation, Science and Research within the framework of the NRW Strategieprojekt BioSC (No. 313/323-400-00213). RK and EK are supported by CEPLAS, LF and KJC were supported by a doctoral fellowship of the DFG International Research Training Group 1525 iGRADplant. Research performed at TSL was kindly supported by the 2Blades Foundation (2B3511-KK). Research in the laboratory of Brad Day is supported by a grant from the US National Science Foundation (IOS-1146128). Microscopy was carried out at the 'Center for Advanced Imaging', HHU. Computational support and infrastructure was provided by the 'Centre for Information and Media Technology', HHU and by the Institute for Cyber-Enabled Research, MSU.


Author contributions


VG and MF planned and designed the research. LF and KJC designed and performed the experiments. SG, N Haeger and N Heßler provided infection figures. AB contributed genomic sequences. LF and BU performed the bioinformatic analysis. EK, YKG, HPvE, and BD contributed materials and supported the experimental design. KJC, LF, RK, and VG wrote the manuscript. KJC and LF contributed equally to this work.

ORCID


Andreas Brachmann  <https://orcid.org/0000-0001-7980-8173>


Brad Day  <https://orcid.org/0000-0002-9880-4319>

Michael Feldbrügge  <https://orcid.org/0000-0003-0046-983X>


Lamprinos Frantzeskakis  <https://orcid.org/0000-0001-8947-6934>

Vera Göhre  <https://orcid.org/0000-0002-7118-1609>

Yogesh K. Gupta  <https://orcid.org/0000-0002-8696-9044>

Ronny Kellner  <https://orcid.org/0000-0002-4618-0110>

Eric Kemen  <https://orcid.org/0000-0002-7924-116X>

H. Peter van Esse  <https://orcid.org/0000-0002-3667-060X>

Björn Usadel  <https://orcid.org/0000-0003-0921-8041>

References

- Aichinger C, Hansson K, Eichhorn H, Lessing F, Mannhaupt G, Mewes W, Kahmann R. 2003. Identification of plant-regulated genes in *Ustilago maydis* by enhancer-trapping mutagenesis. *Molecular Genetics and Genomics* 270: 303–314.
- Andrade O, Munoz G, Galdames R, Duran P, Honorato R. 2004. Characterization, *in vitro* culture, and molecular analysis of *Thecaphora solani*, the causal agent of potato smut. *Phytopathology* 94: 875–882.
- Asai S, Rallapalli G, Piquerez SJM, Caillaud MC, Furzer OJ, Ishaque N, Wirthmueller L, Fabro G, Shirasu K, Jones JDG. 2014. Expression profiling during Arabidopsis/downy mildew interaction reveals a highly-expressed effector that attenuates responses to salicylic acid. *PLoS Pathogens* 10: e1004443.
- Bankevich A, Nurk S, Antipov D, Gurevich AA, Dvorkin M, Kulikov AS, Lesin VM, Nikolenko SI, Pham S, Pribelski AD *et al.* 2012. SPAdes: a new genome assembly algorithm and its applications to single-cell sequencing. *Journal of Computational Biology* 19: 455–477.
- Begerow D, Schaefer AM, Kellner R, Yurkov A, Kemler M, Oberwinkler F, Bauer R. 2014. 11 Ustilagomycotina. In: McLaughlin D, Spatafora J, eds. *Systematics and evolution. The mycota: systematics and evolution part A VII*. Berlin/Heidelberg, Germany: Springer.
- Białas A, Zess EK, De la Concepcion JC, Franceschetti M, Pennington HG, Yoshida K, Upson JL, Chanclud E, Wu C-H, Langner T *et al.* 2017. Lessons in effector and NLR biology of plant-microbe systems. *Molecular Plant-Microbe Interactions* 31: 34–45.
- Bleckmann A, Weidtkamp-Peters S, Seidel CAM, Simon R. 2010. Stem cell signaling in Arabidopsis requires CRN to localize CLV2 to the plasma membrane. *Plant Physiology* 152: 166–176.
- Böhm H, Albert I, Oome S, Raaymakers TM, Van den Ackerveken G, Nürnberger T. 2014. A conserved peptide pattern from a widespread microbial virulence factor triggers pattern-induced immunity in Arabidopsis. *PLoS Pathogens* 10: e1004491.
- Bolger AM, Lohse M, Usadel B. 2014. Trimmomatic: a flexible trimmer for Illumina sequence data. *Bioinformatics* 30: 2114–2120.
- Bösch K, Frantzeskakis L, Vraneš M, Kämper J, Schipper K, Göhre V. 2016. Genetic manipulation of the plant pathogen *Ustilago maydis* to study fungal biology and plant-microbe interactions. *Journal of Visualized Experiments* 115: e54522.
- Bowling SA, Clarke JD, Liu Y, Klessig DF, Dong X. 1997. The cpr5 mutant of Arabidopsis expresses both NPR1-dependent and NPR1-independent resistance. *Plant Cell* 9: 1573–1584.
- Bowling SA, Guo A, Cao H, Gordon AS, Klessig DF, Dong X. 1994. A mutation in Arabidopsis that leads to constitutive expression of systemic acquired resistance. *Plant Cell* 6: 1845–1857.
- Brader G, Compant S, Vescio K, Mitter B, Trognitz F, Ma L-J, Sessitsch A. 2017. Ecology and genomic insights into plant-pathogenic and plant-nonpathogenic endophytes. *Annual Review of Phytopathology* 55: 61–83.
- Brefort T, Doehlemann G, Mendoza-Mendoza A, Reissmann S, Djamei A, Kahmann R. 2009. *Ustilago maydis* as a pathogen. *Annual Review of Phytopathology* 47: 423–445.
- Campbell MS, Holt C, Moore B, Yandell M. 2014. Genome annotation and curation using MAKER and MAKER-P. *Current Protocols in Bioinformatics* 48: 4.11.11–14.11.39.
- Chinchilla D, Zipfel C, Robatzek S, Kemmerling B, Nürnberger T, Jones JDG, Felix G, Boller T. 2007. A flagellin-induced complex of the receptor FLS2 and BAK1 initiates plant defence. *Nature* 448: 497–500.
- Choi J, Kim K-T, Jeon J, Lee Y-H. 2013. Fungal plant cell wall-degrading enzyme database: a platform for comparative and evolutionary genomics in fungi and Oomycetes. *BMC Genomics* 14: S7.
- Conforto C, Cazón I, Fernández FD, Marinelli A, Oddino C, Rago AM. 2013. Molecular sequence data of *Thecaphora frezii* affecting peanut crops in Argentina. *European Journal of Plant Pathology* 137: 663–666.
- Delcher AL, Salzberg SL, Phillippy AM. 2003. Using MUMmer to identify similar regions in large sequence sets. In: Baxevanis AD, Davison DB, eds. *Current protocols in bioinformatics, Chapter 10*. Hoboken, NJ, USA: John Wiley & Sons, 10.3.1–10.3.18.
- Djamei A, Kahmann R. 2012. *Ustilago maydis*: dissecting the molecular interface between pathogen and plant. *PLoS Pathogens* 8: e1002955.
- Djamei A, Schipper K, Rabe F, Ghosh A, Vincin V, Kahnt J, Osorio S, Tohge T, Fernie AR, Feussner I *et al.* 2011. Metabolic priming by a secreted fungal effector. *Nature* 478: 395–398.
- Dobin A, Davis CA, Schlesinger F, Drenkow J, Zaleski C, Jha S, Batut P, Chaisson M, Gingeras TR. 2013. STAR: ultrafast universal RNA-seq aligner. *Bioinformatics* 29: 15–21.
- Dodds PN, Rathjen JP. 2010. Plant immunity: towards an integrated view of plant-pathogen interactions. *Nature Reviews Genetics* 11: 539–548.
- Doehlemann G, Reissmann S, Alßmann D, Fleckenstein M, Kahmann R. 2011. Two linked genes encoding a secreted effector and a membrane protein are essential for *Ustilago maydis*-induced tumour formation. *Molecular Microbiology* 81: 751–766.
- Doehlemann G, van der Linde K, Assmann D, Schwambach D, Hof A, Mohanty A, Jackson D, Kahmann R. 2009. Pep1, a secreted effector protein of *Ustilago maydis*, is required for successful invasion of plant cells. *PLoS Pathogens* 5: e1000290.
- Doehlemann G, Wahl R, Horst RJ, Voll LM, Usadel B, Poree F, Stitt M, Pons-Kühnemann J, Sonnwald U, Kahmann R *et al.* 2008. Reprogramming a maize plant: transcriptional and metabolic changes induced by the fungal biotroph *Ustilago maydis*. *The Plant Journal* 56: 181–195.
- Dutheil JY, Mannhaupt G, Schweizer G, M K Sieber C, Münsterkötter M, Güldener U, Schirawski J, Kahmann R. 2016. A tale of genome compartmentalization: the evolution of virulence clusters in smut fungi. *Genome Biology and Evolution* 8: 681–704.
- Earley KW, Haag JR, Pontes O, Opper K, Juchne T, Song K, Pikaard CS. 2006. Gateway-compatible vectors for plant functional genomics and proteomics. *The Plant Journal* 45: 616–629.
- Eden E, Navon R, Steinfeld I, Lipson D, Yakhini Z. 2009. GOrrilla: a tool for discovery and visualization of enriched GO terms in ranked gene lists. *BMC Bioinformatics* 10: 1–7.
- Emms DM, Kelly S. 2015. OrthoFinder: solving fundamental biases in whole genome comparisons dramatically improves orthogroup inference accuracy. *Genome Biology* 16: 157.

- Engler C, Youles M, Gruetzner R, Ehnert TM, Werner S, Jones JDG, Patron NJ, Marillonnet S. 2014. A Golden Gate modular cloning toolbox for plants. *ACS Synthetic Biology* 3: 839–843.
- Fabro G, Steinbrenner J, Coates M, Ishaque N, Baxter L, Studholme DJ, Körner E, Allen RL, Piquerez SJM, Rougon-Cardoso A *et al.* 2011. Multiple candidate effectors from the oomycete pathogen *Hyaloperonospora arabidopsidis* suppress host plant immunity. *PLoS pathogens* 7: e1002348.
- Fedler M, Luh KS, Stelzer K, Nieto-Jacobo F, Basse CW. 2009. The $\alpha 2$ mating-type locus genes *lga2* and *rga2* direct uniparental mitochondrial DNA (mtDNA) inheritance and constrain mtDNA recombination during sexual development of *Ustilago maydis*. *Genetics* 181: 847–860.
- Feldbrügge M, Kämper J, Steinberg G, Kahmann R. 2004. Regulation of mating and pathogenic development in *Ustilago maydis*. *Current Opinion in Microbiology* 7: 666–672.
- Franken P. 2012. The plant strengthening root endophyte *Piriformospora indica*: potential application and the biology behind. *Applied Microbiology and Biotechnology* 96: 1455–1464.
- Frantzeskakis L, Courville KJ, Pluecker L, Kellner R, Kruse J, Brachmann A, Feldbrügge M, Göhre V. 2017. The plant-dependent life cycle of *Thecaphora thlaspeos*: a smut fungus adapted to Brassicaceae. *Molecular Plant–Microbe Interactions* 30: 271–282.
- Gassmann W, Bhattacharjee S. 2012. Effector-triggered immunity signaling: from gene-for-gene pathways to protein–protein interaction networks. *Molecular Plant–Microbe Interactions* 25: 862–868.
- Germain H, Joly DL, Mireault C, Plourde MB, Letanneur C, Stewart D, Morency MJ, Petre B, Duplessis S, Seguin A. 2017. Infection assays in Arabidopsis reveal candidate effectors from the poplar rust fungus that promote susceptibility to bacteria and oomycete pathogens. *Molecular Plant Pathology* 19: 191–200.
- Ghareeb H, Drechsler F, Löffke C, Teichmann T, Schirawski J. 2015. SUPPRESSOR OF APICAL DOMINANCE 1 of *Sporisorium reilianum* Modulates Inflorescence Branching Architecture in Maize and Arabidopsis. *Plant Physiology* 169: 2789–2804.
- Giraldo MC, Valent B. 2013. Filamentous plant pathogen effectors in action. *Nature Reviews Microbiology* 11: 800–814.
- Glazebrook J. 2005. Contrasting mechanisms of defense against biotrophic and necrotrophic pathogens. *Annual Review of Phytopathology* 43: 205–227.
- Grabherr MG, Haas BJ, Yassour M, Levin JZ, Thompson DA, Amit I, Adiconis X, Fan L, Raychowdhury R, Zeng Q *et al.* 2011. Full-length transcriptome assembly from RNA-Seq data without a reference genome. *Nature Biotechnology* 29: 644–652.
- Gutjahr C, Parniske M. 2013. Cell and developmental biology of arbuscular mycorrhiza symbiosis. *Annual Review of Cell and Developmental Biology* 29: 593–617.
- Hemetsberger C, Herrberger C, Zechmann B, Hillmer M, Doehlemann G. 2012. The *Ustilago maydis* effector Pep1 suppresses plant immunity by inhibition of host peroxidase activity. *PLoS Pathogens* 8: e1002684.
- Hemetsberger C, Mueller N, Matei A, Herrberger C, Doehlemann G. 2015. The fungal core effector Pep1 is conserved across smuts of dicots and monocots. *New Phytologist* 206: 1116–1126.
- Holliday R. 1961. Induced mitotic crossing-over in *Ustilago maydis*. *Genetics Research* 2: 231–248.
- Holt C, Yandell M. 2011. MAKER2: an annotation pipeline and genome-database management tool for second-generation genome projects. *BMC Bioinformatics* 12: 491.
- Huang L, Zhang H, Wu P, Entwistle S, Li X, Yohe T, Yi H, Yang Z, Yin Y. 2017. dbCAN-seq: a database of carbohydrate-active enzyme (CAZyme) sequence and annotation. *Nucleic Acids Research* 46: D516–D521.
- Huot B, Yao J, Montgomery BL, He SY. 2014. Growth-defense tradeoffs in plants: a balancing act to optimize fitness. *Molecular Plant* 7: 1267–1287.
- Irani S, Trost B, Waldner M, Nayidu N, Tu J, Kusalik AJ, Todd CD, Wei Y, Bonham-Smith PC. 2018. Transcriptome analysis of response to *Plasmidiophora brassicae* infection in the Arabidopsis shoot and root. *BMC Genomics* 19: 23.
- Jones P, Binns D, Chang H-Y, Fraser M, Li W, McAnulla C, McWilliam H, Maslen J, Mitchell A, Nuka G *et al.* 2014. InterProScan 5: genome-scale protein function classification. *Bioinformatics* 30: 1236–1240.
- Jurka J, Kapitonov V, Pavlicek A, Klonowski P, Kohany O, Walichiewicz J. 2005. Repbase Update, a database of eukaryotic repetitive elements. *Cytogenetic and Genome Research* 110: 462–467.
- Kämper J, Kahmann R, Bölker M, Ma L-J, Brefort T, Saville BJ, Banuett F, Kronstad JW, Gold SE, Müller O *et al.* 2006. Insights from the genome of the biotrophic fungal plant pathogen *Ustilago maydis*. *Nature* 444: 97–101.
- Karimi M, Inze D, Depicker A. 2002. GATEWAY vectors for Agrobacterium-mediated plant transformation. *Trends in Plant Science* 7: 193–195.
- Katagiri F, Thilmony R, He SY. 2002. The Arabidopsis thaliana–*Pseudomonas syringae* interaction. *Arabidopsis Book* 1: e0039.
- Kellner R, Vollmeister E, Feldbrügge M, Begerow D. 2011. Interspecific sex in grass smuts and the genetic diversity of their pheromone-receptor system. *PLoS Genetics* 7: e1002436.
- Kim D, Langmead B, Salzberg SL. 2015. HISAT: a fast spliced aligner with low memory requirements. *Nature Methods* 12: 357–360.
- Knepper C, Savory EA, Day B. 2011. The role of NDR1 in pathogen perception and plant defense signaling. *Plant Signaling and Behavior* 6: 1114–1116.
- Koncz C, Schell J. 1986. The promoter of T₁-DNA gene 5 controls the tissue-specific expression of chimaeric genes carried by a novel type of *Agrobacterium* binary vector. *Molecular and General Genetics* 204: 383–396.
- Koren S, Walenz BP, Berlin K, Miller JR, Bergman NH, Phillippy AM. 2017. Canu: scalable and accurate long-read assembly via adaptive k-mer weighting and repeat separation. *Genome Research* 27: 722–736.
- Korf I. 2004. Gene finding in novel genomes. *BMC Bioinformatics* 5: 1–9.
- Lahrman U, Ding Y, Banhara A, Rath M, Hajirezaei MR, Döhlemann S, von Wirén N, Parniske M, Zuccaro A. 2013. Host-related metabolic cues affect colonization strategies of a root endophyte. *Proceedings of the National Academy of Sciences, USA* 110: 13965–13970.
- Langmead B, Trapnell C, Pop M, Salzberg SL. 2009. Ultrafast and memory-efficient alignment of short DNA sequences to the human genome. *Genome Biology* 10: R25.
- Lanver D, Müller AN, Happel P, Schweizer G, Haas FB, Franitz M, Pellegrin C, Reissmann S, Altmüller J, Rensing SA *et al.* 2018. The biotrophic development of *Ustilago maydis* studied by RNAseq analysis. *Plant Cell* 30: 300–323.
- Lanver D, Tollot M, Schweizer G, Lo Presti L, Reissmann S, Ma LS, Schuster M, Tanaka S, Liang L, Ludwig N *et al.* 2017. *Ustilago maydis* effectors and their impact on virulence. *Nature Reviews Microbiology* 15: 409–421.
- Laur J, Ramakrishnan GB, Labbé C, Lefebvre F, Spanu PD, Bélanger RR. 2017. Effectors involved in fungal-fungal interaction lead to a rare phenomenon of hyperbiotrophy in the tritrophic system biocontrol agent-powdery mildew-plant. *New Phytologist* 217: 713–725.
- Lee E, Helt GA, Reese JT, Muñoz-Torres MC, Childers CP, Buels RM, Stein L, Holmes IH, Elisk CG, Lewis SE. 2013. Web Apollo: a web-based genomic annotation editing platform. *Genome Biology* 14: R93.
- Lefebvre F, Joly DL, Labbé C, Teichmann B, Linning R, Belzile F, Bakkeren G, Bélanger RR. 2013. The transition from a phytopathogenic smut ancestor to an anamorphic biocontrol agent deciphered by comparative whole-genome analysis. *Plant Cell* 25: 1946–1959.
- Linning R, Lin D, Lee N, Abdennadher M, Gaudet D, Thomas P, Mills D, Kronstad JW, Bakkeren G. 2004. Marker-based cloning of the region containing the *UvAvr1* avirulence gene from the basidiomycete barley pathogen *Ustilago hordei*. *Genetics* 166: 99–111.
- Lo Presti L, Lanver D, Schweizer G, Tanaka S, Liang L, Tollot M, Zuccaro A, Reissmann S, Kahmann R. 2015. Fungal effectors and plant susceptibility. *Annual Review of Plant Biology* 66: 513–545.
- Love MI, Huber W, Anders S. 2014. Moderated estimation of fold change and dispersion for RNA-seq data with DESeq2. *Genome Biology* 15: 1–21.
- Okmen B, Doehlemann G. 2014. Inside plant: biotrophic strategies to modulate host immunity and metabolism. *Current Opinion in Plant Biology* 20: 19–25.
- Oome S, Raaymakers TM, Cabral A, Samwel S, Böhm H, Albert I, Nürnberger T, Van den Ackerveken G. 2014. Nep1-like proteins from three kingdoms of

- life act as a microbe-associated molecular pattern in Arabidopsis. *Proceedings of the National Academy of Sciences, USA* 111: 16955–16960.
- Oome S, Van den Ackerveken G. 2014. Comparative and functional analysis of the widely occurring family of Nep1-like proteins. *Molecular Plant–Microbe Interactions* 27: 1–51.
- Ottmann C, Luberacki B, Küfner I, Koch W, Brunner F, Weyand M, Mattinen L, Pirhonen M, Anderlüh G, Seitz HU *et al.* 2009. A common toxin fold mediates microbial attack and plant defense. *Proceedings of the National Academy of Sciences, USA* 106: 10359–10364.
- Patron N, Orzaez D, Marillonnet S, Warzecha H, Matthewman C, Youles M, Raitskin O, Leveau A, Farre G, Rogers C *et al.* 2015. Standards for plant synthetic biology: a common syntax for exchange of DNA parts. *New Phytologist* 208: 13–19.
- Pertea M, Kim D, Pertea GM, Leek JT, Salzberg SL. 2016. Transcript-level expression analysis of RNA-seq experiments with HISAT, StringTie and Ballgown. *Nature Protocols* 11: 1650–1667.
- Qutob D, Kamoun S, Gijzen M. 2002. Expression of a *Phytophthora sojae* necrosis-inducing protein occurs during transition from biotrophy to necrotrophy. *The Plant Journal* 32: 361–373.
- Rabe F, Bosch J, Stirnberg A, Guse T, Bauer L, Seitner D, Rabanal FA, Czedik-Eysenberg A, Uhse S, Bindics J *et al.* 2016. A complete toolset for the study of *Ustilago bromivora* and *Brachypodium* sp. as a fungal-temperate grass pathosystem. *eLife* 5: 1–35.
- Raffaele S, Kamoun S. 2012. Genome evolution in filamentous plant pathogens: why bigger can be better. *Nature Reviews Microbiology* 10: 417–430.
- Redkar A, Hosler R, Schilling L, Zechmann B, Krzymowska M, Walbot V, Doehlemann G. 2015. A secreted effector protein of *Ustilago maydis* guides maize leaf cells to form tumors. *Plant Cell* 27: 1332–1351.
- Roberts A, Trapnell C, Donaghy J, Rinn JL, Pachter L. 2011. Improving RNA-Seq expression estimates by correcting for fragment bias. *Genome Biology* 12: R22.
- Robinson MD, McCarthy DJ, Smyth GK. 2009. edgeR: a Bioconductor package for differential expression analysis of digital gene expression data. *Bioinformatics* 26: 139–140.
- Rodriguez RJ, White JF, Arnold AE, Redman RS. 2009. Fungal endophytes: diversity and functional roles. *New Phytologist* 182: 314–330.
- Ryals J, Weymann K, Lawton K, Friedrich L, Ellis D, Steiner HY, Johnson J, Delaney TP, Jesse T, Vos P *et al.* 1997. The Arabidopsis NIM1 protein shows homology to the mammalian transcription factor inhibitor 1 kappa B. *Plant Cell* 9: 425–439.
- Santhanam P, van Esse HP, Albert I, Faino L, Nürnberger T, Thomma BPHJ. 2012. Evidence for functional diversification within a fungal NEP1-like protein family. *Molecular Plant–Microbe Interactions* 26: 278–286.
- Schipper K. 2009. *Charakterisierung eines Ustilago maydis Genclusters, das für drei neuartige sekretierte Effektoren kodiert*. PhD thesis, Philipps-Universität Marburg, Marburg, Germany. 1–160.
- Schirawski J, Mannhaupt G, Münch K, Brefort T, Schipper K, Doehlemann G, Di Stasio M, Rössel N, Mendoza-Mendoza A, Pester D *et al.* 2010. Pathogenicity determinants in smut fungi revealed by genome comparison. *Science* 330: 1546–1548.
- Schouten A, van Baarlen P, van Kan JAL. 2007. Phytoxic Nep1-like proteins from the necrotrophic fungus *Botrytis cinerea* associate with membranes and the nucleus of plant cells. *New Phytologist* 177: 493–505.
- Schulz B, Boyle C. 2005. The endophytic continuum. *Mycological Research* 109: 661–686.
- Seitner D, Uhse S, Gallei M, Djamei A. 2018. The core effector Cce1 is required for early infection of maize by *Ustilago maydis*. *Molecular Plant Pathology* 19: 2277–2287.
- Serrano M, Wang B, Aryal B, Garcion C, Abou-Mansour E, Heck S, Geisler M, Mauch F, Nawrath C, Metraux J-P. 2013. Export of salicylic acid from the chloroplast requires the multidrug and toxin extrusion-like transporter EDS5. *Plant Physiology* 162: 1815–1821.
- Sharma R, Xia X, Riess K, Bauer R, Thines M. 2015. Comparative genomics including the early-diverging smut fungus *Ceramosorus bombacis* reveals signatures of parallel evolution within plant and animal pathogens of fungi and oomycetes. *Genome Biology and Evolution* 7: 2781–2798.
- Shimada TL, Shimada T, Hara-Nishimura I. 2010. A rapid and non-destructive screenable marker, FAST, for identifying transformed seeds of *Arabidopsis thaliana*. *The Plant Journal* 61: 519–528.
- Simão FA, Waterhouse RM, Ioannidis P, Kriventseva EV, Zdobnov EM. 2015. BUSCO: assessing genome assembly and annotation completeness with single-copy orthologs. *Bioinformatics* 31: 3210–3212.
- Smith-Unna R, Boursnell C, Patro R, Hibberd JM, Kelly S. 2016. TransRate: reference-free quality assessment of *de novo* transcriptome assemblies. *Genome Research* 26: 1134–1144.
- Sohn KH, Lei R, Nemri A, Jones JDG. 2007. The Downy Mildew effector proteins ATR1 and ATR13 promote disease susceptibility in *Arabidopsis thaliana*. *Plant Cell* 19: 4077–4090.
- Song L, Florea L. 2015. Rcorrector: efficient and accurate error correction for Illumina RNA-seq reads. *GigaScience* 4: 1–8.
- Stanke M, Morgenstern B. 2005. AUGUSTUS: a web server for gene prediction in eukaryotes that allows user-defined constraints. *Nucleic Acids Research* 33: 465–467.
- Stockenhuber R, Zoller S, Shimizu-inatsugi R, Gugerli F. 2015. Efficient detection of novel nuclear markers for Brassicaceae by transcriptome sequencing. *PLoS ONE* 10: e0128181.
- Supek F, Bošnjak M, Škunca N, Šmuc T. 2011. Revigo summarizes and visualizes long lists of gene ontology terms. *PLoS ONE* 6: e21800.
- Teichmann B, Labbé C, Lefebvre F, Bölker M, Linne U, Bélanger RR. 2011. Identification of a biosynthesis gene cluster for flocculosin a cellobiose lipid produced by the biocontrol agent *Pseudozyma flocculosa*. *Molecular Microbiology* 79: 1483–1495.
- Teichmann B, Linne U, Hewald S, Marahiel MA, Bölker M. 2007. A biosynthetic gene cluster for a secreted cellobiose lipid with antifungal activity from *Ustilago maydis*. *Molecular Microbiology* 66: 525–533.
- Tempel S. 2012. Using and understanding RepeatMasker. *Methods in Molecular Biology* 859: 29–51.
- Thalhammer A, Bryant G, Sulpice R, Hinch DK. 2014. Disordered cold regulated 15 proteins protect chloroplast membranes during freezing through binding and folding, but do not stabilize chloroplast enzymes *in vivo*. *Plant Physiology* 166: 190–201.
- Thomma BPHJ, Eggermont K, Penninckx IAMA, Mauch-Mani B, Vogelsang R, Cammue BPA, Broekaert WF. 1998. Separate jasmonate-dependent and salicylate-dependent defense-response pathways in Arabidopsis are essential for resistance to distinct microbial pathogens. *Proceedings of the National Academy of Sciences, USA* 95: 15107–15111.
- Tsuda K, Somssich IE. 2015. Transcriptional networks in plant immunity. *New Phytologist* 206: 932–947.
- Urban M, Kahmann R, Bölker M. 1996. Identification of the pheromone response element in *Ustilago maydis*. *Molecular and General Genetics* 251: 31–37.
- Vanky K, Lutz M, Bauer R. 2008. About the genus *Thecaphora* (Glomosporiaceae) and its new synonyms. *Mycological Progress* 7: 31–39.
- Vie AK, Najafi J, Winge P, Cattan E, Wrzaczek M, Kangasjärvi J, Miller G, Brembu T, Bones AM. 2017. The IDA-LIKE peptides IDL6 and IDL7 are negative modulators of stress responses in *Arabidopsis thaliana*. *Journal of Experimental Botany* 68: 3557–3571.
- Wagner S, Stuttmann J, Rietz S, Guerois R, Brunstein E, Bautor J, Niefind K, Parker JE. 2013. Structural basis for signaling by exclusive EDS1 heteromeric complexes with SAG101 or PAD4 in plant innate immunity. *Cell Host & Microbe* 14: 619–630.
- Walker BJ, Abeel T, Shea T, Priest M, Abouelliel A, Sakthikumar S, Cuomo CA, Zeng Q, Wortman J, Young SK *et al.* 2014. Pilon: an integrated tool for comprehensive microbial variant detection and genome assembly improvement. *PLoS ONE* 9: e112963.
- Weber T, Blin K, Duddela S, Krug D, Kim HU, Bruccoleri R, Lee SY, Fischbach MA, Müller R, Wohlleben W *et al.* 2015. antiSMASH 3.0 – a comprehensive resource for the genome mining of biosynthetic gene clusters. *Nucleic Acids Research* 43: 1–7.
- Wu Y, Zhang D, Chu JY, Boyle P, Wang Y, Brindle ID, De Luca V, Després C. 2012. The Arabidopsis NPR1 protein is a receptor for the plant defense hormone salicylic acid. *Cell Reports* 1: 639–647.

- Yin Y, Mao X, Yang J, Chen X, Mao F, Xu Y. 2012. dbCAN: a web resource for automated carbohydrate-active enzyme annotation. *Nucleic Acids Research* 40: W445–W451.
- Zhang Z, Feechan A, Pedersen C, Newman MA, Qiu JL, Olesen KL, Thordal-Christensen H. 2007. A SNARE-protein has opposing functions in penetration resistance and defence signalling pathways. *The Plant Journal* 49: 302–312.
- Zipfel C. 2014. Plant pattern-recognition receptors. *Trends in Immunology* 35: 345–351.
- Zuo W, Chao Q, Zhang N, Ye J, Tan G, Li B, Xing Y, Zhang B, Liu H, Fengler KA *et al.* 2014. A maize wall-associated kinase confers quantitative resistance to head smut. *Nature Genetics* 47: 151–157.

Supporting Information

Additional Supporting Information may be found online in the Supporting Information section at the end of the article:

Fig. S1 Map of the mitochondrial genome of *T. thlaspeos* strain LF1.

Fig. S2 The mating type locus *a* of *T. thlaspeos*.

Fig. S3 Genome to genome alignments between *T. thlaspeos* and other Ustilaginomycotina species.

Fig. S4 *T. thlaspeos* unique effector THTG_04398 is absent in strain LF2 and in isolates from Hohe Leite, Germany, while present in LF1.

Fig. S5 Principal component analysis (PCA) for the fungal RNA samples collected during axenic culture and infection of *Ar. hirsuta*.

Fig. S6 Transgenic *A. thaliana* lines used in this study accumulate mRNA of each respective effector.

Table S1 Datasets used in this study.

Table S2 Scaffolds with telomeric repeats.

Table S3 BUSCO analysis of the genomic assembly and annotation for the genomes of LF1 and LF2.

Table S4 Functional annotation of the LF1 predicted proteome.

Table S5 List of secreted proteins of *T. thlaspeos* LF1.

Table S6 Count of predicted secreted proteins of other smut fungi species.

Table S7 Number of carbohydrate-active enzyme coding genes in several smut fungi genomes including *T. thlaspeos*.

Table S8 Genes related to secondary metabolism in *T. thlaspeos*, *U. maydis* and *A. flocculosa* as predicted by ANTI-SMASH 4.0.2.

Table S9 Repetitive content of the *T. thlaspeos* LF1 genome.

Table S10 *U. maydis* genes involved in mating and their putative orthologues in *T. thlaspeos*.

Table S11 Whole-genome alignments between *T. thlaspeos* LF1 and other Ustilaginomycotina species.

Table S12 Orthologue genes to *U. maydis* known effector clusters and effectors.

Table S13 Orthology analysis between the *T. thlaspeos* LF1 and 20 Ustilaginomycotina proteomes.

Table S14 *T. thlaspeos* LF1 genes with no homologues to other smut fungi.

Table S15 Summary of differences between the genomes of *T. thlaspeos* LF1 and LF2.

Table S16 *T. thlaspeos* gene models with no hits in the genomic assembly of the opposite isolate.

Table S17 DESEQ2 analysis of the fungal transcriptome during infection of *Ar. hirsuta* with *T. thlaspeos* spores.

Table S18 Fungal genes upregulated during infection of *Ar. hirsuta* with *T. thlaspeos* spores.

Table S19 DESEQ2 analysis of the plant transcriptome of Tue1-expressing *A. thaliana*.

Table S20 Transcriptome analysis of *Ar. hirsuta* plants infected with *T. thlaspeos* spores.

Please note: Wiley Blackwell are not responsible for the content or functionality of any Supporting Information supplied by the authors. Any queries (other than missing material) should be directed to the *New Phytologist* Central Office.

Results

5. Functional characterization of nuclear localized effectors

5.1 Results

5.1.1 Inventory of *T. thlaspeos* NLS effectors

Modulation and reprogramming of host nuclear processes by interacting fungi is a prevalent mechanism for their survival. The discovery and functional validation of nuclear localized effectors was accomplished via a series of experiments, starting with the identification of nuclear-targeted effector proteins. Presence of a predicted nuclear localization sequence (NLS) was my starting point for selecting putative effector candidates.

Identification of 51 secretory proteins has set the foundation for specific characterization of effectors. Eleven candidates were excluded due to presence of known functional domains and remaining 40 genes were considered as potential effector candidates (Courville et al., 2019). Conservation analysis in smut fungi showed 19 *Thecaphora*-unique effector (Tue), 9 conserved effectors of *T. thlaspeos* and its closest homolog *A. floculosa* (Tae), and 12 conserved effectors among *Thecaphora* and smut fungi (Cep). After translocation into host cells, effectors localize to different subcellular compartments and interact with host molecules (see introduction section 1.6.2).

I started my project by predicting nuclear localization signals (NLS) in the 40 effector candidates in three different online prediction tools, Localizer (Sperschneider et al., 2017), cNLSmapper (Kosugi et al., 2009), and NLStradamus (Nguyen Ba et al., 2009). Since protein prediction programs have a certain degree of uncertainty, it was decided that confirmation of the same NLS by at least two programs was required to more accurately identify the NLS within the effector sequence. From these 7 effectors, presence of NLS sequence was confirmed by all 3 programs for 6 effector candidates while *TtTue1* had the NLS identified by two programs: Localizer and cNLSmapper. The NLS is depicted by the green box, and has a different amino acid sequence for each effector candidate (Fig. 5-1).

An overall comparison of NLS prediction was done in total 355 secreted proteins of *T. thlaspeos* and 41 candidates were identified that carried predicted NLS (11 % as opposed to 18 % in the effector candidates), so there is no clear enrichment, but a comparison to all proteins would be interesting. A similar pipeline was used in Ökmen et al by analyzing a transcriptome data of barley leaves infected by *U. hordeii*, ended up with 21 nuclear localized effectors out of 273 upregulated secreted proteins (Ökmen et al., 2018).

The NLS sequences were checked and compared for *U. maydis* homologs of conserved effectors Cep3 and Cep5. *UmCep3* had very short (1 amino acid) NLS sequence while *UmCep5* didn't show any NLS sequence at all which might give hint towards specificity of NLS sequences in conserved effectors of *T. thlaspeos*.

Since all 7 effector candidates have both the signal peptide and the NLS sequence, it is highly likely that they all exit *T. thlaspeos* and localize to the nucleus once they enter the host plant cells. In order to further characterize and prioritize to most promising effector candidates the following experimental strategy was designed: 1. verification of nuclear localization 2. Investigation of virulence activity 3. Analysis of growth phenotype.

Results

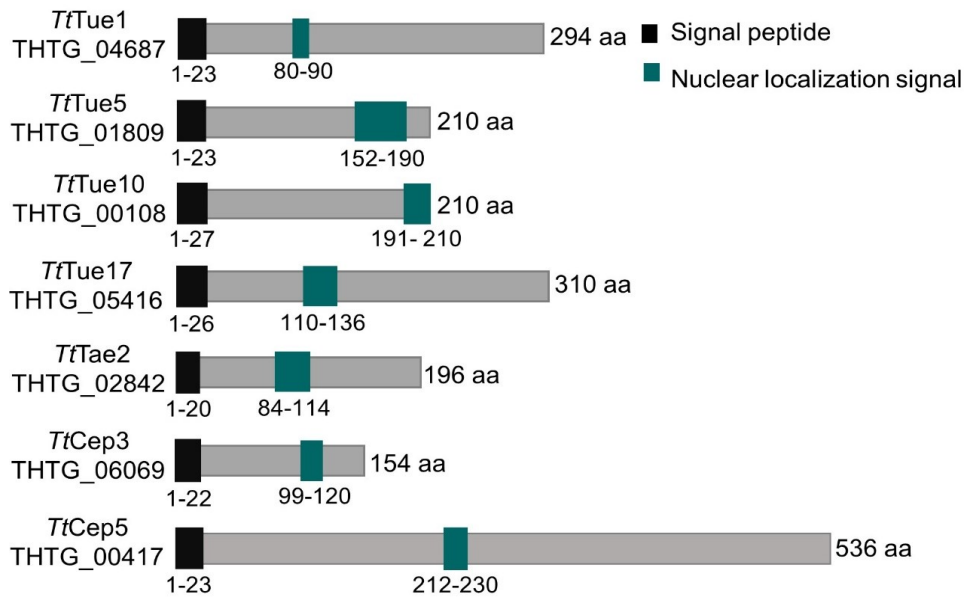


Fig 5-1. Gene models of predicted seven nuclear localized effector candidates. Nuclear localization signals were predicted by three different programs: Localizer (Sperschneider et al., 2017), cNLSmapper (Kosugi et al., 2009) and NLStradamus (Nguyen Ba et al., 2009). Green box denotes Nuclear localization signals. SMART (SignalP) (Nielsen et al., 1997) was used to predict the signal peptide which is denoted by black box. Five candidates were predicted to have similar NLS in all three programs while two carry the same signals in at least two programs. The amino acids positions of respective signals are denoted by their numbers.

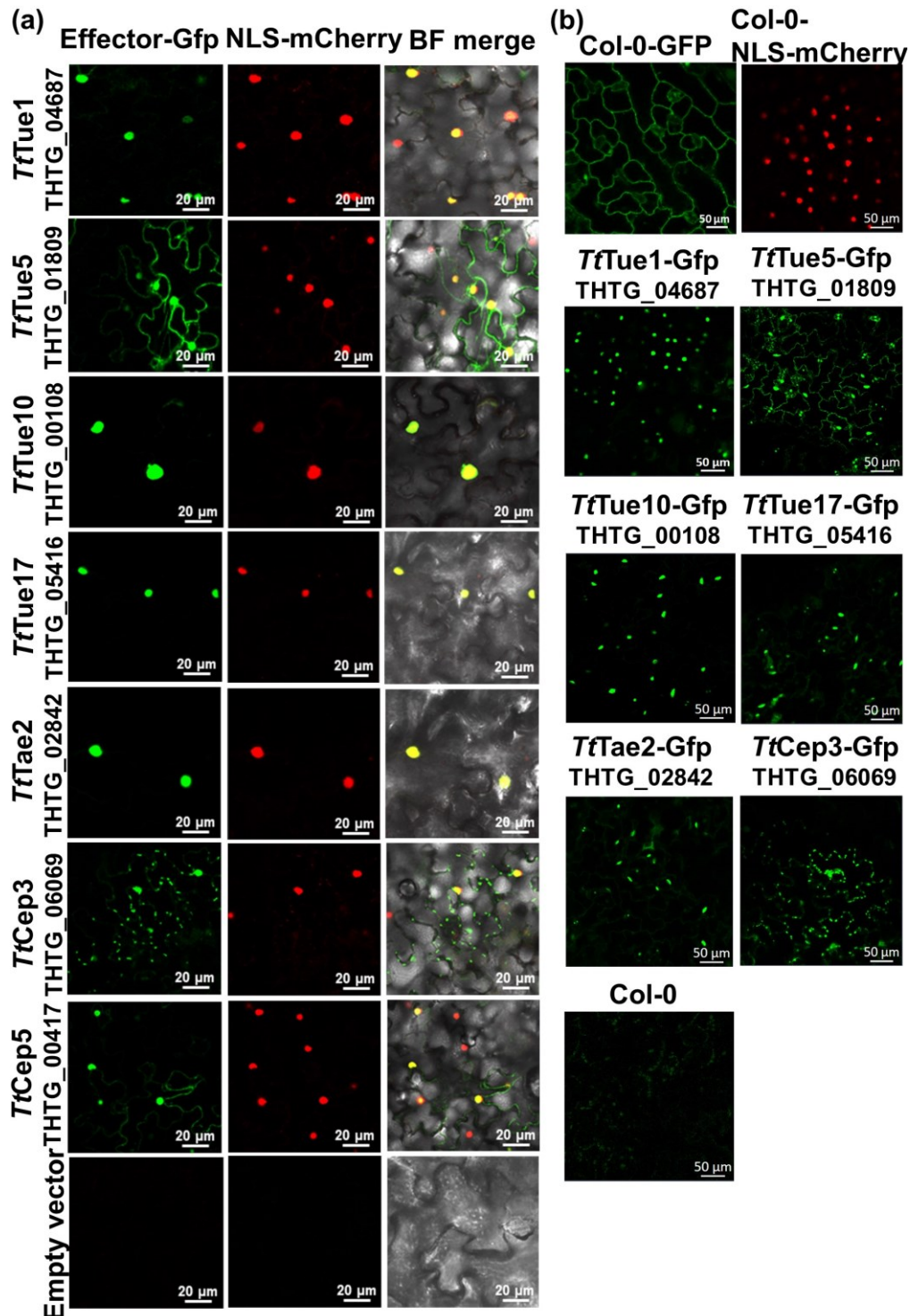
5.1.2 Effectors candidates are targeted to the nuclei of the plant cells in both stably transformed *A. thaliana* and in a heterologous expression system

To verify the accumulation of my selected seven effector candidates in the host plant nucleus, the predicted nuclear localization of *TtTue1*, *TtTue5*, *TtTue10*, *TtTue17*, *TtTae2*, *TtCep3* and *TtCep5* was experimentally tested by *Agrobacterium*-mediated transient expression in *N. benthamiana*. All effector candidates were expressed under the control of the 35S promoter without a signal peptide and were visualized by fusion with the green fluorescent protein (Gfp), which results in green fluorescence at the location within the cell where the effector accumulated. An NLS sequence (Lampropoulos et al., 2013) was tagged with mCherry to use as a nuclear marker. Confocal laser scanning microscopy showed that *TtTue1*, *TtTue10*, *TtTue17*, *TtTae2*, are exclusively localized to the nucleus and clearly co-localized with my nuclear marker. *TtTue10* and *TtTae2* show specific and distinct accumulation in the nucleolus as well, while *TtTue1* has clear exclusion of signal from the nucleolus (Fig. 5-3a). On other hand *TtTue5*, *TtCep3* and *TtCep5* were partially localized to the nucleus, having the co-localization signals with nuclear marker. However, all three candidates also showed distinct fluorescence outside the nucleus. *TtTue5* and *TtCep5* show fluorescence that is likely localized to the cytoplasm, whilst *TtCep3* shows strong fluorescence that appears to localize to the chloroplasts. Control plant infiltrated by *Agrobacterium* strain carrying empty destination vector didn't show any fluorescence signals. I conclude that all seven effector candidates localized to the nucleus, confirming the presence of an NLS, only that *TtTue1*, *TtTue10*, *TtTue17*, *TtTae2* exhibit exclusive accumulation to the nucleus (Fig. 5-2a).

Nuclear localization of six NLS effectors except *TtCep5* was verified by stable expression of Gfp-fusion proteins in *A. thaliana* Col-0. Transgenic lines for *TtCep5* were not obtained in three

Results

independent transformations, which might be due to lethal effect of overexpression of *TtCep5* on the host plant. Free Gfp and NLS-mCherry lines were generated as a controls. All effectors have shown similar pattern of localization as in the transient expression system. *TtTue1*, *TtTue10*, *TtTue17*, *TtTae2* have the exclusive nuclear localization. In addition to nuclear localization, *TtTue5* and *TtCep3* have cytoplasmic and chloroplast accumulation, respectively (Fig. 5-2b). Furthermore, fluorescence microscopy images of transgenic lines showed more protein accumulation pattern in stable lines in comparison to transient expression. Thus, it was confirmed in two independent systems that four effectors are localized to the host plant nucleus solely while three effectors have dual localization pattern.



Results

Fig 5-2. Predicted NLS effector candidates are localized to the nucleus. (a) Selected effectors were visualized by fusion with Gfp in the transient expression in *N. benthamiana*. Left panel shows localization of effectors within the cell at 3 days post infiltration. Red fluorescence in the middle panel shows the location of the nucleus, visualized by a NLS (At4g19150/N7 nuclear localization signal) (Lampropoulos et al., 2013) marker fused to mCherry. The right panel show overlay of the effector localization with the nuclear marker. Yellow spots indicated co-localization of effectors with NLS marker, showing effector localization to the nucleus. Infiltration with an empty vector was included as a negative control. Four effector candidates localize solely in the nucleus, while the other three show dual localization signal in other organelles as well. (b) Subcellular localization of six effector candidates in transgenic lines. Microscopic analysis of the stable lines confirmed the localization of all effector candidates. *TtTue1*, *TtTue10*, *TtTue17* and *TtTae2* were verified the exclusive localization of the protein to the nucleus while rest of the two effectors *TtTue5* and *TtCep3* also showed the dual localization pattern in cytoplasm and chloroplast, respectively, in addition to nuclear localization. Transgenic lines showed consistent results and verified the outcome of transient expression. Effector candidates were visualized by fusion with GFP, and green fluorescence shows effector localization within the cell. Col-0, Free GFP and NLS (At4g19150/N7 nuclear localization signal) fused with mCherry were used as control.

5.3 Predicted NLS sequence is responsible for both nuclear and nucleolar localization of effectors.

To verify that predicted NLS is require for accumulation of protein in the nucleus, an NLS deletion experiment was performed by using transient expression system in *N. benthamiana*. The NLS candidates were selected for this experiment on the basis of their role in promoting virulence (Fig. 5-4) and their exclusive localization in the nucleus (Fig.5-2). *TtTue1*, *TtTue10* and *TtTae2* were shortlisted for testing the requirement of predicted NLS for their nuclear accumulation. These three candidates localize solely to the nucleus (Fig. 5-2, 5-3). Additionally, Gfp signal was also detected in the plant nucleolus for *TtTue10* and *TtTae2* while the signal was completely excluded from nucleolus for plant expressing *TtTue1* (Fig. 5-3a). The NLS sequences of *TtTue1* (80-90 aa) *TtTue10* (191-210 aa) and *TtTae2* (84-114 aa) were deleted in the Gfp constructs. The localization of these truncated proteins was then compared to wild type proteins. Transient expression in *N. benthamiana* showed that, upon NLS deletion, *TtTue1* did not localize to the nucleus, and instead appears to localized mainly in the cytoplasm, while *TtTue10* and *TtTae2* still mainly localized to the nucleus. However, the signal was completely excluded from nucleolus. Additionally, weak fluorescence signal was detected in the cytoplasm for *TtTue10*, indicating that localization might disrupt severely for *TtTue10* then *TtTae2* in the absence of NLS. A similar study showed exclusion of fluorescence signal from the nucleolus upon NLS deletion for the effector Mlp124478 from the poplar leaf rust fungus (Ahmed et al., 2018). Mlp124478 has role in suppression of defense responsive genes via DNA binding and modulating the transcription machinery.

Out of the three effector candidates showing significant virulence activity and nuclear localization, only *TtTue1* showed complete elimination of nuclear localization when the NLS was deleted. Plant infiltrated with the empty plasmid didn't show any florescence signal. However, variations in the signal accumulation pattern with in different effectors confirm the true Gfp signal (Fig. 5-3a). Anti-Gfp immunoblotting for proteins extracted from all three candidates with both intact and deleted NLS version and free GFP control revealed the bands signal at the expected size. This indicated the accumulation of full length protein in the plant cell upon NLS deletion which might not disturb the protein confirmation (Fig. 5-3b).

Results

These results suggest that predicted nuclear signal is responsible for nuclear localization of *TtTue1*, while it is required only for nucleolar localization of *TtTue10* and *TtTae2* and might have functional redundancy for nuclear accumulation.

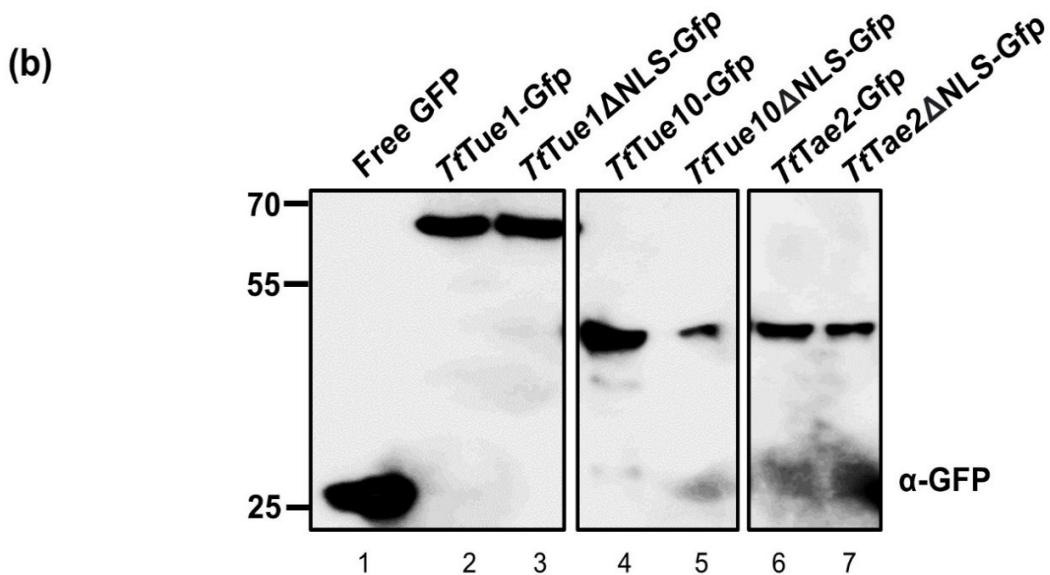
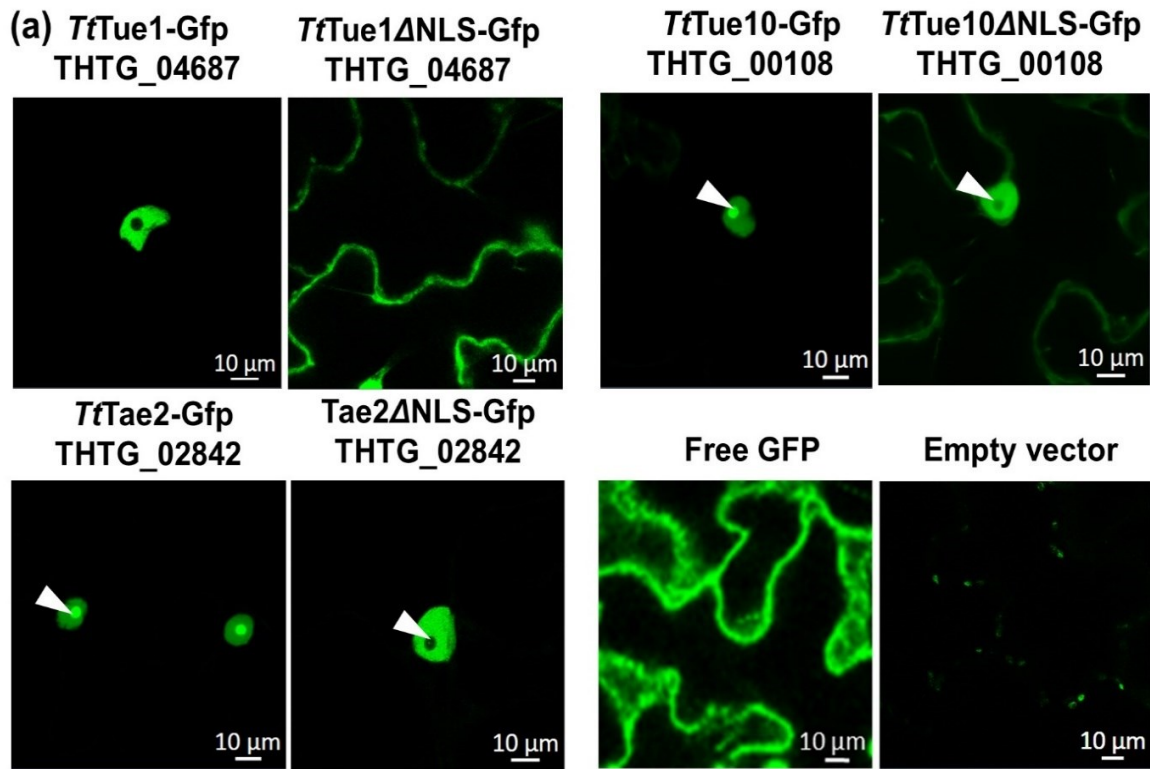


Fig 5-3. NLS signal is responsible for nuclear and nucleolar accumulation of effectors.
 (a) *TtTue1*, *TtTue10*, *TtTae2* were fused with C terminal Gfp. For each effector candidate, the image on the left shows the full-length effector localization, and the image on the right shows the effector localization of NLS deletions. White arrow heads indicate the position of the nucleolus within the nucleus.

Results

Infiltration with an empty vector that did not contain an effector candidate was included as a negative control. NLS deletion in case of *TtTue1* cause exclusion of signal from nucleus completely and instead changed its localization to cytosol. Nuclear localization of *TtTue10* and *TtTae2* were not abolished completely by NLS deletion. Fluorescence signal was still present in nucleus but it was completely excluded from nucleolus in both *TtTue10* and *TtTae2*. (b) Immunoblot analysis of both full-length and NLS deleted version of effectors. Expected sizes for effector candidates are as follows: free GFP 27 KDa (Lane 1), *TtTue1*-Gfp 59.8 kDa (Lane 2), *TtTue1* of Δ NLS-Gfp 58.7 KDa (Lane 3), *TtTue10*-Gfp 50 KDa (Lane 4), *TtTue10* Δ NLS -Gfp 48.1 KDa (Lane 5), *TtTae2*-Gfp 49.5 KDa (Lane 6), *TtTae2* Δ NLS -Gfp 46.5 KDa (Lane 7). Western blot: Anti-GFP

5.4 NLS effectors delivered via *Pst*-LUX enhances bacterial proliferation in *A. thaliana*.

The virulence activity of the effector candidates was examined to see whether nuclear localized effectors have any role in disease progression. Therefore, NLS effectors were translocated to the host cell via a heterologous bacterial delivery system (EDV) (see introduction sec 1.6.1).

The *Pst*-LUX strain containing effector as a fusion protein (without signal peptide) was spray inoculated on to *A. thaliana* Col-0, and luminescence was measured by counting the number of photons produced per second per gram of fresh weight (Fig. 5-4a).

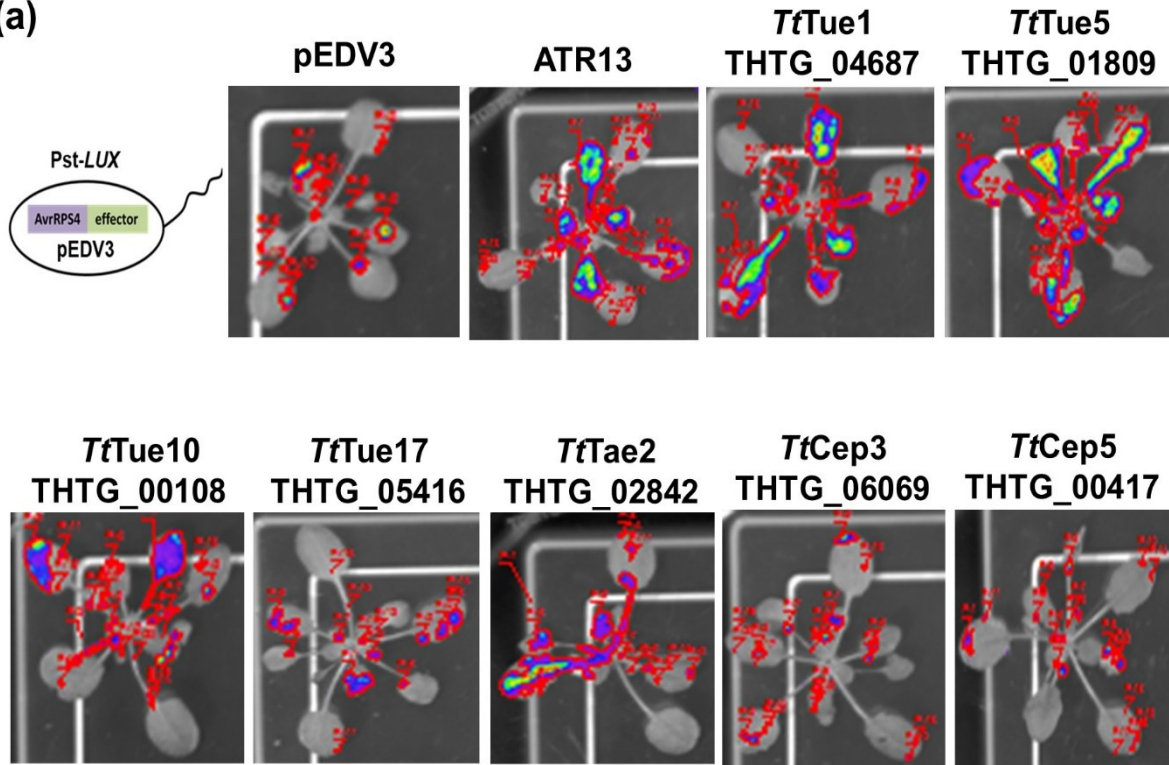
The photon count of the effector candidates was compared against the pEDV3 empty vector control, and the bona fide effector ATR13 from *H. parasitica* as a positive control. Bioluminescence was measured 2 days after spray inoculation and correlated with the number of bacteria (Fabro et al., 2011). ATR13 significantly increased the bacterial count upon delivery to plant cell through EDV system.

A significant impact on proliferation of *Pst*-LUX strain was observed in presence of *TtTue1*, *TtTue5*, *TtTue10* and *TtTae2* indicating they have conserved virulence activity. *TtTue1* and *TtTue5* have more pronounced effect on bacterial proliferation which was shown by high photon counts. Previously, the effect of *TtTue1* and 5 other effectors on virulence activity were measured by infecting their overexpression lines (Courville et al., 2019). Enhanced bacterial growth of *Pst*-LUX containing *TtTue1* in EDV system was comparable to the high bacterial count of *TtTue1* transgenic lines infected with wild type *Pst*-LUX while rest of the 5 transgenic lines expressing effector candidates did not have any effect on bacterial proliferation. However, these 5 transgenic lines expressing effectors did not have a predicted NLS sequence (Courville et al., 2019). Since the microscopic analysis of *TtTue1*-Gfp transgenic line showed a high expression of the fusion protein, the *TtTue1* line without a tag probably has the same level of expression and could cause the pleiotropic effects. This data showed that *TtTue1* positively influences virulence regardless of the virulence detection system.

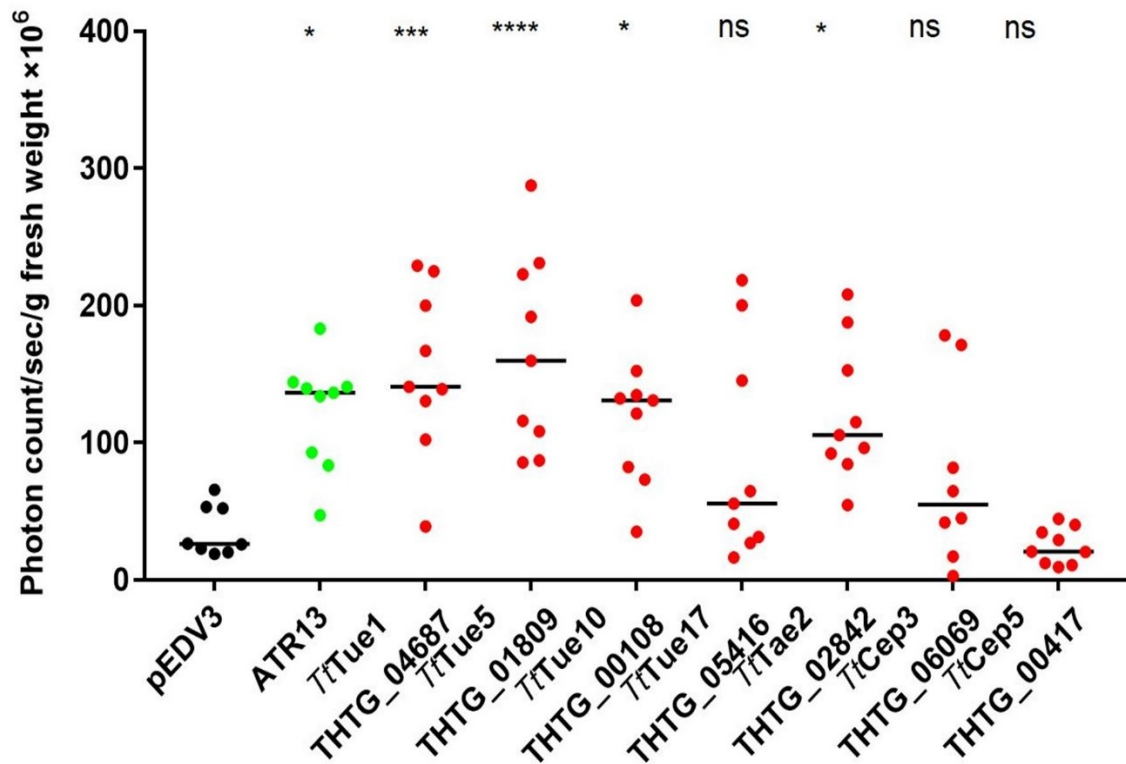
TtTue17, *TtCep3* and *TtCep5* did not contribute to bacterial proliferation in comparison to the control and other candidates. Out of the 7 effector candidates, only *TtTue1*, *TtTue5*, *TtTue10* and *TtTae2* showed high virulence activity, indicating that they are able to promote bacterial infection (Fig. 5-4b).

Results

(a)



(b)



Results

Fig 5-4. Virulence activity of effector candidates (a) Inoculation of *A. thaliana* with *Pst*-LUX strain containing the effector candidate fused N-terminally with AvrRps4, resulting in bioluminescence signals detected due to luciferase activity of *Pst*-LUX. Images were taken at the photon counting chamber NightOwl (LB983NC100U, Berthold). Plant images visualize the location and intensity of luminescence. (b) Extent of effector virulence measured by counting the number of photons produced per second by the *Pst*-LUX vector system. pEDV3 empty vector is a negative control and ATR13 used as a positive control (Fabro et al., 2011). Effector candidates marked by asterisks significantly increased the virulence activity of bacterial strain while non-significant differences are marked by ns and did not have any effect on bacterial proliferation. Statistical analysis was done by one-way ANOVA (Bonferroni's post test) * $P < 0.05$, *** $P < 0.001$, **** $P < 0.0001$, ns=not significant. Experiment was repeated for three biological replicates.

5.5 Expression of *TtTue1*-Gfp in *A. thaliana* results in pronounced phenotypes in both early and late growth phases.

To examine the effect of NLS effectors on developmental phenotype of plants, they were stably expressed in *A. thaliana*. Verification of nuclear localization of effectors in these transgenic line was described in section 5.2. Transgenic lines were generated by expressing all Gfp-tagged NLS effectors except *TtCep5* under the control of the 35S promoter. There were no single transformants received for *TtCep5* in three independent transformation attempts. Interestingly six transgenic lines of effectors exhibited a distinct growth phenotype in comparison to the control lines observed in four-week-old plants (Fig. 5-5a).

The plant transformed with the NLS-mCherry and free GFP did not show any growth difference to the wild type, whilst the *TtTue1*-Gfp line exhibits a clear dwarf phenotype, their rosette size of four weeks old plants was significantly smaller than controls and other effectors lines. It has been shown previously that *TtTue1* without a Gfp tag also possesses a similar dwarf phenotype (Courville et al., 2019) which suggests that the Gfp-fusion is not interfering with effector function. Also, the primary leaves showed clear symptoms of chlorosis, indicated by arrowhead (Fig. 5-5a). This result clearly indicates that *TtTue1* altered the growth and development of the plants. In addition, the plant expressing *TtTue5*-Gfp, *TtTue10*-Gfp, *TtTue17*-Gfp, *TtTae2*-Gfp, and *TtCep3*-Gfp appear to have a slightly smaller rosette. This reduction in the growth also have a significant difference from the wild type but not that obvious as showed by *TtTue1*-Gfp. Microscopy data has verified the protein expression and shown that all six effectors were expressed in *A. thaliana* (Fig. 5-2b).

In addition, the phenotype in the generative growth phase of *A. thaliana* was also observed in transgenic plants. All lines expressing effector candidates including NLS-mCherry and free GFP controls have grown for three months under normal dark and light conditions. Each line expressing effector candidates has produced flowers and siliques in the normal life span of *A. thaliana* which is comparable to controls, except the *TtTue1*-Gfp line, which did not have shoot formation and the rosette size was also small (Fig. 5--5c). *TtTue1* interfered with the whole developmental process of the plant and delayed the plant's life cycle. It has been observed that after more than four months the plant forms a small shoot with less number of siliques. Overall phenotype analysis showed that *TtTue1* severely affected both the vegetative and generative growth phases of plants.

Verification of nuclear localization, virulence activity and specially a noticeable growth phenotype set the basis for selection of *TtTue1* as a top candidate for further characterization. To assess the molecular function of *TtTue1*, several aspects of its possible function were

Results

covered which includes their translocation to the host plant, finding plant interaction partners, analyze the DNA-binding activity and characterization of the deletion mutant. Unfortunately, some experiments could not be completed with success or with an expected outcome.

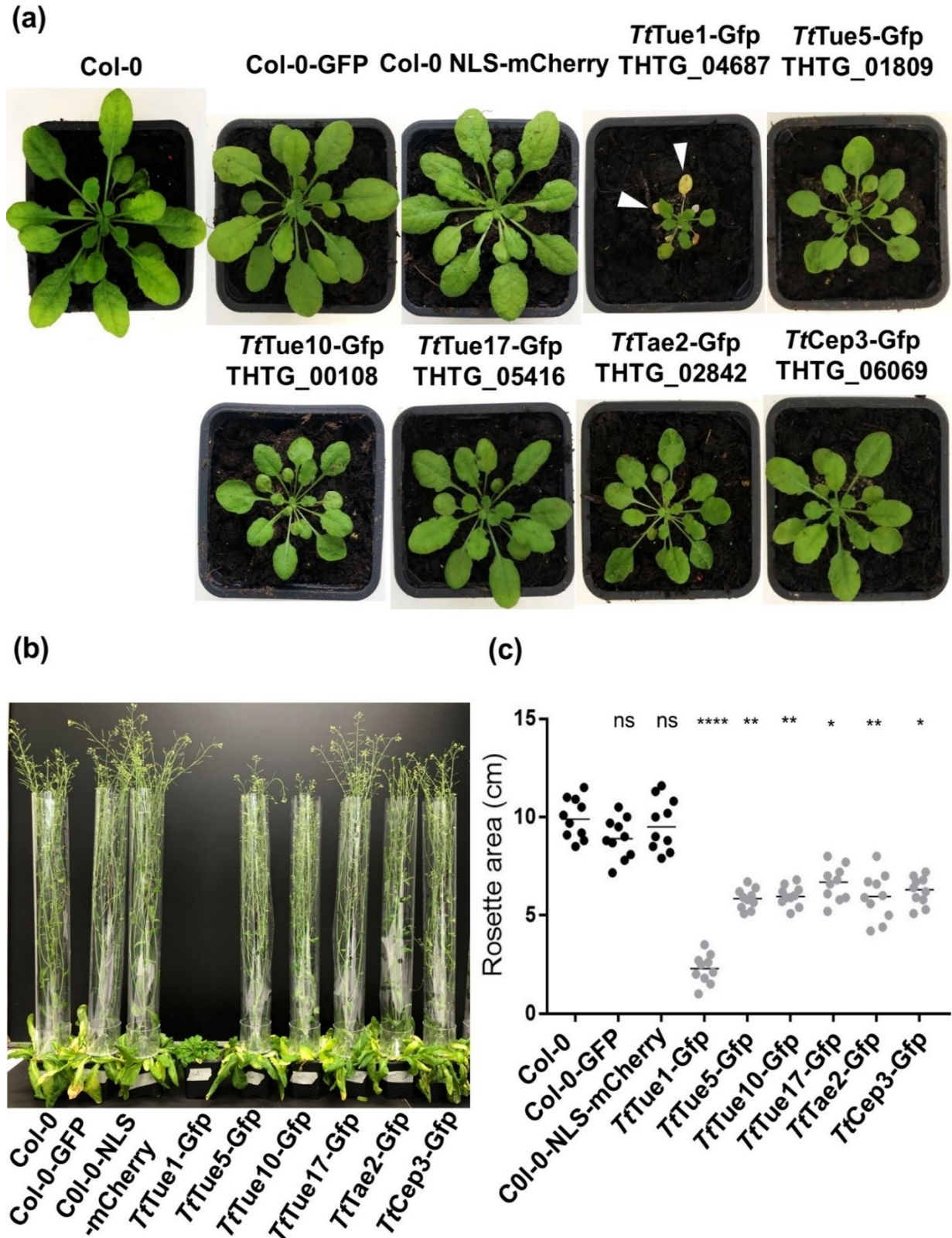


Fig 5-5. Expression of *TtTue1* severely affects the vegetative and generative growth phase of *A. thaliana* (a) Phenotype of four weeks old plants. *A. thaliana* constitutively expressed effector candidates fused to Gfp, free GFP, or an NLS (At4g19150/N7 nuclear localization signal) marker

Results

fused with a mCherry used as negative controls. All the lines were generated in *col-0* background. The *TtTue1-Gfp* line exhibits a dwarf phenotype, which is consistent with previous result for the line expressing *TtTue1* without a tag (Courville et al., 2019). White arrow heads indicate leaf necrosis on primary leaves. Remaining five effector candidates have slight difference in their rosette size (b) Phenotype of three months old flowering plants. *TtTue1* induced late flowering while other 5 effectors have normal span of life cycle and have produced flowers. There was no obvious difference found with controls (*Col-0*, *Col-0-GFP*, *Col-0-mCherry*) other than *TtTue1* for flowering phase of plant. (c) Measurement of rosette area verified that *TtTue1* has pronounced effect on phenotype while rest of the effectors have slight differences with controls. Black dots: wild type control and lines with integration of fluorescence proteins, grey dots: lines expressing effector proteins. Statistical analysis was done by using one-way ANOVA (Bonferroni's post test) * $P < 0.05$, *** $P < 0.001$, **** $P < 0.0001$, ns=not significant. 10 plants were used as biological replicates for each line.

5.6 Genetic modification of *TtTue1* in *T. thlaspeos*

5.6.1 *TtTue1* deletion strain

To characterize the direct role of *TtTue1* on its natural host *Ar. hirsuta* as well as *A. thaliana*, an attempt was made to generate the *Tttue1* Δ deletion strain by following the *T. thlaspeos* transformation protocol (Plücker et al., 2021). For that purpose, both wild type strains of *T. thlaspeos*, LF1 and LF2, were used as progenitors for genetic transformation. The *Tttue1* Δ deletion construct was generated by a student Anna Wendel in her master thesis (Anna Wendel Master thesis, 2020) by using Golden Gate strategy. In this construct, the hygromycin resistance cassette is flanked by around 1kb upstream and downstream regions of the *Tttue1* coding sequence for homologous recombination. Protoplastation and transformation was done according to (Plücker et al., 2021). There were no transformants found for both FB1 and FB2 backgrounds in any transformation attempt although the protoplasts had regenerated properly in the control plates. A self-replicating plasmid (pUMa 2790) was used as a positive control and there were only few satellite colonies found but no real transformants were obtained. Transformation has been repeated 12 times for both LF1 and LF2 strains without obtaining any transformants. Though the protoplasts were capable of regeneration, they might not be viable enough to take up the plasmid DNA. Therefore, by optimizing the enzyme concentrations and finding a suitable time point of stopping protoplastation reaction for each preparation might help in getting the transformants. An alternate approach could be usage of CRISPR-Cas9 system consist of a guide RNA and Cas9 nuclease. A representative images of transformation plates are shown in (Fig. S1).

5.6.2 Translocation of *TtTue1* to the host plant

To find out whether effectors are secreted from the fungus and translocate into the host plant cell, a GFP strand system was planned to use to directly visualize the effector delivery. This system facilitates the characterization of effectors in the natural infection system, both translocation and localization of effectors in the host plant can be studied. GFP is a beta barrel protein of 11 β -strands and assembly of their complementary fragments use for GFP strand system (Cabantous et al., 2005). In this system GFP strand 11 (here after GFP11, 16 amino acids) is fused C terminally with the effector protein. GFP strands 1-10 (GFP1-10) are expressed separately in the host plant. The two parts can assemble into functional GFP protein upon delivery of the effector into the host cell (Henry et al., 2017). It has been shown for several bacterial effectors e.g *Salmonella* effectors PpB2 and SteA that GFP11 does not interfere with the effector translocation (Van Engelenburg and Palmer, 2010).

Results

TtTue1 fused with the C terminal tagged GFP11 under the control of the native promoter. GFP1-10 was expressed separately in *A. thaliana* and the stable line was obtained from Gitta Coaker (UC Davis) for this study. Before generating *TtTue1*-Gfp11 strains in *T. thlaspeos*, the functionality of *TtTue1*-Gfp11 fusion protein was checked in *Agrobacterium* mediated transient expression system in *N. benthamiana*. *TtTue1*-Gfp11 and GFP1-10 were co-expressed from two different bacterial strains in *N. benthamiana* which resulted in GFP fluorescence signal in the nucleus of the plant, while *TtTue1*-Gfp11 and GFP1-10 alone did not show any fluorescence signal. This result demonstrated that GFP strand system is also functional for *T. thlaspeos* effector and that subcellular localization of *TtTue1* is also consistent with previously found nuclear localization (Fig. S2).

Therefore, *T. thlaspeos* LF1 and LF2 strains were separately transformed with *TtTue1*-Gfp11 construct after verification. Transformation was done according to the same protocol as mentioned in the section 4.6.1. *TtTue1*-Gfp11 construct was flanked by 1kb upstream and downstream sequence of *TtTue1* and it was expected that *TtTue1*-Gfp11 will replace the original copy of *TtTue1* in the fungal genome via homologous recombination. Similar to the transformation for the deletion construct of *TtTue1*, no transformants were obtained for *TtTue1*-Gfp11 construct in 6 independent transformations. There were no transformants found for pUMa 2790 except few satellite colonies which turned into contamination after prolong incubation (Fig. S2).

This data showed that GFP strand system worked for investigating the potential subcellular localization of the fungal effector by expression *in planta* but secretion of *TtTue1* effector could not be confirmed in the natural system.

5.7 *TtTue1* interaction screening by using *A. thaliana* root library

So far, from all effectors that I have characterized for virulence activity, nuclear localization, and most importantly phenotype analysis, *TtTue1* was selected as the most promising candidate for further characterization based on its most significant role in promoting virulence, its sole localization in the host plant nucleus and an obvious effect on the growth of plant.

Since protein-protein interaction plays a vital role in predicting the function of an effector protein, identification of *TtTue1* interaction partners was done by a yeast 2-hybrid screen (Y2H). There were two independent screens performed by using different sources of cDNA library.

1. Iron deficient root cDNA library of *A. thaliana*
2. Biotic and abiotic stress-induced cDNA library of *A. thaliana*

To identify the interaction partner of *TtTue1* in the host plant, a cDNA library from *A. thaliana* was used because *T. thlaspeos* can colonize *A. thaliana* under lab conditions (Frantzeskakis et al., 2017). Secondly, *A. thaliana* is a model system, in which stress response genes have been well characterized. Furthermore, by homology search, we have found that *Ar. hirsuta* has homologs for all of the shortlisted candidates.

The initial screen was performed with the root library because *T. thlaspeos* can infect roots of host plant and show systemic infection, and secondly due to local availability of the library material, while the stress-induce library was received with a big time delay due to restrictions

Results

in SARS-CoV-2 pandemic. The root library was kindly provided by Prof. Dr. Petra Bauer's group working at the department of Botany Heinrich-Heine-University (Lingam et al., 2011). The cDNA library was constructed from 17-day old *A. thaliana* roots mRNA, that were stressed three days before harvesting by limiting the iron amount available (iron deficient conditions) to the plant (Lingam et al., 2011). In this system, conducting the yeast 2-hybrid screen by mating was considered to be more effective, instead of co-transformation.

Since the provided library was stored as a yeast culture at -80 °C for a long time, it was important to first test and validate the experimental conditions to achieve good mating efficiencies. For this reason, several test mating experiments were done with the two control plasmids for the optimization of mating conditions. The observed mating efficiency during the test experiment with the controls murine p53 in AH109 and SV40 T-antigen in Y187 was 7.5 %, resulting in 1.5×10^6 mated cells which meets the requirement of 10^6 cells (according the given efficiency in the Matchmaker manual, Table2, Matchmaker™ GAL4 Two- Hybrid System).

Based on these results, screening with *TtTue1* as a bait against the library was done according to the Lingam protocol with the goal of 10^6 screened mated cells for each screen. Surprisingly, during the three screens, the mating efficiencies was much lower than in the test experiment and the number of mated cells did not reach 10^6 . Hence the screens were not saturated, and it cannot be guaranteed that each library protein was screened for interaction with the bait protein (*TtTue1*). A total of 195 colonies were found on plates selecting for expression of the HIS3 reporter only, which is lower than almost 700 candidates found when the library was freshly screened with another protein under the same conditions previously (Lingam et al., 2011). After transferring the candidates to the plates with the same histidine selection, all candidates exhibited growth, but almost all showed red coloring of varying intensity, suggesting a lack of adenine production in the colonies. The candidates were also transferred to plates for selecting of both *HIS3* and *ADE* reporters. Here only seven candidates showed growth. Sequencing of the extracted plasmid revealed, that four of the seven matched to rRNA sequences from *A. thaliana*. The other three showed 100 % similarity to the genes *TTN5*, *PYK10* and *EIL1* of *A. thaliana*. When the interaction of these candidates was tested by co-transforming of the extracted plasmid with the effector candidate *TtTue1*, none of them showed activation of the reporter genes.

Since the interaction of the candidate plant genes and *TtTue1* could not be verified in three independent co-transformations, it was concluded that the found candidates do not interact with the putative effector *TtTue1*. These negative results raised the question about the quality of this cDNA library. Since the mating efficiency should be independent from the transformed construct, the decade-long storage at -80 most likely had a negative effect on the functional efficacy of the library. Therefore, it was concluded that library source was not good enough to find the true interaction partners of *TtTue1*, and in general it is recommended to avoid the use of this source for further future studies.

Therefore, I moved to the biotic and abiotic stress-induced cDNA library of *A. thaliana*. This library was obtained from the group of Prof. Dr. Maëli Melotto at University of California.

Results

Table. 1 Iron deficient *A. thaliana* root library screen in Y2H system for *TtTue1*

Sr. no	Selection criteria	Number of candidates
1	1st reporter gene <i>His</i>	195
2	Selection for dual reporter genes <i>His, Ade</i>	7
3	Final candidates	3
4	Final verification by co-transformation with <i>TtTue1</i>	0

5.8 *TtTue1* interaction screening identifies potential plant targets by using stress-induced cDNA library

The stress-induced cDNA library of *A. thaliana* is in the LexA system, and was used for the second screen. The library was constructed from mRNA extracted from *A. thaliana* leaves treated with different chemicals and bacterium inoculum (Matiolli and Melotto, 2018).

Matiolli and Melotto, performed quality assessment test of the library by finding a good representation of total and stress-associated transcripts of *Arabidopsis* (Matiolli and Melotto, 2018). The library yield was confirmed by finding 2.8×10^7 primary clones and 95% of the clones contained an average insert size of 1kb. Additionally, validation of the stress induced transcripts was performed by doing a test Y2H screen with JAZ4 (At1g48500) as a bait to find its previously reported interaction partners (Zhang et al., 2017). Re-finding the previously identified targets as well as new interaction partners indicated that the library is a good source of material to use for identification of targets of stress-related proteins (Matiolli and Melotto, 2018).

Reconfirmation of the cDNA library material was done by a few small tests. First, the presence of *A. thaliana* stress-related gene *PR1* and the housekeeping gene encoding Actin (*ACT1*) in the plasmid library were checked by PCR analysis. Amplification of right sizes of genes and the comparable band intensity of *PR1* indicated the presence of stress-induced transcripts in the plasmid library. Next, to validate the backbone of the library, the yeast reporter gene in the prey plasmid (tryptophan) and its upstream and downstream regions were verified by sequencing. In addition, the antibiotic resistance was checked by re-transformation of library in *E. coli* and growing on antibiotic selection media (Ampicillin) (Fig. S3a). It has been verified in all these tests that the correct library material was received for the Y2H screen.

To identify the plant protein targeted by *TtTue1*, its coding sequence lacking the signal peptide was used as a bait and cloned in frame with LexA-DBD in a bait vector pGILDA under the control of GAL1 promotor. A yeast strain EGY48 was co-transformed with a bait plasmid carrying *TtTue1* and a prey plasmid pB42AD without any insert. *TtTue1* did not show any auto-activity upon reporter gene expression analysis (Fig. S3b). To verify the expression of *TtTue1* in yeast, a western blot was done on total protein extracted from yeast. Anti-HA immunoblot analysis confirmed the *TtTue1* expression in yeast with detection of band size of 59 KDa (Fig. 5-7c).

The yeast strain EGY48 expressing *TtTue1* was co-transformed with the aforementioned stress induced cDNA library of *A. thaliana* having a concentration of 10 μ g. Transformants were selected on triple dropout media (-His-Trp-Ura). The calculated transformation efficiency

Results

was 2.4×10^6 which is a good representation of having sufficient transformants to screen for the interaction. Further screening for the selection of the first reporter gene *LEU2* was done on quadruple dropout induction media (-His-Trp-Ura-Leu). Induction media improves the chances of detecting AD fusion proteins which were transiently or weakly expressed in yeast. A mix of 3000 small and big colonies were selected for the first reporter gene. For more stringent selection, selected clones were subjected to further screening for second reporter marker *LacZ* on quadrupledropout induction media containing X-Gal. To eliminate the false positive in the first round of blue-white selection *LacZ* expression was carefully determined based on the intensity of the blue color. All the white colonies were excluded and further dividing them into categories of dark and light blue helped to select the true interactors. Out of 3000 colonies, 1100 were selected with light and dark blue colors. Re-patching of all dark blue color colonies further excluded the colonies which did not accumulate proper blue product in the second round. Therefore, several rounds of selections on dropout and X-Gal media finalized the 160 candidates as potential interaction partners for plasmid isolation and identification.

To identify and amplify the extracted plasmids from yeast, the *E. coli* strain KC8 was transformed. KC8 is a defective *trpC* strain and is used to rescue the prey plasmids by complementing the TRP from yeast (LexA Takara manual PT3040-1). However, 7 candidates isolated from yeast did not transform into KC8 strain. A colony PCR was performed on KC8 transformants by using the primer pairs which were binding in the prey plasmid backbone. This was the second exclusion point of the candidates which 3 candidates did not show any band in the colony PCR.

Hence, after excluding candidates from 160 colonies (no transformants of KC8 strain and negative colony PCR results) 150 candidates have been selected. The most important elimination step was checking the auto-activation of the prey plasmid. Therefore, EGY48 yeast strain was co-transformed with 150 selected candidates and *TtTue1* in a targeted Y2H assay. To check the auto-activity of prey plasmids an empty bait vector was used instead of *TtTue1* for co-transformation. There were 3 auto-active candidates found in the more stringent *LacZ* selection on X-Gal containing media (Fig. S4). Co-transformation of the non-autoactive candidates with *TtTue1* excluded 7 additional candidates as false-positives (Fig. S4). The promoters of reporter genes (*LEU2* and *lacZ*) are different in the sequences that flanking the LexA operator. These differences help in the selection and eliminated many false positive to confirm the positive two-hybrid interactions. The remaining 140 candidates were sequenced, and 129 have proper in-frame sequence with the activation domain (Table. 2). Sequencing analysis and identification have been done by aligning the obtained sequencing with *A. thaliana* genome on TAIR (<https://www.arabidopsis.org>) (Table. S1). A high proportion of the reads were from RUBISCO, which is a highly abundant protein, that makes up more than 50% of the soluble leaf proteins (Feller *et al.*, 2008). Furthermore, light harvesting subunits were found in the screen, which could be the non-specific targets due to their enrichment in the plant cell.

Nevertheless, functionally related targets of *TtTue1* were selected by using a functional enrichment analysis via tool g:Profiler (Raudvere *et al.*, 2019) where all the sequenced candidates were scanned against the whole *Arabidopsis* genome to identify significantly overrepresented genes. A filter of P value <0.05 led to the selection of significantly enriched 36 categories of genes (Fig. S5, Table. 2). The gene representation showed a large overlapped in most of these categories therefore percentage of genes in each category were used instead

Results

of number of genes to present the overall coverage (Fig. S5). Due to the same reason, the enrichment analysis was shown as categories in the table. 2 as well. *TtTue1* overexpression in planta activates stress responses and it has been shown in Courville *et al.*, 2019 that in the overexpression line, 12 cold-responsive genes are downregulated. Therefore, the three most relevant categories of biological process (Response to stress, biotic stimulus, and cold) were selected to narrow down the list of top candidates. Overall 38 non-overlapping genes were found in these 3 categories.

There were 12 candidates chosen manually from the aforementioned 3 categories based on the following criteria:

1. Number of hits found for individual yeast colony (Table. S1)
2. Exclusively or partially localizing to the nucleus (Table. 3).
3. Specific function of each gene e.g. role in plant immunity, involve in cold responses.

So overall, twelve plant interacting partners were selected as top-ranked interactors of *TtTue1* (Table. 3).

Table. 2 A. *thaliana* stress-induced cDNA library screen in Y2H system for *TtTue1*

S.no	Selection criteria	Number of candidates
1	1st reporter gene <i>LEU2</i>	3000
2	2nd reporter gene <i>LacZ</i>	1100
3	False positive selection	160
4	Targeted Y2H	150
5	Selected for sequencing	140
6	Correct in-frame sequences	129
7	Functional enrichment analysis via g:Profiler	129
8	Enriched categories with P <0.05	36 (Category)
9	Selection of three stress category	38
10	Top ranked final candidates	12

5.9 Targeted Y2H verifies strong interaction of *TtTue1* with the 12 candidates.

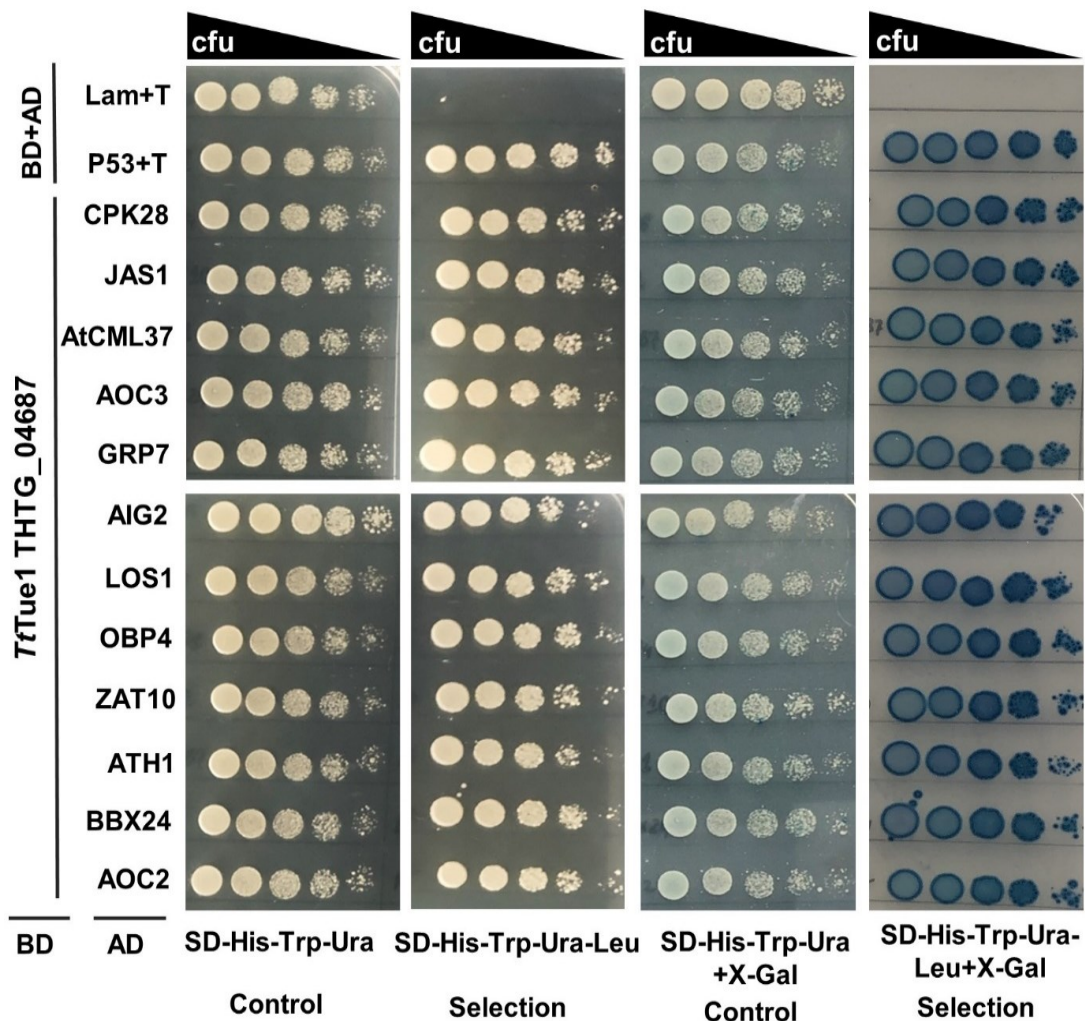
The interaction of selected 12 candidates was already verified in a targeted assay, however their strength of interaction still need to be investigated. Therefore, yeast co-transformation was repeated and a dilution series was made by using the starting OD600 of 0.5 up to five 1:5 dilutions. Negative control Lam+SV40 T-antigen did not show any growth on selection media while P53+SV40 T-antigen was used as a positive control which has accumulated dark blue color in the last and more stringent selection for *LacZ*. The control panel for the selection of both reporter genes has a consistent growth patterns for all candidates with decreasing dilution series which indicated the presence of both bait and prey plasmids (Fig. 5-6). All the twelve candidates (Table. 3) show similar growth pattern with decreasing dilution series on dropout induction media for the selection of the first reporter gene *LEU2*, which showed that selected candidates have a strong degree of interaction with *TtTue1*. More stringent selection for second reporter gene *LacZ* has proved the strength of interaction of selected candidates with *TtTue1* on basis of the accumulation of blue color (Fig. 5-6). Intensity of blue color and growth pattern in the dilution series were almost comparable to the strong interaction between P53 and SV40 T-antigen which verified these twelve candidates for further exploration in the future.

Results

However, confirmation of these interactions through other independent techniques still necessary to be done for detailed characterization at molecular level.

Table. 3 Twelve top-ranked interactors of *TtTue1* in *A. thaliana*

Target	Gene ID	Localization	Function (TAIR)
CPK28	AT5G66210	Plasma membrane	BIK1 innate immune response pathway
JAS1	AT5G13220	Nucleus	Regulation of JA mediated signaling pathway
CML37	AT5G42380	Nucleus, Cytoplasm	Positive regulator in Ca ²⁺ signaling
AOC3	AT3G25780	Plasma membrane	Involve in JA biosynthesis pathway
GRP7	AT2G21660	Nucleus, Cytoplasm	Gene expression is induced by cold
AIG2	AT3G28930	Nucleus, Cytoplasm	Exhibits RPS2-and avrRpt2-dependent induction after infection
LOS1	AT1G56070	Nucleus, Cytoplasm	Involve in cold induced translation
OBP4	AT5G60850	Nucleus	Negatively regulates cell proliferation
ZAT10	AT1G27730	Nucleus	Responsive to chitin
ATH1	AT4G32980	Nucleus	Responsible for delay in flowering
BBX24	AT1G06040	Nucleus	Involved in phytohormone regulation
AOC2	AT3G25770	Cytosol, Chloroplast	Involve in JA biosynthesis



Results

Fig. 5-6. Top 12 selected candidates showed strong interaction with *TtTue1*. Yeast strain EGY48 co expressing pB42AD-Prey and pGILDA-*TtTue1* fusions were plated on triple dropout media (SD-His-Trp-Ura) for control and quadruple dropout media (SD-His-Trp-Ura-Leu) for selection of the first reporter gene *LEU2* X-Gal overlay assay was performed as a second selection marker for *LacZ* expression. Blue intensity indicates the expression of *LacZ* and the strength of interaction. Dilution series was made by using the culture OD 0.5 and 1:5 dilutions were made to detect the differences in the strength of interaction. All candidates showed a strong interaction with *TtTue1* for both selection markers. Lam (BD) and SV40 T-antigen (AD) were used as a negative control while P53 (BD) and SV40 T-antigen (AD) served as a positive control. Selection was done on induction media which contains galactose and raffinose instead of glucose to detect the weak expression in presence of interaction. CfU stands for colony forming unit.

5.10 CPK28 and JAS1 full-length proteins do not affect the strength of interaction with *TtTue1*

The detailed characterization of 2 genes CPK28 and JAS1 from the list of 12 candidates was done. CPK28 was selected on basis of multiple hits, it was found in three independent clones during the library screen. Two independent clones have shown overlapping sequence in the region encoding the N-terminus of the protein, while the third clone has only covered the region encoding the C-terminal part of the protein. This indicates that the full-length CPK28 is interacting with *TtTue1*. CPK28 is a calcium dependent protein kinase that acts a negative regulator of plasma membrane associated kinase BIK1 by phosphorylating it (Monaghan et al., 2014). In addition, CPK28 is involved in manipulating the growth responses of *A. thaliana* and perform its function as a negative regulator of plant development processes (Matschi et al., 2015). By looking more detailed into the functions of each gene, the second candidate JAS1 (one clone in the screen) was chosen based on its exclusive localization in the plant nucleus and its known signaling pathway. It has been identified as an interaction partner of some other effectors e.g HopX1 targets JAZ repressors and facilitate infection in *A. thaliana* (Gimenez-Ibanez et al., 2014). *JAS1* is an early JA-responsive gene which act as a negative regulator of jasmonic acid signaling. Together with a protein complex, JAS1 inhibits the downstream transcription factor MYC2 which is responsible for normal expression of jasmonic acid responsive genes (Chung et al., 2009). Jasmonic acid signaling is involved in many defense-related pathways which also induces other secondary metabolites and pathogen-related proteins expression (Yang et al., 2019).

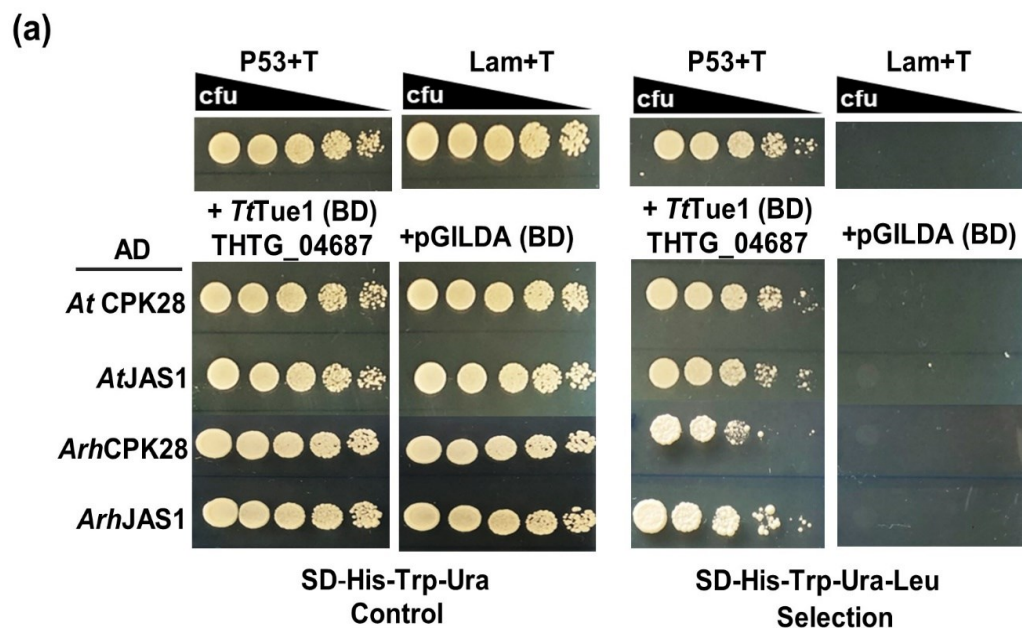
The genome of *Ar. hirsuta* is not available, yet, therefore our group has done a pilot genome sequencing analysis of *Ar. hirsuta*. Preparation of final annotated draft is still in progress (unpublished data). A homolog search of CPK28 and JAS1 were done by using the first version of our genome assembly. *Ar. hirsuta* homologs of CPK28 and JAS1 have shown 92 % and 78 % identity with *A. thaliana* (Fig. S6).

To analyze the interaction with the full-length protein, a targeted Y2H assay was performed with full-length proteins of both *A. thaliana* and *Ar. hirsuta* homologs. Selection of the first reporter gene showed that JAS1 homologs of both plant species have the same strength of interaction as it was found in Y2H screen. *A. thaliana* CPK28 full-length protein also exhibits the same degree of interaction with *TtTue1*, while CPK28 homolog of *Ar. hirsuta* has shown reduced growth of yeast cells in the dilution series. In addition, full-length proteins of both plant species did not show auto-activity upon co-transformation with empty bait vector pGILDA,

Results

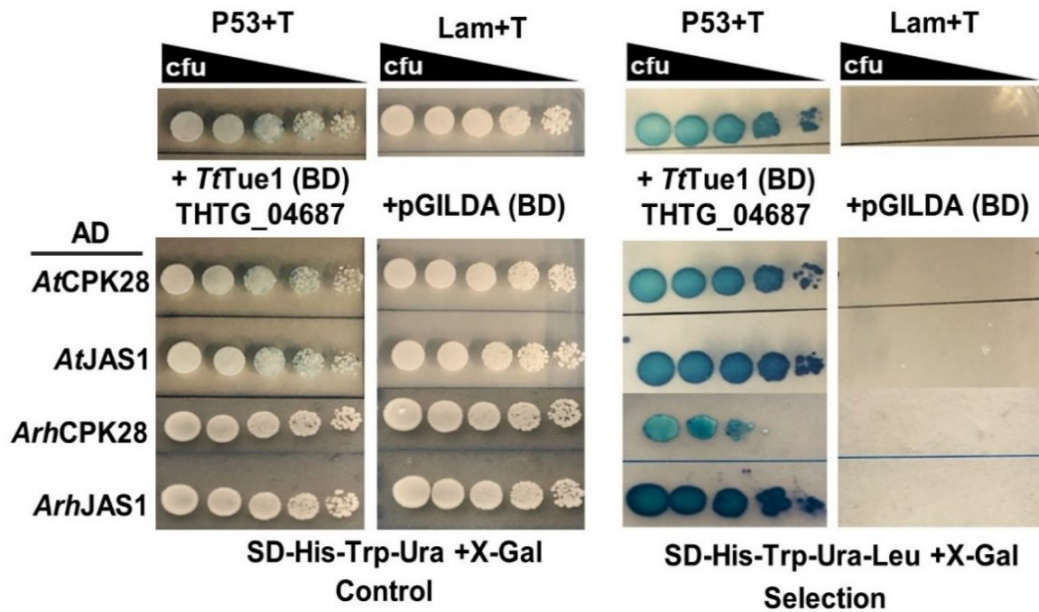
although the control panel showed the presence of both prey plasmid pB42AD containing inserts and an empty bait vector pGILDA (Fig. 5-7a). Full-length protein of CPK28 and JAS1 homologs of both species confirm the strength of interaction with *Tt*Tue1 by expressing the LacZ protein. The intensity of the blue color indicated a strong interaction which was comparable to the positive interactor P53 and T SV40 antigen. Interestingly, *Tt*Tue1 and *Ar. hirsuta* JAS1 full-length proteins were interacting with much higher affinity which is shown by the accumulation of more blue color in comparison to other proteins. X-Gal overlay assay on control plates did not accumulate any blue color except a slight change in the background which pointed out towards true interaction only in the presence of expression of reporter gene *LEU2* (Fig. 5-7b).

Immunoblot analysis on total protein extracted from yeast cells co-transformed with LexA-*Tt*Tue1-HA in pGILDA and full-length AD-CPK28 and AD-JAS1 of *A. thaliana* and *Ar. hirsuta* in pB42AD confirmed the presence of all expressed proteins in yeast. All proteins showed the right size bands AD- *At*CPK28-HA 71.7 kDa, AD- *At*JAS1-HA 34.6 kDa, AD- *Arh*CPK28-HA 73.5 kDa, AD- *Arh*JAS1-HA 35.4 kDa, LexA-Tue1-HA 55 kDa. (Fig. 5-7c). Thus, it was concluded that full-length proteins of CPK28 and JAS1 can bind with *Tt*Tue1 with the same strength as the fragmented proteins in the Y2H screen, except for CPK28 homolog of *Ar. hirsuta*, which has slightly less binding affinity.



Results

(b)



(c)

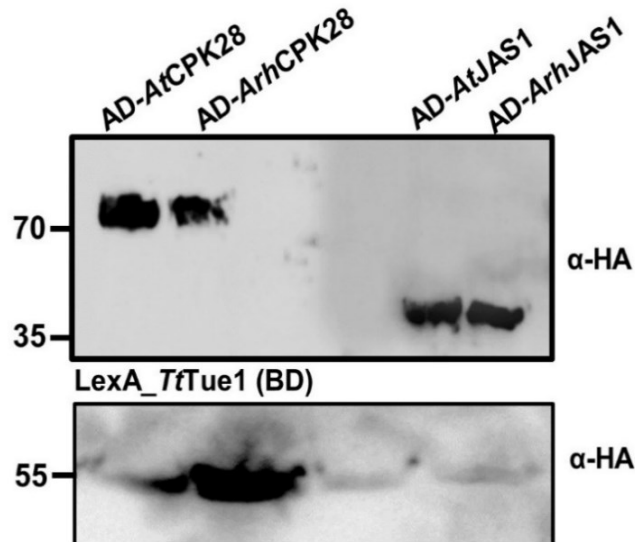


Fig. 5-7. Full-length CPK28 and JAS1 proteins have the same strength of interaction with *TftTue1* as cDNA library fragments. Full length proteins of both *A. thaliana* and *Ar. hirsuta* homologs were used for targeted Y2H assay. Triple dropout media (SD-His-Trp-Ura) was used for control and quadruple dropout media (SD-His-Trp-Ura-Leu) was used for the selection. Images on the right sides of both panels show auto-activity test of full-length prey proteins in pB42AD and empty bait vector (pGILDA). Left side images of both panels show *TftTue1* interaction with selected full-length prey proteins. Growth pattern in the dilution series showed strength of interaction of full-length proteins. Lam (BD), SV40 T-antigen (AD) as a negative control and P53 (BD), SV40 T-antigen (AD) as a positive control were shown on the top of each panel. Selection was done on induction media containing galactose and raffinose instead of glucose. CfU stands for colony forming unit. (a) Selection for first reporter gene showed the strong interaction of JAS1 of both plant species and *AtCPK28* while *ArhCPK28* have slightly weak interaction with *TftTue1* (b) Stringent selection via X-Gal overlay assay for expression of second reporter gene *LacZ* which also showed the comparable results by accumulating the blue color with different intensities. X-Gal overlay assay on control plates produced tiny blue spots. (c) Western blot analysis of yeast cells expressing AD-CPK28 and AD-JAS1 from both plant species showed the right size of bands pattern. Similarly, LexA-*TftTue1* is also expressed in the corresponding yeast cells. Western blot: Anti-HA. Sizes: AD- *AtCPK28*-HA 71.7 kDa, AD- *AtJAS1*-HA 34.6 kDa, AD- *ArhCPK28*-HA 73.5 kDa, AD- *ArhJAS1*-HA 35.4 kDa, LexA-*TftTue1*-HA 55 kDa.

Results

5.11 *In planta* confirmation of *TtTue1* interaction with CPK28 and JAS1

In a yeast two-hybrid screen, CPK28 and JAS1 were selected as the most promising interacting partners of *TtTue1* from the list of twelve candidates. To test whether this interaction also takes place *in planta*, bimolecular fluorescence complementation (BiFC) was performed. This technique is based on the interaction of two non-fluorescent segments of mVenus (mV). The N- and C-terminal fragments of mVenus are fused to two different proteins. When the interacting proteins come in close proximity the split mVenus is reconstituted and gives the fluorescence signal.

For the purpose to perform the BiFC assay, both *TtTue1* and the target proteins were cloned into the destination vector of the GreenGate system (Lampropoulos et al., 2013) with the modules that were expressing the split mVenus, under the control of 35S promoter. *TtTue1* was tagged with N-terminal fragment of mVenus (split 1, NTmV) and all the interaction partners were tagged with C-terminal part of mVenus (split 2, CTmV). Co-infiltration in *N. benthamiana* was done by using the transformed *Agrobacterium* strains of *TtTue1*-NTmV and CPK28-CTmV or *TtTue1*-NTmV and JAS1-CTmV.

Confocal microscopy analysis at 3 dpi showed accumulation of mVenus signal in the nucleus of *N. benthamiana* for JAS1 proteins from both *A. thaliana* and *Ar. hirsuta*. It has already been shown that *AtJAS1* localizes to the plant cell nucleus (Chung et al., 2009) that matching the localization of the *TtTue1*-*AtJAS1* complex. *ArhJAS1* localized to the plant nucleus upon transient expression in *N. benthamiana* (Fig. 5-11) which is also consistent with the *TtTue1*-*ArhJAS1* complex. *AtCPK28* is a plasma membrane-localized protein (Monaghan et al., 2014), but the reconstituted mVenus signal during interaction with *TtTue1* accumulated in the nucleus, which hints at re-localization of CPK28 of both *A. thaliana* and *Ar. hirsuta* upon interaction with *TtTue1*. It has been shown by (Pelgrom et al., 2020) that several target proteins re-localize to different compartments instead of original localization upon interaction such as *LsFLX-like2* targeted by a nuclear-localized effector of *Bremia lactucae* BLR38 caused its re-localization to the nucleus. It was anticipated that strong nuclear localized signal of *AtCPK28* might be due to re-localization of protein upon interaction with *TtTue1* while individual *ArhCPK28* protein was already found with partial nuclear localization (Fig. 5-11). However signal reconstitution of split mVenus was found for both *AtCPK28* and *ArhCPK28*.

It is important to use an appropriate negative control, therefore two different genes, *TtTue16* and *AtCPK7*, were selected from the family of *T. thlaspeos* unique effector and calcium-dependent protein kinase family, respectively. *TtTue1* is part of a cluster and consist of four members, THTG_04687 (*TtTue1*), THTG_04686, THTG_04669 (*TtTue16*), THTG_04670. THTG_04669 (*TtTue16*) has 62% identity with *TtTue1* and is also upregulated during the infection while THTG_04686 and THTG_04670 showed 69% identity with *TtTue1* but they were not induced during the infection. In contrast to *TtTue1*, THTG_04669 (*TtTue16*) did not show a growth phenotype upon expression in *A. thaliana* (Courville et al., 2019). There was no mVenus signal detected upon co-expression of *TtTue16* and both interaction partners. To find the specificity of *TtTue1* interactions, another negative control from plant, *AtCPK7*, was used. As expected, there was no mVenus signal detected above background in any sub-cellular compartment (Fig. 5-8). In all combination of positive interactions rejoining of split mVenus and giving a strong fluorescence signal have verified the *TtTue1* interaction with CPK28 and JAS1 of both plant species.

Results

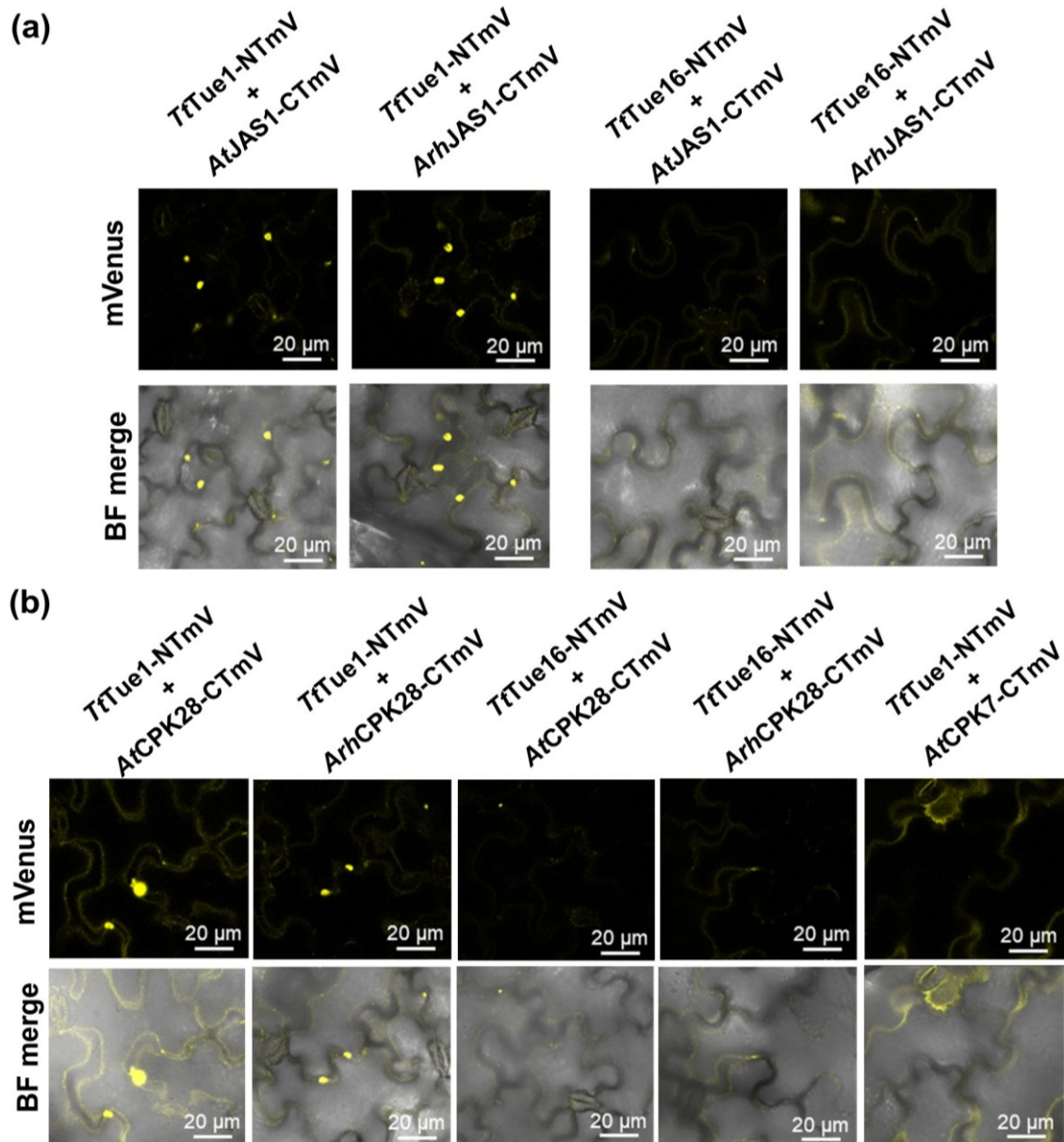


Fig. 5-8. Bimolecular fluorescence complementation analysis of *TtTue1*-JAS1 and *TtTue1*-CPK28 interaction *in planta*. Homologs of both plant species *A. thaliana* and *Ar. hirsuta* were used in the assay. mVenus signal was detected in *N. benthamiana* leaves co-infiltrated with *Agrobacterium* strains expressing *TtTue1*-NTmV and CPK28-CTmV or *TtTue1*-NTmV and JAS1-CTmV. (a) Images on top showed the mVenus signal in the nucleus for JAS1 of both *A. thaliana* and *Ar. hirsuta*. Both split parts of mVenus reconstituted and accumulated the signal in the nucleus upon interaction. *TtTue16* another member of the *TtTue1* family co-infiltrated with JAS1 of both species and it did not show any fluorescence signal. (b) The lower panel showed the interaction of CPK28 of both *A. thaliana* and *Ar. hirsuta* with *TtTue1*. Similar to JAS1, mVenus signal accumulation for CPK28 of both species also occurs in the nucleus of the host plant. *TtTue16*-NTmV was used in the same experimental setup with CPK28 which did not show any fluorescence signal. CPK7-CTmV was used as an additional negative control and no signal was detected upon co-expression with *TtTue1*-NTmV. Upper panel: mVenus, lower panel: Brightfield.

5.12 *In vitro* analysis of *TtTue1* interaction with CPK28 and JAS1

To further quantify the strength of *TtTue1* interaction with CPK28 and JAS1 protein an *in vitro* analysis was performed. Glutathione S-transferase (GST) pull-down is a suitable and fast

Results

method for directly determining the binding affinity (Yong Kim and Hakoshima, 2019). All proteins were expressed and purified in *E. coli* and subjected to GST pull-down assay. GST-tagged *TtTue1* was used as bait and HIS-tagged interaction partners were used as prey. Purified proteins were passed over a size exclusion chromatography (SEC) column and the size-specific fraction was collected for GST pull-down assay. GST beads bound with *TtTue1* were incubated with purified protein of CPK28 and JAS1 of *A. thaliana* and *Ar. hirsuta*. JAS1 of both species has an MBP solubility tag while CPK8 was tagged with GB1 because both proteins alone were present only in the insoluble fraction.

5.12.1 *AtJAS1* and *ArhJAS1* bind *TtTue1*

AtJAS1 and *ArhJAS1* show binding to GST-*TtTue1* (Fig. 5-9a, lane 1 and 3). A Coomassie brilliant blue staining of pull-down samples showed a clear band of both prey proteins in the co-incubated samples with *TtTue1*. Rrm4, an RNA binding protein of *U. maydis* tagged with GST was used as a negative control. Rrm4 did not show any extra band in the pull-down fractions (Fig. 5-9a, lane 4-5) with JAS1 which indicated that *TtTue1* interaction with JAS1 of both plant species was specific. All the lanes either loaded with only *TtTue1* or both prey proteins alone did not show any band corresponding to any bait protein (for *AtJAS1* and *ArhJAS1*) or prey protein (for *TtTue1*) (Fig. 5-9a). Immunoblot with anti-His antibodies also showed the interaction of *TtTue1* with JAS1 from both plant species. Respective size bands have appeared in both pull-down fractions and protein alone. The lane corresponding to the negative control Rrm4 was completely empty though a high concentration of Rrm4 protein was present in the Coomassie brilliant blue stained gel.

5.12.2 CT-*AtJAS1* has a slightly strong binding affinity for *TtTue1*

In addition to the full-length *AtJAS1* protein, a truncated version of *AtJAS1* (CT-*AtJAS1*) was also subjected to pull down with GST-*TtTue1*. The splice variant *AtJAS1.1* which was found in the Y2H screen consisted of 3 known domains, an N-terminal core CMID domain, a central ZIM/TIFY, and a C-terminal Jas domain. The CMID and Jas motifs interact with MYC transcription factor (Zhang et al., 2017). Therefore, on basis of structure homology of *TtTue1* to MYC3 interacting domain, I decided to split the *AtJAS1* sequence into two parts for analyzing two important binding domains, CMID and Jas. Protein purification of N-terminal part of *AtJAS1* (1-58 amino acid) had some complications and could not get optimized due to limited time, while the C-terminal part consisted of the TIFY and Jas domain, was purified by fusing with GB1 solubility tag. The C-terminal part with both motifs was purified for the protein stability. CT-*AtJAS1* (Fig. 5-9a, lane 2) showed slightly stronger interaction with *TtTue1* as compared to the full-length protein. The band intensities in both Coomassie brilliant blue staining and western blot indicated a slightly strong interaction (Fig. S7). This increase in the binding affinity by using the truncated version of protein gave hint for the involvement of the Jas binding motif in the interaction (Fig. 5-9a) because the ZIM domain does not bind directly to MYC TFs. However, testing Jas motif independently, is suggested for the further verification in future.

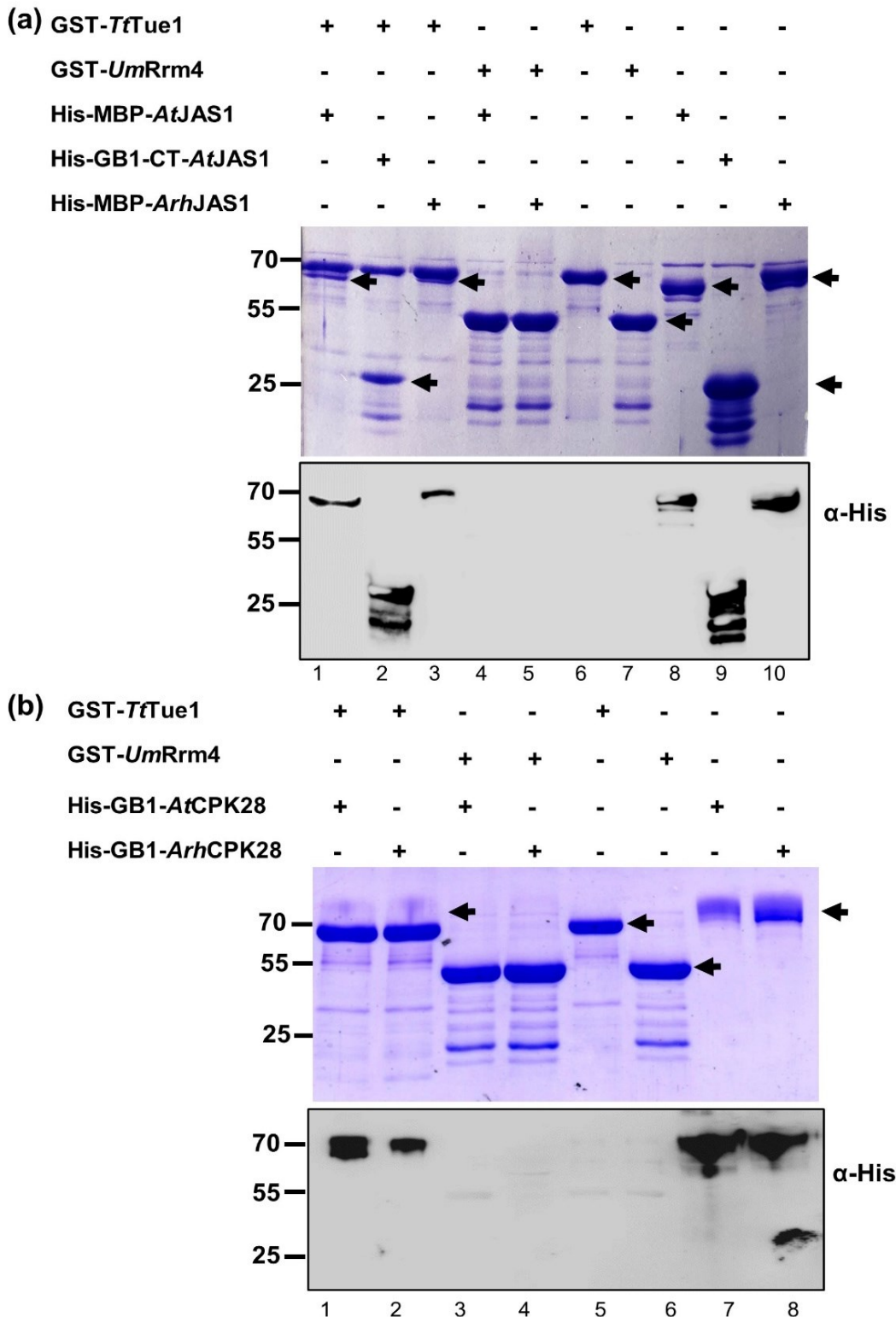
5.12.3 *AtCPK28* and *ArhCPK28* bind *TtTue1*

Similar to JAS1, the interactions of *AtCPK28* and *ArhCPK28* were also analyzed in Coomassie brilliant blue stained gel as well as via Western blot. Pull-down fraction of *AtCPK28* (lane1) and *ArhCPK28* (lane 2) in the stained gel showed a very faint band that appeared on top of the *TtTue1* bands. It showed that *AtCPK28* and *ArhCPK28* still interacted with *TtTue1* which was

Results

not that obvious in Coomassie brilliant blue stained gel therefore, a western blot analysis clarified the results and both homologs displayed bright bands present in pull-down fraction. A negative control GST-Rrm4 did not pull down both *At*CPK28 (lane 3) and *Arh*CPK28 (lane 4) and verified the specific interaction of CPK28 from both plant species (Fig. 5-9b).

Thus *in vitro* verification of interactions also provided evidence and support of the *Tt*Tue1 binding with CPK28 and JAS1, of *A. thaliana* as well as its natural host *Ar. hirsuta*. Most importantly the truncated version of *At*JAS1 provided evidence for finding the exact binding region of JAS1 in future.



Results

Fig. 5-9. *TtTue1* interacts with CPK28 and JAS1 proteins of *A. thaliana* and *Ar. hirsuta* *in vitro*. All proteins were expressed and purified in *E. coli*. His-tagged prey proteins were pulled down with GST tagged *TtTue1* (bait). Interaction was directly detected via Coomassie blue staining. Prey proteins were also detected in the pull-down fractions in Western blot analysis by using anti-His antibodies. GB1 solubility tagged was used for CPK28 and MBP fusion was used for JAS1 proteins. JAS1 (a) and CPK28 (b) of both plant species showed interaction with *TtTue1* with different binding intensities in a GST pull down experiment. (a) Protein band corresponding to His-MBP-*AtJAS1* (lane 1), His-MBP-*ArhJAS1* (lane 3) and the N terminally truncated His-GB1-CT-*AtJAS1* (lane 2) were detected in the respective pull down fractions. A slight increase in the binding intensity was seen for His-GB1-CT-*AtJAS1*. Rrm4, a well-characterized RNA binding protein studies at our institute, was used as a negative control. Lane 4 and 5 show pull down of His-MBP-*AtJAS1* and His-MBP-*ArhJAS1* with GST-Rrm4. Lane 6-10 show all the mentioned proteins without interaction partners (b) *AtCPK28* (lane1) and *ArhCPK28* (lane 2) displayed a strong interaction in the Western blot, while a faint band of CPK28 above the *TtTue1* band is visible in the Coomassie brilliant blue staining. Lane 3-4 represent pull down of *AtCPK28* and *ArhCPK28* with GST-Rrm4. Lane 5-8 show all proteins of this blot without their interaction partners. Black arrows on the right show the band size for each purified protein. Lane numbers corresponding to both stained gels and western blots. Sizes: GST-*TtTue1* 57.6 kDa, GST-Rrm4 46.8 kDa, His-MBP-*AtJAS1* 64.6 kDa, His-GB1-CT-*AtJAS1* 25.4 kDa, His-MBP-*ArhJAS1* 65.4 kDa, His-GB1-*AtCPK28* 69 kDa, His-GB1-*ArhCPK28* 70.8 kDa

5. 13 Quantitative analyses of *TtTue1* binding to JAS1 and CPK28

To obtain quantitative data on the *TtTue1*-protein interactions, a microscale thermophoresis (MST) measurement was performed in collaboration with Dr. Mohanraj Gopalswamy and Prof. Holger Gohlke. The purified proteins of *AtJAS1*, CT-*AtJAS1*, *ArhJAS1*, *AtCPK28* and *ArhCPK28* were used as ligands of *TtTue1*. MST is based on the directed movement of the molecules along the generated temperature gradient which detect the changes and depend on the charge, size and solvation shell of the molecule (Magnez et al., 2017). *TtTue1* was labelled by Alexa Fluor® 488 dye and titrated with the above mentioned ligands which showed changes in the fluorescence upon binding. The labelled *TtTue1* protein titrated only with the MST buffer and no indication for binding was observed.

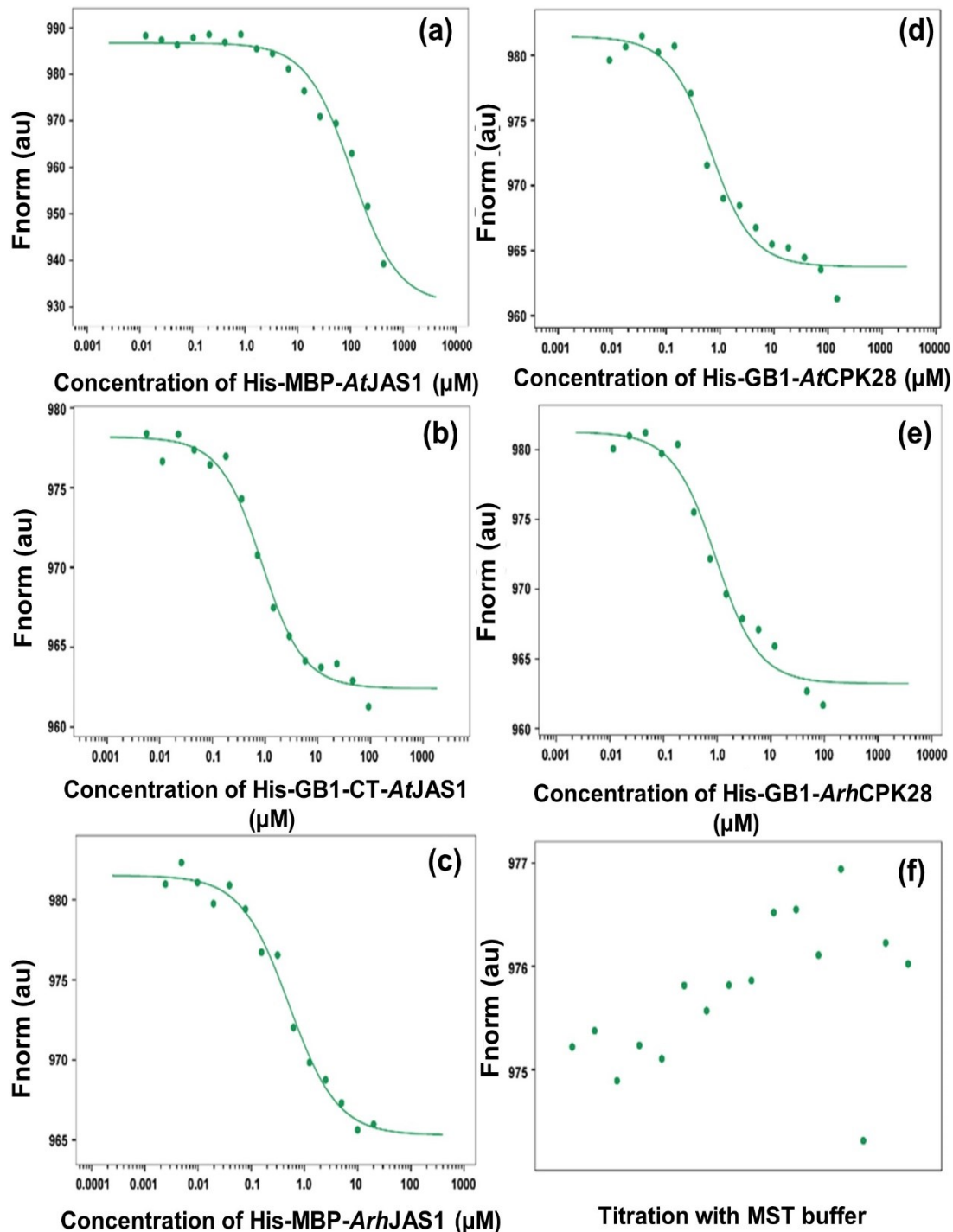
MST was recorded for each sample, the binding constant K_D and the binding stoichiometry were calculated from the non-linear regression curves. The Hill coefficient indicated a 1:1 ratio model between *TtTue1* and the binding partner except His-MBP-*AtJAS1* (Table. 4). All the proteins bind in a nanomolar range while His-MBP-*AtJAS1* showed values in micromolar. The high K_D 107.9 μ M of His-MBP-*AtJAS1* and low K_D 717 nM of His-GB1-CT-*AtJAS1* indicated that full length protein might have hindered the binding domain of *AtJAS1* and decreased the binding affinity. The C-terminal region of *AtJAS1* could be more exposed to binding upon cleaving the N-terminal part of *AtJAS1*, thus showed strong binding with *TtTue1*. The low K_D demonstrated the sequence specificity of the truncated CT-*AtJAS1*. The strong binding of CT-*AtJAS1* is also in line with the observation from GST pull-down experiment (Fig. 5-9). This suggests that C-terminally located Jas domain of *AtJAS1* might be essential for *TtTue1* binding. Similarly, His-MBP-*ArhJAS1* revealed a K_D of 356 nM and indicated a stronger binding affinity. Although the binding domains of *AtJAS1* and *ArhJAS1* are conserved (Fig. S6). *ArhJAS1* might have different protein confirmation and the interacting domain is accessible in full length protein. However, the truncated version of *ArhJAS1* is suggested to check for the specificity of binding domains.

The second interaction partner of *TtTue1*, His-GB1-*AtCPK28* and His-GB1-*ArhCPK28* revealed a K_D of 529 nM and 795 nM respectively. The low K_D values suggested a strong

Results

binding affinity of both *At*CPK28 and *Arh*CPK28. Thus, the binding behavior of all proteins showed a clear binding specificity and consistent with the results of other techniques used for the verification of *Tt*Tue1 binding.

The pattern of binding curves of 1:1 model indicated that *Tt*Tue1 might have two binding sites therefore the MST data was fitted to the 1:2 model. The purpose of this simulation was to determine the two-site binding of a protein. The model indicated that *Tt*Tue1 could have two binding sites for the ligands, thus two K_D 's, K_D (1) and K_D (2), may be expected. It is also speculated that site 1 might have the higher binding affinity which is also evident from the K_D values (Fig. S8) However, there could be less data points to fit to 1:2 model and clearly resolve a second binding step. Nevertheless, 1:2 model also support the supposition of more than one target of *Tt*Tue1.



Results

Fig. 5-10. *TtTue1* binding to JAS1 and CPK28 detected by MST. The panels (a-e) showed non-linear regression curves of *TtTue1* binding with the mentioned proteins on x-axis. Panel (f) showed titration with MST buffer as a control. These binding curves were calculated from the gradual difference of thermophoresis which is plotted as F_{norm} on Y-axis. F_{norm} is defined as $F_{\text{hot}}/F_{\text{cold}}$ against the ligand concentration. The dissociation constant (K_D) was derived from the binding curve by using the MO affinity analysis software (NanoTemper, Germany). The fitted values and standard deviation of three technical replicates were shown in the Table. 4. An approximate 1:1 ratio of Hill coefficients was obtained from the fits. This experiment was performed using GST-or His-tagged proteins in collaboration with Prof. Dr. Holger Gholke and Dr. Mohanraj Gopalswamy.

Table. 4 Dissociation constant and Hill coefficients calculated from the binding curves

Sr. no	<i>TtTue1</i> targets	K_D (nM)	Hill coefficient
1	His-MBP- <i>AtJAS1</i>	107960 ± 26252	ND
2	His-GB1- <i>AtCPK28</i>	529 ± 146	1.119
3	His-GB1-CT- <i>AtJAS1</i>	717 ± 126	1.277
4	His-GB1- <i>ArhCPK28</i>	795 ± 205	0.855
5	His-MBP- <i>ArhJAS1</i>	356 ± 76	0.952

ND - Not determined (Fail to fit to the Hill Model)

5.14 *ArhJAS1* localized to the nucleus while *ArhCPK28* is targeted to both nucleus and plasma membrane of plant

To compare the functions of *Ar. hirsuta* homologs of CPK28 and JAS1 with *A. thaliana*, it was necessary to first investigate their compartmentalization and whether they have a similar localization as *A. thaliana* CPK28 and JAS1 proteins. For that purpose, the *Ar. hirsuta* homologs of CPK28 and JAS1 were C terminally tagged with eGFP and transiently expressed in four weeks old *N. benthamiana* leaves under the control of the 35S promoter. Microscopic analysis of infiltrated leaves at 3 dpi showed that *ArhJAS1* localized solely to the nucleus which was expected and consistent with the localization pattern of *AtJAS1* (Chung et al., 2009). Nuclear localization of *Ar. hirsuta* homolog of JAS1 showed that *TtTue1* interaction with *ArhJAS1* gave hint towards the same pathway involved in the natural host as well. In contrast, *ArhCPK28* accumulated mainly in the plasma membrane, but also in the nucleus up to some extent (Fig. 5-11a). Plasma membrane localization of *AtCPK28* was reported, and it negatively regulates other membrane associated kinase such as *AtBIK1* to manipulate the pathogen-triggered immunity (Monaghan et al., 2014). Western blot analysis using anti-GFP-antibodies showed that full-length fusion proteins of *ArhCPK28* and *ArhJAS1* were produced in the plant. Also, there was a minor fraction of free GFP present for both proteins suggesting that the observed nuclear signal in CPK28 could be true signal and not a result of free GFP (Fig. 5-11b).

Usually, the target proteins localize to the same compartments, are most likely considered to be true interactors (Pelgrom et al., 2020). *TtTue1* interacted with the plasma membrane localized protein CPK28, which is exclusively localized to the plasma membrane in *A. thaliana* while a nuclear localized signal was also found in addition to the plasma membrane localization in *Ar. hirsuta*. The term re-localization has been used for several proteins where their localization was changed during the interaction and they moved to the compartment of their respective interacting partners (Pelgrom et al., 2020). This observation can apply on the similar behavior of *TtTue1* interaction with CPK28 where either of the interacting partner can relocate themselves in order to interfere with the plant immune responses.

Results

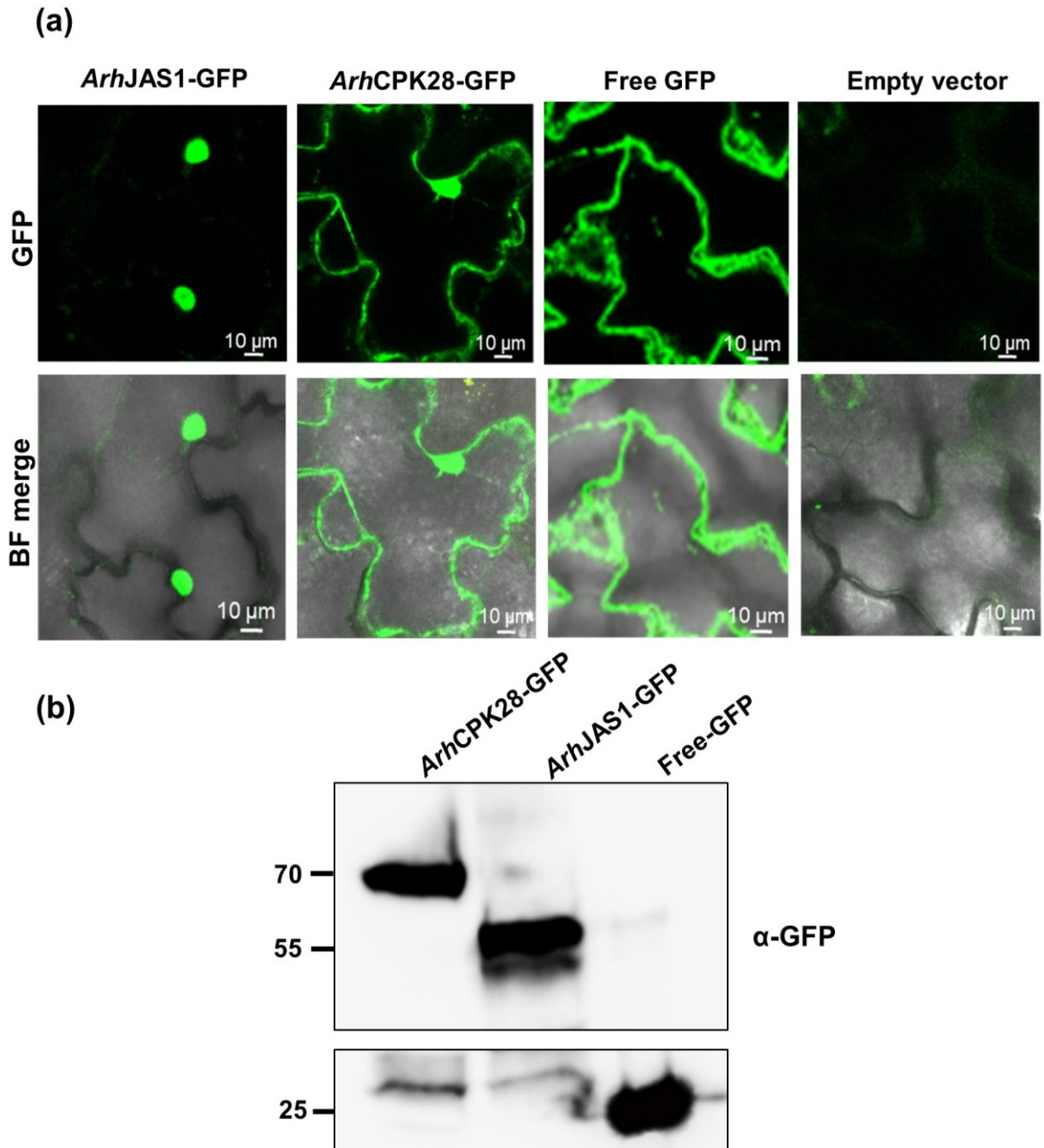


Fig. 5-11. Subcellular localization of *Ar. hirsuta* CPK28 and JAS1 homologs via transient expression in *A. thaliana* (a) *ArhJAS1* and *ArhCPK28* were transiently expressed in *N. benthamiana*. Constructs were prepared by tagging the protein with GFP under the control of 35S promoter. Agrobacterium mediated transformation has done by infiltrating the 4 weeks old plant leaves. Microscopic analysis was done at 3 days post-infiltration. GFP and brightfield channels displayed JAS1 localization in the nucleus while CPK28 was seen to localize in the plasma membrane and nucleus both. An empty vector was used a negative control. Scale bar- 10 μ m. (b) Full length protein expression was detected by western blot analysis using anti-GFP antibodies. Free GFP control was loaded to compare the band intensity of free GFP in *AtCPK28*-GFP and *ArhCPK28*-GFP. Sizes: *ArhCPK28*-GFP 91.5 KDa, *ArhJAS1*-GFP 53.4 KDa, GFP 27 KDa

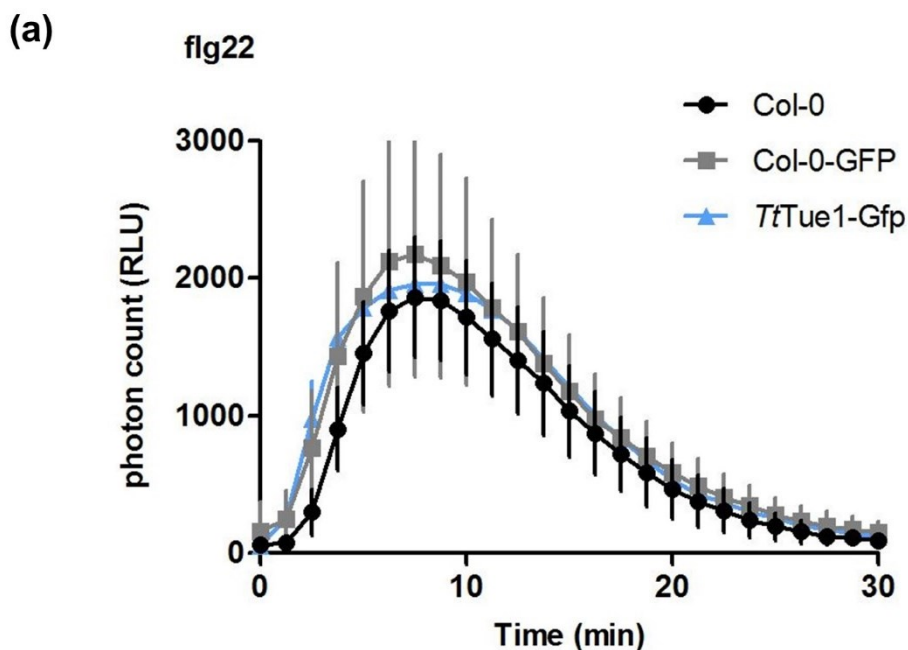
Results

5.15 PTI response remain unchanged in presence of *TtTue1*

To assess the role of *TtTue1* in PTI responses, PAMP-induced ROS burst was analyzed in *A. thaliana* line expressing *TtTue1*. It is known that CPK28 is responsible for the negative regulation of PAMP induced calcium burst (Monaghan et al., 2014) and it is identified as an interacting partner of *TtTue1* (Section 5.10). Therefore, two hypotheses were formulated to evaluate the contribution of *TtTue1* in regulation of PTI responses:

1. *TtTue1* interacts with CPK28 to stabilize its function in order to facilitate the blocking of PTI responses.
2. *TtTue1* could degrade or destabilize the CPK28 protein (Fig. 5-15) and ultimately results in induction of PTI responses.

The initial defense responses are triggered by PAMP which got recognized by PRRs that ultimately led to the accumulation of ROS and resulted in an extensive transcriptional reprogramming in the host (Lo Presti et al., 2015). ROS induction by PAMPs such as flg22 or elf18 was measured as an example for a PTI response. Therefore, reaction of the stable lines expressing *TtTue1*-Gfp upon PAMP perception was analyzed in the luminescence ROS assay (Smith and Heese, 2014). *A. thaliana* wild type and free GFP lines were used as controls. ROS production increased after treatment of plant lines with bacterial flg22 and elf18. There was no significant difference observed in flg22 treated *TtTue1* and controls lines, and the accumulation of ROS was similar in all the cases (Fig. 5-12a). The same trend was observed after treating the plants with elf18 (Fig. 5-12b). These results indicated the sensitivity of *TtTue1* line towards PAMPs and similar responses as controls showing that the presence of *TtTue1* has no effect on plant response towards perception of PAMPs. In general, accumulation of ROS supported the hypothesis that *TtTue1* is recognized by plant protein that can activate initial PTI responses which might be due to destabilization of CPK28.



Results

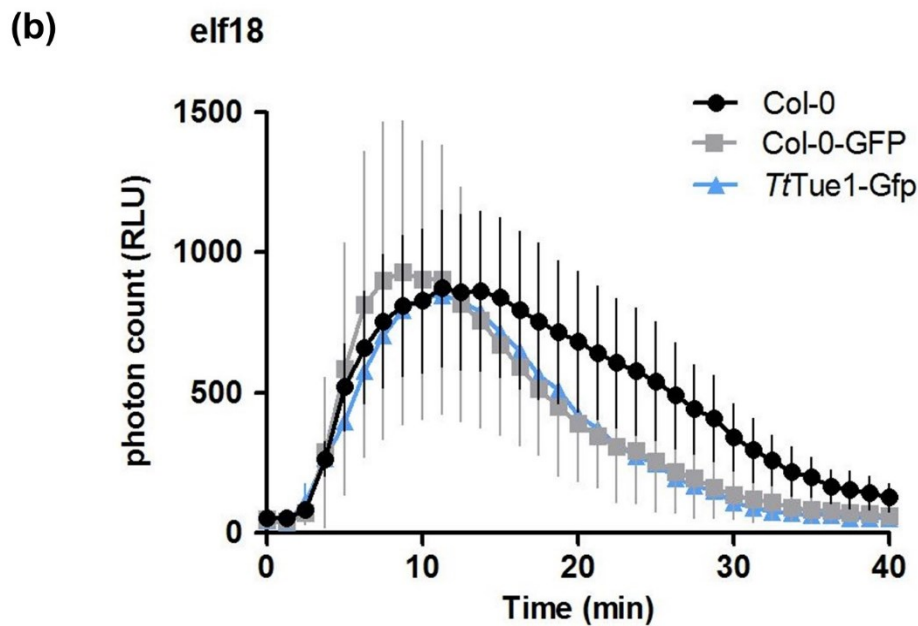


Fig. 5-12. ROS accumulation in *TtTue1-Gfp* transgenic line. Leaf discs of *TtTue1-Gfp*, Col-0-Gfp, and Col-0 were treated with 100 nM flg22 and 100 nM elf18. Photon count (RLU) was measured in the luminometer (Berthold LB 940). All the lines showed similar responses upon perception of flg22 and elf18. The same level of ROS production was observed in *TtTue1-Gfp*, Col-0-Gfp and Col-0 which indicated the activation of plant immune responses. Values are means \pm SDs (n = 8).

5.16 *TtTue1* triggered the secondary metabolite accumulation in plants.

To study the effect of *TtTue1* on more downstream defence signaling, the level of secondary metabolites was checked by GCMS (Gas chromatography mass spectrometry) analysis. JAS1 is involved in the JA signaling pathway therefore *TtTue1* interaction with JAS1 was the basis for the analysis of phytohormones.

Leaf material of four weeks old *TtTue1-Gfp* stable lines in comparison to Col-0 and Col-0-GFP controls were used in the vapor-phase extraction method (Hartmann et al., 2018). The levels of salicylic acids and derivatives salicylic acid O- β -glucoside (SAG), piperolic acid and its derivatives N-hydroxypiperolic acid (NHP) and Camalexin, were analyzed by Karin Kiefer and Prof. Jürgen Zeier (Institute of Molecular ecophysiology of plants). Salicylic acid and N-hydroxypiperolic acid (NHP) are directly involved in multiple aspects related to the growth-defense balance in the plants (Shields et al., 2022). Elevated level of these stress related hormones was detected such as, level of SA and its derivative SAG were significantly high in *TtTue1-Gfp* transgenic line in comparison to the controls (Fig. 5-13) which might activate the SA signaling. Enhance level of SA and its derivatives might suppress the JA biosynthesis which was not detected in this experimental setup. Hence, *TtTue1* might stabilize JAS1 and thereby influence the cross-talk between SA and JA. The jasmonic acid (JA) signaling is antagonistic to salicylic acid (SA) pathway and due to JAS1 function, less JA accumulation was expected.

In addition, to crosstalk between SA and JA, SA and Piperolic acid derivatives are also considered to play a pivotal role in maintaining the balance between plant immunity and plant growth (Shields et al., 2022). Piperolic acid and its derivative NHP and NHPG have shown significant elevated levels in *TtTue1-Gfp* lines, while no such accumulation of any of these

Results

hormones was detected in the control lines. The phytoalexin camalexin is an important component in defending plants against necrotrophic fungal pathogens (Ferrari et al., 2003). It is locally induced to protect the plant from microbial invader (Stotz et al., 2011). *TtTue1* stable line induced a high level of camalexin. Taken together, these findings provide evidence for the accumulation of stress related metabolites in presence of *TtTue1*, however their downstream responses still need to be investigated. This data set can verify by analyzing the metabolites accumulation in infected plant tissues. Infection with wild type *T. thlaspeos* and *TtTue1* Δ strain would be helpful to examine the impact of *TtTue1* on hormone levels in the natural environment.

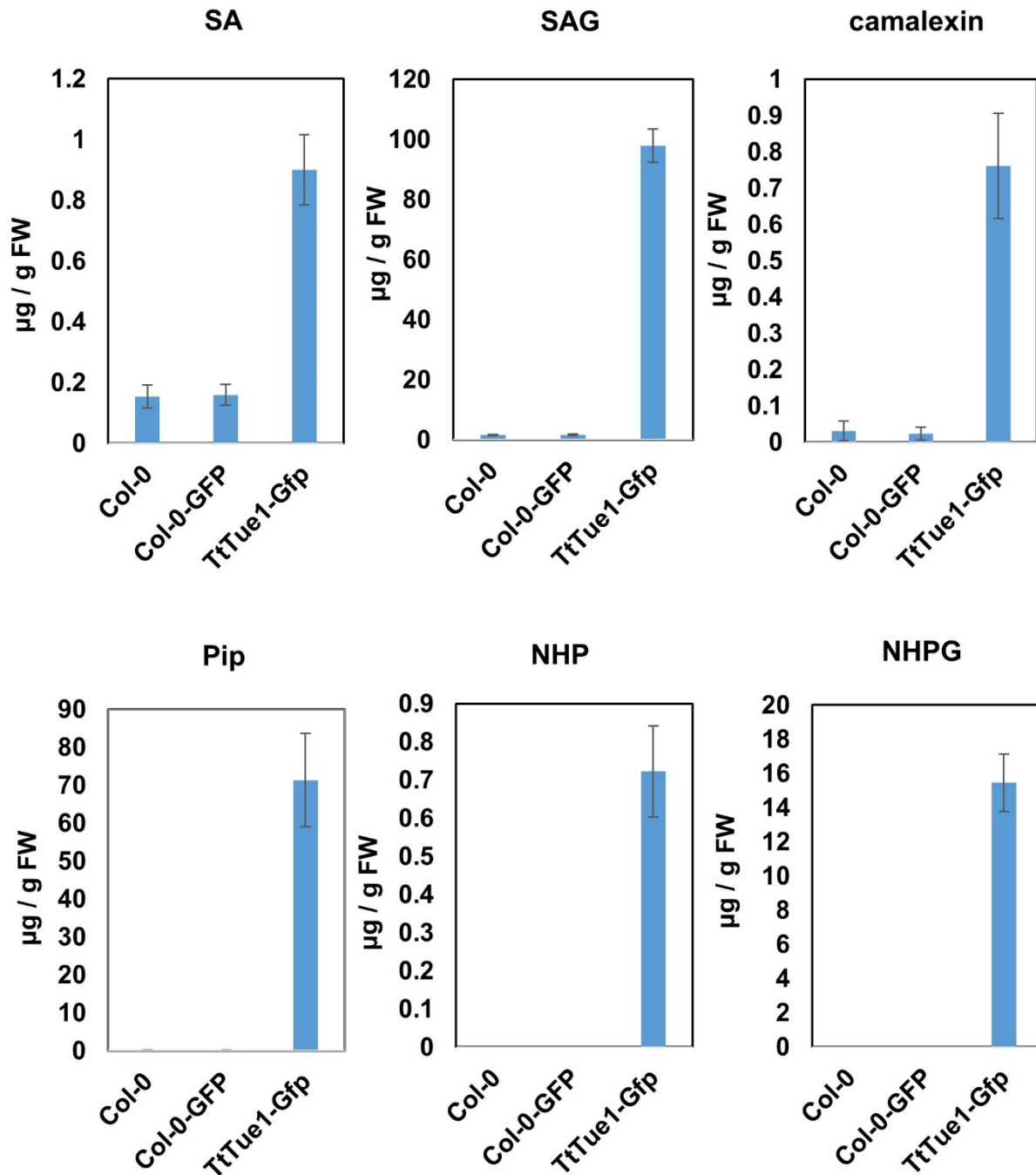


Fig. 5-13. *TtTue1* induced accumulation of significant level of secondary metabolites. Four weeks old leaf sample were used for VPE analysis (Vapor-phase extraction) and secondary metabolites accumulation were measured by GCMS. *TtTue1*-Gfp line accumulated high levels of SA

Results

and its derivatives, pipecolic acid and derivatives and camalexin, in comparison to the control lines Col-0 and Col-0-GFP. Mean value was taken from 4 biological replicates and their standard deviation was shown by error bars. The level of metabolites was measured in $\mu\text{g/g}$ fresh weight. This experiment was done at Institute of Molecular ecophysiology of plants and data was analyzed by Prof. Dr. Jürgen Zeier.

5.17 Effect of CPK28 on colonization of *T. thlaspeos* upon culture infection

To investigate the effect of CPK28 on the colonization of *T. thlaspeos* in *A. thaliana* a culture infection system was used. As described above, CPK28 is a negative regulator of pathogen-triggered immune responses (Monaghan et al., 2014) which means it can facilitate disease development in the plant.

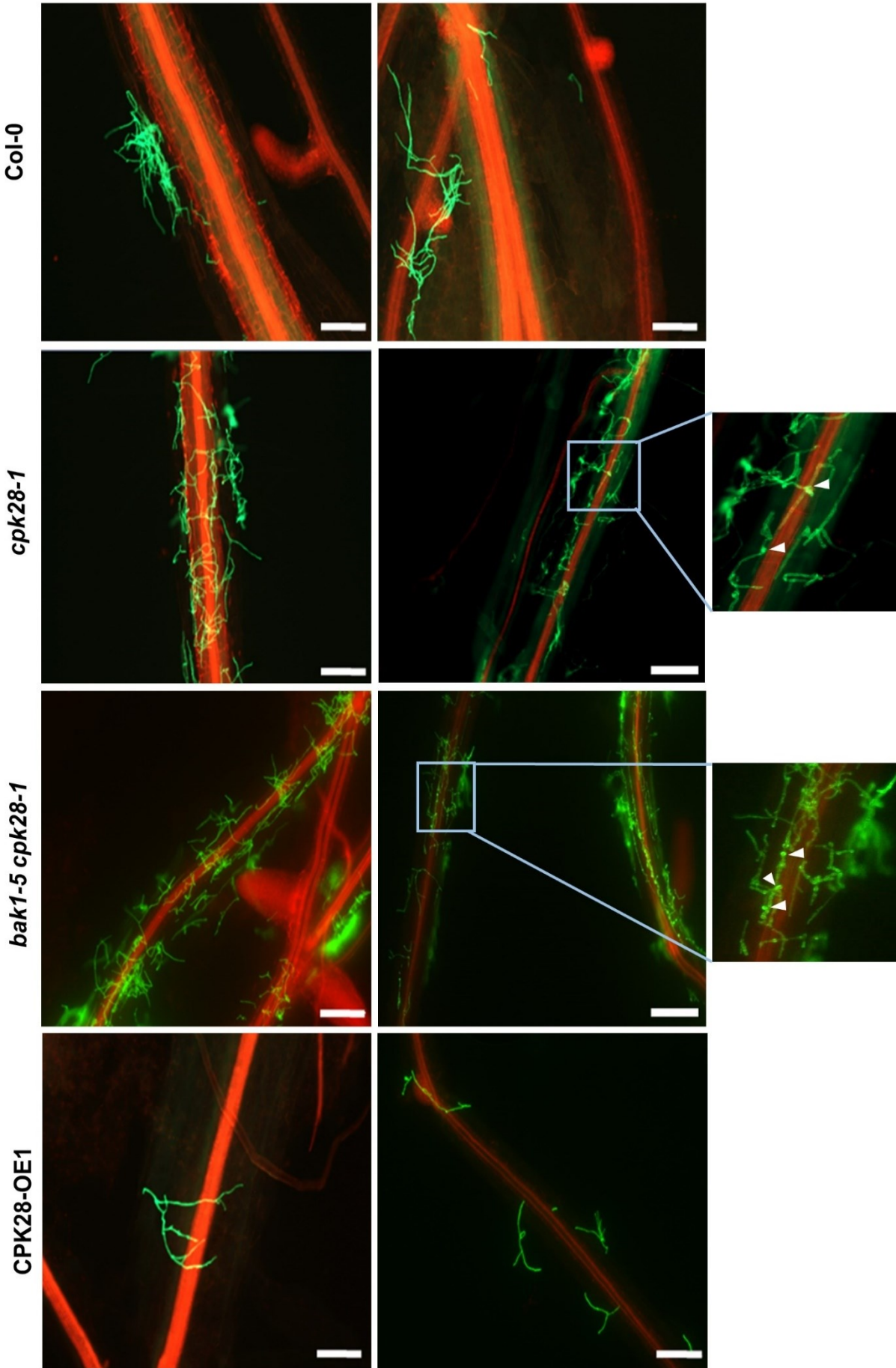
In the culture infection system, roots of one-week old seedlings were inoculated with LF1 culture at 0.5 OD₆₀₀ for 15-20 minutes. After removing the fungal cultures and washing, plants were incubated for 3 more weeks. Microscopic analysis of roots and shoots of 4 weeks old seedlings showed different fungal growth patterns in mutants and control lines. WGA and PI staining distinguish the plant and fungal cells by accumulating the red and green colour respectively. There was only an external fungal hyphal mass found in Col-0 roots which was sticking on the surface of the root, while few samples have developed proper hyphae with round head tips.

cpk28-1 mutant accumulated more fungal hyphae and the spreading pattern of its hyphae along the roots were completely different from Col-0. Both small and long hyphal structures were found and most of them were growing inside the plant cortex. Interestingly round bulb like structures were found in the mutant plant which might be the aspersorium like structure and act as a penetration site. Continuous or fragmented hyphal structures covered most part of the roots. In addition to the proper hyphal structures, a big fungal mass was also found sticking on the surface of the roots.

Further verification of the similar growth pattern of *T. thlaspeos* was done on a double mutant *bak1-5 cpk28-1* which did not show much difference to hyphal growth in *cpk28-1*. The double mutant also responds to the fungus in an almost similar manner as *cpk28-1* however, the small bulbous structures were more prominent in the double mutant.

An opposite growth pattern was expected to be detected in CPK28-OE1 line. Over-expression line did not promote any fungal growth and it is almost comparable to wild type. Only small external hyphal structure was found on the surface of the root. A few were found to have round head hyphal tip which resemble the one found in mutant plants. (Fig. 5-14). The major difference detected in the mutants and wild type plant was accumulation of more fungal mass and presence of more aspersorium like round structures in the mutants however, the hyphal growth completely inside the root was not verified. These results showed that in contrast to the known function of CPK28, it hindered the fungal growth inside the plant instead of facilitating it.

Results



Results

Fig. 5-14. CPK28 caused fungal growth reduction upon culture infection of *T. thlaspeos*. *cpk28-1*, *bak1-5 cpk28-1*, CPK28-OE1 and Col-0 lines were inoculated with LF1 culture and plants were grown for 3 weeks. WGA and PI staining was used to stain the fungal and plant tissue respectively. The plant material was stained 3 weeks post infection. *cpk28-1* mutant showed more hyphal structures grown along the plant roots. The double mutant *bak1-5 cpk28-1* showed almost the same pattern of both short and long hyphae. White head arrow in the zoom in section showed that both mutant plants developed round head structures which could be the penetrating site of hyphae. CPK28-OE1 did not show any hyphae growing along the vasculature but instead of that both overexpression and Col-0 has mostly surface grown hyphae. Two representative overlay images were chosen for each plant line. 60 plants were infected and microscopically analyzed for each line. Green hyphal structures of *T. thlaspeos* have different growth patterns depending on each mutant line. Merged image, WGA: green, PI: Red. Scale bar 100 μ m.

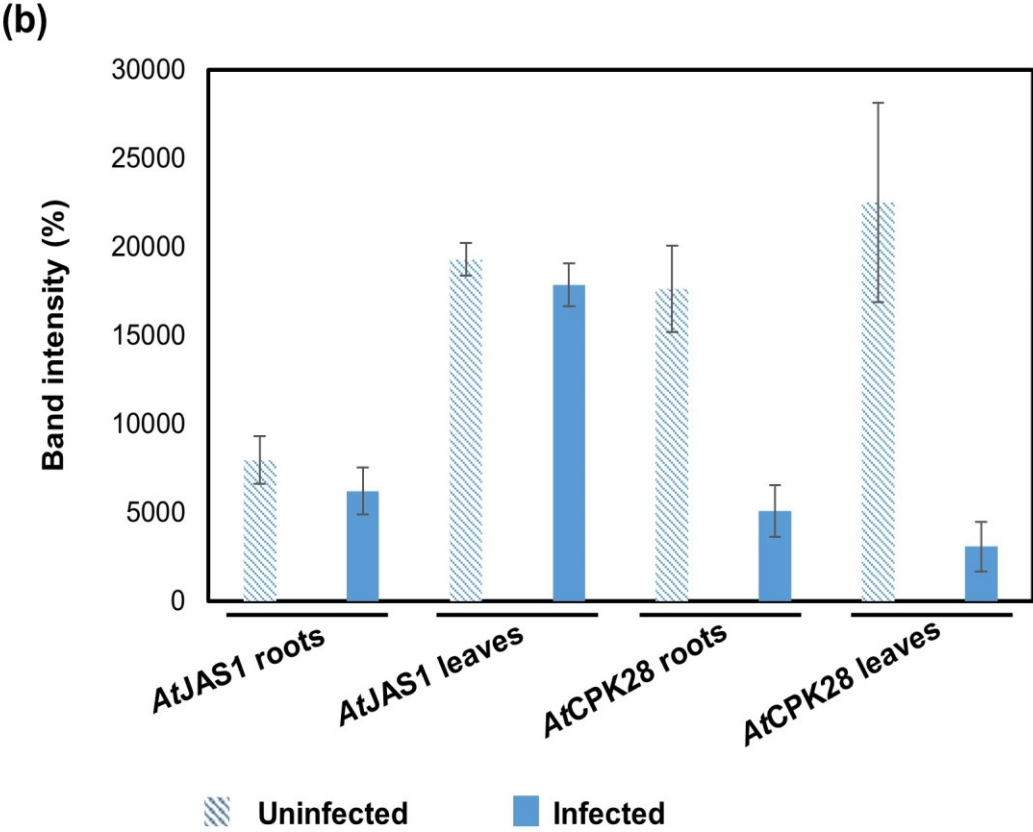
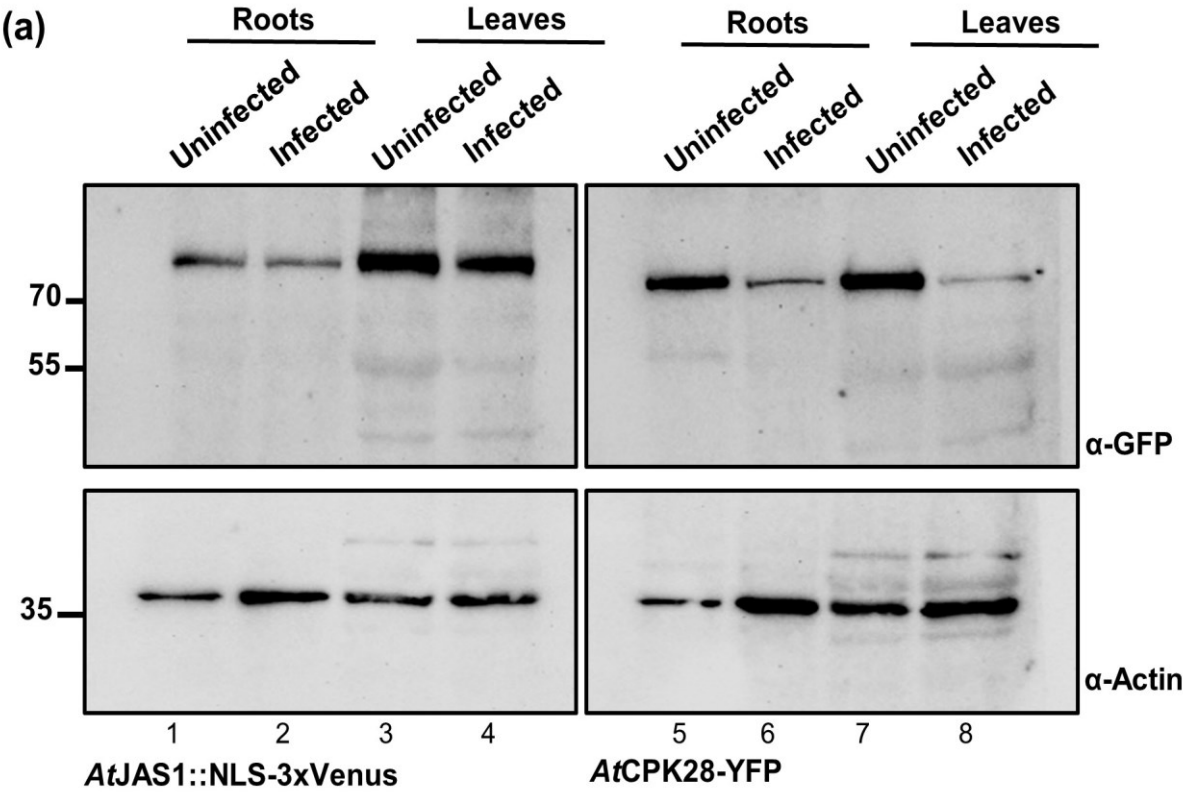
5.18 CPK28 is degraded while JAS1 remains unaffected upon incubation with *T. thlaspeos*

In order to investigate the effect of *T. thlaspeos* on protein level of CPK28 and JAS1, immunoblotting was done on the total protein of the plant material expressing JAS1 tagged with 3x mVenus and YFP tagged CPK28 under the control of 35S promotor upon culture infection. Both tagged lines were inoculated with LF1 culture and plant material (leaves and roots) were harvested after 4 weeks. Healthy leaves and roots of both plant lines were used as a control. Microscopic analysis showed more appressorium like structures in infected *AtJAS1::NLS-3xVenus* line in comparison to wild type plant while the presence of external hyphal mass was comparable to Col-0 (Fig. 5-15c). Afterwards, an equal concentration of protein (1ug) was loaded for each sample, which was controlled by anti-actin for both lines (Fig. 5-15a).

There was no difference observed between inoculated and healthy samples of roots and leaves of *AtJAS1::NLS-3xVenus* (Fig. 5-15a, lane 1-4). Band intensity was same for treated and untreated samples. By contrast, low protein level of CPK28 was observed in the roots and leaves samples inoculated with LF1 culture (Fig. 5-15a, lane 6 and 8). The band intensity of inoculated leaves of *AtCPK28-YFP* line was less than the treated roots of the respective plant and uninfected control samples (Fig. 5-15b). The infection pattern of *AtCPK28-OE1* and *AtCPK28-YFP* was the same (Fig. 5-15c). It is speculated that an unaltered effect of *T. thlaspeos* culture on JAS1 might showed its stability while CPK28 could be degraded partially in the presence of *T. thlaspeos*. These results are also consistent with the fungal growth on *AtJAS1::NLS-3xVenus* lines in culture infections. However, the partial degradation of CPK28 did not affect the growth pattern of *T. thlaspeos* in culture infection and protein level was sufficient to maintain the superficial growth of *T. thlaspeos* in CPK28-OE1 line (Fig. 5-14).

Nevertheless, culture infection system is not established yet and we do not know whether the fungal hyphae is truly colonizing the plant. In addition, no direct colonization has been seen in the leaves during the culture infection but the root colonization might cause an overall stress response and affect the processes occurs in the leaves. However, these results need to be verified by spore infection method for the final conclusion.

Results



Results

(c)

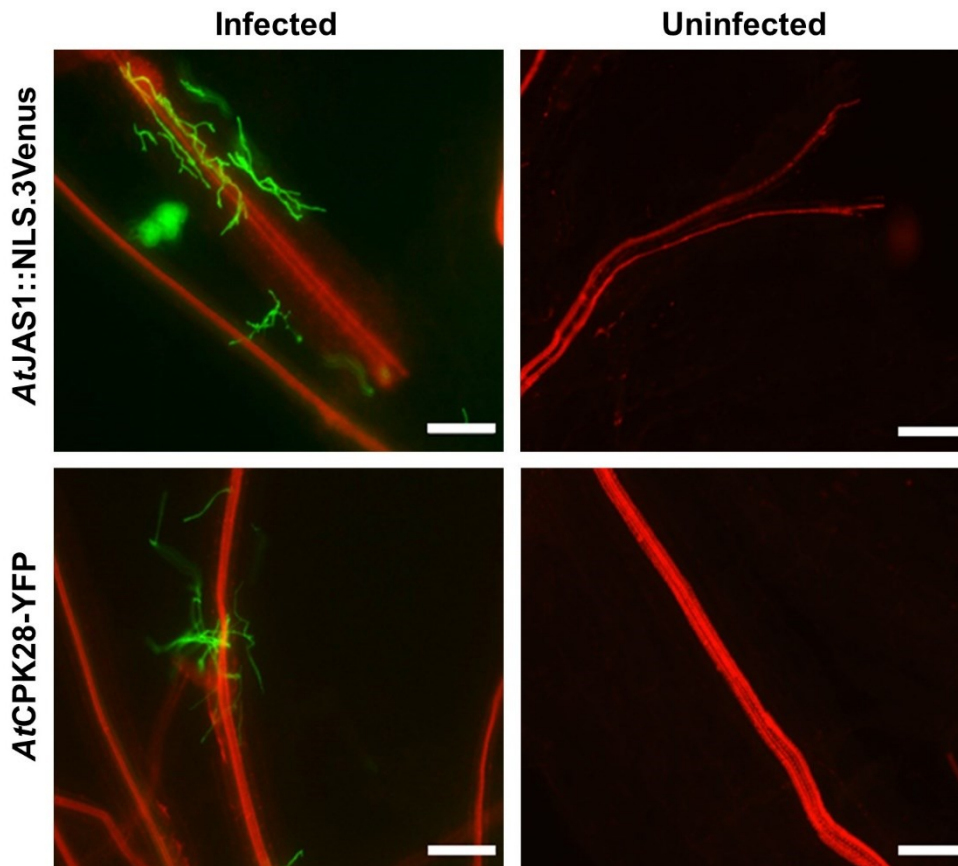


Fig. 5-15. Stabilization of *AtJAS1* and *AtCPK28* upon colonization with *T. thlaspeos*. (a) One-week old seedlings were subjected to *T. thlaspeos* culture infection. Plant tissue were collected from both infected roots and leaves. Uninfected roots and leaf samples were used as a control. Total protein was extracted from 4 weeks old plants. 1 μ g of total protein were loaded for each sample. Western blot was done by using anti-GFP antibodies. The anti-actin antibody was used as a loading control. There was no change found in *AtJAS1* protein in untreated and fungal inoculated root (lane 1-2) and leaves samples (lane 3-4). *AtCPK28* protein expression was less in root (lane 6) and leaves samples (lane 8) treated with LF1 culture in comparison to untreated plant tissues (lane 5 and 7). Sizes: *AtJAS1::NLS.3Venus* 100.4 kDa, 35S *AtCPK28-YFP* 95.6 kDa. (b) Band intensity quantification of infected and uninfected samples of *AtJAS1* and *AtCPK28*. Bands were quantified by imageJ. Error bars represent SD of mean of three replicates. Values showed consistent results as described above. (c) *AtJAS1* and *AtCPK28* colonization by LF1 culture. *AtJAS1* line showed some hyphal and appressorium like structure upon inoculation while very few round head structures were found in *AtCPK28* line. Uninfected control samples of both lines didn't show any fungal mass upon WGA and PI staining. Scale bar 100 μ m.

5.19 *TtTue1* has binding affinity towards host plant DNA

To analyze the DNA binding activity of *TtTue1*, ChIP-Seq was planned but due to time limitations, the sequencing part was not carried out. Nuclear localization of *TtTue1* and prediction analysis of DNA binding residues in *TtTue1* done by Phyre 2 pointed towards DNA binding activity of *TtTue1* (Fig. 5-16e). Leaf tissues of *TtTue1*-Gfp and free GFP line were crosslinked with 1% formaldehyde and further used in the immunoprecipitation experiment. Immunoblotting on total protein extract by anti-GFP antibodies displayed the difference

Results

between crosslinked and non-crosslinked samples. The crosslinked free GFP control has an unspecific shifted faint band (Fig. 5-16a, lane 2), which did not disappear upon DNase treatment on the cross-linked samples (Fig. 5-16a, lane 3). *TtTue1* crosslinked sample showed a shifted band, higher than 130 kDa (Fig. 5-16a, lane 5). DNase treatment of crosslinked *TtTue1* sample caused omission of the shifted band which could be due to the presence of DNA that got degraded by DNase treatment (Fig. 5-16a, lane 6). Due to this quick test a hint for DNA binding affinity of *TtTue1* set the basis for chromatin immunoprecipitation.

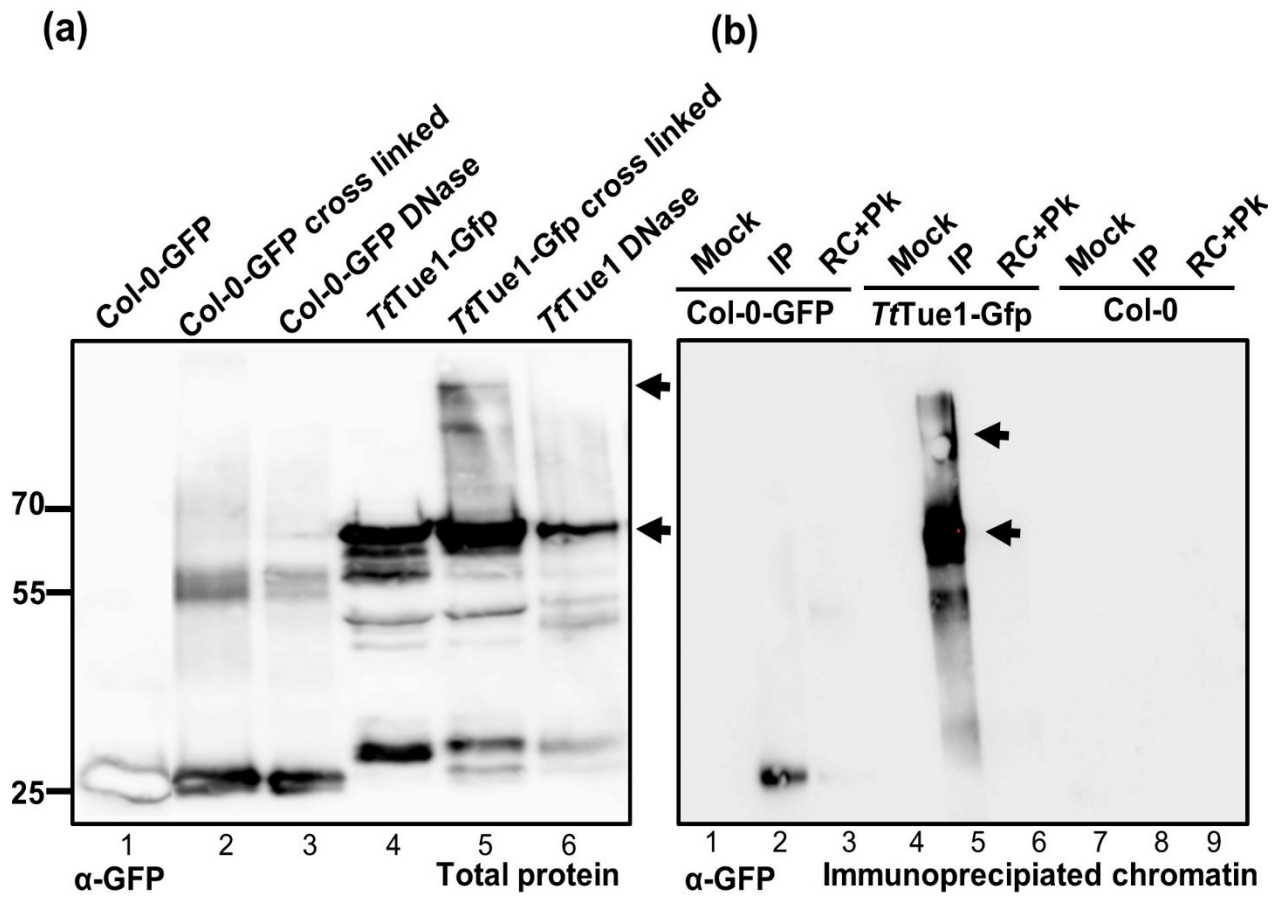
Chromatin material was extracted from crosslinked samples of *TtTue1* and free GFP line and subjected to sonication. A band size in the range of 0.8-1.7 kb was obtained upon sonication (Fig. 5-16d). GFP trap beads were used to pull down the GFP tagged *TtTue1* along with the bound sheared chromatin. To separate the bound chromatin from protein reverse crosslinking and proteinase K treatment were performed which led to the pure DNA sample extracted from DNA-protein complex. In the mock control, samples were treated with agarose control beads and no pull down was expected.

The DNA-protein complex samples after pull down by GFP antibodies were analysed by immunoblot. In *TtTue1*-Gfp samples the extracted chromatin was bound by protein, which appeared in the pull-down fraction in the western blot. DNA-protein complex of free GFP showed free Gfp without any shifted band in the IP fraction (Fig. 5-16b, lane 2), while the mock treated samples did not appear in the blot (Fig. 5-16b, lane 1), which clarified the specificity of only GFP-fused protein binding to the chromatin. Similarly, reverse crosslinking and simultaneous degradation of protein with Proteinase K also caused degradation of bound protein and only DNA was left behind. Therefore, mock control, reverse crosslinking and Proteinase K treatment did not show any band for both free GFP and *TtTue1*-Gfp (Fig. 5-16b, lane 3 and 6). *TtTue1*-Gfp IP fraction showed more or less the same pattern of bands and also a smear ((Fig. 5-16b, lane 5) as it was found in immunoblot done on total protein of extracted from transgenic line before and after cross linking. The expected size of *TtTue1*-Gfp appeared as a thick band with a very clear smear and shifted band which is again higher than the upper most band of the ladder. This type of smear pattern was already provided an indication of nucleic acid binding. All the controls samples: mock, reverse crosslinking and proteinase K treated samples of *TtTue1*-Gfp did not show any bands. A wild type plant Col-0 was used as a control to exclude the possibility of any background noise (Fig. 5-16b, lane 7-9).

The DNA was purified from each sample of DNA-protein complex after degrading the GFP bound protein. The invisible pellet of purified DNA was visualized by glycoblue and eluted for further quantification. DNA concentrations of all input/mock and immunoprecipitated samples were checked by nanodrop and there was difference in DNA concentrations of the control and IP samples. DNA concentration of purified samples were higher as compared to the controls which gave a hint of the presence of more specific targets in the immunoprecipitated samples (Fig. 5-16c).

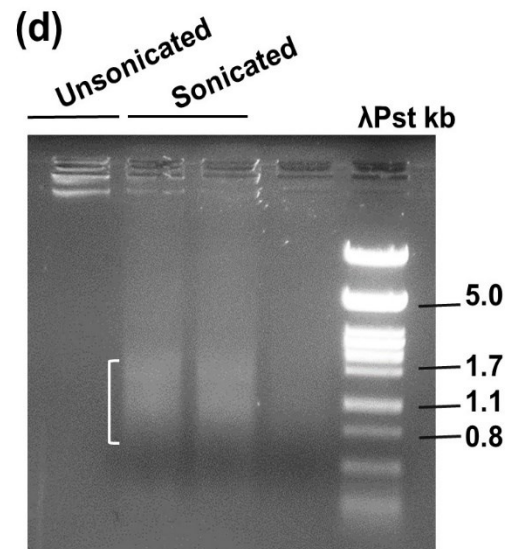
By combining all these results, it seems possible that *TtTue1* displays binding affinity towards DNA, which need to be verified in the future by performing the last set of tests on purified DNA. To identify the targets, qPCR analysis can be done on both DNA samples from free GFP and *TtTue1*-Gfp.

Results



(c)

Sample	Concentrations (ng/ul)
Col-0 Input	0.1
Col-0 IP	0.13
Col-0-GFP Input	0.4
Col-0-GFP IP	14
TtTue1-Gfp Input	0.6
TtTue1-Gfp IP	28



Discussion

Fig. 5-16. *TtTue1* has binding tendency for DNA. (a) Testing DNA binding affinity by total protein analysis of cross linked sample. The cross linking was done with 1% formaldehyde. Total protein and DNase treated samples were used as a control. Western blot done on extracted total protein showed a shifted band in *TtTue1*-Gfp (lane 5) in addition to the expected size band while free GFP control also showed a faint shifted band of a different size (lane 2). The shifted band was disappeared in the DNase treated sample of *TtTue1*-Gfp (lane 6) while it was present in the cross lined GFP sample (lane 3) (b) DNA binding of *TtTue1* was detected by Chromatin immunoprecipitation. GFP-trap magnetic beads were used for immunoprecipitation assay. Similarly, the shifted band pattern for *TtTue1*-Gfp was also detected in the immunoblot analysis of chromatin immunoprecipitated sample (lane 5). The expected protein band disappeared in the sample treated with PK (lane 6). Black arrows indicate the right size of *TtTue1* protein and the shifted band. Mock: agarose control beads samples, IP: immunoprecipitated samples, RC: reverse crosslinked, PK: protinase K. Western blot was done by using Anti-GFP antibodies. Sizes: Col-0-GFP 27 kDa, *TtTue1*-Gfp 59.8 KDa. (c) The DNA was extracted from immunoprecipitated samples and the concentrations were measured by Nanodrop. (d) Sonicated chromatin material of *TtTue1*-Gfp and free GFP line used in the immunoprecipitation. Sonicated samples showed a smear with distinguishable bands in the range of 0.8-1.7 kb while unsonicated sample used as a control. Unsonicated control has running pattern similar to concentrated genomic DNA. (e) DNA binding residues of *TtTue1* predicted by Phyre 2. Alignment with the model residues was based on the hidden Markov models and the different colors indicated the prediction confidence of the program.

6. Discussion

The plant cell depends on the integrated translocation of proteins through various compartments including mitochondria, chloroplast, endoplasmic reticulum and nucleus to coordinate the defense responses. During alarm conditions or upon recognition of pathogen associated molecules, a signal array conveys a message to the plant nucleus to decode the information into a cascade of defense responses of the plant (Deslandes and Rivas, 2011). The effector repertoire of phytopathogenic fungi is often associated with the manipulation of host cellular processes via targeting metabolic signaling and defense pathways (Pradhan et al., 2021). Effectors translocate to the hosts cellular compartments, among them the plant nucleus, which is considered a control panel of all plant processes including the immune responses against various pathogens. In addition, other essential cellular processes such as DNA replication, regulation of the epigenetic state of chromatin, and gene expression are also affected by nuclear effectors (De Mandal and Jeon, 2022). Due to the potential role of effectors in manipulation of nucleus specific plant defense responses, nuclear targeted effectors of *T. thlaspeos* were characterized within the frame of this thesis.

The knowledge of molecular characterization of nuclear localized effectors is limited and only a few examples have been characterized to date such as PopP2, HaRxL44 and well known TAL effectors (see introduction section 1.6.3). Strong interaction of effectors with host plant proteins and exploitation of nuclear regulatory functions indicate that effectors translocate to the plant and provide clues where to look specifically for exploring their molecular mechanism (De Mandal and Jeon, 2022).

My PhD project was driven by the hypothesis that nuclear effectors of *T. thlaspeos* are secreted from the fungus and localize to the plant nucleus where they interfere with the host immune system by protein interaction or by binding the host DNA. On the basis of this hypothesis, the aim was to uncover the role of nuclear localized effectors of *T. thlaspeos* in triggering or suppressing the defense responses of host plants. Initially, I identified 7 putative nuclear localized effectors and confirmed their localization to the plant nucleus, so here after they are

Discussion

called NLS effectors of *T. thlaspeos*. Four out of 7 NLS effectors showed significant disease progression of *P. syringae* (*Pst*-Lux) by promoting the susceptibility of the plant and thus have virulence activity. Lastly *TtTue1* was considered as a top NLS effector candidate from the list of 7 effectors due to its virulence activity and its ability to induce a well pronounced growth phenotype *in planta*. Detailed characterization of *TtTue1* has identified several functionally interesting host targets through Y2H screen. JAS1 and CPK28, which are associated with the host immune system, were the top plant targets of *TtTue1* and are the main highlights of this study. In addition, accumulation of stress related hormones in response to *TtTue1* expression provide evidence for the activation/suppression of immune responses of plants.

Identification of several interesting plant targets of *TtTue1* now opens an avenue to understand the possible multiple/single functions of this effector. Characterization of *TtTue1* provided the foundation for understanding the underlying molecular mechanisms of modulation of the host immune system. Involvement of stress hormonal pathways is another relevant aspect to explore the function of the effector. Evidence of strong and independent interactions with JAS1 and CPK28 found in this study can be used to find the contribution of the novel effector *TtTue1* in *T. thlaspeos* infection.

6.1 Effectors accumulate in the plant nucleus

The *T. thlaspeos* genome shares common characteristics and features typical for smut fungi (Courville et al., 2019). Its predicted functional categories and gene content have overlap with the smut fungi of monocot grasses, despite its adaptation to a dicot host. Nonetheless *T. thlaspeos* genome assembly and annotation brought two unique features to the front. One of them is the lack of conservation of its effectors with the known grass smuts, resulting in the adoption of a unique effector repertoire to maintain its long lasting biotrophic lifestyle (Courville et al., 2019). The catalog of *T. thlaspeos* effector proteins was constructed by using the transcriptome data and 40 genes were shortlisted according to the computational pipeline for identification of effectors (no functional annotation, SignalP and TMHMM). These 40 genes included 19 *Thecaphora*-unique effector (Tue), 9 conserved effectors of *Thecaphora* and its closest homolog *A. flocculosa* (Tae), and 12 conserved effectors of smut fungi (Cep) (Courville et al., 2019).

Such secreted effector proteins of plant pathogenic fungi can remain in the apoplastic space or translocate into the plant cytosol, from where they can move to different intracellular compartments e.g mitochondria, chloroplast or the nucleus (De Mandal and Jeon, 2022). Medium-throughput cell biology screens through transient expression in *N. benthamiana* have been applied on effector libraries of two rust fungi *Puccinia striiformis f. sp. Tritici* and *Melampsora larici-populina* and oomycetes species *Hyaloperonospora arabidopsidis* and *Phytophthora infestans* (Caillaud et al., 2012; Petre et al., 2015). The targeted plant compartments of these 4 pathogens were nuclei, endoplasmic reticulum, tonoplast, chloroplasts, and plasma membranes (Robin et al., 2018).

The allocation of proteins to the nucleus is essential for maintenance of basic cellular processes of eukaryotic cells such as transformation, differentiation, and control of gene expression. It has been shown that nuclear effectors are essential for pathogenesis, but the molecular mechanism of fungal pathogenicity of nuclear effectors is a crucial topic with limited knowledge (Qin et al., 2018; Kim et al., 2020).

Discussion

The catalog of 40 putative effectors (Courville et al., 2019) provided a starting point to identify putative nuclear localized effectors and reveal their role in host-fungus interaction. Presence of an NLS (nuclear localization signal) is a characteristic feature of nuclear proteins (Vargas et al., 2016). The NLS is essential for active transport into the nucleus, which is assisted by importin receptors for efficient migration (Gasiorowski and Dean, 2003). Translocation of proteins occurs through nuclear pore complex which serves as a sieve and controls the transportation of water soluble molecules. Transport is started by binding of importin α to the protein containing an NLS and serves as a bridge for importin β to bind. This trimeric importins/cargo complex crosses the nuclear pore complex and moves to the nucleus (Liu and Coaker, 2008). However, there are some small proteins which can migrate to the nucleus independently of an NLS. Passive diffusion of molecules (up to 60 kDa) can occur through the nuclear pore complex, but the rate of passive transport is very slow for large proteins (over 50 kDa) (Gasiorowski and Dean, 2003). Another study showed that passive diffusion was dramatically reduced beyond a threshold of 30-60 kDa (Timney et al., 2016).

NLS mediated localization of nuclear proteins is a tightly regulated process and several physiological activities are found to be associated with nuclear accumulation of proteins (De Mandal and Jeon, 2022). Scanning of mature effector proteins with three independent prediction tools (NLStradamus, Localizer and cNLSmapper) and the signal comparison in each program identified 7 putative NLS effectors of *T. thlaspeos*. The use of multiple tools is often helpful for prediction of NLS and has been successfully applied to phytopathogenic fungi (De Mandal and Jeon, 2022). The prediction of nuclear effector proteins of *M. oryzae* MoHTRs via three prediction tool identified sixteen NLS proteins from a list of MoHTR1-20 which was previously sorted for transcriptional regulation (Kim et al., 2020). Similarly, the effector repertoire of the smut fungus *U. hordei* was shown to contain NLS candidates. Transcriptome data of infected barley leaves identified 21 out of 273 upregulated effector proteins as nuclear localized effectors (Ökmen et al., 2018). Therefore, prediction of NLS via different tools provided a route to first focus on verification of NLS mediated localization of effectors. Since effectors are defined as small proteins, the possibility of NLS independent transport of protein cannot be excluded (described at the end of this section).

Localization of the 7 NLS effectors *TtTue1*, *TtTue5*, *TtTue10*, *TtTue17*, *TtTae2*, *TtCep3* and *TtCep5* of *T. thlaspeos* to the plant nucleus upon transient and stable expression suggests their interference with host nuclear localized proteins and DNA. Effector localization in heterologous systems can be affected by strong over expression of the protein. However, validation of localization in *A. thaliana* verified the same pattern of signal distribution for all 7 effectors (Fig. 5-2) which support the notion that effectors truly localize to the plants nucleus, if they are translocated into the plant cell. Interestingly, distribution of these 7 effectors in the nucleus was not identical; distinct patterns were found with dual and exclusive localization as detailed here:

- *TtTue5* and *TtCep5* have a dual localization pattern. They accumulate in the nucleus and cytoplasm. A nucleo-cytoplasmic pattern of localization is common, and the majority of the proteins adopts this pattern. Robin et al have provided an inventory of sub-cellular localization of 61 putative effectors of a hemibiotrophic fungus *C. higginsianum*. 40 out of 61 localize both in the nucleus and the cytoplasm, 9 effectors have exclusive nuclear localization, and the rest were distributed in the different cytoplasmic organelles. This distribution indicates that effector proteins can migrate to the specific organelle to carry out their physiological function in the plant cell (Robin et al., 2018). See1, a secreted effector of *U. maydis*, has a role in tumor

Discussion

progression in infected maize. *UmSee1* and its interaction partner SGT1 have dual localization in the nucleus and cytoplasm. *UmSee1* inhibits the MAPK triggered phosphorylation of SGT1, interferes with DNA synthesis and ultimately activates cell division in infected maize leaves. A truncated version of SGT1 lacks MAPK phosphorylation sites which eventually alters the subcellular localization of SGT1. Therefore, *UmSee1* based inhibition of SGT1 phosphorylation might affect the protein localization and interaction (Redkar et al., 2015).

- *TtCep3* shows fluorescence signal in the chloroplast and nucleus. In addition to its central function as the site of photosynthesis, the chloroplast acts as a sensor of environmental and developmental signaling which transmits signals across the nucleus. Thus expression of many nuclear encoded genes is regulated by the chloroplast (Chan et al., 2016). To date, no fungal effector is known with such dual localization pattern of chloroplast and nucleus. However, effectors from many pathogens can have either exclusive chloroplast accumulation or dual targeting in combination with mitochondria. Mitochondria and chloroplast regulate several stress responses through stimulation of fundamental defense signaling e.g, salicylic acid and nitric oxide and accumulation of reactive oxygen species (Littlejohn et al., 2021). Three secreted proteins (CTP1, CTP2, and CTP3) of the rust fungus *Melampsora larici-populina* are imported into the chloroplast upon cleavage of their N terminal signal sequence, which mimics the chloroplast targeting sequence (Petre et al., 2015). *Sntf2*, a secreted effector of *C. gloeosporioides*, migrates to the plant chloroplast when transiently expressed in *N. benthamiana* and performs its role as a suppressor of plant defense mechanisms (Wang et al., 2022). *RsCRP1*, an effector of *Rhizoctonia solani*, a fungus of the Basidiomycota, localizes to both mitochondria and chloroplast and is associated with the disease promotion at early stage of infection (Tzelepis et al., 2021). Hence, it is possible that the observed dual localization of *T. thlaspeos* NLS effectors is important for their function to interfere with cellular processes in the nucleus and cytoplasm or chloroplast.
- Most importantly, I have found four bona fide effectors *TtTue1*, *TtTue10*, *TtTue17* and *TtTae2* that were entirely localized to the nucleus. Notably, the nucleus was the most frequently targeted compartment of the cell in a screen of total 49 effectors from *H. arabidopsidis* with an exclusive nuclear localization of 16 effector candidates (Caillaud et al., 2012). In the nucleus, such effectors can affect a variety of crucial processes for the pathogens benefit, which include coordination of host chromatin in favor of disease development, regulation of gene expression, and DNA replication (De Mandal and Jeon, 2022). *UmNkd1* target maize TPLs (Navarrete et al., 2022) and *UmMer1* target RF12 (Navarrete et al., 2021) are exclusively localized to the nucleus (see section 6.2 for the detailed description). Similarly, *Tip1* and *Tip4* from *U. maydis* accumulate in the plant nucleus, target the host TPL proteins, and induce auxin signaling (Bindics et al., 2022).
- Interestingly, *TtTue10* and *TtTae2* also accumulate in the nucleolus (Fig. 5-3a). The nucleolus is associated with management of several major biological process including regulation of gene expression both at transcriptional and post transcriptional level, ribosome production, mRNA regulation, and spliceosome formation (Kalinina et al., 2018). The role of this nuclear domain is very prominent and therefore considered an important control panel of plant growth and development, and of various disease responses via regulation of signaling pathways (Kalinina et al., 2018). Notably, effector proteins encoded by several pathogens as exemplified below, and especially viral proteins accumulate in the nucleoli, however their molecular

Discussion

mechanisms in regard to the host defense response is still unclear (Kalinina et al., 2018). Nuclear and nucleolar localization of RXLR effectors has been observed and described in the obligate biotrophic oomycete *H. arabidopsidis*. HaRxLR44 localizes to the nucleus and nucleolus of the plant cells (Leonelli et al., 2011; Caillaud et al., 2012). In the nucleolus, it interacts with MED19a, a subunit of the mediator complex, which is responsible for the RNA polymerase II and association of transcriptional regulation. The association between MED19a and HaRxLR44 causes degradation of this mediator complex and leads to switching off the transcription of defense genes to promote plant susceptibility (Caillaud et al., 2013). Thus, it has been shown that not only nuclear localization, but also nucleolar migration of effector proteins has a role in interference with the plant immune system. This specific nuclear and nucleolar localization of two NLS effectors *TtTue10* and *TtTae2* suggests their distinct nucleolar dependent role and they might interfere with nucleolar regulated immune responses of plants.

Although the nuclear localization of all 7 NLS effector candidates was confirmed and it might be interesting to do detailed analysis of both sole and partially nuclear localized effectors, 3 effector candidates *TtTue1*, *TtTue10* and *TtTae2* were prioritized for further analysis based on their significant virulence activity and exclusive nuclear accumulation. To confirm the NLS mediated nuclear localization of effectors, the corresponding NLS sequence was deleted in all 3 effector candidates. NLS deletion of *TtTue1* showed complete exclusion of the fluorescence signal from the nucleus and instead the signal was distributed in the cytoplasm, while *TtTue10* and *TtTae2* NLS deletion only affected the nucleolar accumulation of protein. This deletion analysis indicated that *TtTue1* accumulation in the nucleus occurred through NLS mediated active transport mechanism, while the predicted NLS was only responsible for the nucleolar localization of *TtTue10* and *TtTae2*. Translocation of *TtTue10* and *TtTae2* to the nucleus upon deletion of the predicted NLS might be due to either passive transport to the nucleus or other specific NLS required. A similar observation has been found by Ahmad et al where upon NLS deletion of a poplar rust effector Mlp124478 exclusion of the protein only from the nucleolus was observed. However, virulence activity of the effector was not affected by protein exclusion from the nucleolus (Ahmed et al., 2018).

6.2 Nuclear effectors promote susceptibility and act as virulence factors

A growing number of studies shows that nuclear localized proteins from both host and pathogens, such as effectors, associated R proteins, and other central components of the host e.g regulators and transcription factors, are crucial for the plant immunity. This nuclear dynamic plays an essential role in the regulation of the plant defense system (Deslandes and Rivas, 2012). The success of phytopathogenic fungi mostly depends on virulence factors that are delivered into the host to promote colonization. Nuclear localized effectors either destabilize crucial host components directly or modify host transcription to promote virulence activity. They can also target the resistance protein mediated plant immunity via affecting their sub cellular localization (Rivas and Genin, 2011). The effectorome of *U. maydis* is well studied, including several recently characterized examples such as the a nucleo-cytoplasmic localized effector *UmRip1* (ROS burst interfering protein 1) (Saado et al., 2022). *UmRip1* is a conserved effector of smut fungi infecting monocot species. It is associated with the suppression of PTI responses and interferes with the immunity of maize plants. Nuclear ZmLOX3 interacts with *UmRip1*, which causes the reduction of PAMP-triggered ROS burst responsiveness in maize. *UmMer1*, a member of a cluster of 10 effectors of *U. maydis*, is associated with the suppression of ROS

Discussion

production and the proteosomal degradation pathway in the maize nucleus. *UmMer1* interacts with RF12, a conserved family of E3 ligases which has a role in PAMP triggered ROS-burst. *UmMer1* inhibits the RF12 activity through facilitating its auto-ubiquitination activity, causing proteosomal degradation of E3s and ultimately reducing the ROS burst (Navarrete et al., 2021). *UmVp1*, a nuclear localized effector identified by (Hoang et al., 2021), is upregulated during infection and maintains high expression level throughout the life cycle of the fungus. NLS-mediated localization promotes virulence activity of *UmVp1* which suggested the importance of its nuclear localization. *UmNkd1*, an effector and characterized virulence factor localizes exclusively to the nucleus in heterologous expression systems. *UmNkd1* interacts with maize TPL/TPRs (transcriptional co-repressors TOPLESS/TOPLESS-related) and is responsible for blocking the recruitment of transcriptional repressor of hormone signaling (Navarrete et al., 2022). Besides that, other nuclear localized effectors of *U. maydis* such as *Jsi1* and *See1* are also associated with suppression of plant immune responses (description mentioned in section 6.4.1 and 6.1 respectively according to their specific role). All these effectors of *U. maydis* are highly upregulated during the biotrophic development phase. Similarly, transcriptome analysis has shown that NLS effectors of *T. thlaspeos* were also induced during the infection of the host plant *Ar. hirsuta* (Courville et al., 2019). However, the natural infection system could not be used for *T. thlaspeos* due to some limiting factors such as transformation.

To demonstrate the virulence activity of effector candidates from non-transformable pathogens, heterologous expression systems like the EDV system in bacteria (effector detector vector system or EDV system described in introduction section 1.5.1) are suitable tools. *Pst*-LUX infection of *A. thaliana* transgenic lines expressing the corresponding effector, or effector delivery via *Pst*-LUX into wild type plants are the two different approaches that are used for the virulence activity of NLS effectors of *T. thlaspeos*. This system has been used successfully for detection of virulence activity of several pathogens. For example, Kemen et al showed high virulence activity of several classes of *Albugo laibachii* effectors in a *Pst* DC3000 based heterologous expression system (Kemen et al., 2011). Similarly, another study from Fabro et al., 2011 has shown detailed analysis of virulence function of several nuclear localized HaRxL effectors from *H. arabidopsidis* by observing the enhanced susceptibility of the plant upon delivery of effectors through *Pst*-LUX (Fabro et al., 2011). The virulence activity of 16 effectors CSEPs of poplar rust fungi *Melampsora larici-populina* were analyzed in the EDV system and 5 candidates significantly enhanced the bacterial growth in *planta* (Germain et al., 2018). Thus, it has been observed in several studies that virulence function of the effectors can be detected in heterologous expression system. Similarly, the virulence activity of 7 NLS effector candidates has been observed successfully in the EDV system and 4 candidates have shown significant virulence activity and positively affect the disease progression of *Pst*-LUX.

In *planta*, expression of single effector can affect the plant developmental processes. For example, *TtTue1* causes visible changes in the plant while the other NLS effectors did not have a growth phenotype. A strong dwarf phenotype of untagged *TtTue1* transgenic lines during the vegetative phase had been observed previously (Courville et al., 2019). Similarly, expression of *TtTue1*-Gfp in plant affects both initial and reproductive phases of the plant and causes a strong growth phenotype. Stunted growth of rosettes and shoot and very late flowering with partially abolished seed production of plants expressing *TtTue1* resemble the growth phenotype of a group of nuclear effectors *HaRxLs* with diverse morphological changes. Developmental phenotypes of *A. thaliana* lines expressing *HaRxL* effectors have highlighted

Discussion

the interference of effectors with plant growth regulatory processes. For example, *HaRxLL60*-lines develop smaller and serrated leaves, and both *HaRxLL3*- and *HaRxLL60*-expressing plants show bushy, stunted appearance of shoots during the flowering stage of the plant. *HaRxLL73* expression leads to formation of albino leaves and induces early flowering (Caillaud et al., 2012). *HaRxL106* has been reported to be responsible for susceptibility of *Arabidopsis* (Fabro et al., 2011; Mukhtar et al., 2011) and their expression in *A. thaliana* alters the plant growth in response to light (Wirthmueller et al., 2018). In addition to the observed growth phenotypes, primary leaves of plants expressing *TtTue1* show chlorotic symptoms which turn necrotic in the late growth phase. The overall developmental phenotype highlights the fact that *TtTue1* might interfere with important plant regulatory processes in order to promote virulence (effect of hormones on developmental phenotype described in sec 4.3).

Transgenic lines expressing the other NLS effectors from *T. thlaspeos* have non-significant growth differences. Generation of transgenic line was not successful for *TtCep5* which might be due to lethal effects for the plant. These NLS effectors could have adopted the strategy of weakening the defense responses of the plant instead of interfering with the plant growth. The dilemma of plants to grow or defend has been interpreted a long time ago with a simple model, where most of the metabolic resources consumed upon pathogen attack are for the defense elevation of the plant (Wasternack, 2017). Growth and defense are strongly interconnected processes, therefore *TtTue1* plant might sacrifice the growth of the plant in a transgenic system as a tradeoff for defense, and instead resource allocation has occurred for defense elevation (see section 6.4.2 for the effect of stress hormones on growth of plant). This effect could be due to overexpression of *TtTue1* and might not be obvious in native expression conditions. Conversely, other NLS effectors did not develop any growth phenotypes in the over expression lines which also pointed towards interference of *TtTue1* specifically with the developmental processes. The normal growth of other NLS effectors lines might indicate the consumption of metabolic resources for the morphological development of plant or an alternative explanation could be that they are not recognized by plant receptor protein.

6.3 Identification of plant proteins targeted by *TtTue1*

Migration of effector proteins to the host cellular compartment and specifically to the nucleus is the indication of manipulation of cellular process by interacting with nuclear proteins or the DNA of the host. The DNA binding tendency of *TtTue1* was shown by Chromatin immunoprecipitation (Fig. 5-16) but the qPCR analysis was not done on the obtained DNA sample which identifies and confirm the plant targeted promoters. Therefore, further investigation is suggested for future experiment to confirm the plant promoters bind by *TtTue1*. Hence, this study mainly focuses on the interaction between *TtTue1* and plant proteins to elucidate its molecular function. Nuclear accumulation, virulence activity and a strong developmental growth phenotype ranked the *TtTue1* on top, which indicates that *TtTue1* could manipulate cellular processes by interfering with nuclear plant proteins. Such interactions of many nuclear effectors and the corresponding host defense responses have been described for several effectors and their interaction partners respectively e.g Nkd1 and TPLs, Tip1, Tip4 and TPLs, See1 and SGT1, Rip1 and ZmLOX3, Jsi1 and TPLs, and Mer1 and RF12 (find detailed description and references in section 6.1, 6.2 and 6.4.1).

To identify potential plant interaction partners of *TtTue1*, a Y2H screen was carried out using a stress induced library of *A. thaliana* (Matiolli and Melotto, 2018). This screen initially identified

Discussion

129 targets and their enrichment analysis identified several stress related categories. Within these the most relevant were; response to stress, response to cold, and response to biotic stimuli. These stress related categories indicated that *TtTue1* might trigger plant immune responses in *A. thaliana*. Manual evaluation of the targets from the mentioned categories resulted in the selection of 12 significantly abundant potential *TtTue1* interaction partners (Table. 3) that function in defense related cellular processes. Based on their cellular function, manipulation by *TtTue1* with these targets could likely result in interference with the plant immune response. A cDNA library screen for lettuce proteins against the effectors of *Bremia lectucae* revealed total of 21 interaction partners and an average of 3 targets were found for an individual effector. Y2H screen for other pathogens also show an average of 3.4 interacting partners per effector of *H. arabidopsidis*, *P. syringae* and *G. orontii* against an *A. thaliana* library of ~8000 immune- related full-length proteins (Mukhtar et al., 2011; Weßling et al., 2014). The obtained number of *TtTue1* interactors is significantly higher. Although the selected interactors were verified in targeted Y2H assays but their interaction should be confirmed via other techniques e.g CoIP and BiFC. The quantitative analysis (MST) of *TtTue1* binding to verified plant targets indicated the possibility of two-sites binding (Fig. S8) which support the perception of more than one target of *TtTue1*. PopP2 is a multi-plant target effector encoded by *R. solanacearum* that suppress the host plant immunity by acetyltransferase activity. RD19, RRS1, some of WRKY transcription factors and recently characterized EDS1 and PAD4 physically interact with PopP2 (Huh, 2021). This example indicated that effectors can targets more than one proteins and interfere with different cellular functions.

Large scale approaches such as Y2H screens and mass spectrometry can provide preliminary data for putative interaction partners (Weßling et al., 2014; Petre et al., 2016) which is usually verified by at least two independent techniques in a heterologous system or in the host plant (Kudla and Bock, 2016). Nevertheless, the large scale screen provided a potential lead in the form of the two prime candidates JAS1 and CPK28 from the list of selected 12 targets. JAS1 was selected on the basis of exclusive localization in the nucleus, and its biological function as an important component of the stress hormone signaling pathway. CPK28 was selected due to the highest number of hits found in Y2H screen for independent yeast transformants. Interaction of *TtTue1* and both targets JAS1 and CPK28 were validated by targeted Y2H assay (Fig. 5-7), BiFC (*In vivo*) (Fig. 5-8), GST pull down assay (Fig. 5-9) and microscale thermophoresis (MST) (*In vitro*) (Fig. 5-10). Since *A. thaliana* is not a natural host of *T. thlaspeos*, the interaction of *TtTue1* with *Ar. hirsuta* homologs of both JAS1 and CPK28 were also tested in the mentioned four independent systems including targeted Y2H assays. *TtTue1* showed strong interaction with JAS1 and CPK28 homologs of *Ar. hirsuta* and indicated that it can target the similar pathways in the natural infection system.

JASMONATE ZIM-domain (JAZ) proteins are repressors of jasmonate (JA) signaling (see introduction section 1.5.2, Fig. 1-2, 1-3) (Chung et al., 2009), and it is a family of 13 members called JAZ1-JAZ13 (Chini et al., 2016; Howe et al., 2018). JAZ proteins interact with and cause repression of various transcription factors under low JA-Ile levels, the active form of JA (Chini et al., 2007; Thines et al., 2007). Until now, the well-studied transcription factor is MYC2 and its paralogs that interact with JAZs (Kazan and Manners, 2013; Figueroa and Browse, 2015). JAZ proteins on one hand regulate jasmonate signaling via JAZ-MYC2 and on other hand inhibit the transcriptional activity of EIN3 in ethylene signaling that activate the ORA59/ERF1 to induces the expression of *PLANT DEFENSIN 1.2 (PDF1.2)* (Yang et al., 2019). JAS1(JAZ10), one of the members of the JAZ family is a negative regulator of jasmonic acid (JA) signaling and development of disease symptoms in response to *P. syringae* strain

Discussion

DC3000 (Agnes et al., 2012). *AtJAS1* is a nuclear localized protein (Moreno et al., 2013), and my transient expression in *N. benthamiana* showed that *ArhJAS1*-Gfp also localized to the plant nucleus (Fig. 5-11). Therefore, the co-localization signal for both *AtJAS1* and *ArhJAS1* were detected in the plant nucleus upon interaction with *TtTue1* as depicted by BiFC data. Similarly, targeted Y2H assay and GST pull down also showed strong interaction between *TtTue1* and *JAS1* of both *A. thaliana* and *Ar. hirsuta*. Likewise, a GST pull down assay showed strong interaction between *P. syringae* effector HopZ1 and *GmJAZ1* which was verified by BiFC data that shown the co-localization of both proteins in the nucleus of *N. benthamiana* (Jiang et al., 2013). The dissociation constant (KD) values of *TtTue1* and *JAS1* binding in MST experiment showed much higher binding affinity (Table. 4). The CT-*AtJAS1* and *ArhJAS1* have binding affinity in nanomolar except full length *AtJAS1* which showed that truncated version of *AtJAS1* strongly interact in comparison to full length protein (See section 6.4.1). However, the protein folding could be different in *ArhJAS1* and its binding domain is easily accessible to show strong interaction in full length *ArhJAS1*. This quantitative analysis detected the strong interaction which is hard to identify by qualitative methods and it also varies among *in vitro* and *in vivo* techniques.

CPK28 is a member of the calcium dependent protein kinase family, and acts as a negative regulator of pathogen triggered immune responses (PTI). CPK28 targets and phosphorylates BIK1, a plasma membrane associated cytoplasmic kinase which is associated with PRR complexes (Monaghan et al., 2014). Besides that, CPK28 is also considered a key negative regulator of growth phase-dependent defense responses (Matschi et al., 2015). At the seedling stage, ROS mediated defense signaling is regulated by CPK28 while in mature plants, CPK28 controls plant developmental processes by maintaining the balance between the phytohormones JA and GA (gibberellic acid) without interfering with jasmonic acid-related defense responses (Matschi et al., 2015). JA and GA act antagonistically to keep the balance between triggering defense and growth induction (Kazan and Manners, 2012). JA accumulation in plants leads to the reduction of GA biosynthesis (Heinrich *et al.*, 2013) and wild type plants treated with JA showed accumulation of GA repressor DELLA proteins (Yang et al., 2012). In a *cpk28* mutant the consecutively repressed activity of DELLA proteins lead to an elevated JA gene expression (Navarro et al., 2008). Constitutive activation of DELLA proteins stabilizes it and could be a cause of an increased level of JA signaling in the *cpk28* mutant (Matschi et al., 2015). CPK28 is a plasma membrane localized protein, and the interaction of NLS effector *TtTue1* with both *AtCPK28* and *ArhCPK28* might caused their re-localization to the nucleus, which is obvious from the detection of nuclear localized fluorescence signal upon interaction in BiFC assay (Fig. 5-8). Similarly, transient expression of CPK28-GFP of *Ar. hirsuta* showed nucleo-cytoplasmic localization in *N. benthamiana*. It has been shown (Pelgrom et al., 2020) that several target proteins re-localized to different compartments instead of the original localization upon interaction with effectors. For example, co-localization of a nuclear localized effector of *B. lactucae* BLR38 with its host interacting partner LsFLX-like2 caused re-localization of the host protein to the nucleus. LsFLX-like2 is predominantly localized to punctate cytoplasmic structures and co-expression with its interacting effector shifted the localization to nucleus (Pelgrom et al., 2020). Verification of re-localization of CPK28 to the nucleus can be done by *T. thlaspeos* spore infection of the *AtCPK28*-YFP transgenic line.

Additionally, the targeted Y2H assay, GST pull-down and MST also confirmed the interaction between *TtTue1* and CPK28 of both *A. thaliana* and *Ar. hirsute*. The dilution series of targeted Y2H assay (Fig. 5-7) showed slightly weak interaction of *ArhCPK28*. Similarly, the dissociation

Discussion

constant of *ArhCPK28* is little higher than *AtCPK28* (Table. 4, Fig. 5-10) in MST experiment which also indicated a slightly less binding affinity between *TtTue1* and *ArhCPK28*. Although both *AtCPK28* and *ArhCPK28* were detected in the immunoblot blot analysis of GST pull-down assay of *TtTue1* but their coomassie brilliant blue staining showed faint bands (Fig. 5-9). This might be due to the less protein used and can be improve by increasing the protein concentration to several fold. The GST pull-down can also perform by using the cell lysate of *TtTue1* and *ArhCPK28*.

Both interacting partners JAS1 and CPK28 are involved in regulation of plant hormone signaling. Therefore, it was anticipated that *TtTue1* might alter the stress related phytohormones in order to facilitate the pathogen proliferation or only trigger the plant immune responses.

6.4 Modification of plant hormone signaling in response to *TtTue1*

Plant pathogens can modulate host cell biology through various means including manipulation of plant hormonal signaling which consist of primary defense hormones JA (jasmonic acid), SA (salicylic acid), and ET (ethylene), while ABA (abscisic acid), GA (gibberellic acid), IAA (auxin), CK (cytokyanin), BR (brassinosteroid), and SLs (strigolactones) either independently regulate the defense responses or perform a combined role with primary defense hormones (Kazan and Lyons, 2014). Here, I will focus on primary defense hormones due to their relevance for this study. The primary defense hormones are the major players in plant immunity. The SA- and JA/ ET-mediated signaling pathways are considered key modules of the plant immune system (Li et al., 2019). The SA mediated defense responses contribute to defense against biotrophic pathogens and perform a function in developing local and systemic-acquired resistance, while JA/ET-mediated responses are affective against necrotrophic pathogens. SA and JA/ET often perform their functions antagonistically (Li et al., 2019) while SA and JA also interact synergistically to fine tune plant immunity, which can be exploited by pathogens to increase plant susceptibility (Berens et al., 2017).

6.4.1 SA and JA/ET signaling and related transcriptional profile of *TtTue1*

Previous and recent studies have uncovered several bacterial and fungal effectors that target and manipulate the phytohormone signaling by modifying or hijacking it, such as the fungal effectors *UmCmu1* (Tanaka et al., 2015), *UmJsi1* (Darino et al., 2019), *UmNkd1* (Navarrete et al., 2022), *FoSix8* (Gawehns et al., 2014) and *VdVdIsC1* (Liu et al., 2014), and bacterial effectors *PsHop11* (Zhou and Chai, 2008), *PsHopZ1a* (Jiang et al., 2013), *PsHopX1* (Gimenez-Ibanez et al., 2014), *EAAvrRpt2_{EA}* (Schröpfer et al., 2018), Oomycete effectors *PsPsIsC1* (Liu et al., 2014), *HpaHaRxL44* (Caillaud et al., 2013) and a symbiotic effector *LbMiSSP7* (Plett et al., 2014) interfere with plant hormone signaling. However, this study mainly focuses on hormonal pathways targeted by nuclear effector. The stress related hormones were examined in transgenic lines expressing *TtTue1*, and elevated levels of salicylic acid (SA) and its derivatives salicylic acid O- β -glucoside (SAG) were found. Similarly, the level of the entire stress related hormonal cascade including pipecolic acid and its derivative N-hydroxypipecolic acid (NHP) and camalexine was high (Fig. 5-13), which is the common stress responses of a plant against biotrophic (Shields et al., 2022) and hemibiotrophic fungi (Bohman et al., 2004) respectively. Similar hormonal alteration has been noted for other effectors upon colonization of their host plants, including *UmJsi1*, *FoSix8* and *EAAvrRpt2_{EA}* (described below in this section).

Discussion

The upstream component of the JA signaling pathway was identified through protein-protein interaction. *TtTue1* targets JAS1 which binds MYC transcription factors and represses the expression of downstream JA responsive genes. JAS1.1, the splice variant of JAS1 found in the Y2H screen, consist of three domains: N-terminal CMID, central ZIM and C-terminal Jas domain. The protein alignment of *AtJAS1* and *ArhJAS1* showed that these three domains are conserved in *ArhJAS1* (Fig. S6). The C-terminal part is highly conserved; Jas motif is involved in repression of JA signaling through binding MYC transcription factor (Chung and Howe, 2009). The strong interaction between CMID and N-terminal MYC was also shown but the sequences of the CMID and Jas motifs have dissimilarities and also the mode of action differs (Zhang et al., 2017). While the central ZIM domain is important for JAZ homo- and heterodimerization (Demianski et al., 2012). An increased binding affinity of JAS1 and *TtTue1* was detected in the N-terminally truncated version of CT-*AtJAS1* protein having only central ZIM domain and C-terminal Jas domain (Fig. 5-9, 5-10, S7). The C-terminal *AtJAS1* with both ZIM and Jas motifs was selected for protein purification due to less stability of small truncations. Recently, the crystal structure of *TtTue1* was solved by Dr. Florian Altegoer in our group suggesting that *TtTue1* has structural homology to the JAS interacting domain (JID) of MYC3 transcription factor, which indicates that *TtTue1* could compete with MYC3 for binding to JAS1. Conversely, the higher binding affinity between *TtTue1* and CT-*AtJAS1* suggests that *TtTue1* binds to JAS1 through Jas domain. The similarity between *TtTue1* and MYC3 interacting domain strongly suggests that *TtTue1* can bind either to CMID or Jas domain of JAS1 while the high binding affinity of CT-*AtJAS1* clearly indicated the binding via Jas domain. The ZIM domain can not bind directly to MYC transcription factors therefore probability of interaction with ZIM domain is rather low. However, analysis of Jas motif independently, is suggested for the further verification in future. Moreover, Jas domain is also necessary for binding of COI1 to JAS proteins for its subsequent degradation (Melotto et al., 2008). *TtTue1* binding at jas domain can also mask this site from COI1 binding and might protect the JAS1 from getting targeted by SCF-COI1 complex. Hence, JAS1 could be present in a stable and functional state. The JAS1 protein content was checked in its transgenic lines colonized by *T. thlaspeos* which showed the same protein level in both colonized and healthy samples (Fig. 5-15). This protein level indicated that JAS1 is stable and not degraded in the stressed condition however this is an indirect evidence for stabilization of JAS1 upon *TtTue1* interaction. The CMID domain of JAS1 could be available to bind to MYC3 together with *TtTue1* and work as a complex to repress the downstream JA-responsive genes, thus favoring the suppression of JA signaling (Fig. 6-1). However, the hypothesis of competition between *TtTue1* and MYC transcription factor is based on the crystal structure of *TtTue1* and needs to be experimentally verify.

Transcriptome analysis of infected *Ar. hisuta* plants showed low transcript level of early JA-responsive genes JAZ5, JAZ6 and JAZ9 which indicated that less accumulation of JA is expected. Absence of MYC2 or MYC3 transcripts in the transcriptomic data of *TtTue1* transgenic line also pointed towards repression of their transcription activity. Similarly, the JA-responsive genes that act downstream of MYC transcription factor and regulate various JA dependent cellular process were not induced in the infected *Ar. hisuta* as well as in the transgenic *TtTue1* line. These genes set include ERF2, ERF3, MYB51, MYB34 (Raza et al., 2021), WRKY26, WRKY33 (Dombrecht et al., 2007) and NAC TFs (ANAC019 and ANAC055) (Raza et al., 2021). ERF2 encodes a positive regulator of JA-responsive defense genes and overexpression of ERF2 leads to increase resistance against *F. oxysporium* in transgenic lines (McGrath et al., 2005). ERFs are involved in JA synthesis and plant defences responses. The MYB transcription factors control the synthesis of secondary metabolite such as

Discussion

glucosinolates. WRKYs play vital role in plant defence responses and JA synthesis. Similarly, NACs transcription factors are also involved in plant development and defence response (Ruan et al., 2019) and specifically modulate the cell division, seed growth and secondary cell wall synthesis (Raza et al., 2021). Most importantly the marker gene *PDF1.2* of JA signaling was not expressed in the transcriptome of *TtTue1* transgenic line and neither found in transcriptional data of infected *Ar. hirsuta*. All these evidences strongly support the downregulation of JA signaling during the *T. thlaspeos* infection as well as in response to *TtTue1*.

Furthermore, JAZs also target the EIL2/EIN3 to inhibit their transcriptional activity in the ET signaling pathway. EIL2/EIN3 activate the downstream genes such as *ORA59/ERF1* which also induces the expression of *PDF1.2* thus activate immune responses against hemibiotrophic and necrotrophic pathogens (Zhu et al., 2011). JA and ET transcriptionally control the activation of *ERF1* and *ORA59* (Lorenzo et al., 2003; Pré et al., 2008). In response to *TtTue1* overexpression *in planta*, *ERF1*, a transcriptional regulator of ERF branch of JA signaling (see introduction section 1.5.2) was highly induced and also in the transcriptome analysis of *Ar. hirsuta* homologs (Courville et al., 2019). This signaling pathway is generally associated with the resistance against necrotrophic pathogens (Hou and Tsuda, 2022). It has been shown that ERF and MYC branch are antagonistic to each other (Aerts et al., 2021). Therefore, upregulation of *ERF1* and absence of *MYC3* transcripts in *TtTue1* transgenic line and in the infected *Ar. hirsuta*, indicated the interference of *JAS1* with MYC branch of JA signaling. *JAS1* could get stabilized upon interaction with *TtTue1* and might inhibit the MYC branch of JA signaling which is also evident from their non-induced downstream JA-responsive genes. Thus, *TtTue1* might stabilize *JAS1* which normally get degraded by SCF-CO11 complex in the stressed condition (Fig. 6-1). In contrast, upregulation of *ERF1* but no expression of their marker gene *PDF1.2* and *VSP2* might suggest post-transcriptional regulation of ERF branch of JA signaling.

The transcriptome analysis of infected *Ar. hirsuta* and *TtTue1* transgenic line showed there might be less accumulation of JA upon *T. thlaspeos* infection which ultimately facilitate plant colonization. Most pathogens can interfere with plant hormone signaling at different level. There are examples of hemibiotrophic fungi that metabolize plant produced jasmonic acid: *M. oryzae* synthesizes an antibiotic biosynthetic monooxygenase (Abm) which depletes JA by converting it into inactive 12-OH-JA in order to facilitate host colonization (Patkar et al., 2015; Zhang et al., 2017). In contrast, in the incompatible interactions between *M. oryzae* and rice, Abm undergoes degradation after secretion, ultimately leading to the accumulation of methyl jasmonate signaling and the activation of plant immune responses (Yang et al., 2019). These examples gave evidence that effector mediated downregulation of JA signaling pathway promotes colonization. The effect of *TtTue1* on *Ar. hirsuta* or *A. thaliana* colonization can be detected by analyzing the changes in deletion mutant. Related to hormone crosstalk, the interaction of *Hpa* NLS effector HaRxL44 and the nucleolar Mediator subunit 19a (MED19a) was described above. Their interaction activates the transcription of plant defense genes and switches salicylic acid signalling to JA/ET responsive pathways. Lastly, parallel activation of both hormone pathways was observed: Liu et al. showed that Vd424Y, a secreted NLS protein of *V. dahliae* responsible for full virulence, can induce cell death of the plant dependent on BAK1 and SOBIR1, and activates both SA and JA signaling pathways of the host (Liu et al., 2021). JA and ET act synergistically and are well-coordinated for the regulation of stress responses (Yang et al., 2019). Therefore, I would expect that ethylene will also be

Discussion

downregulated in response to *TtTue1* and facilitate the infection, similarly to PsAvh238, an effector of *P. sojae* targeting soybean Type2 ACSs (GmACSs) which is a precursor of ET biosynthesis. This interaction lead to the suppression of ET biosynthesis and eventually promotes the infection of *P. sojae*. Similarly, inhibition of ET synthesis or signaling through chemical and silencing of GmACSs also results in elevated virulence activity of *P. sojae* (Yang et al., 2019). However, ethylene levels were not measured in this study, thus it would be interesting to include ethylene measurements in future experiments.

TtTue1 expression in *A. thaliana* leads to the activation of SA signaling as evident from an increase of total SA and its derivatives (Fig. 5-13). Transcriptome analysis of natural host *Ar. hirsuta* infected by *T. thlaspeos* revealed an upregulation of SA responsive genes such as SA reporter genes *PR1* and *PR2*, the receptor and co-activator *NPR1/NIM1*, responsive gene of systemic acquired resistance *NPR1*, *EDS1* and *PAD4* (Courville et al., 2019). In contrast, *PR1* expression was not highly induced in the *TtTue1* overexpression line, indicating that the transcriptional regulation of SA responsive genes might be different in this line compared to *T. thlaspeos* infected *Ar. hirsuta* (Courville et al., 2019). Overall increase in the total SA level and expected low JA indicate that there might be cross talk between SA and JA (see introduction section 1.5.3) (Caarls et al., 2015) in reponse to *TtTue1*. Reciprocal crosstalk of SA and JA also exist in rice and seems to be conserved (Yuan et al., 2007) but each hormone offers resistance against pathogens with different lifestyles (De Vleeschauwer et al., 2014). SA acts antagonistically to JA/ET, and thus high SA levels decrease the accumulation of ethylene responsive transcription factor ORA59 while ERF remains active in the high SA environment (Van der Does et al., 2013). Similar trend of these genes expression has been found in the transcriptome dataset of the *TtTue1* transgenic line and infected *Ar. hirsuta*. An upregulation of *ERF1* but no *ORA59* was detected, which might be due to high SA levels. Thus gene expression analysis of SA and JA regulatory pathway correlates with the total increase the of SA level and its derivatives in *A. thaliana* expressing *TtTue1*. Overall transcriptome analysis of infected *Ar. hirsuta* and *A. thaliana* expressing *TtTue1* presented consistent results regarding the induction of JA/ET responsive genes while some differences were found in SA marker genes expression in both transcriptomic data. The co-relation between the transcriptomic and metabolomic datasets either in response to fungal attack (*T. thlaspeos*) or in presence of a single effector (*TtTue1*) support the coordination between SA and JA/ET responsive genes and their hormones level. The elevation of SA levels can be initiated due to the interaction of *TtTue1* and *JAS1*, which triggers the host immune system. *TtTue1* can stabilize the *JAS1* which is responsible for repression of transcription factors of MYC branch of JA signaling pathway and importantly high SA level also cause degradation of ORA59 which is a positive regulator of ERF branch of JA signaling pathway (Caarls et al., 2015). A similar effect on the plant immune system has been observed by Darino et al, upon *UmJsi1* and TPL interaction. *UmJsi1* is a nuclear effector that interacts with TOPLESS in maize and activates the ERF branch of the JA/ET signaling pathway (Darino et al., 2019). Overexpression of *TtTue1* *in planta* or their translocation through bacterial delivery, both increased the susceptibility to biotrophic infection which shows that high SA might not interfere with susceptibility in this context. However, the SA level was not measured in the *TtTue1* transgenic lines challenged with *Pst-LUX* infection, nor in the *A. thaliana* wild type plant that has *TtTue1* delivered through *Pst-LUX*, which is suggested for future verification. Supporting this hypothesis, high SA signaling in *UmJsi1* expressing plants also did not affect the plant susceptibility towards *P. syringae* infection (Darino et al., 2019).

Discussion

TtTue1 in *A. thaliana* might trigger the plant immune system and inhibit JA/ET signaling by inducing high SA levels (Caarls et al., 2015) which might result in balanced growth of the fungus in the plant. Another explanation for high SA and expected low JA levels in the plants expressing *TtTue1* might be the result of the tradeoff between growth or defense. Therefore, plant might has adopted the defense strategy by utilizing resources to fuel the defense responses instead of morphological development, which could be a different scenario to the natural infection system. While on the other hand, downregulation of the JA pathway was shown to be an important strategy for successful infection, which is obvious from the susceptibility of plants in the presence of *TtTue1*. Six8, an effector of *F. oxysporum* interacts with TOPLESS, activating SA defense signaling in *A. thaliana* and has a temperature dependent stunted phenotype (Gawehns et al., 2014). An elevated SA level and low JA was observed in the plant expressing *AvrRpt2_{EA}* which showed a severe necrotic phenotype and was declared as a virulence factor (Schröpfer et al., 2018). Similarly, *TtTue1* might equally contribute to both susceptibility and altered morphology of the plant. The host plant infection with the wild type *T. thlaspeos* did not show any growth or infection phenotype except replacement of the seeds with spores however, infection with the *TtTue1* mutant strain might give some interesting insights.

Pipecolic acid, a non-protein amino acid, and its hydroxylated derivative NHP (*N*-hydroxypipecolic acid) are also involve in plant immunity and induce SA accumulation (Návarová et al., 2012; Hartmann et al., 2018). An increased level of Pip and NHP in response to *TtTue1* (Fig. 5-13) is consistent with the finding that high SA levels also favor NHP elevation during the stress condition. Both SA and NHP have common regulators and they can perform their functions synergistically in order to induce SAR (Zeier, 2021). SA accumulation also requires the NHP biosynthetic enzymes *ALD1*(*AGD2-LIKE DEFENSE RESPONSE PROTEIN 1*) and *FMO1*(*FLAVIN-DEPENDENT MONOOXYGENASE1*), which explains the association between these two metabolites (Mishina and Zeier, 2006; Cecchini et al., 2015). The cooperation between SA and NHP-mediated signaling depends on the common coactivator NPR1 (Návarová et al., 2012; Yildiz et al., 2021). Additionally, *EDS1* and *PAD4* also control SA/NHP accumulation (Hartmann and Zeier, 2019; Zeier, 2021). Therefore, the transcriptional activation of these protein could also be responsible for upregulation of NHP and its precursor Pip.

In addition to transcriptome analysis, other potential interaction partners of *TtTue1* identified in Y2H screen were AOC2 and AOC3, and enrichment analysis showed their significant abundance. However, the interaction between *TtTue1* and AOCs was confirmed by targeted Y2H assay and not verified yet through other independent techniques. ALLENE OXIDE CYCLASE (AOC) are catalyzing components of JA synthesis. AOCs are the enantiomeric structures of jasmonates and 4 genes encode for individual functional polypeptides, including AOC2 and AOC3. AOCs temporally and spatially fine tune the JA synthesis by possible heteromerization of AOCs and their differential expression (Stenzel et al., 2012). The non-induced transcriptional profile of JA regulatory components also indicates that the interaction of *TtTue1* with the catalyzing components (AOCs) of JA synthesis might cause an inhibitory effect on AOCs that could results in dropping of the JA level. Additionally, cold induces expression of AOCs are also involve in JA biosynthesis (Pandita, 2022). Cold induces the expression of JA synthesis-related genes, AOS1, DAD1, AOC, LOX2, and AOS1, that synthesizes the bioactive JA-Ile. JA-Ile activates the JA receptor COI1 which bind to JAZ1, resulting in JAZ1 degradation via the 26S proteome after ubiquitination (Zhu, 2016; Hu et al., 2017). Transcriptomic data of *TtTue1* transgenic lines also provided 4 out of 12 downregulated

Discussion

genes which represented the cold acclimation. However, the protein interaction of those 4 genes were not detected in Y2H screen. The overall scenario could be different in the natural infection system of *T. thlaspeos* for the hormone level.

CPK28 is a plasma membrane localized protein and a negative regulator of PTI responses as described above. In this study, assays were done to correlate its previously identified function in presence of *T. thlaspeos*. CPK28-YFP plants treated with *T. thlaspeos* culture showed protein accumulation to a lesser extent in comparison to untreated plants, which could give a clue about destabilization of CPK28 (Fig. 5-15). However, this is not a direct evidence for the effect of *TtTue1* on CPK28. To support this hypothesis, the experiment could be repeated by doing a comparison between wild type and deletion strain of *TtTue1*. The growth phenotype of *cpk28* (described in sec 6.4.2) also correlates with the *TtTue1* phenotype and is in favor of the hypothesis that CPK28 degradation is facilitated by *TtTue1* interaction. The protein analysis showed less accumulation of CPK28 upon colonization by *T. thlaspeos* as compared to uninfected controls (Fig. 5-15) which also pointed towards degradation of CPK28. Another indirect explanation for CPK28 destabilization by *TtTue1* came from accumulation of ROS in transgenic plants expressing *TtTue1* (Fig. 5-12). According to the function of CPK28 (explained above), pathogen triggered immunity should be compromised in presence of CPK28 as it is a negative regulator of PTI responses. A functional CPK28 protein could help *TtTue1* in inhibition of PAMP triggered immunity after interaction, but *TtTue1* plants showed normal ROS production in three independent experiments which also supports that *TtTue1* might destabilizes or degrade CPK28. ROS production is also linked with the accumulation of stress related hormones, which is consistent with the observed high SA levels. However, there is not much known about the interaction of CPK28 with other effectors and *TtTue1* is the first novel smut fungal effector that interacts with CPK28 to date.

Discussion

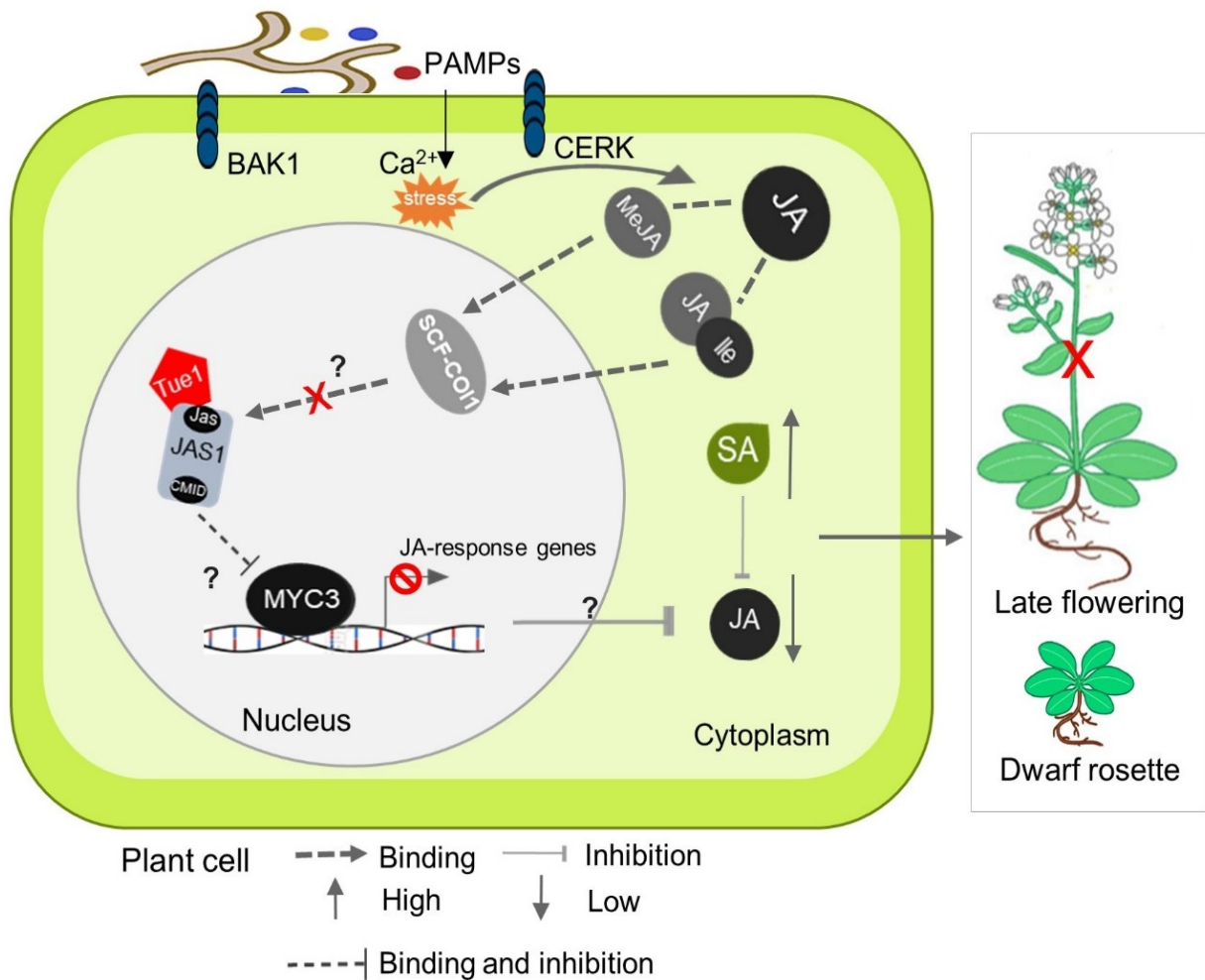


Fig. 6-1 Proposed model for the modulation of plant hormonal signaling in response to interaction between *TtTue1* and *JAS1*. JA synthesis is initiated by fungal attack, upon perception of PAMPs and Ca^{2+} influx. JA derivatives are modified to their active forms MeJA and JA-Ile which subsequently bind to the JA receptor complex SCF-COI1 in the nucleus. During the normal condition, this receptor complex targets the JAS proteins which are subsequently degraded via the 26S proteasome (not depicted here). In the stressed condition, *TtTue1* binds to *JAS1* in the nucleus and might shield it from degradation by JA receptor complex. Structural homology of *TtTue1* with the binding domain (JID) of MYC3 suggests competition for binding to *JAS1*. While *TtTue1* interact with *JAS1* through Jas domain and the CMID domain of *JAS1* is available to be occupied by MYC3. Therefore, both proteins *TtTue1* and *JAS1* can bind as a complex to MYC3. *JAS1* could be stable upon *TtTue1* interaction and represses the transcription activity of MYC3 which lead to suppression of JA responsive genes. Finally, JA signaling is downregulated in response to the inhibitory effect of *JAS1* together with *TtTue1*. High SA level can result in decreased growth of plant with dwarf phenotype. Question mark signs showed that the suggested scenario is not experimentally verified yet. Abbreviations: PAMP = pathogen associated molecular pattern, JA = jasmonic acid, SA = salicylic acid

Discussion

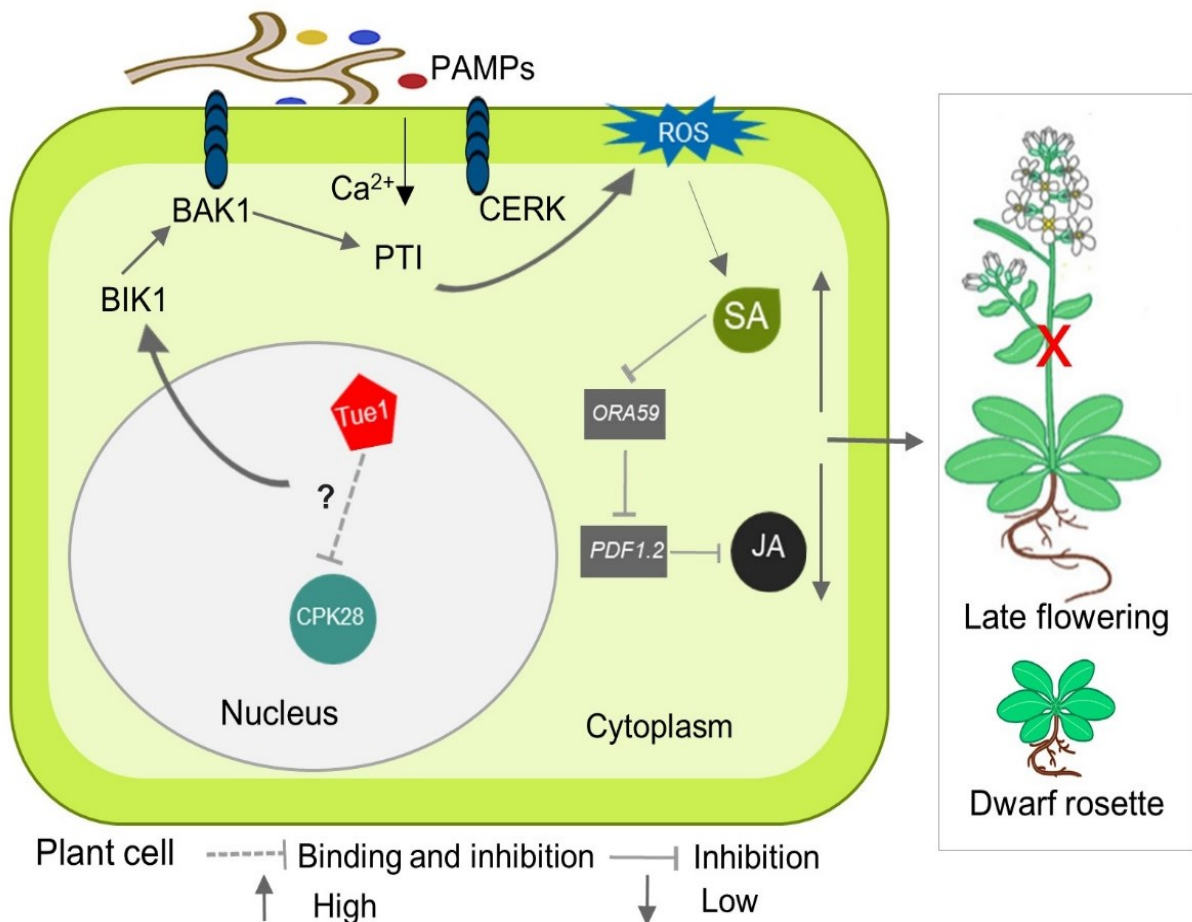


Fig. 6-2 Proposed model for the modulation of plant hormonal signaling and PTI responses upon interaction of *TtTue1* and CPK28. CPK28 is a negative regulator of PTI responses and causes degradation of Bik1 via phosphorylating it. High levels of SA and ROS production showed that *TtTue1* overexpression plants develop PTI responses which suggest that CPK28 was destabilized upon interaction with *TtTue1*. This then allows CPK28 target receptors like BAK1 to perceive PAMPs and induce PTI responses. Additionally, the high SA levels can cause the down regulation of JA signaling via repression of JA/ET induced gene *PDF1.2*. High SA signaling could lead to retarded growth of expressing *TtTue1* plants during the vegetative- as well as the reproductive phase. Question mark signs showed that the suggested scenario is not experimentally verify yet. Abbreviations: PAMP = pathogen associated molecular pattern, JA = jasmonic acid, SA = salicylic acid, PTI =Pathogen triggered immunity.

6.4.2 The Hormonal modification and the developmental phenotype of *TtTue1* is interconnected

TtTue1 mediated phytohormone alterations are ultimately linked to the phenotype of the plant expressing *TtTue1*. *TtTue1* transgenic line served as a great tool and provide bases for specific focus in host plant infection with *TtTue1* mutant strain. Elevated SA levels and no detection of JA-response components in the presence of *TtTue1* might promote the dwarf phenotype of rosette and induces the delayed flowering due to association of both these hormones with developmental phenotypes. Extensive work has been done on the involvement of jasmonates in plant developmental processes such as root growth, senescence of leaves and reproductive development (Wasternack and Hause, 2013; Kim et al., 2015). The previous investigations have shown that exogenous application of JAs suppress the cell proliferation thereby inhibit

Discussion

the plant growth (Patil et al., 2014). Nevertheless, high rate of cell division was observed in the young organs accumulating high level of endogenous jasmonates, thus positive impact of JAs on growth promotion of plant cannot be excluded which could be a consequence of variation in endogenous cytokinins that interrupt to regulate the cell cycle (Avalbaev et al., 2016). In *Arabidopsis*, lateral root formation is stimulated by JA through transcriptional regulation of ERF109 that induces *YUCCA2* and *ANTHRANILATE SYNTHASE A1 (ASA1)* genes involve in auxin biosynthesis (Cai et al., 2014). The vegetative to reproductive phase maturation of *Arabidopsis* is affected by JAZ proteins, which are involve in the inhibition of flowering by targeting TOE1 and TOE2 as well as APETALA2/ERF transcription factors that control flowering thus cause transcriptional inactivation of FLOWERING LOCUS T (Zhai et al., 2015). A pronounced and early interfascicular cambium activity was observed in *Arabidopsis* upon silencing JAS1. Similarly, phloem formation get triggered in wild type plant by exogenous application of JA (Sehr et al., 2010). These observations pointed towards interference of JAS1 in modulation of plant morphology and that growth phenotype of plant expressing *TtTue1* might be an effect of *TtTue1* and JAS1 interaction. Similarly, SA also affects the morphology of plants. For example, high SA levels in plants overexpressing the SA-inducible genes DOF and OBP3 in roots and shoots results in a decreased growth rate that can lead to cell death in severe cases (Kang and Singh, 2000). *Arabidopsis* mutants such as *cpr5*, *acd6-1* and *agd2* constitutively accumulate high SA levels and show a dwarf phenotype (Rate and Greenberg, 2001).

Additionally, high levels of SA and NHP also lead to a dwarf phenotype in plants (Rivas-San Vicente and Plasencia, 2011; Cai et al., 2021). There is a gap of knowledge particularly at the molecular level regarding the effect of NHP on growth and development in plants. According to recent findings, the common growth related molecular components that are targeted by SA and NHP are not known yet (Shields et al., 2022) However, the effect of high Pip levels is described during biotic stress conditions such as drought stress, where Pip accumulation in the roots of sorghum leads to root growth suppression (Caddell et al., 2020). Similarly, a stunted growth phenotype of strawberry showed high levels of Pip upon chilling and maleic hydrazide treatment (Yatsu and Boynton, 1959). The dwarf and stunted phenotypes in Pip accumulating plants are consistent with the dwarf rosette of *TtTue1* expressing plants.

In transgenic lines, an effector can cause prolonged and high accumulation of SA which could lead to a cell death phenotype. In the *TtTue1* line a cell death phenotype was not obvious. Instead, the plants developed chlorosis in primary leaves throughout the vegetative phase which changed to browning or slight necrosis during the generative phase of the plants. The chlorosis and necrosis symptoms were restricted to primary leaves and did not affect the rest of the plant. Necrotic and shepherd's crook shoot tips and browning of the leaves was observed in an apple cultivar that expressed the *AvrRpt2_{EA}* effector of *E. amylovora*. The disease associated necrosis caused by *AvrRpt2_{EA}* caused an increase in SA dependent responses, which helps colonization of the host plant (Schröpfer et al., 2018). The cell death like symptoms of the *A. thaliana* expressing *TtTue1* plant might be due to the activation of SA signaling.

CPK28 regulates the initial defense responses of the plant on the one hand and serves as a phytohormone-mediated plant growth regulator during the generative phase on the other hand. Several developmental phenotypes have been observed in a *cpk28* mutant such as a dwarf rosette, and a stunted shoot (Matschi et al., 2015). However, in contrast to my observations for *TtTue1*, the *cpk28* mutant accumulates high levels of endogenous JA only in the central

Discussion

rosette area during the early growth phase. *cpk28* mutant showed a spatially and temporally defined accumulation of JA and a stage specific reduction of GA synthesis. This observation clearly demonstrated that accumulation of JA showed a very specific response and might not be same in other condition. CPK28 appears essential for the regulation of JA signaling and JA-Ile biosynthesis is important for the *cpk28* phenotype. Nonetheless this phenotype and the accumulation of hormones is a specific response for the *cpk28* mutant and the authors have suggested a disturbance in JA/GA hormone balance would be the cause of altered growth responses in *cpk28* (Matschi et al., 2015). *TtTue1* strongly binds to CPK28 and thus might destabilize CPK28 in order to maintain the dwarf and stunted growth phenotype of the plant, however high JA accumulation in the early growth phase of *cpk28* could be different from hormone analysis of *TtTue1*. High JA levels corresponding to a dwarf phenotype is also not consistent with its affect shown in previous studies described in the above examples, however this could be a very specific response of JA and only related to the *cpk28* mutant.

Despite an obvious effect of *TtTue1* in transgenic line, its activity need to explore in the natural infection system. *TtTue1* might have spatio-temporal effect and its activity can vary in different organs of the plant. Furthermore, investigating molecular basis of the developmental effects of *TtTue1* transgenic line can also provide useful insights.

Conclusion and outlook

6.5 Conclusion and outlook

Smut fungi present a prevalent group of plant pathogenic fungi that mostly infect the monocot species including important crop plants. *U. maydis* is one of the well-studied members of this group with genetically tractable tools for studying the varieties of topics such as cell cycle regulation, mating, transcriptional and translational regulation and pathogenicity. Unlike other smut fungi, *T. thlaspeos* is the only member of *Thecaphora* clade and smut fungi that can infect species of Brassicaceae family. Most importantly, colonization of *A. thaliana* by *T. thlaspeos* under lab conditions reduced the complexity of the system by utilizing an easily accessible and well-annotated genome of *A. thaliana*. Availability of a wealth of information on plant-microbe interactions is beneficial for analyzing the host responses which has been evident from this study as well. Therefore, combining the knowledge of smut fungi, *A. thaliana* and its available data and resources of *T. thlaspeos* presents it as a potential new pathosystem.

Plant pathogen coexistence has developed an intimate relationship which is tightly linked to the translocated molecules of pathogens to establish this strong contact. Effectorome, a field which is identified but not well investigated yet in *T. thlaspeos*. There are some great discoveries in the effector biology such as identification of TAL effectors and Kiwellins proteins as interaction partners greatly contributed to the effector research thereby, this field is still regularly leads to great innovations that change paradigms. Identification and functional characterization of nuclear localized effectors and detailed analysis of *TtTue1* have addressed novel questions of plant-microbe interaction. Using model system, *A. thaliana* for characterization of *T. thlaspeos* effectors offers a new avenue for exploring the molecular mechanism with more readily available genetic tools.

TtTue1 interactome suggests that its targeted plant defense associated components has a broad impact on the host cell immune system. Susceptibility of plant upon infection, upregulation of SA signaling, no expression of JA-responsive genes and an expected downregulation of JA suggest a different or modified regulation of plant hormones which could help *T. thlaspeos* to maintain its less destructive lifestyle without any macroscopic disease symptoms. The phytohormone signaling is a complex and variable process, consequently pathogens either adopt the conventional hormonal pathways or modify the phytohormone regulation for their own benefit. Suppressing or activating certain plant proteins by a single effector ultimately affects the plant hormonal cascade. Therefore, I proposed a model in which presence of single effector generates an array of signals for the benefit of pathogen.

Taken together this study has greatly contributed to *T. thlaspeos* effector biology mainly by identifying the plant novel interactions. This investigation provides a working model for the detailed molecular activity of *TtTue1* and novel insight into modification of targeted plant hormones signaling. It has set the foundation for dissecting the molecular mechanism of identified JAS1 proteins upon interaction with *TtTue1*, its other regulatory components and most importantly CPK28 which to date has not interacted with effectors of other smut fungi.

An interesting result of this study is the binding of *TtTue1* with JAS1 of both *A. thaliana* and *Ar. hirsuta*, which has opened the door for investigation of underlying molecular mechanisms. JAZ proteins interact with the other components of JA responsive elements and are involved in the regulation of JA signaling pathway, which is described above. An important component of this machinery is MYC transcription factor which is directly bound by JAZ proteins. The recently solved structure of *TtTue1* (by Dr. Florian Altegoer) has shown homology with the binding

Conclusion and outlook

domain (JID) of MYC3 transcription factor. JAZ can bind to the MYC transcription factor through both N-terminal CMID domain and C-terminal Jas domain. I found that *TtTue1* has shown strong binding with N-terminally truncated version of JAS1 protein (5-9, 5-10). *TtTue1* crystal structure homology with MYC3 binding domain and its strong binding affinity with the C-terminal part of JAS1 suggests that there might be a competition between *TtTue1* and MYC3 or JAS1 binding to MYC3 can be possible through available CMID domain. To experimentally verify these hypotheses, the binding affinity of MYC3 with truncated versions of JAS1 can be checked in presence of *TtTue1*. Additionally, a complex binding experiment can be performed to check if *TtTue1* and JAS1 together suppress the MYC transcription factor and its downstream activity. Most importantly, JAZ proteins might be stable and performed their role in the suppression of JA signaling during stress. Therefore, it is essential to first verify the JAS1 stabilization by *TtTue1* via infecting JAS1 transgenic line with the *TtTue1* overexpression strain. As a result of JAS1 stabilization and on basis of non-induced JA-responsive genes, checking JA hormone level is strongly suggested to solve the last piece of puzzle of *TtTue1*-JAS1 model (Fig. 6-1). Similarly, verification of CPK28 destabilization upon *TtTue1* interaction can help in dissecting their molecular mechanism. Moreover, CPK28 mediates H₂O₂ and Ca²⁺ signals during biotic stress which can convert in to appropriate responses in biotic interactions therefore effect on Ca²⁺ signaling can be tested in presence of *TtTue1* in future studies.

Nonetheless, the overall response of the plant against a single effector, which is not connected to the rest of the effectorome of the system, may lead to the initial complex responses from an effector action. The initial action extends to an array of recognition responses by the plant immune system, which would be counteracted by functionally redundant effectors in the natural context (Thordal-Christensen, 2020). As described above in the results section, *TtTue16* is the member of *TtTue1* family which consist of total 4 members. *TtTue16* has 62% identity with *TtTue1* and is also upregulated during the infection. In contrast to *TtTue1*, THTG_04669 (*TtTue16*) did not show a growth phenotype upon expression in *A. thaliana* (Courville et al., 2019). Besides that, THTG_04669 (*TtTue16*) did not show binding affinity towards interacting partners of *TtTue1* in a protein-protein interaction (BiFC) experiment (Fig. 5-8). However, it could be possible that in *TtTue1* mutant, its function is rescue by other family members in the natural environment. Therefore, *TtTue1* function was mainly characterized in its independent overexpression lines. Similar effect has been observed for the *UmJsi1* mutants which do not show any disease symptoms upon infection, while facilitating the susceptibility of *A. thaliana* expressing *UmJsi1* upon *P. syringae* infection (Darino et al., 2019). Besides this limitation, generation of *TtTue1* mutant strain can verify some findings of this study, such as virulence activity of *TtTue1* in natural environment would be possible to observe through established transformation protocol (Plücker et al., 2021) and the culture infection system (PhD project of Natascha Heßler, currently in progress). Secondly, more detailed analysis of hormonal cross talk can be done by using the *Ar. hirsuta* tissues infected by *TtTue1* deletion strain, although the current study provided the fundamental information about *TtTue1* interactome.

Additionally, an effector translocation and visualization in the natural host plant was a topic of debate. Therefore, I have initiated an experiment to verify the *TtTue1* translocation from *T. thlaspeos*. The use of a GFP strand system has been planned and their functionality was verified in *N. bethamiana*. Full length GFP is large protein in comparison to effectors and could mask the function of effectors, however GFP11 helices cannot interfere with the function and effector protein can easily translocate to the host. Another advantage of the system is detection of true fluorescence signal because GFP can fluoresce only upon fusion of split strands.

Conclusion and outlook

Although *TtTue1* accumulation in the nucleus of *N. benthamiana* has verified the GFP strand system, transformation of *T. thlaspeos* was not successful with *TtTue1-Gfp11*. Now that the transformation protocol is well established, *TtTue1-Gfp11* strain generation and infection of GFP1-10 line can provide the evidence that *TtTue1* migrates to the host plant nucleus upon secretion from *T. thlaspeos*.

Additionally, the chloroplast targeted effector *TtCep3* could be an interesting candidate to study the interference of *T. thlaspeos* effector with photosynthetic machinery of plants. As described above, chloroplast regulate plant immune responses, transmit signal to the nucleus and also involve in signal transduction of phytohormones therefore finding plant targets of *TtCep3*, analyzing its effect on ROS production and chloroplast metabolism can reveal several unexplored queries.

Materials and Methods

7. Materials and Methods

7.1 Materials

This study has been done by using the following material:

Plant lines, strains, plasmids, oligonucleotides, antibiotics, antibodies, enzymes, kits, markers, media, solutions and buffers.

7.1.1 Plant lines

Plant lines listed below were used for physiological and molecular analysis in this study. *A. thaliana* ecotype Columbia (Col-0) has been used as wild-type

Plant ID	Specie	Ecotype	Name	source
At0051	<i>A. thaliana</i>	Col-0	35S::JAZ210.1-YFP	Prof. Gregg Howe MSU, USA
At0050	<i>A. thaliana</i>	Col-0	jaz1-1	NASC UK, Prof. Gregg Howe MSU, USA
At0049	<i>A. thaliana</i>	Col-0	35S:CPK28†-YFP	Prof. Tina Romeis, IPB Halle
At0048	<i>A. thaliana</i>	Col-0	bak1-5 cpk28-3 #33	Prof. Cyril Zipfel
At0047	<i>A. thaliana</i>	Col-0	bak1-5 cpk28-1 #19	Prof. Cyril Zipfel
At0046	<i>A. thaliana</i>	Col-0	CPK28-OE1	Prof. Cyril Zipfel
At0045	<i>A. thaliana</i>	Col-0	cpk28-1/35S:CPK28-YFP	Prof. Cyril Zipfel, Prof. Tina Romeis, IPB Halle
At0044	<i>A. thaliana</i>	Col-0	cpk28-3	Prof. Cyril Zipfel, (WiscDsLox_264D03)
At0043	<i>A. thaliana</i>	Col-0	cpk28-1	Prof. Cyril Zipfel, Prof. Tina Romeis, IPB Halle, (GABI_523B08)
At0030	<i>A. thaliana</i>	Col-0	Col-0_35S_MYC2_GFP	Max Planck institute Cologne
At0029	<i>A. thaliana</i>	Col-0	Col-0 35S::GFP1-10	Gitta Coaker Lab, UC Daivs California
At0028	<i>A. thaliana</i>	Col-0	Col-0_35S_Cep3_GFP	This study
At0027	<i>A. thaliana</i>	Col-0	Col-0_35S_Tae2_GFP	This study
At0026	<i>A. thaliana</i>	Col-0	Col-0_35S_Tue17_GFP	This study
At0025	<i>A. thaliana</i>	Col-0	Col-0_35S_Tue10_GFP	This study
At0024	<i>A. thaliana</i>	Col-0	Col-0_35S_Tue1_GFP	This study
At0023	<i>A. thaliana</i>	Col-0	Col-0_35S_3xmCherry_linker NLS	This study
At0022	<i>A. thaliana</i>	Col-0	Col-0_35S_GFP	This study

7.1.2 Strains

7.1.2.1 Bacteria

Strain	Genotype	Source
<i>E. coli</i> TOP10	F-, <i>mcrA</i> , (<i>mrr-hsdRMSmcrBC</i>), 80 <i>lacZ</i> M15, <i>lacX74</i> , <i>deoR</i> , <i>recA1</i> , <i>araD139</i> , (<i>ara-leu</i>) 7697, <i>galJ</i> , <i>galK</i> , <i>rpsL</i> (StR), <i>endA1</i> , <i>nupG</i>	(Life Technologies)
LOBSTR	Derived from <i>E. coli</i> BL21(DE3) strain and carries genomically modified copies of <i>arnA</i> and <i>slyD</i>	(Kerafast EC1002)

Materials and Methods

KC8	<i>hsdR, leuB600, trpC9830, pyrF::Tn5, hisB463, lacΔX74, strA, galU, K</i>	Prof. David Holden From Imperial college London
<i>P. syringae</i> Pst-LUX	<i>P. syringae</i> pv. tomato DC3000, luxCDABE	(Fabro et al., 2011) From TSL
C58PMP90pSoup A. <i>Tumefaciens</i>	GV2260	Prof. Dr. Rüdiger Simon HHU

7.1.2.2 Yeast

Strain	Genotype	Reference
EGY48	<i>MAT α, his3, trp1, ura3, LexAop(x6)-LEU2</i>	(Estojak et al., 1995)
AH109	<i>MATα, trp1-901, leu2-3, 112, ura3-52, his3-200, gal4Δ, gal80Δ, LYS2:: GAL1UAS-GAL1TATA-HIS3, GAL2UAS-GAL2TATA-ADE2, URA3::MEL1UAS-MEL1 TATA-lacZ</i>	(James et al., 1996) A. Holtz, unpublished

7.1.2.3 *Thecaphora thlaspeos*

Strain	Genotype	Number	Reference
<i>Thecaphora thlaspeos</i> LF1	Wt	UMa2019	(Frantzeskakis et al., 2017)
<i>Thecaphora thlaspeos</i> LF2	Wt	UMa2020	(Frantzeskakis et al., 2017)

7.1.2.4 *Ustilago maydis*

Strain	Genotype	Number	Locus	Progenitor strain	Reference
SG200 <i>stp1Δ-hyg</i>	<i>Stp1Δ</i>	Uma2488	UMAG_02475	SG200	This study
SG200 <i>stp1Δ-Umstp1-gfp-NatR</i>	<i>Stp1Δ Umstp1-gfp</i>	Uma2928	UMAG_02475	Uma2488	This study
SG200 <i>stp1Δ-Ttstp1-gfp-NatR</i>	<i>Stp1Δ Ttstp1-gfp</i>	Uma2929	UMAG_02475	Uma2488	This study
SG200-3xGFP	<i>egfp</i>	UMa587	IP ^S	-	Stephan Genin
SG200	<i>a1 mfa2 bWe bE1</i>	Uma67	-	-	(Kämper et al., 2006)

7.1.3 Plasmids

7.1.3.1 Plasmids for protein expression in *U. maydis* and *T. thlaspeos*

Plasmids	Number	<i>E. coli</i> resistance	Fungal resistance	Purpose	Reference
<i>Umstp1Δ-Hyg</i>	pUMa3529	AmpR	HygR	Knockout of UMAG_02475 with Hyg cassette	This study
<i>Umstp1-Gfp-NatR</i>	pUMa4146	AmpR	NatR	Expression of <i>Umstp1</i> in the	This study

Materials and Methods

				endogenous locus under control of native promotor	
Ttstp1_Gfp_NatR	pUMa4147	AmpR	NatR	Expression of <i>Ttstp1</i> in the endogenous locus of Um under control of native promotor	This study
TfTue1Δ-Hyg	pUMa4371	AmpR	HygR	Knockout of THTG_4687 with Hyg cassette	This study
TfTue1_Gfp11_Hyg	PUMa4392	AmpR	HygR	Expression of <i>Ttstp1_Gfp11</i> in the endogenous locus under control of native promotor	This study
Storage vector-NatR-eGfp-SapI	pUMa4343	GentR	NatR	Generation of storage vector with SapI sites for goldenGate cloning	This study
pDestI	pUMa1467	AmpR	-	destination vector for BsaI Golden Gate cloning	(Terfrüchte et al., 2014)
pStorI	pUMa1507	GentR	HygR	storage vector for HygR cassette with BsaI and SfiI sites	(Terfrüchte et al., 2013)
PStorII	pUMa1546	GentR	HygR	storage vector for egfp-HygR cassette for C-terminal fusion with BsaI and SfiI sites	(Terfrüchte et al., 2013)
PStorIII	pUMa1694	GentR	NatR	storage vector for egfp-NatR cassette for C-terminal fusions with BsaI sites	Carl Haag
pDestII	pUMa2074	AmpR	-	destination vector for SapI Golden Gate cloning	Kira Müntjes

7.1.3.2 Plasmids for protein expression in plants

Plasmids	Number	<i>E. coli</i> resistance	Purpose	Reference
TfTue1-pEDV3	pUMa3665	GentR	Transient expression of <i>TfTue1</i> in <i>A. thaliana</i>	Katilyne Courville (TSL)
TfTue5-pEDV3	pUMa3669	GentR	Transient expression of <i>TfTue5</i> in <i>A. thaliana</i>	This study
TfTue10-pEDV3	pUMa3674	GentR	Transient expression of <i>TfTue10</i> in <i>A. thaliana</i>	This study
TfTue17-pEDV3	pUMa3681	GentR	Transient expression of <i>TfTue17</i> in <i>A. thaliana</i>	This study

Materials and Methods

TtTae2-pEDV3	pUMa3684	GentR	Transient expression of <i>TtTae2</i> in <i>A. thalaina</i>	This study
Ttcep3-pEDV3	pUMa4456	GentR	Transient expression of <i>TtCep3</i> in <i>A. thalaina</i>	This study
Ttcep5-pEDV3	pUMa4457	GentR	Transient expression of <i>TtCep5</i> in <i>A. thalaina</i>	This study
35s_TtTue1_Gfp_pGGZ001	pUMa4366	SpecR	Transient expression of <i>TtTue1</i> in <i>N. benthamiana</i> for localization	This study
35s_TtTue5_Gfp_pGGZ001	pUMa4078	SpecR	Transient expression of <i>TtTue5</i> in <i>N. benthamiana</i> for localization	This study
35s_TtTue10_Gfp_pGGZ001	pUMa4221	SpecR	Transient expression of <i>TtTue10</i> in <i>N. benthamiana</i> for localization	This study
35s_TtTue17_Gfp_pGGZ001	pUMa4152	SpecR	Transient expression of <i>TtTue17</i> in <i>N. benthamiana</i> for localization	This study
35s_TtTae2_Gfp_pGGZ001	pUMa4149	SpecR	Transient expression of <i>TtTae2</i> in <i>N. benthamiana</i> for localization	This study
35s_TtCep3_Gfp_pGGZ001	pUMa4591	SpecR	Transient expression of <i>TtCep3</i> in <i>N. benthamiana</i> for localization	This study
35s_TtCep5_Gfp_pGGZ001	pUMa4592	SpecR	Transient expression of <i>TtCep5</i> in <i>N. benthamiana</i> for localization	This study
35s_mCherry_Nls_pGGZ001	pUMa4363	SpecR	Identification of position of nuclei via transient expression in <i>N. benthamiana</i>	This study
35s_mCherry_pGGZ001	pUMa4364	SpecR	Cytosolic localization of mCherry via transient expression in <i>N. benthamiana</i>	This study
35s_GFP_pGGZ001	pUMa4767	SpecR	Cytosolic localization of GFP via transient expression in <i>N. benthamiana</i>	This study
ATR13-pEDV3	pUMa4365	GentR	Transient expression of ATR13 in <i>A. thalaina</i>	This study
35s_linker_gfp11_pGGZ001	pUMa4490	KanR	Expression of fusion protein of effectors with <i>gfp11</i> strand	This study
35s_TtTue1_NlsD_GFP_pGGZ001	pQL33	SpecR	Transient expression of <i>TtTue1_NlsD</i> in <i>N. benthamiana</i> for localization	This study
35s_TtTae2_NlsD_Gfp_pGGZ001	pUMa4586	SpecR	Transient expression of <i>TtTae2_NlsD</i> in <i>N. benthamiana</i> for localization	This study
35s_TtTue10_NlsD_Gfp_pGGZ001	pUMa4588	SpecR	Transient expression of <i>TtTue10_NlsD</i> in <i>N. benthamiana</i> for localization	This study
35s_GFP1-10_pGGZ001	pQL31	SpecR	Transient expression of GFP1-10 strands in <i>N. benthamiana</i>	This study

Materials and Methods

35s_TfTue1_GFP11_pGGZ001	pQL30	SpecR	Transient expression of <i>TfTue1_Gfp11</i> in <i>N. benthamiana</i>	This study
35S_TfTue1_NTmVen_pGGZ001_BiFC	pQL113	SpecR	Transient expression of <i>TfTue1</i> with split mVenus in <i>N. benthamiana</i> for Interaction	This study
35S_AtCPK28_CTmVen_pGGZ001_BiFC	pQL114	SpecR	Transient expression of <i>AtCPK28</i> with split mVenus in <i>N. benthamiana</i> for Interaction	This study
35S_AtJAS1_CTmVen_pGGZ001_BiFC	pQL115	SpecR	Transient expression of <i>AtJAS1</i> with split mVenus in <i>N. benthamiana</i> for Interaction	This study
35S_AtCPK7_CTmVen_pGGZ001_BiFC	pQL116	SpecR	Transient expression of <i>AtCPK7</i> with split mVenus in <i>N. benthamiana</i> for Interaction	This study
35S_TfTue16_NTmVen_pGGZ001_BiFC	pQL117	SpecR	Transient expression of <i>TfTue16</i> with split mVenus in <i>N. benthamiana</i> for Interaction	This study
35s_ArhCPK28_CTmVen_pGGZ001_BiFC	pQL130	SpecR	Transient expression of <i>ArhCPK28</i> with split mVenus in <i>N. benthamiana</i> for Interaction	This study
35s_ArhJAS1_CTmVen_pGGZ001_BiFC	pQL131	SpecR	Transient expression of <i>ArhJAS1</i> with split mVenus in <i>N. benthamiana</i> for Interaction	This study
35s_ArhCPK28_GFP_pGGZ001	pQL132	SpecR	Transient expression of <i>ArhCPK28</i> in <i>N. benthamiana</i> for localization	This study
35s_ArhJAS1_GFP_pGGZ001	pQL133	SpecR	Transient expression of <i>ArhJAS1</i> in <i>N. benthamiana</i> for localization	This study

7.1.3.3 Plasmids for protein expression in *S. cerevisiae*

Plasmids	Number	<i>E. coli</i> resistance	<i>S. cerevisiae</i> marker	Purpose	Reference
TfTue1_pGBKT7_Y2H	pUMa4669	KanR	Trp	Expression of <i>TfTue1</i> in Ah109	This study
TfTue1_HA_pGILDA_Y2H	pQL50	AmpR	His	Expression of <i>TfTue1</i> in EGY48	This study
pGILDA-Att-Gateway	pQL26	AmpR	His	Bait vector for Gateway cloning used in LexA system	Prof. Maeli Melotto UC Davis, California
pB42AD-Att-Gateway	pQL28	GentR	Trp	Prey vector for Gateway cloning used in LexA system	Prof. Maeli Melotto UC Davis, California
AtcDNA stress induced library_pB42AD	pQL83	AmpR	Trp	Co-transformation with <i>TfTue1</i> in bait vector	This study

Materials and Methods

AtCPK28_pEN TR221	pQL96	KanR	-	Entry clone of <i>AtCPK28</i> for generation of expression clone	This study
AtCPK28_pEX PpB42AD_Y2H	pQL97	AmpR	Trp	Expression of B42AD_AtCPK28 in EGY48	This study
AtJAS1_pENT R221	pQL98	KanR	-	Entry clone of <i>AtJAS1</i> for generation of expression clone	This study
AtJAS1_pEXPP B42AD_Y2H	pQL99	AmpR	Trp	Expression of B42AD_AtJAS1 in EGY48	This study
ArhCPK28_pE NTR221	pQL120	KanR	-	Entry clone of <i>ArhCPK28</i> for generation of expression clone	This study
ArhCPK28_pE XPpB42AD_Y2H	pQL121	AmpR	Trp	Expression of B42AD_ArhCPK28 in EGY48	This study
ArhJAS1_pENT R221	pQL122	KanR	-	Entry clone of <i>ArhJAS1</i> for generation of expression clone	This study
ArhJAS1_pEXP pB42AD_Y2H	pQL123	AmpR	Trp	Expression of B42AD_ArhJAS1 in EGY48	This study

7.1.3.4 Plasmids for protein expression in *E. coli*

Plasmids	Number	<i>E. coli</i> resistance	Backbone	Purpose	Reference
TtTue1_GST	pQL0102	AmpR	pUMa4789	Expression of GST_TtTue1 in LOBSTR under control of T7 promotor	This study
AtJAS1_NT6xHisM BP	pQL0103	KanR	pUMa3818	Expression of MBP_AtJAS1 in LOBSTR under control of T7 promotor	This study
AtJAS1_CTpart_NT 6xHispEMGB1	pQL0108	AmpR	pIL0017	Expression of GB1_CTAtJAS1 in LOBSTR under control of T7 promotor	This study
AtCPK28_NT6xHisp EMGB1	pQL0112	AmpR	pIL0017	Expression of GB1_AtCPK28 in LOBSTR under control of T7 promotor	This study
ArhJAS1_NT6xHis MBP	pQL0124	KanR	pUMa3818	Expression of MBP_ArhJAS1 in LOBSTR under control of T7 promotor	This study

Materials and Methods

ArhCPK28_NT6xHis pEMGB1	pQL0129	AmpR	pIL0017	Expression of GB1_ArhCPK28 in LOBSTR under control of T7 promotor	This study
--------------------------------	---------	------	---------	---	------------

7.1.4 Oligonucleotides

Number	Name	Sequence
UP506	Stp1-U2	GGTCTCGCCTGCAATATTGACCATGATCAACCAGG
UP507	Stp1-U3	GGTCTCCAGGCCCGTGTCTCTGCTTTATTTTCTC
UP508	Stp1-D1	GGTCTCCGGCCAGCTCTGCTGTAAAGAATCAC
UP509	Stp1-D2	GGTCTCGCTGCAATATTATCAACATTTCTCTCGTTGTC
UP838	<i>Ttstp1</i> _UG	ATGCTATTCCGCAGCGTCTGCATC
UP840	<i>Ttstp1</i> _R	TGGGCCGGTGTGAAGTTGTTGC
UP934	<i>UmStp1</i> F	GGTCTCGGCCTATGAGAGCCGTGCTCTCGCTCAAC
UP935	<i>UmStp1</i> R	GGTCTCCTGGCACGAGAAGGAGGAGGTGCCATGGT
AB305	Tue5_Fw_Sall	GTCGACATGCAGGACCCTCTTCTGGACCAGT
UP982	Tue5_R_BamHI	GGATCCGTTGCCGTCCATCTCCTTCTC
UP989	Tue10_F_Sall	GTCGACACAGCCCCGGTCAAACAC
UP990	Tue10_R_BamHI	GGATCCTGGCGCTTTGGCTTGGCGC
UP1005	Tue17_F_Sall	GTCGACGCGCCTGTGCGAGAACAGATCA
UP1006	Tue17_R_BamHI	GGATCCGACGTATTGGCTGTCGTGGC
UM412	<i>TtStp1</i> _Fw	GGTCTCGGCCTATGATCTTCACGCCTTCCCTTC
UM413	<i>TtStp1</i> _Rev	GGTCTCCTGGCCGGCTTTTTCGCGCGGCGGGGATTA
UM470	<i>TtStp1</i> _Mut_Bsa1_F	GGTCTCAGACGTTTTCTCATGCTATTCCGC
UM471	<i>TtStp1</i> _Mut_Bsa1_R	GGTCTCACGTCTCGCCCGTAATGAGAAG
UM472	Tae2_Sall_F	GTCGACGATACCCAGTCCCGCAGCGTTCATCTGATCC
UM473	Tae2_BamHI_R	GGATCCCTTGTAGATGTTGCCCTTCTTC
UM474	Tae2_MutSapI_F	ATCGCTCTTCTGTGGACCCCGGCCTCACCTTTC
UM475	Tae2_MutSapI_R	TAGGCTCTTCCACATCGTTGCACCTGG
UM763	Tae2_F_Bsa1	GGTCTCGAACAATGGATACCCAGTCCCGCAGCGTTC
UM764	Tae2_R_Bsa1	GGTCTCACTGACTTGTAGATGTTGCCCTTCTTC
UM731	Tae2_Mut_F_Bsal	GGTCTCAGACGGAGAGGATCGAGGTGGG
UM732	Tae2_Mut_R_Bsal	GGTCTCCCGTCTCCGAGACTTCGCGGATCAG
UM502	Tue10_F_Bsal	GGTCTCGAACAATGACAGCCCCGGTCAAACAC
UM882	Tue10_Bsal_Rev	GGTCTCCCTGATGGCGCTTTGGCTTGGCGGAGCGTCTG
UM886	<i>Umstp1</i> _Fw_RT-PCR	GCAAACACTCTCACGCCGAGAC
UM887	<i>Umstp1</i> _Rev_RT-PCR	TAGTTGGGCAGATTGGTGATGTCC
UM888	<i>Ttstp1</i> _Fw_RT-PCR	CGGAGGAGGATCTGGCCAAGGATTC
UM889	<i>Ttstp1</i> _Rev_RT-PCR	TGTCCGGTGTCTTGTCAAGTGC
AB125	ATR13_Fw	ggtggaggtaaacgagGTCGACAATCTGCTCCAC
AB126	ATR13_Rev	tacgtcgtacggatagGGATCCCTGTCTGTCAAG
AB132	Tue1 Bsa1-Fw	GGTCTCGAACAATGACAAACCCCCCTCCCCTCAG
AB133	Tue1 Bsa1-Mut-Fw	GGTCTCGTCCCCCGATTACTCTGTGGAAAC
AB134	Tue1 Bsa1_Mut-Rev	GGTCTCCGGGACCTGGCACCCTGGATCCAG
AB135	Tue1 Bsa1-Rev	GGTCTCCCTGAGGGGCCAGGTCCCGCGCGGTCT
AB174	U2-Tue1	CACGCTCTTCCGTGCAATCTTGCCAACGTCGATAGCTTC
AB175	U3-Tue1	CATGCTCTTCCGGCCGGCGGGCAATGCGCTTGCAGA
AB176	D1-Tue1	CACGCTCTTCCCCTCGCTTCCGTCCAGCAGGTTGCG
AB177	D2-Tue1	CACGCTCTTCCGACAATCTGCACATCTGCGACATCTGT
AB271	Tue1-Gfp11-f	TTAGCTCTTCCATGCTGTTTCTCCGCTTCGCCGTCGT

Materials and Methods

AB272	Tue1-Gfp11-r	GGAGCTCTTCGAATGGTGGGGCCAGGTCCC GCGCGGTC
AB378	<i>TtCep3</i> Fw	ATGGCGTCTTTGAGCGTCTGTTTCG
AB379	<i>TtCep3</i> Rev	TGTTGACGGATGGCACTTGTCT
AB380	<i>TtCep5</i> Fw	CGATGAGACAGACCTCGGATATTC
AB381	<i>TtCep5</i> Rev	AGCGGTGGTCTTCTTCTTGAGG
AB520	Tae2_F_Bsa1_NlsD_Gfp	GGTCTCCAAAATTCAAAAAGATCTGCACCCAGGG
AB521	Tae2_R_Bsa1_NlsD_Gfp	GGTCTCCTTTTTCCAGCTGACCAGACGGCA
AB523	Tue10_Bsa1_Fw_no Sp	GGTCTCGAACAATGGCCCCGGTCAAACACCCCGTGGGT
AB628	Tue10_NT_GFP_NLSd_R	GGTCTCAGCAGCTAACTTGAGCAAATTCGGGCTG
AB707	Tue5 F Bsa1	GGTCTCGAACAATGCAGGATCCTCTTCTGGACCAG
AB708	Tue5 R Bsa1	GGTCTCCCTGAGTTGCCGTCCATCTCCTTCTC
AB709	Tue5 F mut Bsa1	GGTCTCAGATCAGGACAACAAGGAGGAC
AB710	Tue5 R mut bsa1	GGTCTCCGATCTCGCTTGTCTTCATGTC
AB711	Cep3 F 1xGfp CT	GGTCTCGAACAATGTCTTTGAGCGTCTGTTTCGATTAA
AB712	Cep3 R 1xGfp CT	GGTCTCCCTGATGTTGACGGATGGCACTTGTCTT
AB713	Cep5 F 1xgfp CT	GGTCTCGAACAATGAGCCACGTTGACCTTGCCCT
AB714	Cep5 R 1xgfp CT	GGTCTCCCTGAATCTTGGAGCTTGCTCGCCTCGA
AB916	Tue1 F Sfil_pGBKT7	GGCCATTACGGCCATGACAAACCCCCCTCCCTC
AB917	Tue1 R Sfil_pGBKT7	GGCCGAGGCGGCCACTAGGGGCCAGGTCCC GCGC
CD429	Tue1-GFP11-Bsal-R	GGTCTCCGCAGTTAGGTGATACCGGCGGCGTTGA
CD430	GFP1-10-Bsal-F	GGTCTCGAACAATGAGCAAAGGAGAAGA ACTTT
CD431	GFP1-10-Bsal-R	GGTCTCCGCAGTTATCTCACTTTTCGTTGGGATCT
CD507	Tue1 NlsD F Bsal	GGTCTCCCACGACACTCCTGGATCCAGTGGT
CD508	Tue1 NlsD R Bsal	GGTCTCCCGTGTTGAGAAGATTCAGGTCGCTCG
CD914	CPK28_F_ATT	GGGGACAAGTTTGTACAAAAAAGCAGGCTATATGGGTGTC TGTTTCTCCG
CD915	CPK28_R_ATT	GGGGACCACTTTGTACAAGAAAGCTGGGTTCTATCGAAGA TTCCTGTGAC
CD916	JAS1-F-ATT	GGGGACAAGTTTGTACAAAAAAGCAGGCTATATGTGCGAAA GCTACCATAGA
CD917	JAS1-R-ATT	GGGGACCACTTTGTACAAGAAAGCTGGGTTTTAGGCCGAT GTCGGATAG
CD975	<i>Arh</i> CPK28#1-F-ATT	GGGGACAAGTTTGTACAAAAAAGCAGGCTATATGGGTGTG TGTTTCTCCGCCATTAG
CD976	<i>Arh</i> CPK28#1-R-ATT	GGGGACCACTTTGTACAAGAAAGCTGGGTTCTACCGAGG ATTCCTGTGGCCTGC
CD977	<i>Arh</i> JAS1#1-F-ATT	GGGGACAAGTTTGTACAAAAAAGCAGGCTATATGTCTCGA GCTACCATAGA ACTTG
CD978	<i>Arh</i> AS1#1-R-ATT	GGGGACCACTTTGTACAAGAAAGCTGGGTTTTAGGCCGAT GTCGGAAAGTAAGG
EF79	<i>Arh</i> CPK28-F-Bsal	GGTCTCGAACAATGATGGGTGTGTGTTTCTCCGC
EF80	<i>Arh</i> CPK28-R-Bsal-HA	GGTCTCCCTGAGGCATAATCTGGCACATCATAAGGGTACC GAGGATTCTGTGGCCTGC
EF81	<i>Arh</i> JAS1#1--F-Bsal	GGTCTCGAACAATGATGTCTCGAGCTACCATAGAAC
EF82	<i>Arh</i> JAS1#1-R-Bsal-HA	GGTCTCCCTGAGGCATAATCTGGCACATCATAAGGGTAGG CCGATGTCGGAAAGTAAG
EF121	Tue16-F-Bsal	GGTCTCGAACAATGACAAACCCCCCTCCCCTCAG
EF122	Tue16-R-Bsal	GGTCTCCCTGAGGGGCCAGGTCCC GCGCGGTC
EF129	<i>Arh</i> CPK28-F-Bsal-Gogate	GGTCTCCCATGGGCGGTGTGTGTTTCTCCGCCATTAG
EF130	<i>Arh</i> CPK28-R-Bsal-Gogate	GGTCTCCTCGAGCCGAGGATTCCTGTGGCCTGC
EF131	<i>Arh</i> JAS1-F-Bsal-Gogate	GGTCTCCCATGGGCTCTCGAGCTACCATAGA ACTTG
EF132	<i>Arh</i> JAS1-R-Bsal-Gogate	GGTCTCCTCGAGGGCCGATGTGCGAAAGTAAGG

Materials and Methods

7.1.5 Antibiotics

Antibiotic	Dissolve in	concentration
Ampicillin	H ₂ O	100 µg/ml
Gentamycin	H ₂ O	50 µg/ml
Kanamycin	H ₂ O	50 µg/ml
Spectinomycin	H ₂ O	100 µg/ml
Rifampicin	DMSO	10 µg/ml
Tetracycline	DMSO	10 µg/ml
Hygromycin	-	100 µg/ml
Noursethricin	-	50 µg/ml

7.1.6 Enzymes

Enzyme	Company
Phusion polymerase	New England Biolabs
Lysozyme	Thermo Fisher Scientific
Restriction enzymes	New England Biolabs
T4 DNA Ligase	New England Biolabs
Rnase A	Boehringer Ingelheim
BP Clonase II Enzyme mix	Thermo Scientific
LR Clonase II Enzyme mix	Thermo Scientific
Yatalase	Takara
Glucanex	Sigma

7.1.7 Antibodies

Mouse Anti-His, SIGMA (Sigma-Aldrich, H1029) 1:1000

Mouse Anti-GFP 1:1000

Mouse Anti-Actin, MP Biomedicals, 08691002, 1:1000

Rabbit Anti LexA, (Sigma-Aldrich) 1:3000

Anti-Mouse IgG, HRP conjugate, Promega W4021, 1:4000

Anti-Rabbit IgG, HRP-linked AB, Cell Signaling #7074, 1:3000

7.1.8 Kits

Monarch® PCR & DNA Cleanup Kit (New England Biolabs, UK)

Monarch® DNA Gel Extraction Kit (New England Biolabs, UK)

NucleoSpin Plasmid (NoLid) (Macherey-Nagel, Germany)

TOPO-TA cloning Kit with pCRII Vector (Thermo Fisher Scientific)

Zero Blunt TOPO-PCR cloning Kit with pCR Blunt II vector (Thermo Fisher Scientific)

PCR DIG Labeling Mix (Roche)

ECL™ Prime Western-Blot-System (Sigma)

CDP Star® (Roche)

7.1.9 Ladders

GeneRuler 1 kb DNA ladder from Thermo Fisher Scientific

GeneRuler 50 kb DNA ladder from Thermo Fisher Scientific

λPstI: genomic λ phage DNA from Thermo Scientific restricted with PstI

Prestained protein ladder

Materials and Methods

7.1.10 Media

YT-Medium (Sambrook, 1989)

0,8 % (w/v) Tryptone
0,5 % (w/v) Yeast extract
0,5 % (w/v) NaCl
1 % (w/v) Bacto Agar
In H₂O
Sterilization: autoclaved for 5 min at 121°C

dYT-Medium (Sambrook, 1989)

1,6 % (w/v) Tryptone
1,0 % (w/v) Yeast extract
0,5 % (w/v) NaCl
In H₂O

YL medium (YEPSlight)

1.0 % (w/v) Yeast-Extract (Difco)
0.4 % (w/v) BactoTM-Peptone (Dico)
0.4 % (w/v) Sucrose
in H₂O
For solid medium: 0.6 % plant agar / 2.0 %
bacto agar
Sterilisation: autoclaved for 5 min at 121°C

YMPG REG medium

0.3 % (w/v) Yeast-Extract (Difco)
0.3 % (w/v) malt extract
0.5 % (w/v) Bacto-Peptone (Difco)
1.0 % glucose
1 M sucrose
0.6 % plant agar (Duchefa)
in H₂O
Sterilisation: autoclaved for 5 min at 121°C

REGlight (Schulz et al. 1990)

1,5 % (w/v) Bacto Agar
1 M Sorbitol
In YL medium
Sterilisation: autoclaved for 5 min at 121°C

½ MSN medium

2.2 g/l Murashig & Skoog medium
(Duchefa)
1 % (w/v) sucrose
adjust pH to 5.7
Sterilisation: autoclaved for 5 min at 121°C

YPD medium

2.5 % (w/v) Bacto peptone
1,25 % (w/v) Bacto Yeast extract
2.0 % (v/v) glucose (added after
autoclaving)
1.3 % (w/v) Bacto Agar (for solid medium)
In H₂O
Sterilization: autoclaved for 5 min at 121°C

Synthetic Dropout medium

0.5 % (w/v) amino acid mix
1.7 % (w/v) Yeast nitrogen base w/o amino
acids
2.0 % (v/v) glucose (added after
autoclaving)
1.3 % (w/v) Bacto Agar (for solid medium)
in H₂O. Adjust pH to 5.8
Sterilization: autoclaved for 5 min at 121°C

Amino acid mix for SD medium

4.2 % (w/w) Alanine
4.2 % (w/w) Lysine
4.2 % (w/w) Arginine
4.2 % (w/w) Phenylalanine
4.2 % (w/w) Asparagine
4.2 % (w/w) Proline
4.2 % (w/w) Aspartate
4.2 % (w/w) Serine
4.2 % (w/w) Cysteine
4.2 % (w/w) Threonine
4.2 % (w/w) Glutamine
4.2 % (w/w) Tyrosine
4.2 % (w/w) Glutamate
4.2 % (w/w) Uracile
4.2 % (w/w) Glycine
4.2 % (w/w) Valine
4.2 % (w/w) (myo)-inositol
4.2 % (w/w) Isoleucine
4.2 % (w/v) Histidine
8.5 % (w/v) Leucine
4.2 % (w/v) Methionine
4.2 % (w/v) Tryptophane
1.1 % (w/v) Adenine
0.42 % (w/w) 4-Aminobenzoic acid
The powder was mixed overnight on a
wheel at 4 °C and stored at 4 °C.

Materials and Methods

7.2 Methods

The culturing conditions, competent cells and transformation methods of all microorganisms used in this study are listed here:

7.2.1 Bacterial and fungal species

7.2.1.1 *E. Coli*

7.2.1.1.1 Culture and transformation

Transformation of *E. coli* cells were done by using the competent Top10 cells which were prepared according to protocol from (Cohen et al., 1972) and readily available in the lab. 50 µl of cells aliquot were used for an individual transformation. Cells were thawed on ice for few minutes and immediately mix with plasmid DNA depending on the method of plasmid generation. *E. coli* cells were incubated on ice for 30 minutes after mixing with the plasmid DNA. A heat shock was given at 42°C for 45 seconds followed by 2 minutes on ice. Cells were recovered by adding 250-300 µl of DYT media and incubated at 37°C on rotator for 30-60 minutes depending on the antibiotic used for the selection. Cells were plated on YT media which were mixed with the required antibiotic for the used plasmids. In case of *LacZ* expression or blue/white selection 2 % X-Gal were used on the media plates. Plates were incubated at 37°C overnight.

7.2.1.2 *Pseudomonas syringae*

7.2.1.2.1 Culture and competent cells

P. syringae was cultivated in DYT media at 28°C. An overnight culture was set up in 5ml media in a test tube. The optical density of the culture was obtained by measuring the absorption at 600 nm. Cultures was diluted to an initial OD of 0.3 in 20 ml DYT media and let them grow for 1 ½ hours at 28°C. OD should be in between 0.5-0.8 after second incubation round. At this point, culture was centrifuge at 4000 rpm for 4 minutes. Pellet was resuspended in 20 ml of 300 mM sterile sucrose solution. From this point onward all the steps were performed on ice. A second round of centrifugation was repeated at 10000 rpm with the resuspended pellet. Sucrose wash was repeated for total of 3 three time with 20ml sucrose solution. At the end pellet was resuspended in 0.5 ml 300 mM sucrose solution.

7.2.1.2.2 Transformation

Plasmid DNA (50-300 ng) was added to 50 µl competent cells followed by 20 minutes incubation on ice. Cells were transformed by giving an electric shock by using the following condition at the electroporator:

Voltage (V)	1.25 kv
Capacitance (uF)	25
Resistance	200
Cuvette (mm)	1

Finally, 1 ml of DYT media added to cuvette and slightly mix it with electroporated mixture by pipetting up and down. Incubated at 28 °C for 2-3 hours with shaking and followed by spreading the cells on antibiotic selection plates. Last incubation was done at 28 °C for 2-3 days until the colonies were appeared.

Materials and Methods

7.2.1.3 *Agrobacterium tumefaciens*

7.2.1.3.1 Culture and competent cells

Agrobacterium tumefaciens strain C58pMP90 was grown in 10 ml DYT media by incubating at 28 °C overnight with shaking at 200 rpm. Cells were transfer to 250 ml DYT media and incubated for 3-4 hours until the OD reaches 0.5-1.0. Grown culture was placed on ice for 5 minutes and followed by centrifugation at 3000 g for 5 minutes at 4 °C. Pellet was rinsed with 10 ml of 20 mM ice-cold CaCl₂ and spinned briefly. Resuspension of pellet was done gently by adding 5 ml of chilled 20 mM CaCl₂.

7.2.1.3.2 Transformation

100 ng plasmid DNA was added to 0.1 ml competent cells and incubated on ice for 5 minutes. A freezing step of 5 minutes was done in liquid nitrogen and proceeded for an immediate heat shock at 37°C for 5 minutes. Added 250 µl DYT media after chilling the cells on ice for 5 minutes. Cells recovery step was done by growing them at 28 °C for 2 hours with shaking. 100 µl of cells were enough to plate on selection media. Plates were incubated at 28°C for 2-3 days.

7.2.1.4 *Saccharomyces cerevisiae*

7.2.1.4.1 Preparation of competent cells

S. cerevisiae strain EGY48 was streaked out from a glycerol stock and grown on a dropout (SD-Ura) yeast solid medium at 28 °C or 30 °C for 3-4 days. A colony from the plate was cultivated overnight in 5ml SD-Ura drop out media on continuous shaking. 50 µl of overnight grown culture was transferred to 50 ml –Ura media in a 250 ml baffled flask and grown for 30 °C for 16 hours at 200 rpm. OD of overnight culture was measured at 600 nm which should be in between 0.5-0.7. An OD₆₀₀ of 0.15 was taken and centrifuged the cells at 700 g for 5 minutes at room temperature. Resuspended the cells pellet in 100 ml of SD-Ura drop out media and transferred the cells to 500 ml baffled flask. Cells were grown at 30 °C with continuous shaking at 200 rpm until OD₆₀₀ reached 0.4-0.5 (approximately 3 hours). Cells were centrifuged at 700 g for 5 minutes and followed by resuspension in 25 ml sterile milliQ water. The same centrifugation step was repeated with resuspension of pellet in 900 µl of 1.1x TE/LiAc solution. At last, a centrifugation step at maximum speed for 30 seconds was done and cells were resuspended in 600 µl of 1.1x TE/LiAc solution. Aliquots were either used directly for the transformation or stored at -80 °C.

LiT

100 mM Lithiumacetat
10 mM Tris-HCl (pH 8,0)
In H₂O

Salmon testis-DNA

10 mg/ml Salmon testis-DNA
(Sigma-Aldrich, D1626)
In TE-Puffer, pH 8,0

7.2.1.4.2 Transformation

This protocol was adopted from big scale transformation for the library screens. Yeast carrier DNA was denatured at 95 °C for 5 minutes and chilled on ice. Following components were added to the pre-chilled eppendorf tubes.

Materials and Methods

Components	Volume for each transformation
pGILDA (binding) 1µg	1 µl
pB42AD (Activation) 1µg	1 µl
Denatured salmon sperm DNA	5 µl
Competent cells	50 µl
80% PEG/ 10% LiAc/ 10% TE solution	500 µl

All the components were mixed by inverting. An incubation at 30 °C for 30 minutes was followed by addition of 20 µl of DMSO. A heat shock was given at 42 °C for 15 minutes by inverting the tubes every 5 minutes. This mixture was spin down at 1000 g for 5 minutes after heat shock and pellet was resuspended in 1 ml of YPDA media. The cells were recovered by growing at 30 °C for 1 hour and centrifuged at 700 g for 5 minutes. Pellet was resuspended in 100 µl 0.9 % NaCl. The cells were plated on the selection drop out media in the dilution series of 1:5, 1:25, 1:125: 1:625. Plates were incubated at 28 °C for 3-4 days or until colonies appeared.

7.2.1.5 *Thecaphora. thlaspeos*

7.2.1.5.1 Culture and protoplast formation

T. thlaspeos strains LF1 and LF2 were used for the transformation, by inoculating 100 ml culture in YMPG with the starting OD₆₀₀ of 0.075. Cultures were grown at 18 °C for 3-4 days until the OD reached 0.5-0.8. A filter sterilized enzyme solution was prepared by dissolving 20 mg/ml glucanex and 10 mg/ml yatalase in citrate buffer. Meanwhile the cells were harvested in a cell strainer of 40 µm pore size followed by washing with 20 ml citrate buffer. 9 ml of enzyme solution were added per 100 ml of culture and incubated at room temperature for 30 minutes while it can turn into protoplast after 10-15 minutes. Protoplast was checked under the microscope and the enzyme reaction was stopped by adding 13 ml of citrate buffer. This mixture was split in 15 ml falcon tubes by transferring 6 ml in each. Each aliquot was carefully overly with 5 ml trapping buffer and centrifuged at 5000 rpm for 15 minutes at 4 °C. The interphase was collected from each tube and mixed with an equal volume of cold STC buffer. Another centrifugation round was done for 10 minutes to collect the required pellet of protoplast which was resuspended in 500 µl STC buffer. *T. thlaspeos* protoplast was immediately used for transformation without any freezing.

Buffers	Compositions
Citrate buffer	0.1 M trisodium citrate 2x H ₂ O 0.01 M EDTA 1.2 M MgSO ₄ In H ₂ O pH was adjusted to 5.8 with Citric acid solution Sterilization: autoclaved for 5 min at 121°C
Trapping buffe	0.6 M sorbitol 0.1 M Tris/HCl, pH 7.0
STC buffer	0.01 M Tris/HCl, pH 7.5 0.1 M CaCl ₂ 1 M sorbitol In H ₂ O Filter sterile

Materials and Methods

7.2.1.5.2 Transformation

Transformation protocol of *T. thlaspeos* was exactly the same as *U. maydis* except the plating medium. Instead of REGligh medium YMPG was used and plates were incubated for several weeks at 18 °C until the colonies appeared on the plates.

7.2.1.6 *Ustilago. maydis*

7.2.1.6.1 Culture and competent cells

U. maydis progenitor strain SG200 was overnight grown in primary culture of 3 ml of YL media at 28 °C. The secondary culture was inoculated in 50 ml YL media with the addition of 25 µl from the primary culture. The optical density was checked by measuring the absorption at 600 nm which should be in between 0.6-0.8. The cells were pelleted by centrifugation at 3000 rpm for 5 minutes. The pellet was resuspended in 20 ml SCS buffer and another round of centrifugation was repeated. To obtain protoplast cells were resuspended in 4 ml of enzyme suspension (12.5 mg/ml glucanex in SCS buffer) and incubated at room temperature for 15 minutes. Protoplast formation was observed under the microscope and reaction was stopped by adding 10 ml cold SCS buffer. From now on, all the steps were carried out on ice. Protoplast was pelleted at 2400 rpm at 4°C for 5 minutes and washed two times with 10 ml cold SCS buffer. Cold STC buffer was used for third wash and finally the cells were resuspended in 1 ml of cold STC buffer. 100 µl aliquots were stored at -80 °C or used directly for the transformation.

Solution	Composition
SCS buffer	0.2 M trisodium citrate 2x H ₂ O 1.0 M sorbitol In H ₂ O pH was adjusted to 5.8 with Citric acid solution
STC buffer	0.01 M Tris/HCl, pH 7.5 0.1 M CaCl ₂ 1 M sorbitol In H ₂ O bidest

7.2.1.6.2 Transformation

The frozen protoplast of *U. maydis* was thawed on ice and mixed with 1 µl heparin and the plasmid DNA of 1-5 µg followed by 10 minutes incubation on ice. Afterwards 500 µl STC/PEG was added gently and incubated for another 15 minutes on ice. At last, the mixture was spreaded on two layered REGligh media plates. The bottom layer of REGligh was supplemented with double concentration of required antibiotic while top layer was spread with only REGligh media. The plates were incubated for 5-7 days at 28 °C.

Solution	Composition
Heparin solution	15 mg/ml heparin In H ₂ O
STC/PEG	15 ml STC 10 g PEG 4000

Materials and Methods

7.2.2 Infection assays

5.2.2.1 Infection of *A. thaliana* with *P. syringae* (Pst-LUX)

A colony of Pst-LUX strain from the freshly streaked plate was inoculated in 100 ml DYT media with required antibiotic and incubated at 28 °C for 24 hours at 200 rpm. The optical density was measured at 600 nm which should be between 1-1.5. The final OD₆₀₀ of 0.2 was used and proceeded with centrifugation at 4000 rpm for 4 minutes. The cells were washed two times with 30 ml distilled water and finally resuspended in 30 ml water. 1.2 ml of 1% Sliwet with the overall concentration 0.04% was added to 30 ml cell suspension. Afterwards 4 weeks old *A. thaliana* plants were spray inoculated and 15 ml of inoculum was used for spraying 5 plants. Plants were covered with the lid and incubated in the plant growth chamber for 3 days.

7.2.2.2 Infection of *A. thaliana* with *T. thlaspeos* culture

7.2.2.2.1 Preparation *A. thaliana* seedlings

Seeds of mutant or tagged lines of *A. thaliana* were surface sterilized with 70% ethanol subsequently followed by 100% ethanol, each with three time washing steps with water. ½ MSN media supplemented with 0.5% sucrose were used for seeds cultivation. A small chamber was made by cutting the agar for pouring the culture. About 10 seeds were placed on each plate and incubated in the growth chamber in the sterile condition. Three weeks old seedling were used for the infection assay.

7.2.2.2.2 Infection assay

T. thlaspeos culture was cultivated in 20 ml YL media for 3-4 days and transferred to the glass homogenizer after checking the contamination. All the clumps were homogenized and the cells were harvested by centrifugation at 3500 rpm for 5 minutes. The pellet was washed with 10 ml sterile water and centrifuged again. The cells were resuspended in 5 ml water and OD₆₀₀ was adjusted to 0.5. About 1.5 ml of culture was poured in each chamber to evenly covered the submerged roots. Plates were incubated for 30 minutes under the clean bench, and the fungal solution was removed. The plant roots were washed with sterile water and carefully removed all the fungal clumps. Plates were sealed with two layers of parafilm to avoid the contamination. Plates were incubated again for 1 week in the sterile growth chamber. Plants were carefully detached from the plant agar and subjected to WGA/PI staining (according to Doehlemann, 2018). The scoring system for the culture Infection of *T. thlaspeos* is not established yet therefore analysis was done according to differences have noticed under the microscope.

7.2.2.3 Infection of *Z. mays* with *U. maydis* SG200 strain

U. maydis strain SG200 with required genetic manipulation were grown in the primary and secondary culture as described in the competent cells preparation section. The cells were grown until they reached the OD₆₀₀ of 1.0. The cells were pelleted at 3500 rpm for 5 minutes followed by three-time washes with sterile water. Final resuspension was done in water with OD₆₀₀ of 3.0. The cells were kept on the continuous shaking until use. 7-8 days old maize plants were infiltrated with 1 ml syringe by injecting 250-500 µl of prepared cell suspension in the stem of each plant (1 cm above the ground). The injection was considered successful if the suspension oozes out at the top of leaves. For the negative control water was injected

Materials and Methods

instead of cell suspension. Plants were kept in the control condition in the assigned growth chambers and first scoring was done at 7 days post infection and subsequently followed by second scoring after 12 days. Scoring system was the analysis of the following symptoms: healthy plants, chlorosis, anthocyanins, small tumors, large tumors and dead plants.

7.2.3 Plant growth condition and assays

7.2.3.1 *Arabidopsis* seed sterilization

Prior to plating in the media, *Arabidopsis* seeds were surface sterilized with 6% sodium hypochlorite, 1% triton X-100, and distilled water for 10 minutes. The seeds were then stratified for a period of two to three days at 4°C in the dark before being placed in 0.1% plant agar. Seeds were grown on soil without sterilization, only stratification was performed for soil grown plants.

7.2.3.2 *Arabidopsis* plant growth

After being sterilized, the seeds were plated on ½ MSN agar medium in the sterile growth chamber at 21°C/24°C and 16 h of dark and 8 h of light (short day condition) with a light intensity of 110-150 mol m⁻²s⁻¹. The same conditions were used for the plant grown on soil or jiffy pellets.

7.2.3.3 *Arabidopsis* transgenic line generation

A. thaliana plants were grown according to the above-mentioned method and waited until they started flowering. Most of the flowers have immature clusters and only few have fertilized siliques which were removed before transformation. *Agrobacterium* strain was freshly transformed with the required construct and culture was grown in DYT media at 28°C for 1-2 days. Culture was grown until the OD₆₀₀ reached 2.0 and poured in to 120 ml of 5% sucrose solution. 0.03% of silwet was added to the culture and sucrose suspension. Inflorescence of the above selected plants were dip inoculated in the sucrose solution containing culture for 1 minute. Plants were immediately covered with the plastic bags and kept in dark overnight. Plants were shifted to the growth chambers and harvested upon production of seeds. Verification of the transformation was done by growing seeds on ½ MSN media supplemented with appropriate antibiotics.

7.2.3.4 *N. benthamiana* infiltration with *A. tumefaciens*

A pre culture of the *A. tumefaciens* transformed with gene of interest was inoculated in 5 ml DYT media at 28 °C for 14 hours followed by secondary culture in 50 ml DYT media with 0.5 ml of inoculum from the pre culture. Appropriate antibiotics were added according to the plasmid selection. The cells were centrifuged at 5000 rpm for 15 min at 4 °C. The pellet was resuspended with 2 ml of tobacco infiltration solution to a final optical density at 600 nm (OD₆₀₀) of 0.5 to 1.0. Following this, the suspension was incubated at room temperature for 2-3 hours with slight shaking at room temperature. Moreover, the tobacco leaves were kept dampish to retain the stomata in an open state. Afterwards, the undersurface (abaxial side) of 2 fully expanded leaves of *N. benthamiana* were slowly infiltrated with 100 µl suspension per spot using needless syringe. The plants were kept in dim light or dark at 23 °C under high humidity

Materials and Methods

for 2-3 days. Confocal microscopy was then performed to check the expression of fluorophore tagged with the gene of interest.

Solution	Compositions
AS or infiltration solution	10 mM MgCl ₂ , 10 mM MES in H ₂ O bidest pH 5.6 100 µM acetosyringone in ethanol

7.2.4 Isolation of nucleic acids

7.2.4.1 Plasmid DNA extraction

Plasmid DNA was extracted through crude method of boiling preparation by using the modified version of Sambrook (1989). Overnight culture was inoculated in 2 ml DYT media supplemented with required antibiotic and incubated at 37°C. The cells were harvested by spinning them at 8000 rpm for 2 minutes. The pellet was resuspended in 200 µl STET buffer and 20 µl lysozyme. This suspension was boiled at 95°C for 1 minute and subjected to a centrifugation step at 13000 rpm for 10 minutes. A slimy pellet formed which was removed with a tooth pick. To precipitate the DNA, 20 µl minilli (3 M sodium acetate pH 5.3) and 500 µl isopropanol were added. The suspension was mixed by inverting the tubes several times followed by centrifugation at 13000 rpm for 10 minutes. The supernatant was discarded and pellet was washed with 70% ethanol and centrifuged again for 3 minutes. Finally, the pellet was dried at 50 °C for 5 minutes and resuspended in 100 µl TE/RNase. Pellet was dissolved in TE/RNase at 50 °C for 10 minutes of shaking at 600 rpm.

Lysozyme solution	STET	TE/RNase A
10 mg/ml lysozyme	50 mM Tris-HCl, pH 8.0	10 mM Tris/HCl, pH 7.9
10 mM Tris-HCl, pH 8,0	50 mM Na ₂ -EDTA	1 mM Na ₂ -EDTA
In H ₂ O	8 % (w/v) sucrose	20 µg/ml RNase A
	5 % (w/v) Triton x-100	In H ₂ O
	In H ₂ O	

7.2.4.2 *A. thaliana* gDNA extraction

Plant (*A. thaliana*, *Ar. hirsuta*) gDNA was extracted by following the CTAB method. 4 weeks old leaf material was snap freeze in the liquid nitrogen and homogenization was done in the tissue lyser. Following components were needed for the extraction:

Components	Volume/Conc
3x extraction buffer	3% CTAB(w/v), 1.4M NaCl, 0.8 M Tris-HCl pH 8.0, 0.5M EDTA pH 8.0
2- beta-Mercaptoethanol	0.3 %
Chloroform:isoamyl alcohol (24:1 v/v)	800 µl
5 M NaCl	350 µl
3 M Potassium acetate	70 µl
Isopropyl alcohol	500 µl
Ethanol	500 µl
TE buffer	50 µl

Materials and Methods

Extraction buffer was preheated at 65 °C and 3% 2-beta-Merceptoethanol was added immediately before use. 50 mg of grinded plant material and mixed with 800 µl preheated CTAB extraction buffer. The sample mixture was incubated at 60 °C for 1 hour and mixed every 20 minutes by inverting the tubes several times. An equal volume of chloroform: isoamylalcohol (24:1) was added and mixed by slight inversion. The mixture was centrifuged at 13000 rpm for 15 minutes at room temperature. The aqueous phase was carefully transferred to the new tube and mixed with 350 µl of 50 M NaCl and 70 µl of 3 M potassium acetate. Afterwards 500 µl ice cold 100% isopropanol was added and followed by gentle inversion until the DNA cloud was visible. This mixture was centrifuged at 13000 rpm for 5 minutes after a 30 minutes incubation step at -20 °C. Supernatant was discarded and DNA pellet was washed with 70% ethanol. Pellet was dried at room temperature for an hour and eluted in 50 µl 1x TE buffer. To quickly resuspend the pellet another incubation step was done at 50 °C for few minutes. DNA was stored at -20 °C.

7.2.4.3 *A. thaliana* RNA extraction

The harvested plant material (50 mg) was snap freezed in liquid nitrogen and homogenize to fine powder. 1 ml trizol was added to the sample and immediately placed them on ice after mixing. Samples were incubated in ice for 5 minutes. 200 µl cold chloroform was added, vortex for 10 seconds and incubated at room temperature for 5 minutes. Samples were centrifuged at 12000 rcf for 15 minutes at 4 °C. The upper aqueous phase was separated carefully and mixed with 500 µl cold iso-propanaol and tubes were inverted several times. An incubation was done at -20 °C for 15-20 minutes and then centrifuged for 10 minutes at 12000 rcf. Pellet was washed two time with 1 ml of 70% ethanol. A centrifugation step of 5 minutes at 12000 rcf was done in between each wash. The pellet was dried for 10 minutes and resuspended in HPLC grade water. This was followed by treatment with RNase-free DNase for the removal of any genomic DNA contamination. The DNase free RNA was either stored immediately at -80 °C or run on 1 % agarose to check the quality of RNA.

7.2.4.4 cDNA synthesis

The protoscript II reverse transcriptase kit was used for cDNA synthesis. According to the manufacturer's instructions, first-strand cDNA synthesis was carried out at 42°C for 60 min in 20 µl of reaction mixture containing 5 or 10 µg of total RNA, 20 pmol of oligo (dT), and 200 units of reverse transcriptase (Invitrogen Life Technologies).

7.2.4.5 Polymerase chain reaction (PCR)

Polymerase chain reaction (PCR) was done according to a modified version of standard protocol (Innis, 1990). A typical PCR reaction was consisted of sequence specific primer pair (10 µM), 10-50 ng template, dNTPs 25 µM, required buffer and NEB Phusion polymerase.

Component	Volume (µl)
NEB Phusion Buffer (5x)	5
dNTPs	0.25
NEB Phusion-Polymerase	0.25
Forward-Primer (10µM)	1.5
Reverse-Primer (10µM)	1.5
DNA-Template (1-50 ng)	1
H ₂ O	add 25 µl

Materials and Methods

Following standard program was used for the reactions. The annealing temperature and final extension temperature was adjusted according to requirement of each reaction.

98 °C	3 min	
98 °C	20 s	
50-70 °C	20 s	35 cycles
72 °C	10 s up to 3 min	
72 °C	8 min	
4 °C	∞	

7.2.4.6 Restriction digestion

A standard restriction digestion was done by using the following components while the amount of used DNA and final volume varied according to the requirement of the experiment. All the enzymes were used from New England Biolabs.

Component	volume (µl)
DNA	1-5
Cutsmart buffer	2
Enzyme	0,25
H ₂ O	Adjusted accordingly
Total	20

7.2.4.7 Gel extraction/PCR purification

Extraction of DNA from agarose gels and purification of PCR products were carried out by using the Monarch Gel extraction kit and Monarch PCR purification kit. The user manuals were followed for the extraction and purification.

7.2.4.8 DNA sequencing

DNA sequencing was done by using the service from Eurofins and LMU Biozentrum Munich. Sequencing analysis was performed in Clone Manager version 9 by using the sequence assemblies.

7.2.4.9 Gene expression analysis (Semi quantitative RT-PCR)

The semi quantitative PCR was done by using cDNA (Synthesis described in sec 5.2.4.4) (1:10) as a template. The primers were designed for coverage of at least 200-300 bp of the gene of interest and fulfilled the requirement of basic synthesis criteria, annealing temperature, GC content, primer dimers and stabilization. The PCR was done according to the standard program as described in sec 5.2.4.5 by using 1 µl diluted cDNA and 250 nM primers. The cycles were reduced to 25 and final extension time was set to 10 seconds. Afterwards the product ran on the 2% agarose gel and the band intensities were compared.

7.2.4.10 Southern blot analysis

Verification of gene deletion or insertion from the genome (*U. maydis*) was carried out by using a modified version of protocol from (Southern, 1975). The genomic DNA was extracted from the strain which needs to be verified and subjected to the restriction digestion with the

Materials and Methods

appropriate enzymes overnight. The digested DNA was run on the 0.8% agarose gel for about 2 hours with low voltage. Afterwards the separation of the DNA was visualized in the UV light. Then the gel was incubated in 0.25 M HCl for 20 minutes and rinsed with water. Incubation in DENAT and RENAT solution was followed for 20 minutes each with the washing step.

At this point the DNA was transferred from gel to the membrane by using the following blotting steps:

Assembly was started from bottom to top.

Weight

Paper towel

2 Whatman paper (3mm)

Nylon membrane

Prepared gel

Salt bridge with Whatman paper soaked in 20xSCS

After overnight blotting the transferred DNA on the membrane was fixed by UV-cross linking at 120 mJ. Afterwards the membrane was incubated in hybridization buffer for 30 minutes at 65 °C. In parallel, probe preparation was done by amplifying the upstream and downstream flank of the gene of interest by using the DIG dNTPs. The probe was denatured at 95 °C for 5 minutes and immediately added to 15 ml hybridization buffer. The membrane was transfer to hybridization buffer containing probe and incubated overnight. The next day membrane was washed in southern wash buffer I, II and III for 15 minutes at 65 °C each. Then membrane was washed in DIG wash buffer for 5 minutes at 25 °C followed by an incubation in DIG2 for 30 minutes at 25 °C. (DIG2 consist of 1% milk powder and used for blocking). 15 ml of DIG2 supplemented with anti-dioxygenin antibody used for 1-hour incubation of membrane. At last membrane was washed two times with DIG wash for 15 minutes and one time with DIG3 buffer for 5 minutes. Membrane was incubated in 8 ml CDP-star solution for 5 minutes and chemiluminescent was detected in ImageQuant LAS 4000.

Solution	Composition
0.25 M HCl	3.26 % (v/v) HCl in H ₂ O bid.
DENAT	1.5 M NaCl 0.4 M NaOH in H ₂ O.
RENAT	1.5 M NaCl 282 mM Tris-HCl 218 mM Tris-Base in H ₂ O
20xSCS	3 M NaCl 0.3 M tri-sodium citrate *2H ₂ O in H ₂ O pH 7
20xSSPE	0.02 M EDTA 2.98 M NaCl in 0.2 M phosphate buffer pH 7.4
Denhardt solution	2 % (w/v) BSA fraction V 2 % (w/v) ficoll 2 % (w/v) polyvinylpyrrolidon in H ₂ O
Hybridization buffer	26 % (v/v) SSPE (20x) 5 % (v/v) Denhardt solution 5 % (v/v) SDS (10 %) in H ₂ O

Materials and Methods

Southern wash I	10 % (v/v) SSPE (20x) 1 % (v/v) SDS (10 %) in H ₂ O
Southern wash II	5 % (v/v) SSPE (20x) 1 % (v/v) SDS (10 %) in H ₂ O
Southern wash III	0.5 % (v/v) SSPE (20x) 1 % (v/v) SDS (10 %) in H ₂ O
DIG1	100 mM maleic acid 150 mM NaCl in H ₂ O. pH 7.5 (adjust with NaOH)
DIG2	1 % (w/v) skim milk powder in DIG1
DIG3	0.1 M Tris-HCl 0.1 M NaCl in H ₂ O bid. pH 9.5 (adjust with NaOH)
DIG wash	0.3 % Tween-20 in DIG1
CDP-Star solution	1 % CDP-Star in DIG3

7.2.5 Isolation of protein

7.2.5.1 Protein extraction from plant

Input plant material for protein extraction was *N. benthamiana* and *A. thaliana*. Plant material (50 mg) was harvested, snap frozen and homogenized in tissue lyser. Protein extraction buffer (600 µl) was added immediately to the lysed plant material and incubated the samples on rotating device at 4 °C for 1 hour. Afterwards the samples were centrifuged at 13000 rpm for 20 minutes at 4 °C. The supernatant was collected in a separate tube and checked for the protein concentration.

Extraction buffer:

50 mM Tris-HCl pH 7.5

150 mM NaCl

1 mM EDTA

10 % Glycerol

0,1 % Nonident 40

5 µM DDT

proteinase inhibitor cocktail

7.2.5.2 Protein extraction from yeast

Protein extraction from yeast was done according to yeast manual (Clontech). Extraction was started by inoculating an overnight 5 ml culture in SD-Ura drop out media. A secondary culture was inoculated in 50 ml SD-Ura drop out media with the entire overnight culture. The culture was incubated at 30 °C at 220 rpm until the OD600 reached 0.4-0.6. Afterwards, the cells were pelleted at 1000 g for minutes at 4 °C, washed with 50 ml ice cold water and centrifuged again. OD600 was measured and 7.5 units of the cells were resuspended in 100 µl of preheated yeast cracking buffer. This suspension was mixed with 80 µl glass beads and shake them on heat block at 70 °C for 10 minutes. The cells were pelleted at 13000 rpm at 4 °C for 5 minutes. Supernatant was collected and checked on SDS gel.

Materials and Methods

Yeast Cracking Buffer	Total volume (10 ml)
40 mM Tris-HCl (pH 6,8)	800 µl (0,5 M Stock)
8 M Urea	4.85 g
5 % (w/v) SDS	0.5 g
0,1 mM Na ₂ -EDTA	2 µl (0,5 M Stock)
0,4 mg/ml Bromphenolblau	4 g
Freshly added	
Mercaptoethanol	88,5 µl
Benzamidin	619,5 µl
Protaseinhibitormix Roche	400 ,0 µl

7.2.5.3 Western blot analysis

The western blot analysis was carried out in accordance with (Sambrook et al., 1989). The transiently expressed protein in *N. benthamiana*, *A. thaliana* and *E. Coli* was extracted. Using 12% SDS-polyacrylamide gel, total protein extract containing the desired protein was separated. Gel electrophoresis was carried out in Tris-Gly buffer (also known as "Running buffer") by using micro gel equipment from Bio-Rad. The proteins were transferred to the PVDF membrane by using anode and cathode buffers at 80-85 mA for 1.5 hours.

The PVDF membrane was blocked for 1 hour with 5% skimmed milk/BSA solution dissolved in TBST to limit nonspecific antibody binding. This was followed by an overnight incubation at 4°C with the required antibody (anti His, anti GFP, anti actin 1:1000, Sigma-Aldrich) in 3-4% milk-TBST. The membrane was then rinsed in TBST four times for ten minutes each. Afterwards, incubation with secondary antibody (anti mouse IgG, HRP conjugate, Promega W4021, 1:4000) was done for 1 hour at room temperature and followed by four time washing steps for 10 minutes each. To detect, GE Health Care's ECL system was used and chemiluminescence imaging were done at LAS.

Anode buffer 1	Anode buffer 2	Cathode buffer
300 mM Tris/HCl, pH 10.4	30 mM Tris/HCl, pH 10.4	25 mM Tris/HCl, pH 9.4
15% MeOH	15% MeOH	40 mM ε-Aminocaproic acid
		15% MeOH
SDS Running buffer	TBST	
25 mM Tris Base	50 mM Tris-Base	
192 mM Glycine	150 mM NaCl	
0.1% SDS	0,6% (w/v) Tris-HCl	
	0,05% (v/v) Tween-20	

7.2.6 Cloning

7.2.6.1 Classical cloning

The gene of interest was PCR amplified by using the required enzymes sites in the primer pair. The same PCR product was subjected to restriction digestion along with corresponding destination vector by mixing the following components:

Materials and Methods

Components	Volume (μ l)
Cutsmart Buffer NEB	2
PCR product/destination vector	0.1- 0.5 μ g
Enzyme	0,25
H ₂ O	16,8
Total	20

Restriction digestion was done by using the enzymes supplied by NEB. Digested PCR product for insert and the backbone vector were incubated at 37 °C for 2 hours and followed by gel purification (0.8 %). Afterwards the purified products were ligated by using the following components:

Components	Volume (μ l)
T4 ligase buffer (10x)	1
DNA insert	3x
DNA vector backbone	x
T4 ligase	0,5
H ₂ O	ad 10 μ l

Ligation of the product was done by using NEB ligation calculators therefore the volume and concentrations were adjusted accordingly for each ligation. Ligation was done in 1:3-1:5 molecular ratio of vector backbone to insert. The reaction was incubated at 16 °C overnight or at room temperature for 30-60 minutes. Afterwards the *E. coli* cells were transformed with the ligated mixture.

7.2.6.2 GoldenGate cloning

Terfrüchte et al., 2013 was followed for the GoldenGate cloning. Primers were designed according to the instruction with type III restriction enzyme BsaI or SapI with compatible overhangs. Both restriction and ligation were carried out together in one reaction which are as followed with the other required components:

Components	Volume (μ l)/(μ g)
T4 ligase buffer (10x, Roche)	1.5 μ l
Destination vector	75 ng
Storage vector	75 ng
Inserts/ flanks	40 ng/kb
T4 DNA ligase (Roche)	0.75 μ l
<i>BsaI</i> -HF	0.5 μ l
H ₂ O	ad 15 μ l

All the components were mixed in one tube and the reaction was carried out in a PCR cycler by using the following program

(37°C 2 min and 16°C 5 min) 50 cycles

37°C 5 min, 50°C 5 min, 80°C 5 min

16°C ∞

The final product of this reaction was used for *E. coli* transformation.

7.2.6.3 GreenGate cloning

GreenGate cloning was done according to the Lampropoulos et al., 2013. The basic principle of GreenGate cloning is same as GoldenGate cloning. The type III restriction enzyme BsaI

Materials and Methods

was used together with T4 ligase. In this system each fragment was available as an independent module in a vector. Each module tagged with Bsal enzyme including the destination vector. Primers were designed for the required gene with Bsal enzyme site and compatible overhang according to the corresponding module. One pot reaction consists of the following components

Component	Volume (ul/ng)
T4 ligase	1 μ l
Bsal-HF	1 μ l
Cutsmart	1.5 μ l
ATP(10mM)	1.5 μ l
Destination vector	100 ng
Promotor (Ubi10)	100 ng
Terminator (Ubi10)	100 ng
PNos-KanR	100 ng
Required module	100 ng
PCR product	100 ng
H ₂ O	Add 15

All these components were added in a tube and subjected to following reaction in a PCR cyclor. (37°C 5 min and 16°C 5 min) 50 cycles

37°C 5 min

50°C 5 min

80°C 5 min

16°C ∞

The final product of this reaction was used for *E. coli* transformation.

7.2.6.4 Gateway cloning

This cloning technique consists of two reactions (BP and LR) for generation of an expression plasmid, it is based on the homologous recombination of the designed overhangs called *att*-sites.

7.2.6.4.1 BP reaction

The BP reaction was performed to clone the insert in to the entry plasmid. Primers were designed with the *attB* sites to amplified the gene of interest. Principle of homologues recombination applied as exchange should occur between *attB* of PCR product *attP* of donor vector (pDONR221) resulting in *attL* sites of entry clone and *attR* as a by-product. The BP reaction was catalyzed by an enzyme BP clonase in the following ratio:

PCR fragment: 3 μ l (10 ng)

Donor vector: 1 μ l (50-150 ng)

BP Clonase: 0.5 μ l (1 U)

All the components were added and incubated at 25°C for 1 hour. The reaction was terminated by adding 1 μ l of Protinase K and incubated at 37°C for 10 minutes. Afterwards, *E. coli* cells were transformed with the product of entry plasmid. Plasmid was extracted and the correct plasmid was confirmed by sequencing.

Materials and Methods

7.2.6.4.2 LR reaction

After successful generation of entry clone, LR reaction was carried out to transfer the cloned gene from entry plasmid to the destination vector for obtaining the final expression plasmid. Homologous reaction was done between *attL* of the entry clone and *attR* of destination vector resulting in *attB* of expression plasmid and *attP* as a by-product. The LR reaction catalyzed by LR clonase and other components were added in the following ratio:

Entry clone: 2.5 μ l (10-150 ng)
Destination vector: 2.5 μ l (50-150 ng)
LR Clonase: 0.5 μ l (1 U)

All the components were mixed and incubated at 25°C for 1 hour. The reaction was terminated by adding 1 μ l of Proteinase K and incubated at 37°C for 10 minutes. The *E. coli* cells were transformed with the expression clone and confirmed by sequencing.

7.2.7 *E. coli* protein expression and purification

7.2.7.1 Expression

E. Coli strain LOBSTR was used to express the GST_His_TtTue1, JAS1_MBP1, CPK28_GB1 protein of *A. thaliana* and *Ar. hirsuta*. To begin, 20 ml culture of freshly transformed cells with the above mentioned IPTG inducible construct inoculated at 37°C overnight. The following day, a fresh 800 ml (Big culture) of DYT medium with required antibiotic was used to dilute the overnight small culture to OD600 0.1. The cells were grown at 37°C to mid-log phase (OD600 = 0.6 to 1.0) with continual shaking at 200 rpm, and after attaining the required OD600 (0.6 - 0.8), expression was induced by adding IPTG at a final concentration of 0.5 mM and let the cells to grow to overnight at 18°C. Afterwards, the cells were centrifuging at 5000 rpm for 15 minutes and pellet was resuspended in 30 ml lysis buffer. Cell disruption was carried out by using the sonicator.

Following sonicator program was used:

Pulse on time 15 sec
Pulse off time 30 sec
Total processing time 10 minutes
Cycles 1
Amplitude 60%

The sonicated cells were centrifuged at 18000 rpm for 30 minutes at 4°C. Before starting the protein purification, solubility test was done by running the resuspended pellet and supernatant on 12% SDS gel. For the above-mentioned constructs protein were in soluble phase and subjected to purification.

7.2.7.2 Purification

Purification was started with equilibrating the 5 ml Ni-NTA column with buffer A at a rate of 200 using the peristaltic pump followed by passing the whole cell lysate at 4°C. Afterwards the column was washed with buffer A and let it run for 10-20 minutes. The pump was washed with buffer B by detaching the column. The protein was eluted in buffer B having total volume of 15 ml. An amicon concentrator of the right cut off according to the size of each protein was used to concentrate the protein. Samples were centrifuged in the concentrator at 5000 rpm at 4°C

Materials and Methods

to final volume of 0.5-2 ml. At this point the concentrated sample was checked on 12 % SDS gel again.

7.2.7.3 Size exclusion chromatography (SEC)

Size exclusion chromatography was performed in SEC-system/Äkta PRIME by using the HiLoad Superdex 200 prep grade column. Column was washed with SEC buffer by selecting the column equilibration program in Äkta PRIME followed by loop wash. Afterwards the concentrated sample was loaded on loop and started the sample application and elution program from the system. According to the chromatogram of protein, the protein fractions were collected and checked on 12% SDS gel. After verification of the correct protein, the collected fractions were pooled and concentrated to final volume of 1 ml. Protein concentration was calculated by using the following formula:

$A = \epsilon \cdot c$ (A: measured absorption; ϵ : extinction coefficient of the protein; c: concentration in mmol/ml). Protein either used directly for the assays or stored at -80°C .

1x Lysis buffer	1x Buffer A	1x Buffer B	1x SEC Buffer
20 mM HEPES pH 8.0	20 mM HEPES pH 8.0	20 mM HEPES pH 8.0	20 mM HEPES pH 7.5
20 mM KCl	20 mM KCl	20 mM KCl	20 mM KCl
250 mM NaCl	250 mM NaCl	250 mM NaCl	200 mM NaCl
40 mM Imidazole	40 mM Imidazole	500 mM Imidazole	
100 mM PMSF			
0.1-1mg/ml Lsozyme			

7.2.8 GST pull down assay

Glutathione agarose beads were used for interaction assays. GST beads (GE Healthcare) were twice washed with SEC buffer. A total amount of 4 nmol of SEC purified GST tagged protein was loaded on the beads and incubated on roller for 30 minutes at 4°C . Then beads were washed twice with SEC buffer contained 0.05% tween and re-loaded with interacting His tagged protein. Another incubation step of 1 hour with constant rotation was done at 4°C followed by washing steps. The supernatant was removed in each step by spinning at 4000 rpm for 1 minute. At last, protein was eluted in 80 μl of GSH elution buffer or 2x SDS loading buffer devoid of DTT and bromophenolblue and incubated at 95°C for 5 minutes to elute bound proteins. The eluted protein was then exposed to SDS-PAGE gels for further analysis.

GSH elution buffer

20	mM HEPES PH 8.0
200	mM NaCl
20	mM KCl
20	mM MgCl ₂
0.05%	Tween
20	M reduced- glutathione

7.2.9 MicroScale Thermophoresis (MST)

The MST measurements were performed according to the protocol described by (Gopalswamy et al., 2022). Prior to the MST experiments, purified *TtTue1* protein was labeled

Materials and Methods

with the dye Alexa Fluor[®] 488 (NHS Ester Protein Labeling kit, ThermoFisher Scientific, USA) by incubating 185 μM of protein and 555 μM of dye (100 μl reaction volume) for 1 h at room temperature ($\sim 22^\circ\text{C}$), followed by 40 min at 30°C . Labelling reaction was performed in a buffer consisting of 50 mM sodium phosphate, 50 mM sodium chloride, pH 8.0 and the same buffer was used for all MST measurements. The dye-labeled proteins were purified using a PD-10 column containing Sephadex G-25 Mini (GE Healthcare Life Sciences) and then centrifuged at 50,000 rpm for 30 min. The concentrations and the efficiency of the labeling were determined as indicated in the manual of the labeling kit.

Thermophoresis was measured for the labeled *TtTue1* protein alone (as a control experiment) or by mixed 600 nM of labeled *TtTue1* with unlabeled binding partners, His-MBP-*AtJAS1* (852 μM), His-GB1-CT-*AtJAS1* (370 μM), His-MBP-*ArhJAS1* (80 μM), His-GB1-*AtCPK28* (588 μM), His-GB1-*ArhCPK28* (758 μM), to 1:1 dilution of 16 serial dilutions. The mixtures were incubated in the dark for about 5 hours or overnight at room temperature. The experiment was carried out using a Monolith NT.115 instrument (NanoTemper Technologies GmbH, Munich, Germany). The measurements were performed with an excitation power of 20-50% for 30 s and MST power of 40% at an ambient temperature of $\sim 24^\circ\text{C}$. Triplicates of the same dilution were measured.

The data was analyzed and the constant of dissociation (K_D) was calculated using the MO affinity analysis software (NanoTemper, Germany), considering a 1:1 model. Same data points were fitted to the Hill Model to obtain the Hill coefficient (n), represent the cooperativity of the binding.

7.2.10 Bimolecular fluorescence complementation (BiFC)

Bimolecular fluorescence complementation (*BiFC*) has been effectively used for *in vivo* protein-protein interaction research for many years. The method is based on the interaction of two non-fluorescent mVenus fragments, which combine to generate fluorescent complexes. The split mVenus constructs were generated by GreenGate cloning as described above in the 5.2.6.3. *TtTue1* was tagged with mVenus split1 and the interaction partners were tagged with mVenus split2. *A. tumifaciens* strain C59pMP90 was transformed with each construct according to the 5.2.1.3.2. and co infiltration of *TtTue1* and each interaction partner in *N. benthamiana* was done according to the 5.2.3.4. After 3 days post infiltration interaction of both proteins were observed via mVenus signal through confocal microscopy described in 5.2.12.

7.2.11 Chromatin immunoprecipitation (ChiP)

Chromatin immunoprecipitation was done by following the (Kaufmann et al., 2010).

A. thaliana transgenic lines expressing *TtTue1*-Gfp, Col-0-GFP; and Col-0 were used for ChiP analysis. 0.8 g of 4 weeks old leaf tissues were crosslinked under vacuum in 25 ml MC buffer containing 1% formaldehyde. Tissue fixation was done for 30 minutes by applying vacuum two times each with 15 minutes. Fixation was stopped by adding 2.5 ml of 1.25 M glycine and followed by vacuum for 2 minutes. Afterwards, tissues were washed thrice with MC buffer and grinded. Tissue powder were mixed with 20 ml M1 buffer and passed through the 55 μm mesh. The filtrate was centrifuged at 1000 g for 20 minutes at 4°C . The supernatant was discarded and pellet was washed five times with 5 ml of M2 buffer, each with a centrifugation step at 1000 g for 10 minutes at 4°C . The last washing step was done with 5 ml of M3 buffer and centrifuged again. Pellet was resuspended in 1 ml of sonic buffer and chromatin was sonicated on ice by using the following settings:

Materials and Methods

Amplitude 50%

Pulse on time 15 sec

Pulse off time 45 sec

3 cycles

The suspension was centrifuged two times at maximum speed for 10 minutes at 4 °C. The supernatant was mixed with an equal volume of IP buffer and 120 µl was set aside as Input DNA. To load clean sample on the beads, centrifugation at 16000 g was done for 10 minutes. Samples were split in to two equal volumes, one treated with control agarose magnetic beads (Chromotek) as a negative control and second sample loaded on 30 µl GFP trap magnetic beads serve as IP sample. Both samples were incubated on rotating device at 4 °C for 1 hour. Then the beads were either separated by centrifugation at 3800 g or by using the magnetic rack at 4 °C. Beads were washed five times with 1 ml of IP buffer for 8 minutes each followed by 2 minutes centrifugation at 3800 g at room temperature. The protein-DNA complex was eluted from the beads in 100 µl cold elution buffer with 1-minute incubation at 37 °C and the supernatant was mixed with 150 µl of 1 M Tris pH 9 to neutralize with 4 minutes of incubation at 37 °C. Proteinase K (0.5 mg/ml) was added to the eluted sample and overnight incubated at 37 °C followed by 6 hours incubation at 65 °C for reverse crosslinking. The separated DNA was precipitated with 100% ethanol (2.5 vol), 3 M NaOAc pH 5.4 (1/10) and 1 µl glycobule overnight at -20 °C and then centrifuged at maximum speed at 4 °C for 30 minutes. DNA pellet was resuspended in 100 µl milliQ water. DNA purification was done by using the Monarch PCR purification kit and samples were eluted in 30 µl elution buffer.

Sodium phosphate buffer pH 7 (1 M stock)

57.7 ml 1 M disodium hydrogen phosphite
(Na₂HPO₄)

42.3 ml 1 M sodium dihydrogen phosphate
(NaH₂PO₄)

Sterile filter

M1 buffer (fresh)

10 mM sodium phosphate, pH 7

0.1 M NaCl

1 M 2-methyl 2,4-pentanediol

10 mM β-mercaptoethanol

½ tablet of protease inhibitor cocktail

Final volume 25 ml

M3 buffer (fresh)

10 mM sodium phosphate, pH 7

0.1 M NaCl

10 mM β-mercaptoethanol

½ tablet of protease inhibitor cocktail

Final volume 25 ml

IP buffer

50 mM HEPES, pH 7.5

150 mM NaCl

5mM MgCl₂

10 µM ZnSO₄

1% Triton X-100

0.05% SDS

MC buffer (fresh)

3.423 g of sucrose

10 mM sodium phosphate, pH 7

50 mM NaCl

0.1 M sucrose

M2 buffer (fresh)

10 mM sodium phosphate, pH 7

0.1 M NaCl

1 M 2-methyl 2,4-pentanediol

10 mM β-mercaptoethanol

10 mM MgCl₂

0.5% Triton X-100

½ tablet of protease inhibitor cocktail

Final volume 25 ml

Sonic buffer

10 mM sodium phosphate, pH 7

1.1 M NaCl

0.5% Sarkosyl

10 mM EDTA

½ tablet of protease inhibitor cocktail

Final volume 50 ml

Elution buffer

0.1 M stock

0.5 stock

0.05% Tween-20

pH 2.8

Materials and Methods

7.2.12 ROS assay

A. thaliana expressing *TtTue1-Gfp*, *Col-0-GFP*; and *Col-0* were used for the ROS assay. Leaf discs of youngest fully expanded 4 weeks old plants were harvested with a cork borer no.1 (3.8 mm). A total of 16 leaf disc were used for each plant line. Leaf discs were transfer to the 96-well plate contained 200 μ l water and incubated overnight at room temperature. Water was replaced with fresh 50 μ l and leaf discs were incubated for 1 hour. 50 μ l of assay solution was added to the each well carrying disc and immediately start measurement in the Berthold Luminometer.

Components	stock solutions	Volume
Luminol 17 μ g.mL ⁻¹	17 mg.mL ⁻¹ in DMSO (100 mM)	6 μ L
HRP 100 μ g.mL ⁻¹	100 mg.mL ⁻¹ in water	6 μ L
PAMP 100 nM	100 μ M in water	6 μ L
Water		2982 μ L

7.2.13 Microscopy

Microscopy imaging of this study was done by using the confocal and light microscope. *Thecaphora* culture infection images were taken at Zeiss Axio imager. M1. This microscope consisted of Plan Neofluar objective lenses, 40x and 100x, NA 1.3; 63x, NA 1.25 and Spot Pursuit CCD camera (Diagnostic Instruments, Sterling Heights, MI, USA). A HXP metal halide lamp (LEj, Jena, Germany) used for excitation of fluorescently-labeled proteins by applying different filter sets for Gfp (ET470/40BP, ET495LP, ET525/50BP) and Rfp/mCherry (ET560/40BP, ET585LP, ET630/75BP). The microscopy imaging was carried out by using a software package MetaMorph version 7.

Confocal microscopy was performed at facility of Center for advanced imaging (CAi) at HHU. GFP, mCherry and mVenus signals were detected in the epidermal cells of *N. Benthamiana* leaves 48–72 hours after transformation by using Zeiss LSM 880 and Zeiss LSM 780.

Both LSM 880 and LSM 780 consisted of GaAsP, PMT and TPMT detectors while LSM 880 has an additional airyscan detector. Laser excitation was carried out at 405, 458, 488, 514, 561 and 633 nm with the corresponding emission filters.

mCherry was excited at 561 nm excitation wavelength and detection filter was 575-615 nm, GFP was excited at 488 nm excitation wavelength by employing detection filter 495-550 nm and mVenus was excited at 514 nm with the detection filter of 520-551 nm. Pinhole (80-120 μ m) and laser power (3-10 %) were adjusted according to the signal strength of different proteins. Images were taken at Plan- Apochromat 40x/1.3 oil/water immersion objective and processed by using the ZEN software

7.2.14 Bioinformatic tool

CloneManager 9 (Scientific and Educational Central Software; Cary, USA)

Ensemble Fungi (<https://fungi.ensembl.org/index.html>)

PEDANT (<http://pedant.helmholtz-muenchen.de/>)

SMART Database (<http://smart.embl-heidelberg.de/>)

Pfam database (<http://pfam.xfam.org/search/sequence>)

Blastn /Blastp (<http://blast.ncbi.nlm.nih.gov/Blast.cgi>)

Phyre2 (<http://www.sbg.bio.ic.ac.uk/~phyre2/html/page.cgi?id=index>)

Materials and Methods

Localizer (<https://localizer.csiro.au/>)

NLStradamus (<http://www.moseslab.csb.utoronto.ca/NLStradamus/>)

cNLSmapper (<https://nls-mapper.iab.keio.ac.jp/cgi-bin/NLS Mapper form.cgi>)

g: Profiler (<https://biit.cs.ut.ee/qprofiler/gost>)

7.2.15 Data analysis, writing and graphical design

Microsoft Office 2016 (Microsoft Corporation)

GraphPad Prism 8 (GraphPad Software Inc.)

ImageJ

ZEN (black edition)

References

8. References

- Aerts N, Pereira Mendes M, Van Wees SC** (2021) Multiple levels of crosstalk in hormone networks regulating plant defense. *The Plant Journal* **105**: 489-504
- Agrios G** (1997) How plants defend themselves against pathogens. *Plant pathology*: 93-114
- Ahmad P, Rasool S, Gul A, Sheikh SA, Akram NA, Ashraf M, Kazi A, Gucel S** (2016) Jasmonates: multifunctional roles in stress tolerance. *Frontiers in plant science* **7**: 813
- Ahmed H, Howton T, Sun Y, Weinberger N, Belkhadir Y, Mukhtar MS** (2018) Network biology discovers pathogen contact points in host protein-protein interactomes. *Nature communications* **9**: 1-13
- Ahmed MB, Santos KCGd, Sanchez IB, Petre B, Lorrain C, Plourde MB, Duplessis S, Desgagné-Penix I, Germain H** (2018) A rust fungal effector binds plant DNA and modulates transcription. *Scientific reports* **8**: 1-14
- Akagi Y, Akamatsu H, Otani H, Kodama M** (2009) Horizontal chromosome transfer, a mechanism for the evolution and differentiation of a plant-pathogenic fungus. *Eukaryotic cell* **8**: 1732-1738
- Albert M** (2013) Peptides as triggers of plant defence. *Journal of experimental botany* **64**: 5269-5279
- Ali S, Laurie JD, Linning R, Cervantes-Chavez JA, Gaudet D, Bakkeren G** (2014) An immunity-triggering effector from the barley smut fungus *Ustilago hordei* resides in an Ustilaginaceae-specific cluster bearing signs of transposable element-assisted evolution. *PLoS pathogens* **10**: e1004223
- Alonso JM, Hirayama T, Roman G, Nourizadeh S, Ecker JR** (1999) EIN2, a bifunctional transducer of ethylene and stress responses in *Arabidopsis*. *Science* **284**: 2148-2152
- Alvarez-Loayza P, White Jr JF, Torres MS, Balslev H, Kristiansen T, Svenning J-C, Gil N** (2011) Light converts endosymbiotic fungus to pathogen, influencing seedling survival and niche-space filling of a common tropical tree, *Iriartea deltoidea*. *PloS one* **6**: e16386
- Anderson JP, Gleason CA, Foley RC, Thrall PH, Burdon JB, Singh KB** (2010) Plants versus pathogens: an evolutionary arms race. *Functional plant biology* **37**: 499-512
- Avalbaev A, Yuldashev R, Fedorova K, Somov K, Vysotskaya L, Allagulova C, Shakirova F** (2016) Exogenous methyl jasmonate regulates cytokinin content by modulating cytokinin oxidase activity in wheat seedlings under salinity. *Journal of Plant Physiology* **191**: 101-110
- Baggs EL, Monroe JG, Thanki AS, O'Grady R, Schudoma C, Haerty W, Krasileva KV** (2020) Convergent loss of an EDS1/PAD4 signaling pathway in several plant lineages reveals coevolved components of plant immunity and drought response. *The Plant Cell* **32**: 2158-2177
- Basse CW, Steinberg G** (2004) *Ustilago maydis*, model system for analysis of the molecular basis of fungal pathogenicity. *Molecular plant pathology* **5**: 83-92
- Begerow D, Schäfer A, Kellner R, Yurkov A, Kemler M, Oberwinkler F, Bauer R** (2014) 11 *Ustilaginomycotina*. In *Systematics and Evolution*. Springer, pp 295-329

References

- Benevenuto J, Teixeira-Silva NS, Kuramae EE, Croll D, Monteiro-Vitorello CB** (2018) Comparative genomics of smut pathogens: insights from orphans and positively selected genes into host specialization. *Frontiers in microbiology* **9**: 660
- Berens ML, Berry HM, Mine A, Argueso CT, Tsuda K** (2017) Evolution of hormone signaling networks in plant defense. *Annual review of phytopathology* **55**: 401-425
- Bernoux M, Timmers T, Jauneau A, Briere C, de Wit PJ, Marco Y, Deslandes L** (2008) RD19, an Arabidopsis cysteine protease required for RRS1-R-mediated resistance, is relocalized to the nucleus by the *Ralstonia solanacearum* PopP2 effector. *The Plant Cell* **20**: 2252-2264
- Berrocal-Lobo M, Molina A, Solano R** (2002) Constitutive expression of ETHYLENE-RESPONSE-FACTOR1 in Arabidopsis confers resistance to several necrotrophic fungi. *The Plant Journal* **29**: 23-32
- Bhandari DD, Lapin D, Kracher B, von Born P, Bautor J, Niefind K, Parker JE** (2019) An EDS1 heterodimer signalling surface enforces timely reprogramming of immunity genes in Arabidopsis. *Nature communications* **10**: 1-13
- Bindics J, Khan M, Uhse S, Kogelmann B, Baggely L, Reumann D, Ingole KD, Stirnberg A, Rybecky A, Darino M** (2022) Many ways to TOPLESS—manipulation of plant auxin signalling by a cluster of fungal effectors. *New Phytologist* **236**: 1455-1470
- Bleecker AB, Kende H** (2000) Ethylene: a gaseous signal molecule in plants. *Annual review of cell and developmental biology* **16**: 1-18
- Bohman S, Staal J, Thomma BP, Wang M, Dixelius C** (2004) Characterisation of an Arabidopsis–*Leptosphaeria maculans* pathosystem: resistance partially requires camalexin biosynthesis and is independent of salicylic acid, ethylene and jasmonic acid signalling. *The Plant Journal* **37**: 9-20
- Bölker M** (2001) *Ustilago maydis*—a valuable model system for the study of fungal dimorphism and virulence. *Microbiology* **147**: 1395-1401
- Bölker M, Genin S, Lehmler C, Kahmann R** (1995) Genetic regulation of mating and dimorphism in *Ustilago maydis*. *Canadian Journal of Botany* **73**: 320-325
- Bölker M, Urban M, Kahmann R** (1992) The a mating type locus of *U. maydis* specifies cell signaling components. *Cell* **68**: 441-450
- Brefort T, Doehlemann G, Mendoza-Mendoza A, Reissmann S, Djamei A, Kahmann R** (2009) *Ustilago maydis* as a pathogen. *Annual review of phytopathology* **47**: 423-445
- Brodersen P, Malinovsky FG, Hématy K, Newman M-A, Mundy J** (2005) The role of salicylic acid in the induction of cell death in Arabidopsis *acd11*. *Plant Physiology* **138**: 1037-1045
- Brückner A, Polge C, Lentze N, Auerbach D, Schlattner U** (2009) Yeast two-hybrid, a powerful tool for systems biology. *International journal of molecular sciences* **10**: 2763-2788
- Caarls L, Pieterse CM, Van Wees SC** (2015) How salicylic acid takes transcriptional control over jasmonic acid signaling. *Frontiers in plant science* **6**: 170

References

- Cabantous S, Terwilliger TC, Waldo GS** (2005) Protein tagging and detection with engineered self-assembling fragments of green fluorescent protein. *Nature biotechnology* **23**: 102-107
- Caddell DF, Louie K, Bowen B, Sievert JA, Hollingsworth J, Dahlberg J, Purdom E, Northen T, Coleman-Derr D** (2020) Drought shifts sorghum root metabolite and microbiome profiles and enriches the stress response factor pipercolic acid. *bioRxiv*
- Cai J, Jozwiak A, Holoidovsky L, Meijler MM, Meir S, Rogachev I, Aharoni A** (2021) Glycosylation of N-hydroxy-pipercolic acid equilibrates between systemic acquired resistance response and plant growth. *Molecular plant* **14**: 440-455
- Cai X-T, Xu P, Zhao P-X, Liu R, Yu L-H, Xiang C-B** (2014) Arabidopsis ERF109 mediates cross-talk between jasmonic acid and auxin biosynthesis during lateral root formation. *Nature Communications* **5**: 1-13
- Caillaud M-C, Asai S, Rallapalli G, Piquerez S, Fabro G, Jones JD** (2013) A downy mildew effector attenuates salicylic acid-triggered immunity in Arabidopsis by interacting with the host mediator complex. *PLoS biology* **11**: e1001732
- Caillaud MC, Piquerez SJ, Fabro G, Steinbrenner J, Ishaque N, Beynon J, Jones JD** (2012) Subcellular localization of the Hpa RxLR effector repertoire identifies a tonoplast-associated protein HaRxL17 that confers enhanced plant susceptibility. *The Plant Journal* **69**: 252-265
- Castroverde CDM, Dina D** (2021) Temperature regulation of plant hormone signaling during stress and development. *Journal of Experimental Botany* **72**: 7436-7458
- Cecchini NM, Jung HW, Engle NL, Tschaplinski TJ, Greenberg JT** (2015) ALD1 regulates basal immune components and early inducible defense responses in Arabidopsis. *Molecular Plant-Microbe Interactions* **28**: 455-466
- Cermak T, Doyle EL, Christian M, Wang L, Zhang Y, Schmidt C, Baller JA, Somia NV, Bogdanove AJ, Voytas DF** (2011) Efficient design and assembly of custom TALEN and other TAL effector-based constructs for DNA targeting. *Nucleic acids research* **39**: e82-e82
- Chakraborty S, Murray G, Magarey P, Yonow T, O'Brien R, Croft B, Barbetti M, Sivasithamparam K, Old K, Dudzinski M** (1998) Potential impact of climate change on plant diseases of economic significance to Australia. *Australasian Plant Pathology* **27**: 15-35
- Chan KX, Phua SY, Crisp P, McQuinn R, Pogson BJ** (2016) Learning the languages of the chloroplast: retrograde signaling and beyond. *Annual review of plant biology* **67**: 25-53
- Chanclud E, Morel JB** (2016) Plant hormones: a fungal point of view. *Molecular plant pathology* **17**: 1289-1297
- Chassot C, Nawrath C, Métraux J-P** (2008) The cuticle: not only a barrier for plant defense, a novel defense syndrome in plants with cuticular defects. *Plant signaling & behavior* **3**: 142-144
- Chinchilla D, Zipfel C, Robatzek S, Kemmerling B, Nürnberger T, Jones JD, Felix G, Boller T** (2007) A flagellin-induced complex of the receptor FLS2 and BAK1 initiates plant defence. *Nature* **448**: 497-500

References

- Chini A, Fonseca S, Fernandez G, Adie B, Chico J, Lorenzo O, García-Casado G, López-Vidriero I, Lozano F, Ponce M** (2007) The JAZ family of repressors is the missing link in jasmonate signalling. *Nature* **448**: 666-671
- Chini A, Gimenez-Ibanez S, Goossens A, Solano R** (2016) Redundancy and specificity in jasmonate signalling. *Current opinion in plant biology* **33**: 147-156
- Chung HS, Howe GA** (2009) A critical role for the TIFY motif in repression of jasmonate signaling by a stabilized splice variant of the JASMONATE ZIM-domain protein JAZ10 in Arabidopsis. *The Plant Cell* **21**: 131-145
- Chung HS, Niu Y, Browse J, Howe GA** (2009) Top hits in contemporary JAZ: an update on jasmonate signaling. *Phytochemistry* **70**: 1547-1559
- Cohen SN, Chang AC, Hsu L** (1972) Nonchromosomal antibiotic resistance in bacteria: genetic transformation of *Escherichia coli* by R-factor DNA. *Proceedings of the National Academy of Sciences* **69**: 2110-2114
- Conforto C, Cazón I, Fernández FD, Marinelli A, Oddino C, Rago AM** (2013) Molecular sequence data of *Thecaphora frezii* affecting peanut crops in Argentina. *European journal of plant pathology* **137**: 663-666
- Cornelis GR** (2010) The type III secretion injectisome, a complex nanomachine for intracellular 'toxin' delivery.
- Courville KJ, Frantzeskakis L, Gul S, Haeger N, Kellner R, Heßler N, Day B, Usadel B, Gupta YK, van Esse HP** (2019) Smut infection of perennial hosts: the genome and the transcriptome of the Brassicaceae smut fungus *Thecaphora thlaspeos* reveal functionally conserved and novel effectors. *New Phytologist* **222**: 1474-1492
- Cui H, Tsuda K, Parker JE** (2015) Effector-triggered immunity: from pathogen perception to robust defense. *Annu. Rev. Plant Biol* **66**: 10.1146
- Darino M, Marques J, Chia K-S, Aleksza D, Soto LM, Uhse S, Borg M, Betz R, Bindics J, Zienkiewicz K** (2019) Fungal effector Jsi1 hijacks plant JA/ET signaling through Topless. *bioRxiv*: 844365
- De Mandal S, Jeon J** (2022) Nuclear Effectors in Plant Pathogenic Fungi. *Mycobiology* **50**: 259-268
- De Vleeschauwer D, Xu J, Höfte M** (2014) Making sense of hormone-mediated defense networking: from rice to Arabidopsis. *Frontiers in plant science* **5**: 611
- Dean R, Van Kan JA, Pretorius ZA, Hammond-Kosack KE, Di Pietro A, Spanu PD, Rudd JJ, Dickman M, Kahmann R, Ellis J** (2012) The Top 10 fungal pathogens in molecular plant pathology. *Molecular plant pathology* **13**: 414-430
- Dean RA, Talbot NJ, Ebbole DJ, Farman ML, Mitchell TK, Orbach MJ, Thon M, Kulkarni R, Xu J-R, Pan H** (2005) The genome sequence of the rice blast fungus *Magnaporthe grisea*. *Nature* **434**: 980-986
- Demianski AJ, Chung KM, Kunkel BN** (2012) Analysis of Arabidopsis JAZ gene expression during *Pseudomonas syringae* pathogenesis. *Molecular plant pathology* **13**: 46-57
- Dempsey DMA, Vlot AC, Wildermuth MC, Klessig DF** (2011) Salicylic acid biosynthesis and metabolism. *The Arabidopsis book/American Society of Plant Biologists* **9**

References

- Deslandes L, Rivas S** (2011) The plant cell nucleus: a true arena for the fight between plants and pathogens. *Plant Signaling & Behavior* **6**: 42-48
- Deslandes L, Rivas S** (2012) Catch me if you can: bacterial effectors and plant targets. *Trends in plant science* **17**: 644-655
- Djamei A, Schipper K, Rabe F, Ghosh A, Vincon V, Kahnt J, Osorio S, Tohge T, Fernie AR, Feussner I** (2011) Metabolic priming by a secreted fungal effector. *Nature* **478**: 395-398
- Dodds PN, Rathjen JP** (2010) Plant immunity: towards an integrated view of plant–pathogen interactions. *Nature Reviews Genetics* **11**: 539-548
- Doehlemann G, Ökmen B, Zhu W, Sharon A** (2017) Plant pathogenic fungi. *Microbiology spectrum* **5**: 5.1. 14
- Doehlemann G, Reissmann S, Aßmann D, Fleckenstein M, Kahmann R** (2011) Two linked genes encoding a secreted effector and a membrane protein are essential for *Ustilago maydis*-induced tumour formation. *Molecular microbiology* **81**: 751-766
- Doehlemann G, Van Der Linde K, Aßmann D, Schwambach D, Hof A, Mohanty A, Jackson D, Kahmann R** (2009) Pep1, a secreted effector protein of *Ustilago maydis*, is required for successful invasion of plant cells. *PLoS pathogens* **5**: e1000290
- Doehlemann G, Wahl R, Horst RJ, Voll LM, Usadel B, Poree F, Stitt M, Pons-Kühnemann J, Sonnewald U, Kahmann R** (2008) Reprogramming a maize plant: transcriptional and metabolic changes induced by the fungal biotroph *Ustilago maydis*. *The Plant Journal* **56**: 181-195
- Dombrecht B, Xue GP, Sprague SJ, Kirkegaard JA, Ross JJ, Reid JB, Fitt GP, Sewelam N, Schenk PM, Manners JM** (2007) MYC2 differentially modulates diverse jasmonate-dependent functions in *Arabidopsis*. *The Plant Cell* **19**: 2225-2245
- Dong X** (2004) NPR1, all things considered. *Current opinion in plant biology* **7**: 547-552
- Doughari J** (2015) An overview of plant immunity. *J. Plant Pathol. Microbiol* **6**: 10.4172
- Dunn KW, Kamocka MM, McDonald JH** (2011) A practical guide to evaluating colocalization in biological microscopy. *American Journal of Physiology-Cell Physiology* **300**: C723-C742
- El Oirdi M, El Rahman TA, Rigano L, El Hadrami A, Rodriguez MC, Daayf F, Vojnov A, Bouarab K** (2011) *Botrytis cinerea* manipulates the antagonistic effects between immune pathways to promote disease development in tomato. *The Plant Cell* **23**: 2405-2421
- Ellis JG, Lagudah ES, Spielmeier W, Dodds PN** (2014) The past, present and future of breeding rust resistant wheat. *Frontiers in plant science* **5**: 641
- Erb M, Reymond P** (2019) Molecular interactions between plants and insect herbivores. *Annu. Rev. Plant Biol* **70**: 527-557
- Estojak J, Brent R, Golemis EA** (1995) Correlation of two-hybrid affinity data with in vitro measurements. *Molecular and cellular biology* **15**: 5820-5829
- Fabro G, Steinbrenner J, Coates M, Ishaque N, Baxter L, Studholme DJ, Körner E, Allen RL, Piquerez SJ, Rougon-Cardoso A** (2011) Multiple candidate effectors from the

References

- oomycete pathogen *Hyaloperonospora arabidopsidis* suppress host plant immunity. *PLoS pathogens* **7**: e1002348
- Farfaring JW, Auffarth K, Basse CW** (2005) Identification of cis-active elements in *Ustilago maydis* *mg2* promoters conferring high-level activity during pathogenic growth in maize. *Molecular plant-microbe interactions* **18**: 75-87
- Ferrari S, Plotnikova JM, De Lorenzo G, Ausubel FM** (2003) Arabidopsis local resistance to *Botrytis cinerea* involves salicylic acid and camalexin and requires EDS4 and PAD2, but not SID2, EDS5 or PAD4. *The Plant Journal* **35**: 193-205
- Figuroa P, Browse J** (2015) Male sterility in Arabidopsis induced by overexpression of a MYC5-SRDX chimeric repressor. *The Plant Journal* **81**: 849-860
- Franken P** (2012) The plant strengthening root endophyte *Piriformospora indica*: potential application and the biology behind. *Applied Microbiology and Biotechnology* **96**: 1455-1464
- Frantzeskakis L, Courville KJ, Plücker L, Kellner R, Kruse J, Brachmann A, Feldbrügge M, Göhre V** (2017) The plant-dependent life cycle of *Thecaphora thlaspeos*: a smut fungus adapted to Brassicaceae. *Molecular Plant-Microbe Interactions* **30**: 271-282
- Fu ZQ, Dong X** (2013) Systemic acquired resistance: turning local infection into global defense. *Annual review of plant biology* **64**: 839-863
- Gaffney T, Friedrich L, Vernooij B, Negrotto D, Nye G, Uknes S, Ward E, Kessmann H, Ryals J** (1993) Requirement of salicylic acid for the induction of systemic acquired resistance. *Science* **261**: 754-756
- Gan P, Ikeda K, Irieda H, Narusaka M, O'Connell RJ, Narusaka Y, Takano Y, Kubo Y, Shirasu K** (2013) Comparative genomic and transcriptomic analyses reveal the hemibiotrophic stage shift of *Colletotrichum* fungi. *New Phytologist* **197**: 1236-1249
- Gao Q-M, Zhu S, Kachroo P, Kachroo A** (2015) Signal regulators of systemic acquired resistance. *Frontiers in plant science* **6**: 228
- Garcion C, Métraux J-P** (2008) Salicylic acid. *Plant Hormone Signaling: Annual Plant Reviews*: 229-255
- Gasiorowski JZ, Dean DA** (2003) Mechanisms of nuclear transport and interventions. *Advanced drug delivery reviews* **55**: 703-716
- Gawehns F, Houterman P, Ichou FA, Michielse C, Hijdra M, Cornelissen B, Rep M, Takken F** (2014) The *Fusarium oxysporum* effector Six6 contributes to virulence and suppresses I-2-mediated cell death. *Molecular Plant-Microbe Interactions* **27**: 336-348
- Germain H, Joly DL, Mireault C, Plourde MB, Letanneur C, Stewart D, Morency MJ, Petre B, Duplessis S, Séguin A** (2018) Infection assays in Arabidopsis reveal candidate effectors from the poplar rust fungus that promote susceptibility to bacteria and oomycete pathogens. *Molecular plant pathology* **19**: 191-200
- Ghareeb H, Becker A, Iven T, Feussner I, Schirawski J** (2011) *Sporisorium reilianum* infection changes inflorescence and branching architectures of maize. *Plant Physiology* **156**: 2037-2052
- Ghorbel M, Brini F, Sharma A, Landi M** (2021) Role of jasmonic acid in plants: The molecular point of view. *Plant Cell Reports* **40**: 1471-1494

References

- Gillissen B, Bergemann J, Sandmann C, Schroeer B, Bölker M, Kahmann R** (1992) A two-component regulatory system for self/non-self recognition in *Ustilago maydis*. *Cell* **68**: 647-657
- Gimenez-Ibanez S, Boter M, Fernández-Barbero G, Chini A, Rathjen JP, Solano R** (2014) The bacterial effector HopX1 targets JAZ transcriptional repressors to activate jasmonate signaling and promote infection in *Arabidopsis*. *PLoS biology* **12**: e1001792
- Giraldo MC, Dagdas YF, Gupta YK, Mentlak TA, Yi M, Martinez-Rocha AL, Saitoh H, Terauchi R, Talbot NJ, Valent B** (2013) Two distinct secretion systems facilitate tissue invasion by the rice blast fungus *Magnaporthe oryzae*. *Nature communications* **4**: 1-12
- Giraldo MC, Valent B** (2013) Filamentous plant pathogen effectors in action. *Nature Reviews Microbiology* **11**: 800-814
- Glazebrook J** (2005) Contrasting mechanisms of defense against biotrophic and necrotrophic pathogens. *Annual review of phytopathology* **43**: 205
- Godfrey D, Böhlenius H, Pedersen C, Zhang Z, Emmersen J, Thordal-Christensen H** (2010) Powdery mildew fungal effector candidates share N-terminal Y/F/WxC-motif. *BMC genomics* **11**: 1-13
- Gopalswamy M, Kroeger T, Bickel D, Frieg B, Akter S, Schott-Verdugo S, Viegas A, Pauly T, Mayer M, Przibilla J** (2022) Biophysical and pharmacokinetic characterization of a small-molecule inhibitor of RUNX1/ETO tetramerization with anti-leukemic effects. *Scientific Reports* **12**: 1-18
- Grbić V, Bleecker AB** (1995) Ethylene regulates the timing of leaf senescence in *Arabidopsis*. *The Plant Journal* **8**: 595-602
- Green JR, Pain NA, Cannell ME, Leckie CP, McCready S, Mitchell AJ, Callow JA, Jones GL, O'Connell RJ, Mendgen K** (1995) Analysis of differentiation and development of the specialized infection structures formed by biotrophic fungal plant pathogens using monoclonal antibodies. *Canadian Journal of Botany* **73**: 408-417
- Guo J, Cheng Y** (2022) Advances in Fungal Elicitor-Triggered Plant Immunity. *International Journal of Molecular Sciences* **23**: 12003
- Gürlebeck D, Szurek B, Bonas U** (2005) Dimerization of the bacterial effector protein AvrBs3 in the plant cell cytoplasm prior to nuclear import. *The Plant Journal* **42**: 175-187
- Gürlebeck D, Thieme F, Bonas U** (2006) Type III effector proteins from the plant pathogen *Xanthomonas* and their role in the interaction with the host plant. *Journal of plant physiology* **163**: 233-255
- Gururani MA, Venkatesh J, Upadhyaya CP, Nookaraju A, Pandey SK, Park SW** (2012) Plant disease resistance genes: current status and future directions. *Physiological and molecular plant pathology* **78**: 51-65
- Hardoim PR, Van Overbeek LS, Berg G, Pirttilä AM, Compant S, Campisano A, Döring M, Sessitsch A** (2015) The hidden world within plants: ecological and evolutionary considerations for defining functioning of microbial endophytes. *Microbiology and molecular biology reviews* **79**: 293-320
- Hartmann M, Zeier J** (2019) N-hydroxypipicolinic acid and salicylic acid: a metabolic duo for systemic acquired resistance. *Current opinion in plant biology* **50**: 44-57

References

- Hartmann M, Zeier T, Bernsdorff F, Reichel-Deland V, Kim D, Hohmann M, Scholten N, Schuck S, Bräutigam A, Hölzel T** (2018) Flavin monooxygenase-generated N-hydroxypipecolic acid is a critical element of plant systemic immunity. *Cell* **173**: 456-469. e416
- Heath MC, Skalamera D** (1997) Cellular interactions between plants and biotrophic fungal parasites. *In* *Advances in botanical research*, Vol 24. Elsevier, pp 195-225
- Hemetsberger C, Herrberger C, Zechmann B, Hillmer M, Doehlemann G** (2012) The *Ustilago maydis* effector Pep1 suppresses plant immunity by inhibition of host peroxidase activity. *PLoS pathogens* **8**: e1002684
- Henry E, Toruño TY, Jauneau A, Deslandes L, Coaker G** (2017) Direct and indirect visualization of bacterial effector delivery into diverse plant cell types during infection. *The Plant Cell* **29**: 1555-1570
- Hoang CV, Bhaskar CK, Ma L-S** (2021) A novel core effector Vp1 promotes fungal colonization and virulence of *Ustilago maydis*. *Journal of Fungi* **7**: 589
- Hou S, Tsuda K** (2022) Salicylic acid and jasmonic acid crosstalk in plant immunity. *Essays in Biochemistry* **66**: 647-656
- Howe GA, Major IT, Koo AJ** (2018) Modularity in jasmonate signaling for multistress resilience. *Annu. Rev. Plant Biol* **69**: 387-415
- Hu Y, Jiang Y, Han X, Wang H, Pan J, Yu D** (2017) Jasmonate regulates leaf senescence and tolerance to cold stress: crosstalk with other phytohormones. *Journal of Experimental Botany* **68**: 1361-1369
- Huang P, Dong Z, Guo P, Zhang X, Qiu Y, Li B, Wang Y, Guo H** (2020) Salicylic acid suppresses apical hook formation via NPR1-mediated repression of EIN3 and EIL1 in *Arabidopsis*. *The Plant Cell* **32**: 612-629
- Hückelhoven R, Panstruga R** (2011) Cell biology of the plant–powdery mildew interaction. *Current opinion in plant biology* **14**: 738-746
- Huh SU** (2021) PopP2 interacts with PAD4 in an acetyltransferase activity-dependent manner and affects plant immunity. *Plant Signaling & Behavior* **16**: 2017631
- Huot B, Yao J, Montgomery BL, He SY** (2014) Growth–defense tradeoffs in plants: a balancing act to optimize fitness. *Molecular plant* **7**: 1267-1287
- Irieda H, Maeda H, Akiyama K, Hagiwara A, Saitoh H, Uemura A, Terauchi R, Takano Y** (2014) *Colletotrichum orbiculare* secretes virulence effectors to a biotrophic interface at the primary hyphal neck via exocytosis coupled with SEC22-mediated traffic. *The Plant Cell* **26**: 2265-2281
- James P, Halladay J, Craig EA** (1996) Genomic libraries and a host strain designed for highly efficient two-hybrid selection in yeast. *Genetics* **144**: 1425-1436
- Jiang S, Yao J, Ma K-W, Zhou H, Song J, He SY, Ma W** (2013) Bacterial effector activates jasmonate signaling by directly targeting JAZ transcriptional repressors. *PLoS pathogens* **9**: e1003715
- Jones JD, Dangl JL** (2006) The plant immune system. *nature* **444**: 323-329

References

- Ju C, Chang C** (2015) Mechanistic insights in ethylene perception and signal transduction. *Plant Physiology* **169**: 85-95
- Kalinina NO, Makarova S, Makhotenko A, Love AJ, Taliansky M** (2018) The multiple functions of the nucleolus in plant development, disease and stress responses. *Frontiers in plant science* **9**: 132
- Kämper J, Kahmann R, Bölker M, Ma L-J, Brefort T, Saville BJ, Banuett F, Kronstad JW, Gold SE, Müller O** (2006) Insights from the genome of the biotrophic fungal plant pathogen *Ustilago maydis*. *Nature* **444**: 97-101
- Kämper J, Reichmann M, Romeis T, Bölker M, Kahmann R** (1995) Multiallelic recognition: nonself-dependent dimerization of the bE and bW homeodomain proteins in *Ustilago maydis*. *Cell* **81**: 73-83
- Kang HG, Singh KB** (2000) Characterization of salicylic acid-responsive, Arabidopsis Dof domain proteins: overexpression of OBP3 leads to growth defects. *The Plant Journal* **21**: 329-339
- Kaufmann K, Muino JM, Østerås M, Farinelli L, Krajewski P, Angenent GC** (2010) Chromatin immunoprecipitation (ChIP) of plant transcription factors followed by sequencing (ChIP-SEQ) or hybridization to whole genome arrays (ChIP-CHIP). *Nature protocols* **5**: 457-472
- Kay S, Hahn S, Marois E, Hause G, Bonas U** (2007) A bacterial effector acts as a plant transcription factor and induces a cell size regulator. *Science* **318**: 648-651
- Kazan K, Lyons R** (2014) Intervention of phytohormone pathways by pathogen effectors. *The Plant Cell* **26**: 2285-2309
- Kazan K, Manners JM** (2012) JAZ repressors and the orchestration of phytohormone crosstalk. *Trends in plant science* **17**: 22-31
- Kazan K, Manners JM** (2013) MYC2: the master in action. *Molecular plant* **6**: 686-703
- Kemen E, Gardiner A, Schultz-Larsen T, Kemen AC, Balmuth AL, Robert-Seilaniantz A, Bailey K, Holub E, Studholme DJ, MacLean D** (2011) Gene gain and loss during evolution of obligate parasitism in the white rust pathogen of *Arabidopsis thaliana*. *PLoS biology* **9**: e1001094
- Kerppola TK** (2008) Bimolecular fluorescence complementation (BiFC) analysis as a probe of protein interactions in living cells. *Annual review of biophysics* **37**: 465
- Kesarwani M, Yoo J, Dong X** (2007) Genetic interactions of TGA transcription factors in the regulation of pathogenesis-related genes and disease resistance in *Arabidopsis*. *Plant physiology* **144**: 336-346
- Khang CH, Berruyer R, Giraldo MC, Kankanala P, Park S-Y, Czymmek K, Kang S, Valent B** (2010) Translocation of *Magnaporthe oryzae* effectors into rice cells and their subsequent cell-to-cell movement. *The Plant Cell* **22**: 1388-1403
- Kim J, Chang C, Tucker ML** (2015) To grow old: regulatory role of ethylene and jasmonic acid in senescence. *Frontiers in Plant Science* **6**: 20
- Kim S, Kim C-Y, Park S-Y, Kim K-T, Jeon J, Chung H, Choi G, Kwon S, Choi J, Jeon J** (2020) Two nuclear effectors of the rice blast fungus modulate host immunity via transcriptional reprogramming. *Nature communications* **11**: 1-11

References

- Klessig DF, Choi HW, Dempsey DMA** (2018) Systemic acquired resistance and salicylic acid: past, present, and future. *Molecular plant-microbe interactions* **31**: 871-888
- Kodama Y, Hu C-D** (2012) Bimolecular fluorescence complementation (BiFC): a 5-year update and future perspectives. *Biotechniques* **53**: 285-298
- Kosugi S, Hasebe M, Tomita M, Yanagawa H** (2009) Systematic identification of cell cycle-dependent yeast nucleocytoplasmic shuttling proteins by prediction of composite motifs. *Proceedings of the National Academy of Sciences* **106**: 10171-10176
- Kou Y, Wang S** (2010) Broad-spectrum and durability: understanding of quantitative disease resistance. *Current opinion in plant biology* **13**: 181-185
- Kudla J, Bock R** (2016) Lighting the way to protein-protein interactions: recommendations on best practices for bimolecular fluorescence complementation analyses. *The Plant Cell* **28**: 1002-1008
- Kuo H-C, Hui S, Choi J, Asiegbu FO, Valkonen J, Lee Y-H** (2014) Secret lifestyles of *Neurospora crassa*. *Scientific Reports* **4**: 1-6
- Lampropoulos A, Sutikovic Z, Wenzl C, Maegele I, Lohmann JU, Forner J** (2013) GreenGate-a novel, versatile, and efficient cloning system for plant transgenesis. *PLoS one* **8**: e83043
- Lanver D, Berndt P, Tollot M, Naik V, Vranes M, Warmann T, Münch K, Rössel N, Kahmann R** (2014) Plant surface cues prime *Ustilago maydis* for biotrophic development. *PLoS pathogens* **10**: e1004272
- Lanver D, Müller AN, Happel P, Schweizer G, Haas FB, Franitza M, Pellegrin C, Reissmann S, Altmüller J, Rensing SA** (2018) The biotrophic development of *Ustilago maydis* studied by RNA-seq analysis. *The Plant Cell* **30**: 300-323
- Lanver D, Tollot M, Schweizer G, Lo Presti L, Reissmann S, Ma L-S, Schuster M, Tanaka S, Liang L, Ludwig N** (2017) *Ustilago maydis* effectors and their impact on virulence. *Nature Reviews Microbiology* **15**: 409-421
- Lapin D, Bhandari DD, Parker JE** (2020) Origins and immunity networking functions of EDS1 family proteins. *Annual review of phytopathology* **58**: 253-276
- Laurie JD, Ali S, Linning R, Mannhaupt G, Wong P, Güldener U, Münsterkötter M, Moore R, Kahmann R, Bakkeren G** (2012) Genome comparison of barley and maize smut fungi reveals targeted loss of RNA silencing components and species-specific presence of transposable elements. *The Plant Cell* **24**: 1733-1745
- Lee H-J, Park Y-J, Seo PJ, Kim J-H, Sim H-J, Kim S-G, Park C-M** (2015) Systemic immunity requires SnRK2. 8-mediated nuclear import of NPR1 in *Arabidopsis*. *The Plant Cell* **27**: 3425-3438
- Lee S, Yang DS, Uppalapati SR, Sumner LW, Mysore KS** (2013) Suppression of plant defense responses by extracellular metabolites from *Pseudomonas syringae* pv. *tabaci* in *Nicotiana benthamiana*. *BMC plant biology* **13**: 1-13
- Lemarié S, Robert-Seilantantz A, Lariagon C, Lemoine J, Marnet N, Jubault M, Manzanares-Dauleux MJ, Gravot A** (2015) Both the jasmonic acid and the salicylic acid pathways contribute to resistance to the biotrophic clubroot agent *Plasmodiophora brassicae* in *Arabidopsis*. *Plant and cell Physiology* **56**: 2158-2168

References

- Leon-Reyes A, Van der Does D, De Lange ES, Delker C, Wasternack C, Van Wees S, Ritsema T, Pieterse CM** (2010) Salicylate-mediated suppression of jasmonate-responsive gene expression in Arabidopsis is targeted downstream of the jasmonate biosynthesis pathway. *Planta* **232**: 1423-1432
- Leonelli L, Pelton J, Schoeffler A, Dahlbeck D, Berger J, Wemmer DE, Staskawicz B** (2011) Structural elucidation and functional characterization of the *Hyaloperonospora arabidopsidis* effector protein ATR13. *PLoS pathogens* **7**: e1002428
- Li M, Yu G, Cao C, Liu P** (2021) Metabolism, signaling, and transport of jasmonates. *Plant Communications* **2**: 100231
- Li N, Han X, Feng D, Yuan D, Huang L-J** (2019) Signaling crosstalk between salicylic acid and ethylene/jasmonate in plant defense: do we understand what they are whispering? *International Journal of Molecular Sciences* **20**: 671
- Li W, Deng Y, Ning Y, He Z, Wang G-L** (2020) Exploiting broad-spectrum disease resistance in crops: from molecular dissection to breeding. *Annu. Rev. Plant Biol* **71**: 575-603
- Liang L** (2013) Die Rolle des sekretierten Effektors Stp1 in der biotrophen Interaktion von *Ustilago maydis* und seiner Wirtspflanze Mais. Philipps-Universität Marburg
- Lin Y, Zhang C, Lan H, Gao S, Liu H, Liu J, Cao M, Pan G, Rong T, Zhang S** (2014) Validation of potential reference genes for qPCR in maize across abiotic stresses, hormone treatments, and tissue types. *PloS one* **9**
- Lingam S, Mohrbacher J, Brumbarova T, Potuschak T, Fink-Straube C, Blondet E, Genschik P, Bauer P** (2011) Interaction between the bHLH transcription factor FIT and ETHYLENE INSENSITIVE3/ETHYLENE INSENSITIVE3-LIKE1 reveals molecular linkage between the regulation of iron acquisition and ethylene signaling in Arabidopsis. *The Plant Cell* **23**: 1815-1829
- Littlejohn GR, Breen S, Smirnoff N, Grant M** (2021) Chloroplast immunity illuminated. *New Phytologist* **229**: 3088-3107
- Liu C, Pedersen C, Schultz-Larsen T, Aguilar GB, Madriz-Ordeñana K, Hovmøller MS, Thordal-Christensen H** (2016) The stripe rust fungal effector PEC 6 suppresses pattern-triggered immunity in a host species-independent manner and interacts with adenosine kinases. *New Phytologist*
- Liu J, Coaker G** (2008) Nuclear trafficking during plant innate immunity. *Molecular plant* **1**: 411-422
- Liu L, Wang Z, Li J, Wang Y, Yuan J, Zhan J, Wang P, Lin Y, Li F, Ge X** (2021) *Verticillium dahliae* secreted protein Vd424Y is required for full virulence, targets the nucleus of plant cells, and induces cell death. *Molecular plant pathology* **22**: 1109-1120
- Liu T, Liu Z, Song C, Hu Y, Han Z, She J, Fan F, Wang J, Jin C, Chang J** (2012) Chitin-induced dimerization activates a plant immune receptor. *science* **336**: 1160-1164
- Liu T, Song T, Zhang X, Yuan H, Su L, Li W, Xu J, Liu S, Chen L, Chen T** (2014) Unconventionally secreted effectors of two filamentous pathogens target plant salicylate biosynthesis. *Nature communications* **5**: 1-10
- Lo Presti L, Lanver D, Schweizer G, Tanaka S, Liang L, Tollot M, Zuccaro A, Reissmann S, Kahmann R** (2015) Fungal effectors and plant susceptibility. *Annual review of plant biology* **66**: 513-545

References

- López-Ráez JA, Verhage A, Fernández I, García JM, Azcón-Aguilar C, Flors V, Pozo MJ** (2010) Hormonal and transcriptional profiles highlight common and differential host responses to arbuscular mycorrhizal fungi and the regulation of the oxylipin pathway. *Journal of experimental botany* **61**: 2589-2601
- Lorang J, Kidarsa T, Bradford C, Gilbert B, Curtis M, Tzeng S-C, Maier C, Wolpert T** (2012) Tricking the guard: exploiting plant defense for disease susceptibility. *Science* **338**: 659-662
- Lorenzo C, Okoloise M, Williams K, Stern MP, Haffner SM** (2003) The metabolic syndrome as predictor of type 2 diabetes: the San Antonio heart study. *Diabetes care* **26**: 3153-3159
- Lorrain C, Gonçalves dos Santos KC, Germain H, Hecker A, Duplessis S** (2019) Advances in understanding obligate biotrophy in rust fungi. *New Phytologist* **222**: 1190-1206
- Lorrain C, Petre B, Duplessis S** (2018) Show me the way: rust effector targets in heterologous plant systems. *Current opinion in microbiology* **46**: 19-25
- Ludwig N, Reissmann S, Schipper K, Gonzalez C, Assmann D, Glatter T, Moretti M, Ma L-S, Rexer K-H, Snetselaar K** (2021) A cell surface-exposed protein complex with an essential virulence function in *Ustilago maydis*. *Nature microbiology* **6**: 722-730
- Lyapina I, Filippova A, Fesenko I** (2019) The role of peptide signals hidden in the structure of functional proteins in plant immune responses. *International Journal of Molecular Sciences* **20**: 4343
- Macho AP, Zipfel C** (2014) Plant PRRs and the activation of innate immune signaling. *Molecular cell* **54**: 263-272
- Martín R, Bermúdez-Humarán LG, Langella P** (2018) Searching for the bacterial effector: The example of the multi-skilled commensal bacterium *Faecalibacterium prausnitzii*. *Frontiers in Microbiology* **9**: 346
- Matei A, Doehlemann G** (2016) Cell biology of corn smut disease—*Ustilago maydis* as a model for biotrophic interactions. *Current opinion in microbiology* **34**: 60-66
- Matiolli CC, Melotto M** (2018) A comprehensive *Arabidopsis* yeast two-hybrid library for protein-protein interaction studies: a resource to the plant research community. *Molecular plant-microbe interactions* **31**: 899-902
- Matschi S, Hake K, Herde M, Hause B, Romeis T** (2015) The calcium-dependent protein kinase CPK28 regulates development by inducing growth phase-specific, spatially restricted alterations in jasmonic acid levels independent of defense responses in *Arabidopsis*. *The Plant Cell* **27**: 591-606
- McGrath KC, Dombrecht B, Manners JM, Schenk PM, Edgar CI, Maclean DJ, Scheible W-R, Udvardi MK, Kazan K** (2005) Repressor-and activator-type ethylene response factors functioning in jasmonate signaling and disease resistance identified via a genome-wide screen of *Arabidopsis* transcription factor gene expression. *Plant physiology* **139**: 949-959
- Melotto M, Mecey C, Niu Y, Chung HS, Katsir L, Yao J, Zeng W, Thines B, Staswick P, Browse J** (2008) A critical role of two positively charged amino acids in the Jas motif of *Arabidopsis* JAZ proteins in mediating coronatine- and jasmonoyl isoleucine-dependent interactions with the COI1 F-box protein. *The Plant Journal* **55**: 979-988

References

- Melotto M, Underwood W, Koczan J, Nomura K, He SY** (2006) Plant stomata function in innate immunity against bacterial invasion. *Cell* **126**: 969-980
- Mine A, Berens ML, Nobori T, Anver S, Fukumoto K, Winkelmüller TM, Takeda A, Becker D, Tsuda K** (2017) Pathogen exploitation of an abscisic acid-and jasmonate-inducible MAPK phosphatase and its interception by Arabidopsis immunity. *Proceedings of the National Academy of Sciences* **114**: 7456-7461
- Mishina TE, Zeier J** (2006) The Arabidopsis flavin-dependent monooxygenase FMO1 is an essential component of biologically induced systemic acquired resistance. *Plant physiology* **141**: 1666-1675
- Miya A, Albert P, Shinya T, Desaki Y, Ichimura K, Shirasu K, Narusaka Y, Kawakami N, Kaku H, Shibuya N** (2007) CERK1, a LysM receptor kinase, is essential for chitin elicitor signaling in Arabidopsis. *Proceedings of the National Academy of Sciences* **104**: 19613-19618
- Monaghan J, Matschi S, Shorinola O, Rovenich H, Matei A, Segonzac C, Malinovsky FG, Rathjen JP, MacLean D, Romeis T** (2014) The calcium-dependent protein kinase CPK28 buffers plant immunity and regulates BIK1 turnover. *Cell host & microbe* **16**: 605-615
- Moreno JE, Shyu C, Campos ML, Patel LC, Chung HS, Yao J, He SY, Howe GA** (2013) Negative feedback control of jasmonate signaling by an alternative splice variant of JAZ10. *Plant physiology* **162**: 1006-1017
- Mou Z, Fan W, Dong X** (2003) Inducers of plant systemic acquired resistance regulate NPR1 function through redox changes. *Cell* **113**: 935-944
- Mukhtar MS, Carvunis A-R, Dreze M, Epple P, Steinbrenner J, Moore J, Tasan M, Galli M, Hao T, Nishimura MT** (2011) Independently evolved virulence effectors converge onto hubs in a plant immune system network. *science* **333**: 596-601
- Mundt CC** (2014) Durable resistance: a key to sustainable management of pathogens and pests. *Infection, Genetics and Evolution* **27**: 446-455
- Návarová H, Bernsdorff F, Döring A-C, Zeier J** (2012) Pipecolic acid, an endogenous mediator of defense amplification and priming, is a critical regulator of inducible plant immunity. *The Plant Cell* **24**: 5123-5141
- Navarrete F, Gallei M, Kornienko AE, Saado I, Khan M, Chia K-S, Darino MA, Bindics J, Djamei A** (2022) TOPLESS promotes plant immunity by repressing auxin signaling and is targeted by the fungal effector Naked1. *Plant communications* **3**: 100269
- Navarrete F, Grujic N, Stirnberg A, Saado I, Aleksza D, Gallei M, Adi H, Alcântara A, Khan M, Bindics J** (2021) The Pleiades are a cluster of fungal effectors that inhibit host defenses. *PLoS pathogens* **17**: e1009641
- Navarro L, Bari R, Achard P, Lisón P, Nemri A, Harberd NP, Jones JD** (2008) DELLAs control plant immune responses by modulating the balance of jasmonic acid and salicylic acid signaling. *Current Biology* **18**: 650-655
- Navarro L, Zipfel C, Rowland O, Keller I, Robatzek S, Boller T, Jones JD** (2004) The transcriptional innate immune response to flg22. Interplay and overlap with Avr gene-dependent defense responses and bacterial pathogenesis. *Plant physiology* **135**: 1113-1128

References

- Naveed ZA, Wei X, Chen J, Mubeen H, Ali GS** (2020) The PTI to ETI continuum in Phytophthora-plant interactions. *Frontiers in Plant Science* **11**: 593905
- Ngou BPM, Ding P, Jones JD** (2021) Channeling plant immunity. *Cell* **184**: 3358-3360
- Nguyen Ba AN, Pogoutse A, Provart N, Moses AM** (2009) NLStradamus: a simple Hidden Markov Model for nuclear localization signal prediction. *BMC bioinformatics* **10**: 1-11
- Nielsen H, Engelbrecht J, Brunak S, Von Heijne G** (1997) Identification of prokaryotic and eukaryotic signal peptides and prediction of their cleavage sites. *Protein engineering* **10**: 1-6
- Niere BI** (2001) Significance of non-pathogenic isolates of *Fusarium oxysporum* Schlecht.: Fries for the biological control of the burrowing nematode *Radopholus similis* (Cobb) Thorne on tissue cultured banana. na
- Nishimura T, Mochizuki S, Ishii-Minami N, Fujisawa Y, Kawahara Y, Yoshida Y, Okada K, Ando S, Matsumura H, Terauchi R** (2016) Magnaporthe oryzae glycine-rich secretion protein, Rbf1 critically participates in pathogenicity through the focal formation of the biotrophic interfacial complex. *PLoS pathogens* **12**: e1005921
- Nomoto M, Skelly MJ, Itaya T, Mori T, Suzuki T, Matsushita T, Tokizawa M, Kuwata K, Mori H, Yamamoto YY** (2021) Suppression of MYC transcription activators by the immune cofactor NPR1 fine-tunes plant immune responses. *Cell Reports* **37**: 110125
- Nomura K, Mecey C, Lee Y-N, Imboden LA, Chang JH, He SY** (2011) Effector-triggered immunity blocks pathogen degradation of an immunity-associated vesicle traffic regulator in Arabidopsis. *Proceedings of the National Academy of Sciences* **108**: 10774-10779
- O'Connell RJ, Thon MR, Hacquard S, Amyotte SG, Kleemann J, Torres MF, Damm U, Buiate EA, Epstein L, Alkan N** (2012) Lifestyle transitions in plant pathogenic *Colletotrichum* fungi deciphered by genome and transcriptome analyses. *Nature genetics* **44**: 1060-1065
- Ökmen B, Doehlemann G** (2014) Inside plant: biotrophic strategies to modulate host immunity and metabolism. *Current opinion in plant biology* **20**: 19-25
- Ökmen B, Mathow D, Hof A, Lahrmann U, Aßmann D, Doehlemann G** (2018) Mining the effector repertoire of the biotrophic fungal pathogen *Ustilago hordei* during host and non-host infection. *Molecular plant pathology* **19**: 2603-2622
- Pandita D** (2022) Jasmonates: key players in plant stress tolerance. *In* *Emerging Plant Growth Regulators in Agriculture*. Elsevier, pp 165-192
- Panzer S, Brych A, Batschauer A, Terpitz U** (2019) Opsin 1 and Opsin 2 of the Corn Smut Fungus *Ustilago maydis* Are Green Light-Driven Proton Pumps. *Frontiers in microbiology* **10**: 735
- Patil RA, Lenka SK, Normanly J, Walker EL, Roberts SC** (2014) Methyl jasmonate represses growth and affects cell cycle progression in cultured *Taxus* cells. *Plant cell reports* **33**: 1479-1492
- Patkar RN, Benke PI, Qu Z, Constance Chen YY, Yang F, Swarup S, Naqvi NI** (2015) A fungal monoxygenase-derived jasmonate attenuates host innate immunity. *Nature chemical biology* **11**: 733-740

References

- Pelgrom AJ, Meisrimler C-N, Elberse J, Koorman T, Boxem M, Van den Ackerveken G** (2020) Host interactors of effector proteins of the lettuce downy mildew *Bremia lactucae* obtained by yeast two-hybrid screening. *PLoS one* **15**: e0226540
- Peng Y, van Wersch R, Zhang Y** (2018) Convergent and divergent signaling in PAMP-triggered immunity and effector-triggered immunity. *Molecular Plant-Microbe Interactions* **31**: 403-409
- Pennington HG, Jones R, Kwon S, Bonciani G, Thieron H, Chandler T, Luong P, Morgan SN, Przydacz M, Bozkurt T** (2019) The fungal ribonuclease-like effector protein CSEP0064/BEC1054 represses plant immunity and interferes with degradation of host ribosomal RNA. *PLoS pathogens* **15**: e1007620
- Perkins DD, Turner BC** (1988) *Neurospora* from natural populations: toward the population biology of a haploid eukaryote. *Experimental Mycology* **12**: 91-131
- Petre B, Saunders DG, Sklenar J, Lorrain C, Krasileva KV, Win J, Duplessis S, Kamoun S** (2016) Heterologous expression screens in *Nicotiana benthamiana* identify a candidate effector of the wheat yellow rust pathogen that associates with processing bodies. *PLoS one* **11**: e0149035
- Petre B, Saunders DG, Sklenar J, Lorrain C, Win J, Duplessis S, Kamoun S** (2015) Candidate effector proteins of the rust pathogen *Melampsora larici-populina* target diverse plant cell compartments. *Molecular Plant-Microbe Interactions* **28**: 689-700
- Petrini O** (1991) Fungal endophytes of tree leaves. *In* *Microbial ecology of leaves*. Springer, pp 179-197
- Pieterse CM, Van der Does D, Zamioudis C, Leon-Reyes A, Van Wees SC** (2012) Hormonal modulation of plant immunity. *Annual review of cell and developmental biology* **28**: 489-521
- Pieterse CM, Zamioudis C, Berendsen RL, Weller DM, Van Wees SC, Bakker PA** (2014) Induced systemic resistance by beneficial microbes. *Annual review of phytopathology* **52**: 347-375
- Plett JM, Daguerre Y, Wittulsky S, Vayssières A, Deveau A, Melton SJ, Kohler A, Morrell-Falvey JL, Brun A, Veneault-Fourrey C** (2014) Effector MiSSP7 of the mutualistic fungus *Laccaria bicolor* stabilizes the *Populus* JAZ6 protein and represses jasmonic acid (JA) responsive genes. *Proceedings of the National Academy of Sciences* **111**: 8299-8304
- Plücker L, Bösch K, Geißl L, Hoffmann P, Göhre V** (2021) Genetic manipulation of the Brassicaceae smut fungus *Thecaphora thlaspeos*. *Journal of Fungi* **7**: 38
- Poloni A, Schirawski J** (2016) Host specificity in *Sporisorium reilianum* is determined by distinct mechanisms in maize and sorghum. *Molecular plant pathology* **17**: 741-754
- Pradhan A, Ghosh S, Sahoo D, Jha G** (2021) Fungal effectors, the double edge sword of phytopathogens. *Current genetics* **67**: 27-40
- Pré M, Atallah M, Champion A, De Vos M, Pieterse CM, Memelink J** (2008) The AP2/ERF domain transcription factor ORA59 integrates jasmonic acid and ethylene signals in plant defense. *Plant physiology* **147**: 1347-1357

References

- Puri A, Padda KP, Chanway CP** (2016) Evidence of nitrogen fixation and growth promotion in canola (*Brassica napus* L.) by an endophytic diazotroph *Paenibacillus polymyxa* P2b-2R. *Biology and Fertility of Soils* **52**: 119-125
- Qiao H, Shen Z, Huang S-sC, Schmitz RJ, Urich MA, Briggs SP, Ecker JR** (2012) Processing and subcellular trafficking of ER-tethered EIN2 control response to ethylene gas. *Science* **338**: 390-393
- Qin J, Wang K, Sun L, Xing H, Wang S, Li L, Chen S, Guo H-S, Zhang J** (2018) The plant-specific transcription factors CBP60g and SARD1 are targeted by a *Verticillium* secretory protein VdSCP41 to modulate immunity. *Elife* **7**: e34902
- Rabe F, Bosch J, Stirnberg A, Guse T, Bauer L, Seitner D, Rabanal FA, Czedik-Eysenberg A, Uhse S, Bindics J** (2016) A complete toolset for the study of *Ustilago bromivora* and *Brachypodium* sp. as a fungal-temperate grass pathosystem. *Elife* **5**
- Raffaele S, Rivas S, Roby D** (2006) An essential role for salicylic acid in AtMYB30-mediated control of the hypersensitive cell death program in *Arabidopsis*. *FEBS letters* **580**: 3498-3504
- Rafiqi M, Ellis JG, Ludowici VA, Hardham AR, Dodds PN** (2012) Challenges and progress towards understanding the role of effectors in plant–fungal interactions. *Current opinion in plant biology* **15**: 477-482
- Rate DN, Greenberg JT** (2001) The *Arabidopsis* aberrant growth and death2 mutant shows resistance to *Pseudomonas syringae* and reveals a role for NPR1 in suppressing hypersensitive cell death. *The Plant Journal* **27**: 203-211
- Raudvere U, Kolberg L, Kuzmin I, Arak T, Adler P, Peterson H, Vilo J** (2019) g: Profiler: a web server for functional enrichment analysis and conversions of gene lists (2019 update). *Nucleic acids research* **47**: W191-W198
- Raza A, Charagh S, Zahid Z, Mubarik MS, Javed R, Siddiqui MH, Hasanuzzaman M** (2021) Jasmonic acid: a key frontier in conferring abiotic stress tolerance in plants. *Plant Cell Reports* **40**: 1513-1541
- Redkar A, Villajuana-Bonequi M, Doehlemann G** (2015) Conservation of the *Ustilago maydis* effector *See1* in related smuts. *Plant signaling & behavior* **10**: e1086855
- Redman RS, Dunigan DD, Rodriguez RJ** (2001) Fungal symbiosis from mutualism to parasitism: who controls the outcome, host or invader? *New Phytologist* **151**: 705-716
- Reuber TL, Plotnikova JM, Dewdney J, Rogers EE, Wood W, Ausubel FM** (1998) Correlation of defense gene induction defects with powdery mildew susceptibility in *Arabidopsis* enhanced disease susceptibility mutants. *The Plant Journal* **16**: 473-485
- Reyes-Fernández EZ, Shi Y-M, Grün P, Bode HB, Bölker M** (2021) An Unconventional Melanin Biosynthesis Pathway in *Ustilago maydis*. *Applied and Environmental Microbiology* **87**: e01510-01520
- Riemann M, Haga K, Shimizu T, Okada K, Ando S, Mochizuki S, Nishizawa Y, Yamanouchi U, Nick P, Yano M** (2013) Identification of rice Allene Oxide Cyclase mutants and the function of jasmonate for defence against *Magnaporthe oryzae*. *The Plant Journal* **74**: 226-238
- Rivas-San Vicente M, Plasencia J** (2011) Salicylic acid beyond defence: its role in plant growth and development. *Journal of experimental botany* **62**: 3321-3338

References

- Rivas S, Genin S** (2011) A plethora of virulence strategies hidden behind nuclear targeting of microbial effectors. *Frontiers in plant science* **2**: 104
- Rizzo DM, Lichtveld M, Mazet JA, Togami E, Miller SA** (2021) Plant health and its effects on food safety and security in a One Health framework: Four case studies. *One Health Outlook* **3**: 1-9
- Robin GP, Kleemann J, Neumann U, Cabre L, Dallery J-F, Lapalu N, O'Connell RJ** (2018) Subcellular localization screening of *Colletotrichum higginsianum* effector candidates identifies fungal proteins targeted to plant peroxisomes, golgi bodies, and microtubules. *Frontiers in plant science* **9**: 562
- Rodriguez PA, Rothballer M, Chowdhury SP, Nussbaumer T, Gutjahr C, Falter-Braun P** (2019) Systems biology of plant-microbiome interactions. *Molecular plant* **12**: 804-821
- Rodriguez R, White Jr J, Arnold AE, Redman aRa** (2009) Fungal endophytes: diversity and functional roles. *New phytologist* **182**: 314-330
- Römer P, Hahn S, Jordan T, Strauß T, Bonas U, Lahaye T** (2007) Plant pathogen recognition mediated by promoter activation of the pepper Bs3 resistance gene. *Science* **318**: 645-648
- Rooney HC, Van't Klooster JW, van der Hoorn RA, Joosten MH, Jones JD, de Wit PJ** (2005) *Cladosporium Avr2* inhibits tomato Rcr3 protease required for Cf-2-dependent disease resistance. *Science* **308**: 1783-1786
- Rouxel T, Balesdent M-H** (2010) Avirulence genes. eLS
- Ruan J, Zhou Y, Zhou M, Yan J, Khurshid M, Weng W, Cheng J, Zhang K** (2019) Jasmonic acid signaling pathway in plants. *International journal of molecular sciences* **20**: 2479
- Saado I, Chia K-S, Betz R, Alcântara A, Pettkó-Szandtner A, Navarrete F, D'Auria JC, Kolomiets MV, Melzer M, Feussner I** (2022) Effector-mediated relocalization of a maize lipoxygenase protein triggers susceptibility to *Ustilago maydis*. *The Plant Cell*
- Saharan GS, Mehta N** (2008) Sclerotinia diseases of crop plants: biology, ecology and disease management. Springer Science & Business Media
- Saitoh H, Fujisawa S, Mitsuoka C, Ito A, Hirabuchi A, Ikeda K, Irieda H, Yoshino K, Yoshida K, Matsumura H** (2012) Large-scale gene disruption in *Magnaporthe oryzae* identifies MC69, a secreted protein required for infection by monocot and dicot fungal pathogens. *PloS pathogens* **8**: e1002711
- Sambrook J, Fritsch EF, Maniatis T** (1989) Molecular cloning: a laboratory manual. Cold spring harbor laboratory press
- Savary S, Willocquet L, Pethybridge SJ, Esker P, McRoberts N, Nelson A** (2019) The global burden of pathogens and pests on major food crops. *Nature ecology & evolution* **3**: 430-439
- Schardl CL, Leuchtmann A** (2005) The *Epichloë* endophytes of grasses and the symbiotic continuum. *Mycology series* **23**: 475
- Schellenberg B, Ramel C, Dudler R** (2010) *Pseudomonas syringae* virulence factor syringolin A counteracts stomatal immunity by proteasome inhibition. *Molecular Plant-Microbe Interactions* **23**: 1287-1293

References

- Scheuermann TH, Padrick SB, Gardner KH, Brautigam CA** (2016) On the acquisition and analysis of microscale thermophoresis data. *Analytical biochemistry* **496**: 79-93
- Schipper K** (2009) Charakterisierung eines *Ustilago maydis* Genclusters, das für drei neuartige sekretierte Effektoren kodiert. Philipps-Universität Marburg
- Schnable PS, Ware D, Fulton RS, Stein JC, Wei F, Pasternak S, Liang C, Zhang J, Fulton L, Graves TA** (2009) The B73 maize genome: complexity, diversity, and dynamics. *science* **326**: 1112-1115
- Schröpfer S, Böttcher C, Wöhner T, Richter K, Norelli J, Rikkerink EH, Hanke M-V, Flachowsky H** (2018) A single effector protein, AvrRpt2EA, from *Erwinia amylovora* can cause fire blight disease symptoms and induces a salicylic acid-dependent defense response. *Molecular Plant-Microbe Interactions* **31**: 1179-1191
- Schultink A, Qi T, Lee A, Steinbrenner AD, Staskawicz B** (2017) Roq1 mediates recognition of the *Xanthomonas* and *Pseudomonas* effector proteins XopQ and HopQ1. *The Plant Journal* **92**: 787-795
- Schulze-Lefert P, Panstruga R** (2003) Establishment of biotrophy by parasitic fungi and reprogramming of host cells for disease resistance. *Annual review of phytopathology* **41**: 641
- Schuster M, Schweizer G, Reissmann S, Kahmann R** (2016) Genome editing in *Ustilago maydis* using the CRISPR-Cas system. *Fungal Genetics and Biology* **89**: 3-9
- Schuster M, Trippel C, Happel P, Lanver D, Reißmann S, Kahmann R** (2018) Single and multiplexed gene editing in *Ustilago maydis* using CRISPR-Cas9. *Bio-protocol* **8**: e2928-e2928
- Scott B** (2001) Epichloë endophytes: fungal symbionts of grasses. *Current Opinion in Microbiology* **4**: 393-398
- Sehr EM, Agusti J, Lehner R, Farmer EE, Schwarz M, Greb T** (2010) Analysis of secondary growth in the *Arabidopsis* shoot reveals a positive role of jasmonate signalling in cambium formation. *The Plant Journal* **63**: 811-822
- Selin C, De Kievit TR, Belmonte MF, Fernando WD** (2016) Elucidating the role of effectors in plant-fungal interactions: progress and challenges. *Frontiers in microbiology* **7**: 600
- Seyfferth C, Tsuda K** (2014) Salicylic acid signal transduction: the initiation of biosynthesis, perception and transcriptional reprogramming. *Frontiers in plant science* **5**: 697
- Shabab M, Shindo T, Gu C, Kaschani F, Pansuriya T, Chintha R, Harzen A, Colby T, Kamoun S, van der Hoorn RA** (2008) Fungal effector protein AVR2 targets diversifying defense-related cys proteases of tomato. *The Plant Cell* **20**: 1169-1183
- Sheard LB, Tan X, Mao H, Withers J, Ben-Nissan G, Hinds TR, Kobayashi Y, Hsu F-F, Sharon M, Browse J** (2010) Jasmonate perception by inositol-phosphate-potentiated COI1-JAZ co-receptor. *Nature* **468**: 400-405
- Shields A, Shivnauth V, Castroverde CDM** (2022) Salicylic Acid and N-Hydroxy-pipecolic Acid at the Fulcrum of the Plant Immunity-Growth Equilibrium.
- Sikora RA, Pocasangre L, zum Felde A, Niere B, Vu TT, Dababat A** (2008) Mutualistic endophytic fungi and in-planta suppressiveness to plant parasitic nematodes. *Biological control* **46**: 15-23

References

- Singh RP, Hodson DP, Jin Y, Lagudah ES, Ayliffe MA, Bhavani S, Rouse MN, Pretorius ZA, Szabo LJ, Huerta-Espino J** (2015) Emergence and spread of new races of wheat stem rust fungus: continued threat to food security and prospects of genetic control. *Phytopathology* **105**: 872-884
- Smith JM, Heese A** (2014) Rapid bioassay to measure early reactive oxygen species production in Arabidopsis leave tissue in response to living *Pseudomonas syringae*. *Plant methods* **10**: 1-9
- Sohn KH, Lei R, Nemri A, Jones JD** (2007) The downy mildew effector proteins ATR1 and ATR13 promote disease susceptibility in Arabidopsis thaliana. *The Plant Cell* **19**: 4077-4090
- Solano R, Stepanova A, Chao Q, Ecker JR** (1998) Nuclear events in ethylene signaling: a transcriptional cascade mediated by ETHYLENE-INSENSITIVE3 and ETHYLENE-RESPONSE-FACTOR1. *Genes & development* **12**: 3703-3714
- Song T, Ma Z, Shen D, Li Q, Li W, Su L, Ye T, Zhang M, Wang Y, Dou D** (2015) An oomycete CRN effector reprograms expression of plant HSP genes by targeting their promoters. *PLoS pathogens* **11**: e1005348
- Southern EM** (1975) Detection of specific sequences among DNA fragments separated by gel electrophoresis. *Journal of molecular biology* **98**: 503-517
- Spanu PD, Abbott JC, Amselem J, Burgis TA, Soanes DM, Stüber K, Loren van Themaat EV, Brown JK, Butcher SA, Gurr SJ** (2010) Genome expansion and gene loss in powdery mildew fungi reveal tradeoffs in extreme parasitism. *Science* **330**: 1543-1546
- Spellig T, Bölker M, Lottspeich F, Frank RW, Kahmann R** (1994) Pheromones trigger filamentous growth in *Ustilago maydis*. *The EMBO journal* **13**: 1620-1627
- Sperschneider J, Catanzariti A-M, DeBoer K, Petre B, Gardiner DM, Singh KB, Dodds PN, Taylor JM** (2017) LOCALIZER: subcellular localization prediction of both plant and effector proteins in the plant cell. *Scientific reports* **7**: 1-14
- Spoel SH, Koornneef A, Claessens SM, Korzelius JP, Van Pelt JA, Mueller MJ, Buchala AJ, Métraux J-P, Brown R, Kazan K** (2003) NPR1 modulates cross-talk between salicylate- and jasmonate-dependent defense pathways through a novel function in the cytosol. *The Plant Cell* **15**: 760-770
- Stenzel I, Otto M, Delker C, Kirmse N, Schmidt D, Miersch O, Hause B, Wasternack C** (2012) ALLENE OXIDE CYCLASE (AOC) gene family members of Arabidopsis thaliana: tissue- and organ-specific promoter activities and in vivo heteromerization. *Journal of experimental botany* **63**: 6125-6138
- Stergiopoulos I, Collemare J, Mehrabi R, De Wit PJ** (2013) Phytotoxic secondary metabolites and peptides produced by plant pathogenic Dothideomycete fungi. *FEMS microbiology reviews* **37**: 67-93
- Stergiopoulos I, Cordovez V, Ökmen B, Beenen HG, Kema GH, De Wit PJ** (2014) Positive selection and intragenic recombination contribute to high allelic diversity in effector genes of *Mycosphaerella fijiensis*, causal agent of the black leaf streak disease of banana. *Molecular plant pathology* **15**: 447-460
- Stergiopoulos I, de Wit PJ** (2009) Fungal effector proteins. *Annual review of phytopathology* **47**: 233-263

References

- Stotz HU, Sawada Y, Shimada Y, Hirai MY, Sasaki E, Krischke M, Brown PD, Saito K, Kamiya Y** (2011) Role of camalexin, indole glucosinolates, and side chain modification of glucosinolate-derived isothiocyanates in defense of Arabidopsis against *Sclerotinia sclerotiorum*. *The Plant Journal* **67**: 81-93
- Struck C** (2015) Amino acid uptake in rust fungi. *Frontiers in plant science* **6**: 40
- Szurek B, Rossier O, Hause G, Bonas U** (2002) Type III-dependent translocation of the *Xanthomonas AvrBs3* protein into the plant cell. *Molecular microbiology* **46**: 13-23
- Tanaka S, Han X, Kahmann R** (2015) Microbial effectors target multiple steps in the salicylic acid production and signaling pathway. *Frontiers in Plant Science* **6**: 349
- Tao Y, Xie Z, Chen W, Glazebrook J, Chang H-S, Han B, Zhu T, Zou G, Katagiri F** (2003) Quantitative nature of Arabidopsis responses during compatible and incompatible interactions with the bacterial pathogen *Pseudomonas syringae*. *The Plant Cell* **15**: 317-330
- Terfrüchte M, Joehnk B, Fajardo-Somera R, Braus GH, Riquelme M, Schipper K, Feldbrügge M** (2014) Establishing a versatile Golden Gate cloning system for genetic engineering in fungi. *Fungal Genetics and Biology* **62**: 1-10
- Thines B, Katsir L, Melotto M, Niu Y, Mandaokar A, Liu G, Nomura K, He SY, Howe GA, Browse J** (2007) JAZ repressor proteins are targets of the SCFCO11 complex during jasmonate signalling. *Nature* **448**: 661-665
- Thomas P** (1988) *Ustilago hordei*, covered smut of barley and *Ustilago nigra*, false loose smut of barley. *In* *Advances in plant pathology*, Vol 6. Elsevier, pp 415-425
- Thomma BP, Eggermont K, Tierens KF-J, Broekaert WF** (1999) Requirement of functional ethylene-insensitive 2 gene for efficient resistance of Arabidopsis to infection by *Botrytis cinerea*. *Plant physiology* **121**: 1093-1101
- Thordal-Christensen H** (2020) A holistic view on plant effector-triggered immunity presented as an iceberg model. *Cellular and Molecular Life Sciences* **77**: 3963-3976
- Thrall PH, Hochberg ME, Burdon JJ, Bever JD** (2007) Coevolution of symbiotic mutualists and parasites in a community context. *Trends in Ecology & Evolution* **22**: 120-126
- Tudzynski P, Scheffer J** (2004) *Claviceps purpurea*: molecular aspects of a unique pathogenic lifestyle. *Molecular Plant Pathology* **5**: 377-388
- Tzelepis G, Holmquist L, Dixelius C** (2021) Plant mitochondria and chloroplasts are targeted by the *Rhizoctonia solani* RsCRP1 effector. *Biochemical and Biophysical Research Communications* **544**: 86-90
- Underwood W** (2012) The plant cell wall: a dynamic barrier against pathogen invasion. *Frontiers in plant science* **3**: 85
- Upadhyaya NM, Mago R, Staskawicz BJ, Ayliffe MA, Ellis JG, Dodds PN** (2014) A bacterial type III secretion assay for delivery of fungal effector proteins into wheat. *Molecular Plant-Microbe Interactions* **27**: 255-264
- Üstün S, Börnke F** (2015) The *Xanthomonas campestris* type III effector XopJ proteolytically degrades proteasome subunit RPT6. *Plant physiology* **168**: 107-119

References

- van Butselaar T, Van den Ackerveken G** (2020) Salicylic acid steers the growth–immunity tradeoff. *Trends in plant science* **25**: 566-576
- Van der Does D, Leon-Reyes A, Koornneef A, Van Verk MC, Rodenburg N, Pauwels L, Goossens A, Körbes AP, Memelink J, Ritsema T** (2013) Salicylic acid suppresses jasmonic acid signaling downstream of SCFCO11-JAZ by targeting GCC promoter motifs via transcription factor ORA59. *The Plant Cell* **25**: 744-761
- Van Engelenburg SB, Palmer AE** (2010) Imaging type-III secretion reveals dynamics and spatial segregation of Salmonella effectors. *Nature methods* **7**: 325-330
- van Esse HP, Van't Klooster JW, Bolton MD, Yadeta KA, van Baarlen P, Boeren S, Vervoort J, de Wit PJ, Thomma BP** (2008) The *Cladosporium fulvum* virulence protein Avr2 inhibits host proteases required for basal defense. *The Plant Cell* **20**: 1948-1963
- Vánky K, Lutz M** (2007) Revision of some Thecaphora species (Ustilaginomycotina) on Caryophyllaceae. *Mycological Research* **111**: 1207-1219
- Vánky K, Lutz M, Bauer R** (2008) About the genus Thecaphora (Glomosporiaceae) and its new synonyms. *Mycological Progress* **7**: 31-39
- Vargas WA, Sanz-Martín JM, Rech GE, Armijos-Jaramillo VD, Rivera LP, Echeverría MM, Díaz-Mínguez JM, Thon MR, Sukno SA** (2016) A fungal effector with host nuclear localization and DNA-binding properties is required for maize anthracnose development. *Molecular plant-microbe interactions* **29**: 83-95
- Vega FE** (2008) Insect pathology and fungal endophytes. *Journal of invertebrate pathology* **98**: 277-279
- Vlot AC, Dempsey DMA, Klessig DF** (2009) Salicylic acid, a multifaceted hormone to combat disease. *Annual review of phytopathology* **47**: 177-206
- Voegelé RT, Struck C, Hahn M, Mendgen K** (2001) The role of haustoria in sugar supply during infection of broad bean by the rust fungus *Uromyces fabae*. *Proceedings of the National Academy of Sciences* **98**: 8133-8138
- Wang KL-C, Li H, Ecker JR** (2002) Ethylene biosynthesis and signaling networks. *The plant cell* **14**: S131-S151
- Wang L, Chen S, Kong W, Li S, Archbold DD** (2006) Salicylic acid pretreatment alleviates chilling injury and affects the antioxidant system and heat shock proteins of peaches during cold storage. *Postharvest Biology and Technology* **41**: 244-251
- Wang M, Ji Z, Yan H, Xu J, Zhao X, Zhou Z** (2022) Effector Sntf2 Interacted with Chloroplast-Related Protein Mdycf39 Promoting the Colonization of *Colletotrichum gloeosporioides* in Apple Leaf. *International Journal of Molecular Sciences* **23**: 6379
- Wasternack C** (2017) A plant's balance of growth and defense–revisited. *New Phytologist* **215**: 1291-1294
- Wasternack C, Feussner I** (2018) The oxylipin pathways: biochemistry and function. *Annual review of plant biology* **69**: 363-386
- Wasternack C, Hause B** (2013) Jasmonates: biosynthesis, perception, signal transduction and action in plant stress response, growth and development. An update to the 2007 review in *Annals of Botany*. *Annals of botany* **111**: 1021-1058

References

- Wasternack C, Strnad M** (2016) Jasmonate signaling in plant stress responses and development—active and inactive compounds. *New Biotechnology* **33**: 604-613
- Wernegreen JJ** (2005) For better or worse: genomic consequences of intracellular mutualism and parasitism. *Current opinion in genetics & development* **15**: 572-583
- Weßling R, Epple P, Altmann S, He Y, Yang L, Henz SR, McDonald N, Wiley K, Bader KC, Gläßer C** (2014) Convergent targeting of a common host protein-network by pathogen effectors from three kingdoms of life. *Cell host & microbe* **16**: 364-375
- Wicker T, Oberhaensli S, Parlange F, Buchmann JP, Shatalina M, Roffler S, Ben-David R, Doležel J, Šimková H, Schulze-Lefert P** (2013) The wheat powdery mildew genome shows the unique evolution of an obligate biotroph. *Nature genetics* **45**: 1092-1096
- Williamson B, Tudzynski B, Tudzynski P, Van Kan JA** (2007) *Botrytis cinerea*: the cause of grey mould disease. *Molecular plant pathology* **8**: 561-580
- Win J, Chaparro-Garcia A, Belhaj K, Saunders D, Yoshida K, Dong S, Schornack S, Zipfel C, Robatzek S, Hogenhout S** (2012) Effector biology of plant-associated organisms: concepts and perspectives. *In* Cold Spring Harbor symposia on quantitative biology, Vol 77. Cold Spring Harbor Laboratory Press, pp 235-247
- Wirthmueller L, Asai S, Rallapalli G, Sklenar J, Fabro G, Kim DS, Lintermann R, Jaspers P, Wrzaczek M, Kangasjärvi J** (2018) Arabidopsis downy mildew effector HaRxL106 suppresses plant immunity by binding to RADICAL-INDUCED CELL DEATH1. *New Phytologist* **220**: 232-248
- Xin X-F, Kvitko B, He SY** (2018) *Pseudomonas syringae*: what it takes to be a pathogen. *Nature Reviews Microbiology* **16**: 316-328
- Yang B, Wang Y, Guo B, Jing M, Zhou H, Li Y, Wang H, Huang J, Wang Y, Ye W** (2019) The Phytophthora sojae RXLR effector Avh238 destabilizes soybean Type2 Gm ACSs to suppress ethylene biosynthesis and promote infection. *New Phytologist* **222**: 425-437
- Yang C, Li W, Cao J, Meng F, Yu Y, Huang J, Jiang L, Liu M, Zhang Z, Chen X** (2017) Activation of ethylene signaling pathways enhances disease resistance by regulating ROS and phytoalexin production in rice. *The Plant Journal* **89**: 338-353
- Yang D-L, Yao J, Mei C-S, Tong X-H, Zeng L-J, Li Q, Xiao L-T, Sun T-p, Li J, Deng X-W** (2012) Plant hormone jasmonate prioritizes defense over growth by interfering with gibberellin signaling cascade. *Proceedings of the National Academy of Sciences* **109**: E1192-E1200
- Yang J, Duan G, Li C, Liu L, Han G, Zhang Y, Wang C** (2019) The crosstalks between jasmonic acid and other plant hormone signaling highlight the involvement of jasmonic acid as a core component in plant response to biotic and abiotic stresses. *Frontiers in plant science* **10**: 1349
- Yang L, Teixeira PJPL, Biswas S, Finkel OM, He Y, Salas-Gonzalez I, English ME, Epple P, Mieczkowski P, Dangl JL** (2017) *Pseudomonas syringae* type III effector HopBB1 promotes host transcriptional repressor degradation to regulate phytohormone responses and virulence. *Cell host & microbe* **21**: 156-168
- Yatsu L, Boynton D** (1959) Pipelicolic acid in leaves of strawberry plant as influenced by treatments affecting growth. *Science* **130**: 864-865

References

- Yildiz I, Mantz M, Hartmann M, Zeier T, Kessel J, Thurow C, Gatz C, Petzsch P, Köhrer K, Zeier J** (2021) The mobile SAR signal N-hydroxypipecolic acid induces NPR1-dependent transcriptional reprogramming and immune priming. *Plant physiology* **186**: 1679-1705
- Yoshimoto R, Ishida F, Yamaguchi M, Tanaka S** (2022) The production and secretion of tRNA-derived RNA fragments in the corn smut fungus *Ustilago maydis*. *Frontiers in Fungal Biology*: 49
- Yuan M, Ngou BPM, Ding P, Xin X-F** (2021) PTI-ETI crosstalk: an integrative view of plant immunity. *Current opinion in plant biology* **62**: 102030
- Yuan Y, Zhong S, Li Q, Zhu Z, Lou Y, Wang L, Wang J, Wang M, Li Q, Yang D** (2007) Functional analysis of rice NPR1-like genes reveals that OsNPR1/NH1 is the rice orthologue conferring disease resistance with enhanced herbivore susceptibility. *Plant biotechnology journal* **5**: 313-324
- Zander M, Thurow C, Gatz C** (2014) TGA transcription factors activate the salicylic acid-suppressible branch of the ethylene-induced defense program by regulating ORA59 expression. *Plant physiology* **165**: 1671-1683
- Zeier J** (2021) Metabolic regulation of systemic acquired resistance. *Current Opinion in Plant Biology* **62**: 102050
- Zhai Q, Zhang X, Wu F, Feng H, Deng L, Xu L, Zhang M, Wang Q, Li C** (2015) Transcriptional mechanism of jasmonate receptor CO11-mediated delay of flowering time in *Arabidopsis*. *The Plant Cell* **27**: 2814-2828
- Zhang F, Ke J, Zhang L, Chen R, Sugimoto K, Howe GA, Xu HE, Zhou M, He SY, Melcher K** (2017) Structural insights into alternative splicing-mediated desensitization of jasmonate signaling. *Proceedings of the National Academy of Sciences* **114**: 1720-1725
- Zhang L, Zhang F, Melotto M, Yao J, He SY** (2017) Jasmonate signaling and manipulation by pathogens and insects. *Journal of experimental botany* **68**: 1371-1385
- Zheng X-y, Spivey NW, Zeng W, Liu P-P, Fu ZQ, Klessig DF, He SY, Dong X** (2012) Coronatine promotes *Pseudomonas syringae* virulence in plants by activating a signaling cascade that inhibits salicylic acid accumulation. *Cell host & microbe* **11**: 587-596
- Zhou J-M, Chai J** (2008) Plant pathogenic bacterial type III effectors subdue host responses. *Current opinion in microbiology* **11**: 179-185
- Zhou Z, Wu Y, Yang Y, Du M, Zhang X, Guo Y, Li C, Zhou J-M** (2015) An *Arabidopsis* plasma membrane proton ATPase modulates JA signaling and is exploited by the *Pseudomonas syringae* effector protein AvrB for stomatal invasion. *The Plant Cell* **27**: 2032-2041
- Zhu J-K** (2016) Abiotic stress signaling and responses in plants. *Cell* **167**: 313-324
- Zhu Z, An F, Feng Y, Li P, Xue L, Jiang Z, Kim J-M, To TK, Li W, Zhang X** (2011) Derepression of ethylene-stabilized transcription factors (EIN3/EIL1) mediates jasmonate and ethylene signaling synergy in *Arabidopsis*. *Proceedings of the National Academy of Sciences* **108**: 12539-12544

References

- Zuccaro A, Lahrmann U, Güldener U, Langen G, Pfiffi S, Biedenkopf D, Wong P, Samans B, Grimm C, Basiewicz M** (2011) Endophytic life strategies decoded by genome and transcriptome analyses of the mutualistic root symbiont *Piriformospora indica*. *PLoS pathogens* **7**: e1002290
- Zuo W, Ökmen B, Depotter JR, Ebert MK, Redkar A, Misas Villamil J, Doehlemann G** (2019) Molecular interactions between smut fungi and their host plants. *Annual Review of Phytopathology* **57**: 411-430

Supplementary figures

9. Supplementary figures

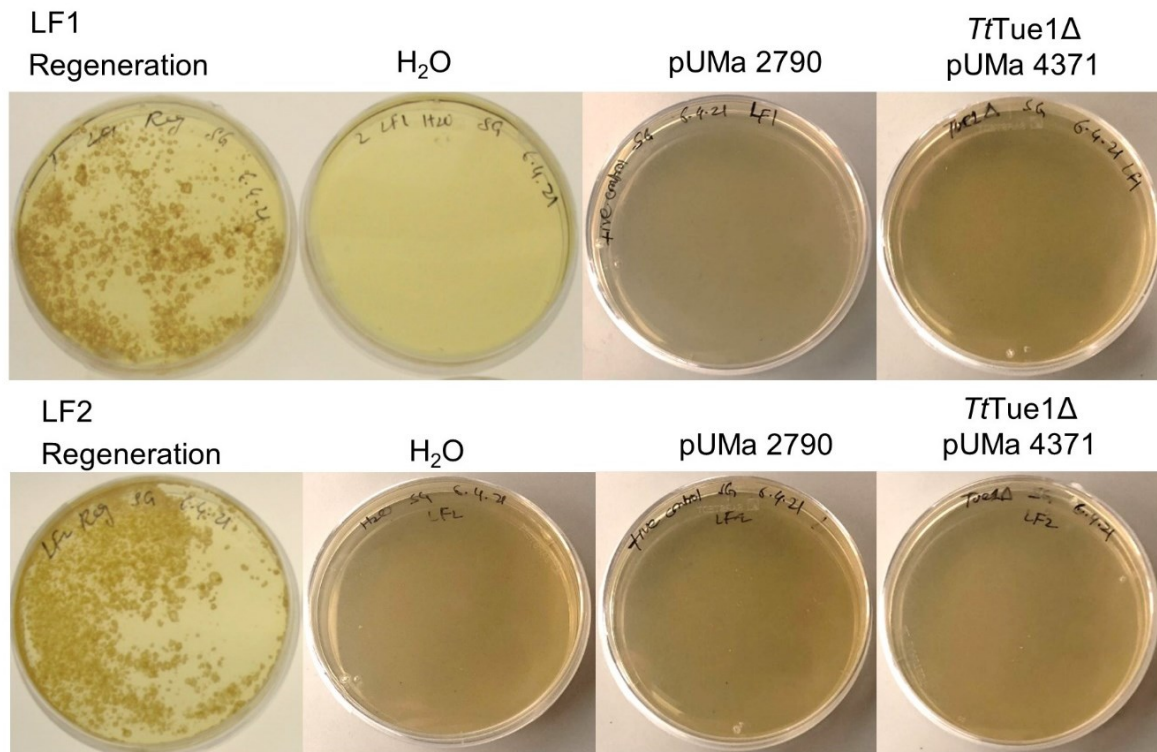
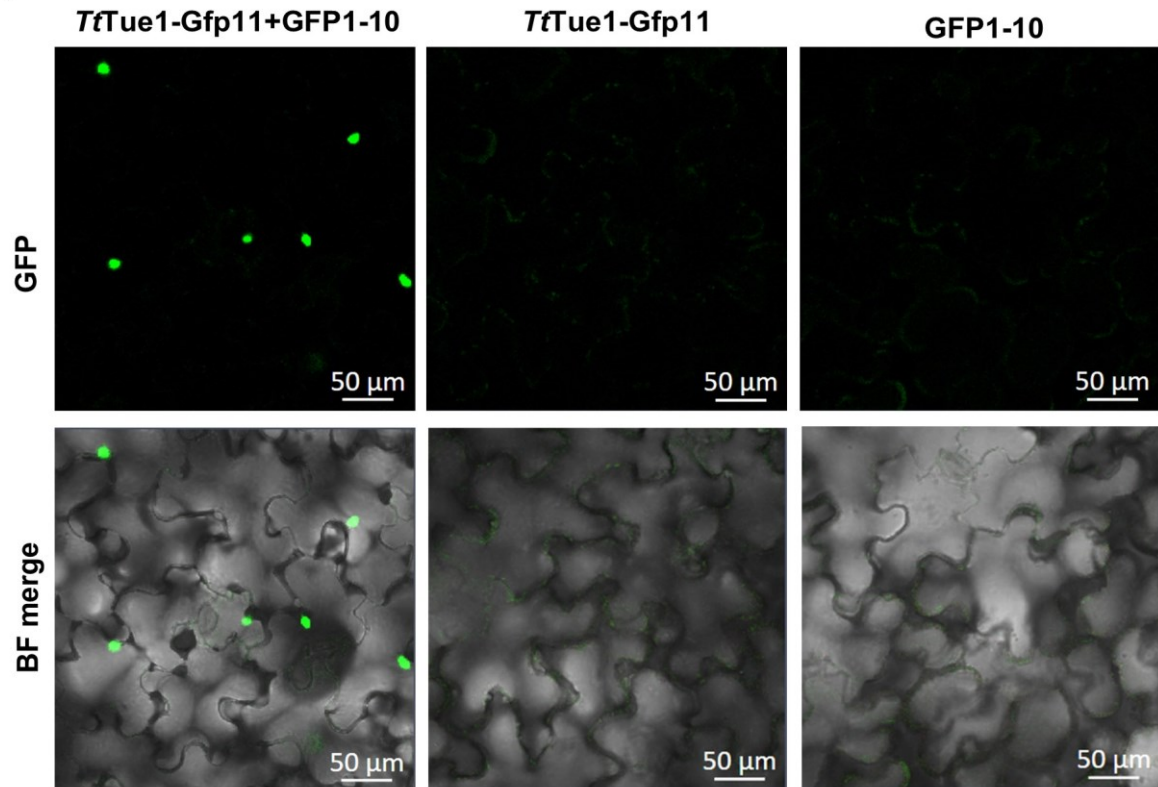


Fig. S1 Generation of *TtTue1Δ* strain by LF1 and LF2 transformation. Upper panel showed the transformation attempts using LF1 culture. There were no colonies found for *TtTue1Δ* construct. Lower panel showed the transformation of LF2 culture and similarly no transformants were found for *TtTue1* deletion construct. Plates were incubated at 16 °C up to 8-12 weeks. Both panels show the representative images of 12 independent transformations attempts for both LF1 and LF2 cultures. pUMa 2790 is self replicating plasmid and used as a control.

Supplementary figures

(a)



(b)

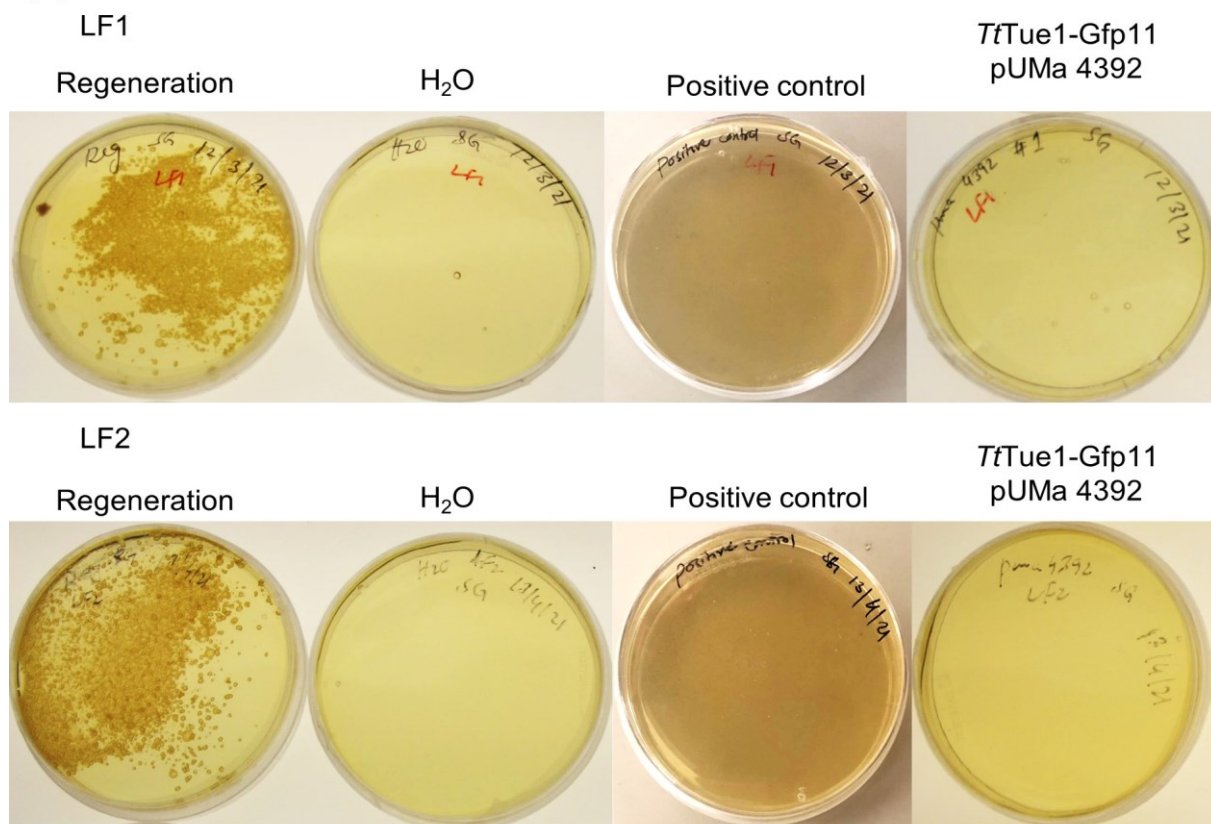
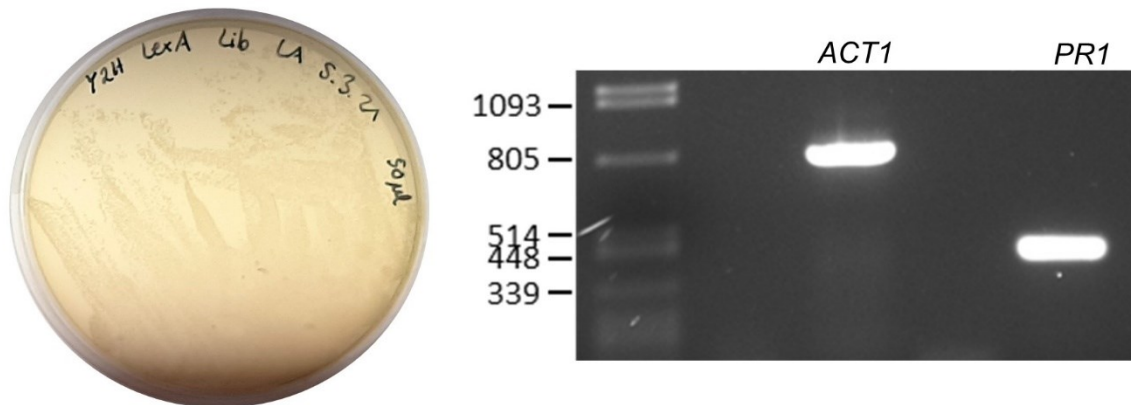


Fig. S2. *TtTue1* translocation to the plant via GFP strand system. (a) *TtTue1*-Gfp11 made functional protein upon fusing with GFP1-10 strands in the transient expression system in *N-benthamaina* under the expression of 35S promoter. Co-expression of *TtTue1*-Gfp11 and GFP1-10 displayed *TtTue1* localization in the nucleus. *TtTue1*-Gfp11 and GFP1-10 alone were used as a negative

Supplementary figures

control. Incomplete GFP strands did not show any fluorescence signal. Experiment was repeated for three biological replicates (b) *T. thlaspeos* strains LF1 and LF2 transformation with *TtTue1*-Gfp11 under the expression of native promoter was carried out. Protoplast mediated transformation shows nicely regenerated protoplast of both strains while no transformants were found for *TtTue1*-Gfp11. Independent transformations were repeated 12 times for each strain. Plates were incubated at 16 °C up to 8-12 weeks. pUMa 2790 is self replicating plasmid and used as a control.

(a)



(b)

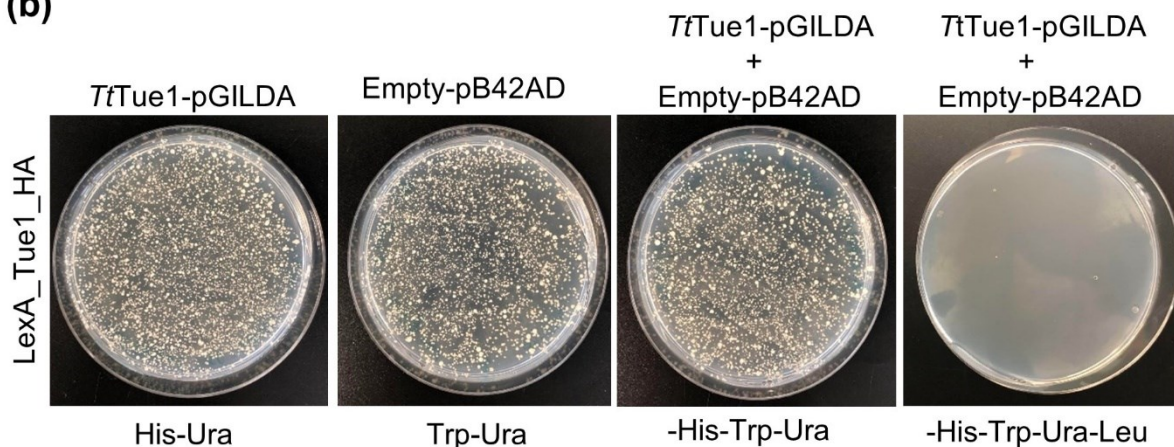


Fig. S3 Validation of infectious *A. thaliana* cDNA library material and auto-activity test of *TtTue1* in yeast. (a) Library material obtained from group of Prof. Dr. Maeli Melotto at University of California and transformed in *E. coli* and cells were plated on Ampicillin containing medium. Expression of stress related gene were verified by a PCR for *PR1* and *ACT1* as a control. Sizes Actin 793 bp, *PR1* 411 bp. Both tests verified the library material for Y2H screen. (b) Auto-activation of *TtTue1* in yeast strain EGY48 was checked by its co-transformation with empty prey vector pB42AD. Transformants were plated on both plasmid selection (three drop out) and a reporter gene selection (four drop out) media. Plate with four drop out for reporter gene selection did not show any growth which verified that *TtTue1* was not auto-active.

Supplementary figures

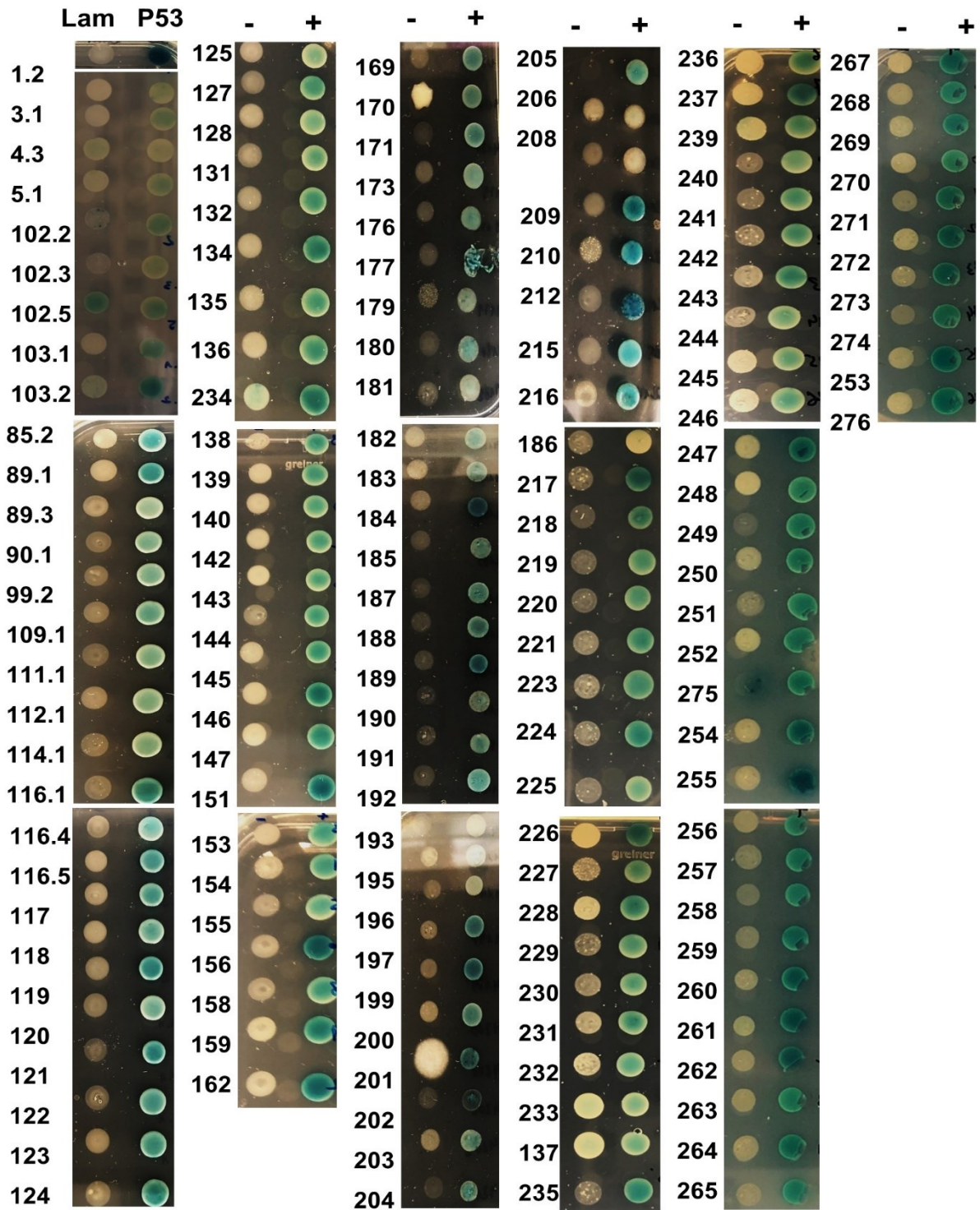


Fig. S4 Targeted Y2H assay and auto-activity test of 150 selected candidates from the Y2H screen. Lam+SV40 T-antigen and P53+SV40 T-antigen were used as negative and positive controls, respectively. Negative sign on the top of each image denotes the interaction of library candidates with empty bait vector (pGILDA) while positive sign shows interaction of library candidates with *TtTue1* in pGILDA. Numbers on left side of each dot were the given numbers during the selection procedure of the promising candidates. Test was done by co-transforming *TtTue1* with prey candidates and as a control empty bait vector was co-transformed with *TtTue1*. Three candidates showed auto-activity and 7 were false positives in the test which were removed from the selection process.

Supplementary figures

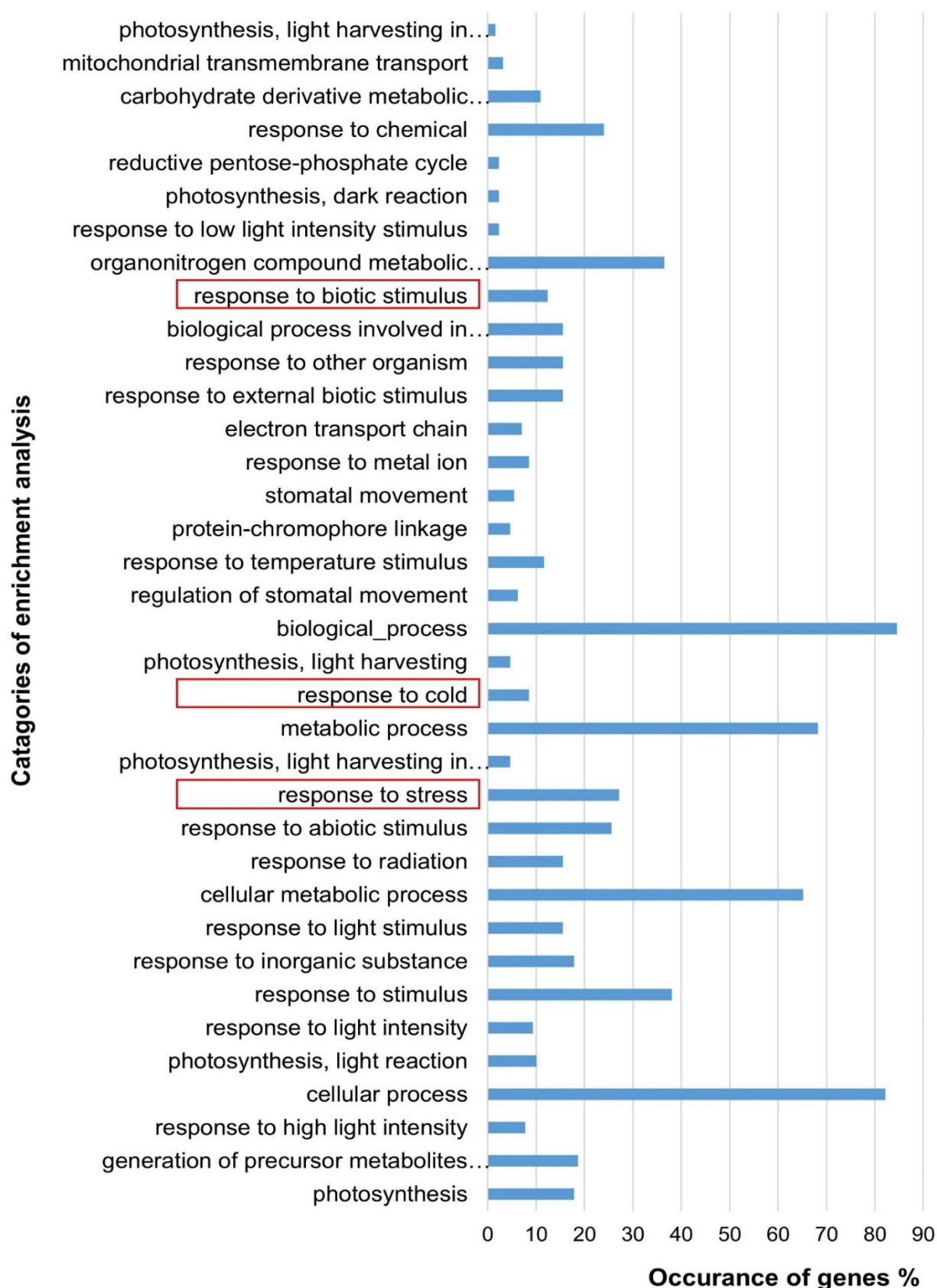


Fig. S5. Enrichment analysis of 129 plant genes found in Y2H library screen of *TtTue1*. List of 129 candidates were subjected to enrichment analysis via g: Profiler. Y axis shows 36 categories shortlisted from the GO biological process on basis of significant $p < 0.05$. X axis shows the percentage of genes in each category. The red boxes show selected three stress related catagories.

Supplementary figures

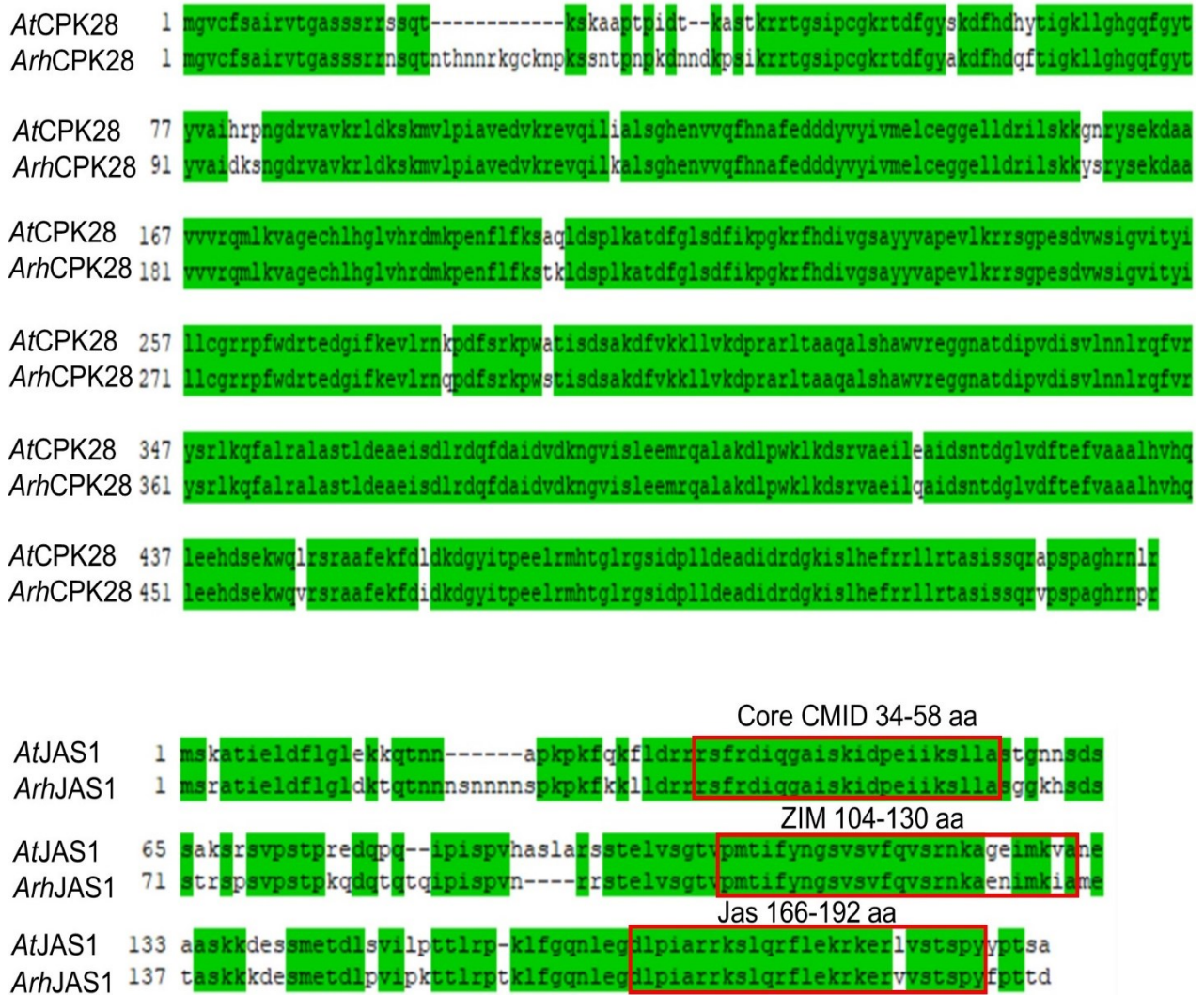


Fig. S6 Sequence similarity of *Ar. hirsuta* and *A. thaliana* homologs of CPK28 and JAS1. Protein alignment was done in clone manager by using scoring matrix BLOSUM 62. *ArhCPK28* protein shows 92% similarity with *AtCPK28* while *ArhJAS1* has 78% similarity with *AtJAS1*. The red boxes show N-terminal Core CMID domain, central ZIM domain, C-terminal Jas domain. These domains were identified in *AtJAS1* and the sequence alignment showed their conservation in *ArhJAS1*. The ZIM domain showed difference of three amino acids while Jas domain has a difference of single amino acid.

Supplementary figures

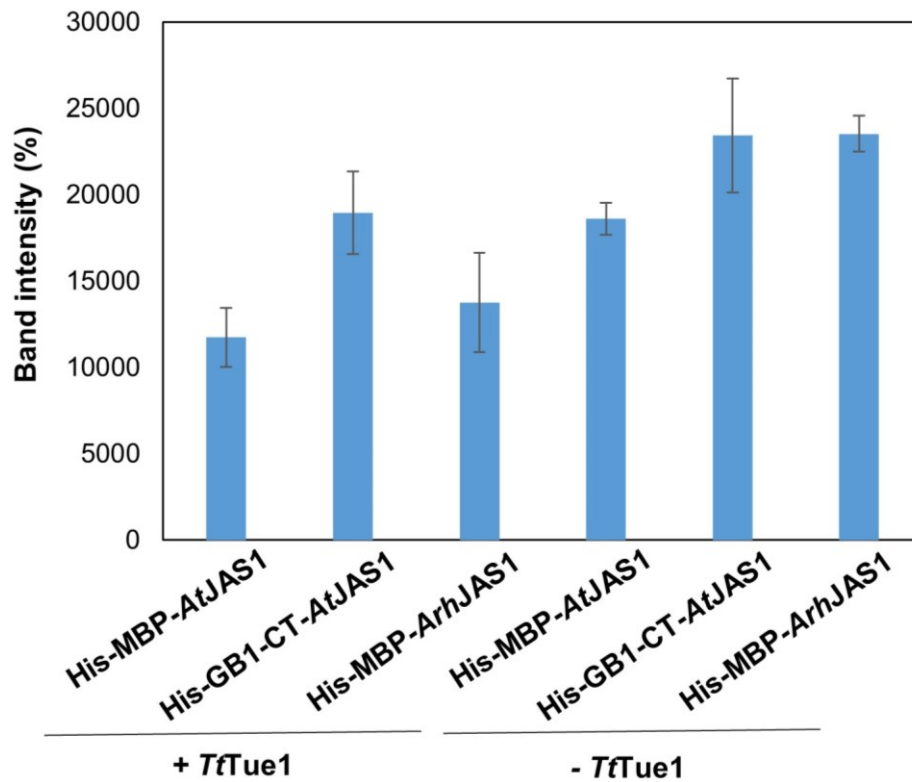
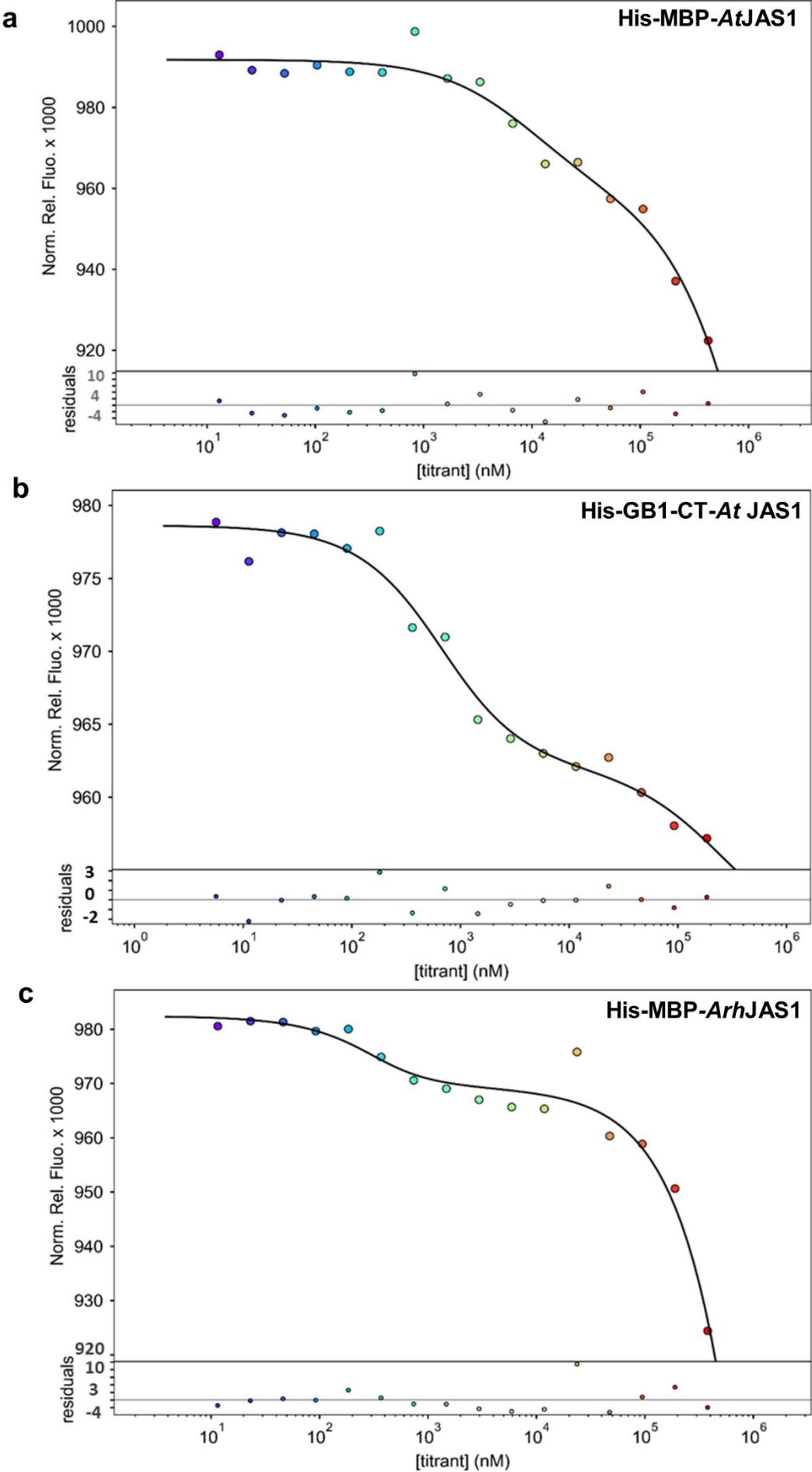


Fig. S7 Band intensity quantification of *TtTue1* interaction partner *JAS1*. Bands were quantified from western blot of GST pull down by using imageJ. First three bars denoted the *AtJAS1*, CT-*AtJAS1* and *ArhJAS1* pull down with GST-*TtTue1*. The last three bars showed the respected proteins loaded as control. CT-*AtJAS1* showed an increase in binding affinity with *TtTue1* in comparison to full length *AtJAS1* and *ArhJAS1*.

Supplementary figures



Supplementary figures

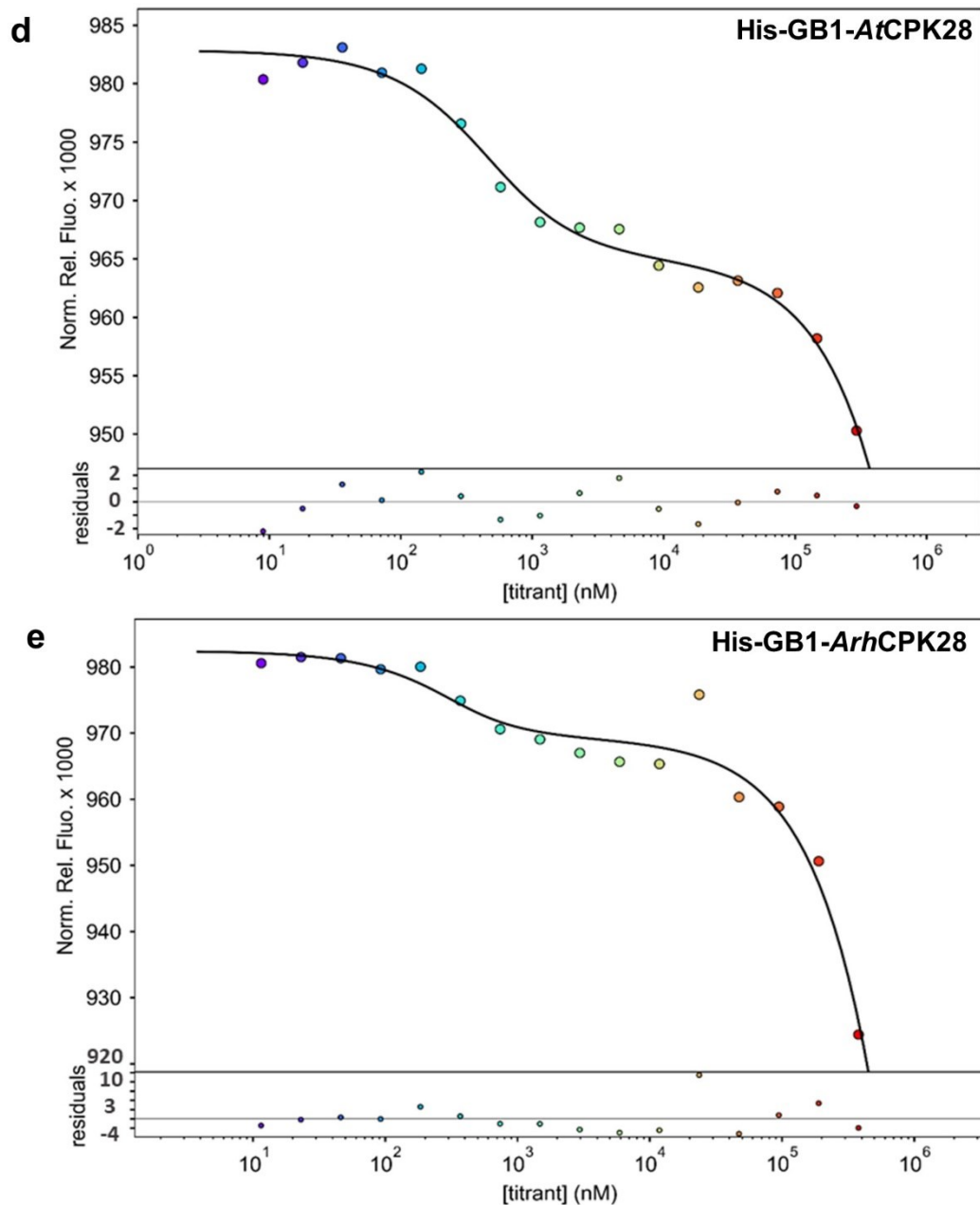


Fig. S8 1:2 binding model of *Tt*Tue1 MST fits to simulated data. The MST data used for 1:1 model (Fig. 5-10) were fitted to a 1:2 binding model by using the PALMIST software (Scheuermann et al., 2016) (Scheuermann et al., 2016). It is postulated that binding curves revealed two binding sites of *Tt*Tue1 thus two K_D 's, $K_D(1)$ and $K_D(2)$ were obtained in 1:2 model. K_D values are as follows: His-MBP-*At*JAS1 $K_D(1)$ 9 μ M $K_D(2)$ 2300 μ M, His-GB1-CT-*At* JAS1 $K_D(1)$ 500 nM $K_D(2)$ 300 μ M, His-MBP-*Arh*JAS1 $K_D(1)$ 300 nM $K_D(2)$ 9953 μ M, His-GB1-*At*CPK28 $K_D(1)$ 300 nM $K_D(2)$ 2000 μ M, His-GB1-*Arh*CPK28 $K_D(1)$ 125 nM $K_D(2)$ 800 μ M. There may be too few data points to fit to 1:2 model and clearly resolve a second binding step. The fit becomes indeterminate if the cooperativity is close to 1 or the MST signal of the protein with one or two bound ligands is too similar to be resolved (see PALMIST manual). The lower plot shows the residuals between the data and the fit.

Supplementary figures

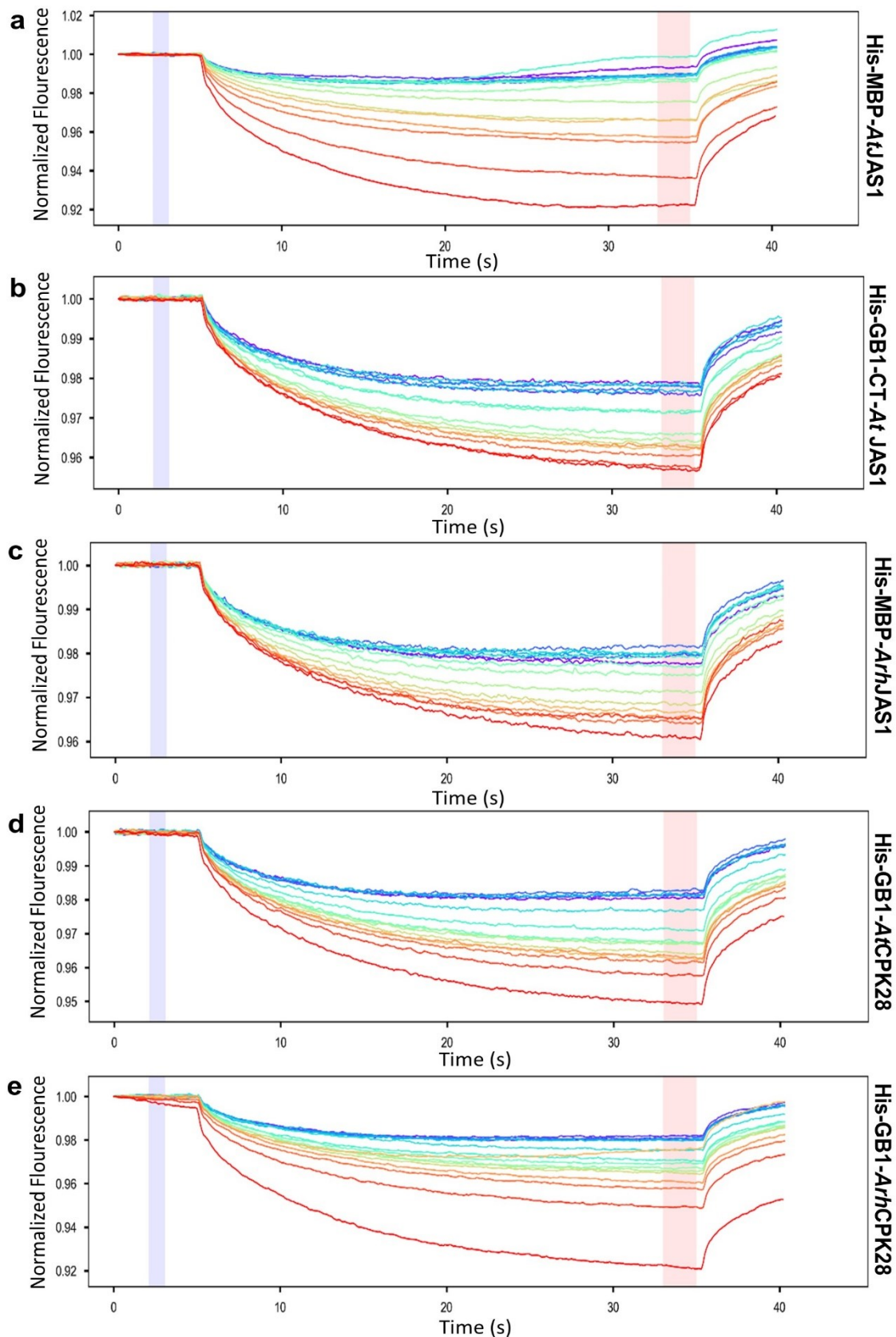


Fig. S9 Thermographs of *TtTue1* binding to mentioned ligands provide well-defined curves. The temperature gradient was not applied at cold spot indicated by blue region at 0 s, and the red region after 30 s shows the hot spot during the thermophoresis. Thermophoresis was measured using a Monolith NT.115 instrument, with an excitation power of 20-50% for 30 s and MST power of 40% at an ambient temperature of 24 °C.

Supplementary tables

Table. S1 List of 129 sequenced and identified candidates from Y2H screen

S. no	Gene ID	Hits	Description (from TAIR)
1	AT4G12800.1	4	PHOTOSYSTEM I SUBUNIT L, PSAL Encodes subunit L of photosystem I reaction centre
2	AT1G79040.1	3	PHOTOSYSTEM II SUBUNIT R, PSBR. located in chloroplast
3	AT5G66210.2	3	CALCIUM-DEPENDENT PROTEIN KINASE 28, CPK28. Calcium Dependent Protein Kinase. Functions in the innate immune response pathway
4	AT3G27830.1	3	RIBOSOMAL PROTEIN L12, the mRNA is cell-to-cell mobile. Located in chloroplast
5	AT1G29930.1	3	AB140, CAB1, CAB140, CHLOROPHYLL A/B BINDING PROTEIN 1, CHLOROPHYLL A/B PROTEIN 140
6	AT5G38410.3	2	RBCS3B, RUBISCO SMALL SUBUNIT 3B, Located in apoplast, cell wall
7	AT3G27850.1	2	RIBOSOMAL PROTEIN L12-C, RPL12-C 50S ribosomal protein L12-C The mRNA is cell-to-cell mobile
8	AT3G54890.1	2	LHCA1, PHOTOSYSTEM I LIGHT HARVESTING COMPLEX GENE 1. Encodes a component of the light harvesting complex associated with photosystem I
9	AT4G09320.1	2	ATNDK1, NDK1, NDPK1, NUCLEOSIDE DIPHOSPHATE KINASE 1 involved in CTP biosynthetic process
10	AT1G06460.1	2	ACD31.2, ALPHA-CRYSTALLIN DOMAIN 31.2, 1 encodes an alpha-crystalline domain containing protein with homology to small heat shock proteins
11	AT3G16140.1	2	PHOTOSYSTEM I SUBUNIT H-1, PSAH-1 Encodes subunit H of photosystem I reaction centre subunit VI
12	AT5G13220.1	1	JAS1, JASMONATE-ASSOCIATED 1, JASMONATE-ZIM-DOMAIN PROTEIN 10, JAZ10, regulation of systemic acquired resistance, response to jasmonic acid
13	AT1G05940.1	1	CAT9, CATIONIC AMINO ACID TRANSPORTER 9, amino acid transport, transmembrane transport
14	AT5G60850.1	1	ATDOF5.4, OBF BINDING PROTEIN 4, OBP4. acts upstream of or within regulation of transcription
15	AT1G31580.1	1	ECS1 Encodes cell wall protein. Response to bacterium
16	AT1G67090.1	1	RBCS1A, RIBULOSE BIPHOSPHATE CARBOXYLASE SMALL CHAIN 1A, response to cold
17	AT4G19200.1	1	GLYCINE AND PROLINE RICH PROTEIN 3, GPRP3, Hormone-mediated signaling pathway
18	AT5G02870.1	1	RIBOSOMAL LARGE SUBUNIT 4, RPL4, response to inorganic substance
19	AT3G21055.1	1	PHOTOSYSTEM II SUBUNIT T, PSBTN, a nuclear-encoded gene
20	AT2G43030.1	1	Ribosomal protein L3 family protein
21	AT3G14415.2	1	GLYCOLATE OXIDASE 2, GOX2. defence response to bacterium
22	AT1G62750.1	1	ATSCO1, ATSCO1/CPEF-G, SCO1, SNOWY COTYLEDON 1
23	AT2G04700.1	1	FERREDOXIN/THIOREDOXIN REDUCTASE CATALYTIC SUBUNIT, FTRB, IMBALANCED NADP STATUS 1, INAP1 Located in chloroplast
24	AT1G01470.1	1	ARABIDOPSIS THALIANA LATE EMBRYOGENESIS ABUNDANT 14, ATLEA14, defence response to fungus
25	AT4G00300.1	1	Located in endoplasmic reticulum, extracellular region
26	AT3G50820.1	1	OEC33, OXYGEN EVOLVING COMPLEX SUBUNIT 33. located in chloroplast
27	AT1G55490.1	1	CHAPERONIN 60 BETA, CHAPERONIN-60BETA1, CPN60B, systemic acquired resistance
28	AT1G73230.1	1	Nascent polypeptide-associated complex NAC, located in mitochondrion
29	AT2G06050.2	1	ATOPR3, DDE1, DELAYED DEHISCENCE 1, OPR3
30	AT5G48800.1	1	Phototropic-responsive NPH3 family protein. maintenance of meristem identity
31	AT4G29350.1	1	ATPRF2, PFN2, PRF2, PRO2, PROFILIN 2 Encodes profilin2 actin monomer-binding protein

Supplementary tables

32	AT1G02920.1	1	ARABIDOPSIS GLUTATHIONE S-TRANSFERASE 11, ATGST11 response to cadmium ion
33	AT2G01290.1	1	RIBOSE-5-PHOSPHATE ISOMERASE 2, RPI2 Cytosolic ribose-5-phosphate isomerase
34	AT3G28930.3	1	AIG2, AVRRT2-INDUCED GENE 2 avrRpt2-induced gene that exhibits RPS2- and avrRpt2-dependent induction early after infection with <i>Pseudomonas syringae</i>
35	AT5G54270.1	1	LHCB3, acts upstream of or within photosynthesis. located in chloroplast
36	AT3G15840.1	1	PIFI, POST-ILLUMINATION CHLOROPHYLL FLUORESCENCE INCREASE acts upstream of or within chloro- respiration
37	AT1G09310.1	1	SVB-LIKE, SVB2, SVBL. ABA responsive trichome formation regulator. acts upstream of or within carboxylic acid metabolic process
38	AT1G78010.1	1	TRME tRNA modification GTPase, involved in tRNA methylation
39	AT3G01850.2	1	Aldolase-type TIM barrel family protein, involved in carbohydrate metabolic process
40	AT3G13050.1	1	ATNIAP, NICOTINATE TRANSPORTER. Encodes a plant nicotinate transporter than can also transport trigonelline
41	AT1G73470.1	1	hypothetical protein acts upstream of or within macromolecule catabolic process
42	AT1G17080.1	1	Ribosomal protein L18ae family. acts upstream of or within organelle organization
43	AT2G26500.1	1	PETM Essential for the stabilization and function of the cytochrome b6f complex
44	AT5G40810.1	1	Cytochrome C1 family. acts upstream of or within cellular localization
45	AT1G56070.1	1	LOS1, LOW EXPRESSION OF OSMOTICALLY RESPONSIVE GENES 1. involved in cold acclimation
46	AT4G05050.3	1	UBIQUITIN 11, UBQ11 polyubiquitin gene, acts upstream of or within ubiquitin-dependent protein catabolic process
47	AT2G35795.1	1	PAM18-1 Chaperone DnaJ-domain superfamily protein, involved in protein import into mitochondrial matrix
48	AT5G13240.3	1	MAF1, Global repressor of RNA polymerase III (Pol III) response to hydroperoxide, response to stress
49	AT3G25780.1	1	ALLENE OXIDE CYCLASE 3, AOC3, encodes allene oxide cyclase
50	AT5G13490.1	1	AAC2, ADP/ATP CARRIER 2 Encodes mitochondrial ADP/ATP carrier
51	AT5G26000.1	1	ATTGG1, BETA GLUCOSIDASE 38, BGLU38, TGG1, THIOLUCOSIDE GLUCOHYDROLASE 1
52	AT4G04020.1	1	FIB, FIB1A, FIBRILLIN, FIBRILLIN 1A, PGL35, PLASTOGLOBULIN 35. Fibrillin precursor protein
53	AT3G25770.1	1	AOC2, catalyzes an essential step in jasmonic acid biosynthesis
54	AT5G28345.1	1	hypothetical protein
55	AT1G32172.1	1	Other_RNA
56	AT1G15970.1	1	DNA glycosylase superfamily protein. involved in base-excision repair
57	AT3G15353.2	1	ATMT3, METALLOTHIONEIN 3, MT3 metallothionein
58	AT2G40060.1	1	CLATHRIN LIGHT CHAIN 2, CLC2 Encodes a clathrin that is localized to the cortical division zone and the cell plate
59	AT1G06040.1	1	B-BOX DOMAIN PROTEIN 24, BBX24, encodes salt tolerance protein (STO) which confers salt tolerance to yeast cells
60	AT2G34480.2	1	L18AB, RPL18AB Encodes a nuclear localized member of the ribosomal L18ae/LX protein family
61	AT5G65990.1	1	ATAVT3 Transmembrane amino acid transporter family protein
62	AT5G04880.1	1	pseudogene of ABC transporter family protein
63	AT5G42380.1	1	ATCML37, CALMODULIN LIKE 37, CML37 acts upstream of or within cellular response to hypoxia
64	AT4G13495.2	1	other_RNA
65	AT2G03470.1	1	ATAVT3 Transmembrane amino acid transporter family protein
66	AT4G25740.1	1	RNA binding Plectin/S10 domain-containing protein. acts upstream of or within cellular component biogenesis

Supplementary tables

67	AT1G01020.1	1	ARV1 ARV1 family protein. acts upstream of or within sphingolipid metabolic process
68	AT3G45030.1	1	AT3G45030.1 Length=717 Identities = 489/490 (99%) Ribosomal protein S10p/S20e family protein. located in chloroplast
69	AT2G26140.1	1	ATFTSH4, FTSH PROTEASE 4, FTSH4 Encodes an FtsH protease that is localized to the mitochondrion
70	AT2G41100.1	1	ARABIDOPSIS THALIANA CALMODULIN LIKE 4, ATCAL4, CALMODULIN-LIKE 12, CML12, TCH3, TOUCH 3
71	AT3G28730.1	1	ATHMG, HIGH MOBILITY GROUP, HMG, NFD, NUCLEOSOME/CHROMATIN ASSEMBLY FACTOR D, SSRP1
72	AT1G19570.1	1	ATDHAR1, DEHYDROASCORBATE REDUCTASE, DEHYDROASCORBATE REDUCTASE 5, DHAR1, DHAR5. Encodes a member of the dehydroascorbate reductase gene family
73	AT4G32980.1	1	ATH1, HOMEBOX GENE 1. Encodes transcription factor involved in photomorphogenesis
74	AT2G38270.1	1	ATGRX2, ATGRXS16, CAX-INTERACTING PROTEIN 2, CXIP2, GLUTAREDOXIN 16, GLUTAREDOXIN 2 Encodes protein homologous to CXIP1. CXIP1
75	AT1G31180.2	1	ARABIDOPSIS ISOPROPYLMALATE DEHYDROGENASE 3, ATIMD3, IMD3, IMDH3, IPMDH1, ISOPROPYLMALATE DEHYDROGENASE 1, ISOPROPYLMALATE DEHYDROGENASE 3
76	AT1G78040.1	1	Pollen Ole e 1 allergen and extensin family protein. acts upstream of or within developmental growth
77	AT4G28750.1	1	PSA E1 KNOCKOUT, PSAE-1 mutant has Decreased effective quantum yield of photosystem II
78	AT3G22890.1	1	APS1, ATP SULFURYLASE 1, ATPS1 encodes ATP sulfurylase
79	AT3G26380.1	1	APSE, ARAPASE APSE is a member of the Glycoside Hydrolase (GH27) family that functions as a β -l-arabinopyranosidase
80	AT2G20890.1	1	PHOTOSYSTEM II REACTION CENTER PSB29 PROTEIN, PSB29, THF1, THYLAKOID FORMATION1
81	AT1G06680.1	1	OE23, OEE2, OXYGEN EVOLVING COMPLEX SUBUNIT 23 KDA, OXYGEN-EVOLVING ENHANCER PROTEIN 2
82	AT3G43720.1	1	GLYCOSYLPHOSPHATIDYLINOSITOL-ANCHORED LIPID PROTEIN TRANSFER 2, LTPG2 Bifunctional inhibitor/lipid-transfer
83	AT3G26980.1	1	MEMBRANE-ANCHORED UBIQUITIN-FOLD PROTEIN 4 PRECURSOR, MUB4
84	AT3G51600.1	1	LIPID TRANSFER PROTEIN 5, LTP5 Predicted to encode a PR (pathogenesis-related) protein
85	AT3G47470.1	1	CAB4, LHCA4, LIGHT-HARVESTING CHLOROPHYLL-PROTEIN COMPLEX I SUBUNIT A4
86	AT2G21660.1	1	ATGRP7, CCR2, COLD, CIRCADIAN RHYTHM, AND RNA BINDING 2, GLYCINE RICH PROTEIN 7, GLYCINE-RICH RNA-BINDING PROTEIN 7
87	AT3G12780.1	1	PGK1, PGKP1, PHOSPHOGLYCERATE KINASE 1 PGK1
88	AT1G12330.1	1	cyclin-dependent kinase-like protein located in chloroplast
89	AT2G05070.1	1	LHCB2, LHCB2.2, LIGHT-HARVESTING CHLOROPHYLL B-BINDING 2
90	AT1G20340.1	1	DNA-DAMAGE-REPAIR/TOLERATION PROTEIN 112, DRT112, PETE2, PLASTOCYANIN 2. acts upstream of or within copper ion homeostasis
91	AT1G80230.1	1	Rubredoxin-like superfamily protein. involved in mitochondrial electron transport
92	AT3G23920.1	1	ATBAM1, BAM1, BETA-AMYLASE 1, BETA-AMYLASE 7, BMY7, TR-BAMY
93	AT1G27730.1	1	SALT TOLERANCE ZINC FINGER, STZ, ZAT10 Related to Cys2/His2-type zinc-finger proteins found in higher plants
94	AT2G21660.1	1	ATGRP7, CCR2, COLD, CIRCADIAN RHYTHM, AND RNA BINDING 2, GLYCINE RICH PROTEIN 7
95	AT2G35370.1	1	GDCH, GLYCINE DECARBOXYLASE COMPLEX H. Encodes glycine decarboxylase complex H protein
96	AT5G23060.1	1	PGK1, PGKP1, PHOSPHOGLYCERATE KINASE 1 PGK1

Supplementary tables

97	AT3G18820.1	1	LHCB2, LHCB2.2, LIGHT-HARVESTING CHLOROPHYLL B-BINDING 2, PHOTOSYSTEM II
98	AT2G23960.1	1	DNA-DAMAGE-REPAIR/TOLERATION PROTEIN 112, DRT112, PETE2, PLASTOCYANIN 2
99	AT5G13220.1	1	Rubredoxin-like superfamily protein
100	AT2G39190.1	1	ATBAM1, BAM1, BETA-AMYLASE 1, BETA-AMYLASE 7, BMY7, TR-BAMY
101	AT5G24314.1	1	SALT TOLERANCE ZINC FINGER, STZ, ZAT10
102	AT3G14930.1	1	ATGRP7, CCR2, COLD, CIRCADIAN RHYTHM, AND RNA BINDING 2, GLYCINE RICH PROTEIN 7
103	AT3G47070.1	1	GDCH, GLYCINE DECARBOXYLASE COMPLEX H. Encodes glycine decarboxylase complex H protein
104	AT3G55440.1	1	PGK1, PGKP1, PHOSPHOGLYCERATE KINASE 1 PGK1
105	AT3G53420.2	1	Cyclin-dependent kinase-like protein
106	AT4G38920.1	1	DNA-DAMAGE-REPAIR/TOLERATION PROTEIN 112, DRT112, PETE2, PLASTOCYANIN 2
107	AT3G07555.1	1	Rubredoxin-like superfamily protein. involved in mitochondrial electron transport
108	AT4G24350.4	1	ATBAM1, BAM1, BETA-AMYLASE 1, BETA-AMYLASE 7, BMY7, TR-BAMY
109	AT2G18020.1	1	SALT TOLERANCE ZINC FINGER, STZ, deprivation, response to wounding
110	AT1G68440.1	1	LHCB2, LHCB2.2, LIGHT-HARVESTING CHLOROPHYLL B-BINDING 2, PHOTOSYSTEM II LIGHT HARVESTING COMPLEX GENE 2.2
111	AT2G43910.1	1	DNA-DAMAGE-REPAIR/TOLERATION PROTEIN 112, DRT112, PETE2, PLASTOCYANIN 2. acts upstream of or within copper ion homeostasis
112	AT4G03280.1	1	ATBAM1, BAM1, BETA-AMYLASE 1, BETA-AMYLASE 7, BMY7, TR-BAMY

Acknowledgments

10. Acknowledgement

Firstly, I would like to express my sincere gratitude to my supervisor **Prof. Dr. Michael Feldbrügge** for accepting my request to do my PhD at the Institute of Microbiology and all his support. My special thanks goes to **Dr. Vera Göhre** for her guidance and support throughout the research process and writing of this thesis. She kindly helped me to obtain financial support during prolongation of my scholarship.

I am thankful to **Prof. Dr. Laura Rose** for being my mentor and for correction of my dissertation. I would like to say thanks to Dr. Sigrun Wegener-Feldbrügge and Dr. Petra Fackendahl for arranging the extended funding sources and all the organisational matters.

I would like to say a big thanks to Schlumberger foundation faculty for the future FFTF for the financial support granted to pursue my Ph.D. I am grateful for being an associated member of iGRADplant Graduate School that allow me to participate in numerous events and to get benefit from the funding at the end of my PhD.

Thanks to all iTIP students, master students Anna Wendel and Anton Kraege for helping me in various parts of my project. Thanks to Elka egger and Minerva arazia for assisting me in the Y2H screen. Special thanks to Woogie, Lesely and Trusha for helping me with different part of my theiss and their feedback. I appreciate the valuable insights and feedback from Lilli and Nina for DNA binding study. I am thankful to our collaborators, Prof. Dr. Jürgen Zeier for the hormones analysis, Prof. Dr. Holger Gholke and Dr. Mohanraj Gopalswamy for generating the MST data.

Thanks to the entire institute for the great cooperation, support, interesting discussions and the friendly atmosphere. Many thanks to the whole Rabattack team for friendly working environment in the lab. Without Uli, it was not possible to work in a fully functional lab, Many thanks to Uli for his technical assistance. I am very grateful to Woogie, Sri, Minerva, Senthil for their countinous support and encouragement in each and every moment.

All of my friends outside the institue who provided me family like environment, I am grateful to have all of you. A huge thanks to my friend Dr. Imran Khan for all his encouragement, guidance and moral support throughout my PhD Journey. Last but not least, a special thanks to my family for their understanding, support and patience which made possible to acheive my goals.

I dedicate this thesis to my Late father Saeed Ur Rehman.